

V. N. Karazin Kharkiv National University

Modern physics

V. M. KUKLIN

**SELECTED CHAPTERS
(THEORETICAL PHYSICS)**

Kharkiv – 2021

PACS 52.35 Mw;41.60.-m;
05.45 Xt;03.65 Sq;47.55 pb
K 89

Reviewers:

V. A. Buts – Head of the laboratory of NSC KIPT, Professor of V. N. Karazin University, PhD, Doctor of Sciences ;

A. V. Tur – Directeur de recherche Emérite CNRS Université Paul Sabatier, Toulouse, France, PhD, Doctor of Sciences.

*Approved for publication by the decision of the Scientific Council
of V. N. Karazin Kharkiv National University
(Rec. No. 3 dated February 22.2021)*

Kuklin V. M.

K 85 Selected chapters (theoretical physics) / V. M. Kuklin. – Kh. : V. N. Karazin KhNU, 2021. – 244 p.

ISBN 978-966-285-700-9

The book considers spontaneous and induced emission of particles and waves. The formation of coherent pulses near a detected new threshold of induced radiation is discussed. It is shown how modulation instabilities generate self-similar structures and anomalous waves. A comparison is made of the dynamics of instability of Langmuir oscillations in plasma and heating of ions in Silin and Zakharov models. Turbulent-wave instability is discussed and a new approach to the description of the Mossbauer effect is presented. The similarity of processes of superradiation and dissipative instability is noted. Structural transitions in the convective layer and the appearance of large-scale vortices during modulation instability of developed convection and other relevant problems are discussed. It is of interest to specialists, graduate students and students of physics departments.

**PACS 52.35 Mw;41.60.-m;
05.45 Xt;03.65 Sq;47.55 pb**

ISBN 978-966-285-700-9

© Kuklin V. M., 2021

© Donchik I. M., design of cover, and layout, 2021

© Translated from Russian by A. Kotova, 2021

CONTENTS

Foreword	7
Introduction	10
PART I. PROCESSES IN NONEQUILIBRIUM MEDIA.....	13
Chapter 1. Spontaneous & induced radiation.....	13
Section 1: Two-Level System.....	13
References to section 1	16
Section 2. Spontaneous and induced radiation of electron beam particles in plasma	16
References to section 2	21
Section 3. Spontaneous and induced effects within the frame of three-wave interaction.....	21
References to section 3	24
Section 4. Semi-classical model	25
<i>Shortened equations</i>	27
<i>Balance equations</i>	27
<i>Excitation of a resonator with an active medium</i>	28
References to section 4	31
Chapter 2. Spontaneous vs induced radiation	32
Section 5. New threshold of induced radiation.....	32
References to section 5.....	36
Section 6. Periodic changes in the luminosity of quantum sources.....	37
References to section 6.....	42
Section 7. Turbulent-wave instability	43
References to section 7.....	46
Chapter 3. Spatial-temporary dynamics of some types instability.....	47
Section 8. Spatial-temporal dynamics of a decay three-wave instability	47
References to section 8.....	51
Section 9. Spatial-temporal dynamics of a beam-plasma instability	51
<i>The development of kinetic instability</i>	51
<i>The development of hydrodynamic instability</i>	52
References to section 9.....	54
Chapter 4. Dissipative instability	55
Section 10. Dissipative beam instabilities	55
<i>Abnormal beam energy loss</i>	55
<i>Multiwave mode</i>	58
<i>Spectrum characteristics</i>	59
References to section 10	60
Section 11. Beam instability in nonlinear and negative dissipations.....	61
<i>Development of beam instability in a hot plasma</i>	61
<i>Change in the nature of beam instability with the excitation of surface waves in plasma with a blurred boundary</i>	62
<i>The "wave – trapped particles" structure in a weakly ionized gas flow</i>	63
References to section 11	64
Chapter 5. Superradiation modes	65

Chapter 5. Superradiation modes	65
Section 12. Formation of the fine structure of electron bunches, injected into plasma	65
<i>Example of negative macroscopic dielectric permittivity</i>	65
<i>Clusters</i>	68
<i>Self-profiling of a short bunch of electron, moving in plasma</i>	68
References to section 12	71
Section 13. Dissipative instabilities and superradiance modes.....	73
<i>Electron beam in a longitudinally bounded system</i>	73
<i>A system of oscillators whose centers are fixed in radiation field</i>	76
<i>The field of the waveguide or resonator</i>	76
<i>Dissipative regime in a quantum system</i>	81
References to section 13	84
Chapter 6. Cyclotron instability of particle flows	85
Section 14. Excitation of TE waves by a beam of charged particles.....	85
References to section 14	94
Section 15. Equations, that describing the excitation of a TM wave	95
<i>Excitation of a longitudinal wave in magnetically active</i> <i>plasma waveguide</i>	97
References to section 15	98
Chapter 7. Modulation instability and self-similar structures	99
Section 16. Modulation Instability.....	99
<i>Origins of instability</i>	103
<i>Modeling a process at high absorption levels</i>	104
<i>Integral and local characteristics of the process instability</i>	106
References to section 16	107
Section 17. Formation of a self-similar field structure	108
<i>The formation of long-lived quasi-stable states.</i>	109
<i>The occurrence of self-similar field structures</i>	109
References to section 17	111
Chapter 8. Modulation instability. Emergence of waves of anomalous amplitudes	112
Section 18. Modulation instability far from the threshold.....	112
<i>Instability of a large-amplitude wave in the 2D Lighthill model</i>	114
<i>Comparison of 1D Lighthill models in cases of applying S-theory</i> <i>and direct calculation of the equation.</i>	115
<i>Instability mode far from the threshold.</i>	116
References to section 18	119
Section 19. Modulation instability of gravitational waves on water surface	119
<i>Numerical analysis of dynamics and statistical</i> <i>indicators using S-theory</i>	122
<i>Comparison of 1D models in cases of applying S-theory</i> <i>and more general description</i>	125
References to section 19	130
Chapter 9. Parametric and / or modulation instabilities	
intense Langmuir oscillations in plasma	131
Section 20. Silin's and Zakharov's models.....	131
<i>Problems of description</i>	132
<i>Equations of the Silin hybrid model</i>	133

	<i>The equations of the hybrid Zakharov model</i>	135
	<i>Nonlinear modes of instabilities</i>	137
	References to section 20	140
Section 21.	Comparison of Silin's and Zakharov's models heating of ions.....	141
	<i>Results of numerical simulation</i>	142
	References to section 21	147
Chapter 10.	Structures of different scales and topologies	
	in thin layer convection	148
Section 22.	Structural-phase transitions in a thin layer	
	of convectively unstable medium.....	148
	<i>The Proctor-Sivashinsky equation</i>	149
	<i>Amorphous state. The mechanism of competition of spectrum modes</i>	152
	<i>Structural-phase transitions</i>	154
	<i>The physical nature of the second order phase transition</i>	159
	References to section 22	160
Section 23.	Modulation instability of the system of convective cells	
	in a thin layer. Hydrodynamic dynamo effect.....	161
	<i>Sivashinsky – Proctor – Pismen model</i>	161
	<i>Modulation instability of a system of convective cells</i>	162
	<i>The effect of a regular hydrodynamic dynamo</i>	163
	References to section 23	164
PART II.	ANNEXES	165
Annex I.	Traditional threshold of induced radiation.....	165
Annex II.	Spontaneous and induced radiation of the electron beam.	
	Landau damping. Equations of kinetic instability	
	of a hot electron beam in plasma.....	166
	References to Annex II.....	169
Annex III.	On spontaneous and induced wave radiation	169
	<i>On the description of self-interaction processes</i>	171
	References to Annex III.....	172
Annex IV.	On the nature of Mossbauer effect	172
	<i>The relaxation processes of LF excitations in continuous media</i>	175
	<i>Effect of jitter of a potential well</i>	176
	References to Annex IV	177
Annex V.	Density matrix and equations of the semi-classical models.....	177
	References to Annex V	179
Annex VI.	Calculation of parameters of pulses induced radiation	179
	<i>Calculation of pulse parameters of a quantum source</i>	179
	<i>Periodic changes in the luminosity of Cepheid stars</i>	180
	References to Annex VI	183
Annex VII.	Equations of turbulent wave instability	183
Annex VIII.	Spatial and temporary dynamics of instability during	
	a three-wave interaction	184
Annex IX.	Space-temporal development of beam instability in plasma.....	186
Annex X.	Multimode interaction of a non-relativistic electron beam with plasma.....	187
Annex XI.	Dissipative generation mode in the resonator, filled with active medium.....	189
	References to Annex XI.....	191

Annex XII. Cavities, formed in the plasma resonance region	191
References to Annex XII.....	193
Annex XIII. Attenuation of a wave package in a resonator filled with an active medium ..	194
References to Annex XIII	196
Annex XIV. Attenuation of a wave package in a resonator filled with a non-isothermal plasma	197
References to Annex XIV	200
Annex XV. Wake field of an electron bunch, moving in a plasma	200
<i>On the applicability of the description</i>	201
References to Annex XV.....	204
Annex XVI. Superradiance mode of oscillator system.....	204
<i>Fields of a single particle and particle bunch</i>	204
References to Annex XVI	206
Annex XVII. Plasma gyrotron equations.....	206
<i>Equation of plasma gyrotron</i>	207
References to Annex XVII.....	209
Annex XVIII. Integrals of equation systems, which describe cyclotron instabilities	209
References to Annex XVIII.....	210
Annex XIX. Modulation instability of a flat wave in a two-dimensional case.....	210
Annex XX. Self-similar structures on surface and in volume of crystals.....	211
References to Annex XX	215
Annex XXI. Nature of forced interference.....	216
References to Annex XXI.....	218
Annex XXII. Waves of anomalous amplitude in the ocean.....	218
References to Annex XXII	224
Annex XXIII. Cold plasma. One-dimensional Silin equations.....	225
References to Annex XXIII.....	230
Annex XXIV. Anomalous oscillations of the coefficient of reflection of an electromagnetic wave from a plasma surface.....	231
References to Annex XXIV	233
Annex XXV. Phase transitions in the Proctor-Sivashinsky model under conditions of dependence of viscosity on temperature.....	233
References to Annex XXV.....	236
Annex XXVI. Defectiveness criteria of spatial periodic structures.....	236
<i>Spectral and visual defectiveness's</i>	236
<i>External noise and instability of system boundaries</i>	236
References to Annex XXVI	237
Annex XXVII. On the applicability of the Proctor-Sivashinsky-Pismen model to the description of the modulated instability of the developed structure of convective cells	238
References to Annex XXVII	238
Annex XXVIII. Semiclassic superradiation model.....	238
References to Annex XXVIII	240
Subject index	241
Instead of conclusion.....	243

FOREWORD

After a long period of studying various phenomena in the field of plasma electronics, under the influence of such renowned scientists and teachers of the Faculty of Physics and Technology as Y. B. Fainberg, V. D. Shapiro, V. G. Baryakhtar, A. G. Sitenko, K. N. Stepanov and others, as a result of joint work with my PhD supervisor A. N. Kindratenko, the range of tasks has somewhat expanded. Remarkable books by V. L. Ginzburg and A. A. Rukhadze (he was a reviewer of the Russian-language version of the presented monograph), V. P. Silin, V. N. Tsitovich and V. I. Karpman, as well as personal contact with some of them, as well as with N. A. Armand, V. M. Yakovenko, Yu. A. Romanov, S. S. Moiseev, Yu. L. Klimontovich, H. Wilhelmson and many others have contributed to this fact.

The internship and preparation of my diploma at the KIPT, work in the IRE, IKI, as well as a participation in the seminar delivered by V.P. Silin, for productive communication with whom I am sincerely grateful, have played an important role in broadening the horizons. Business trips to Haifa to L. M. Pismen and to Hamburg to K. Shuneman were effective. The works that are included in this book are far from all that was performed during the period of scientific activity. However, they seemed the most interesting to the author and have an obvious prospect for further research.

Attention to the role of spontaneous emission in physical processes was attracted by the works by V. L. Ginzburg, A. G. Sitenko, V. N. Tsytovich; this issue was also taught at lectures by V. I. Kurilko and raised in discussions with I. F. Kharchenko. Similar questions also arose during the preparation for publication of the monograph "Fundamentals of Plasma Electronics" in collaboration with A. N. Kindratenko. This made it necessary to understand the general structure of the description of spontaneous and induced phenomena in quantum and, most of all, in classical models. The competition between spontaneous and induced processes was also used in the universal system of equations, which describe turbulent-wave instability, obtained under the influence of S. S. Moiseev's ideas.

A new threshold for the induced radiation emergence, which me and A. G. Zagorodny discovered, due to its competition with spontaneous processes, made it possible to understand the nature of the formation of coherent pulses with intensities comparable to spontaneous emission at extremely low levels of inversion.

The works by A. M. Fedorchenko and N. Ya. Kotsarenko, and later by L. M. Gorbunov, prompted a search for a simpler description of the spatiotemporal dynamics of multi-wave processes.

An interesting effect of anomalous energy extraction from a beam of charged particles in a medium with a noticeable absorption of RF energy,

discovered jointly with A. N. Kindratenko and V. I. Tkachenko, was evaluated by Yu. A. Romanov and colleagues in Nizhny Novgorod. It forced to delve into the details of similar processes. A decrease in the level of absorption of the medium due to nonlinear mechanisms brought to life a number of works on the transitions of dissipative processes to reactive ones.

Great interest to the problems of particle acceleration in wake fields of bunches made it possible to be one of the first who published works on a self-consistent description of the dynamics of bunches in the self-radiation field. Later this made it possible to understand the connection of this phenomenon, first with dissipative regimes of beam instabilities, and then with superradiance, which it is more likely to be.

The emergence of low-density plasma arising from the operation of powerful gyrotrons, the theory of which was previously created by Nizhny Novgorod scientists, made me and my co-authors (K. Shuneman and G. I. Zaginailov) to understand the description of the excitation of cyclotron oscillations. However, the inclusion of the finite Larmor radius in the problems of generation of longitudinal waves in plasma waveguides was previously performed with J. Krusha.

The discovery of the phenomenon of the formation of self-similar structures in wave media as a result of modulation instability allowed us, together with A. V. Kirichok and O. V. Kuklina, to systematically study this phenomenon. Later, it was possible to clarify the nature of the formation of these structures and in collaboration with E. V. Belkin to conduct numerical experiments, which showed agreement with analytical estimates.

The great interest of the scientific community for the emergence of waves of anomalous amplitude in the ocean made us recall the approaches of the S-theory constructed by V. S. Lvov and V. E. Zakharov in order to describe the excitation of spin waves. Using the modified S-theory developed with the help of V. M. Vorobyov, it was possible to understand the nature of stimulated interference and to explain the formation of waves of anomalous amplitude and bursts of modulation, the intensity of which was an order of magnitude higher than average levels. It was not difficult to create a description of the behavior of waves on the surface of the ocean according to the S-theory. The verification of the S-theory was carried out later using wave propagation examples in waveguides and in the ocean by comparing previous data obtained by E. V. Belkin with direct calculations by A. V. Priymak.

The generalization of the system of equations of V. P. Silin and the construction of the so-called Silin model of parametric instability of the Langmuir wave in cold plasma was a successful research result of the mid-80s. First numerical experiments performed in collaboration with I. P. Panchenko and S. M. Sevidov showed a deep modulation of plasma density and energy transfer to ions, which was previously discovered during the development of

modulation instability in various modifications of the V. E. Zakharov's model. The comparison of the parametric instability of V.P. Silin with the well-known model of V. E. Zakharov of the modulation instability of the Langmuir wave in nonisothermal plasma in recent years, carried out with A. G. Zagorodny and A. V. Kirichok with the help of A. V. Priymak, revealed direct connection between these processes.

By analyzing research results of convection in a thin layer of liquid and gas, it was possible to detect the existence of structural-phase transitions between metastable and stable states. Together with I. V. Gushchin and A. V. Kirichok, a state function was found and a model of such phenomena was constructed. Recently, a large volume of new results that provoked some corrections to the sections of the book was carried out in collaboration with E. V. Poklonsky.

The reader may also be interested in a new look at the nature of the Mössbauer effect, presented together with A. G. Zagorodny and A. V. Kirichok. It was the support of V. G. Kirichenko and the calculations carried out with O. V. Kuklina that made it possible to come close to the solution of this problem. With I. P. Panchenko, we estimated V. P. Silin's generalized models describing intense oscillations of the coefficient of reflection of an electromagnetic wave from a plasma surface. Also we discovered the phenomenon of modulation instability in developed convection, where the help of A. V. Kirichok was needed. This task of finding the conditions for the development of a "regular" hydrodynamic dynamo was posed by S. S. Moiseev on the basis of the description model developed by L. M. Pismen.

In conclusion, special thanks should be expressed for the support and attention of A. N. Kindratenko, to my colleagues V. A. Buts, A. G. Zagorodny, V. I. Karas and V. V. Yanovsky, as well as A. V. Kirichok, which have supported me in recent years, especially in the successful publication of a series of scientific works "Problems of Theoretical Physics". Although there is no way to list everyone who supported me in the search for solutions, in discussions and implementation, I am also very grateful to all of them.

Author

INTRODUCTION

The book discusses the problems and tasks to which the author arose interest, and to which he was most directly related. However, the solution of these tasks would be impossible without the devoted participation of both eminent and junior colleagues, as well as students who just started their scientific career. Only a few tasks were solved in a relatively short time, but the bulk of the work continued for years, and sometimes decades. Such a tender interest of the author and his colleagues in certain topics was caused by revealing new sides of the same processes, as well as with the discovery of links between completely different phenomena. It seems that fate did not let go away from the selected topics, predetermining the direction of thought.

In the first chapter of the first part of the book, spontaneous and induced processes in wave-particle and wave-wave interactions are considered. It is shown how, using the expression for spontaneous emission, one can easily and correctly obtain the terms of the equations that determine the induced processes, the procedure of direct calculation of which is sometimes very difficult. Additionally, a description of the radiation of the electromagnetic field by an active medium in the framework of the semiclassical theory is presented.

The second chapter discusses the new threshold of induced radiation. A mechanisms for the formation of coherent pulse is presented; it should be noted that their intensity is comparable or greater than the intensity of the spontaneous field near the detected new threshold of the induced radiation.

Near this threshold, it is also possible to generate periodic pulses of coherent radiation, which are formed as a result of competition between spontaneous and induced processes. The dynamics of instability in the same proximity to the threshold of induced radiation, which leads to an increase in turbulent pulsations under the action of an external wave, is discussed.

The third chapter presents the spatio-temporal dynamics of the development of several types of instabilities. It is noted that the consideration of the nonlinearity of wave motions has little effect on the nature of spatio-temporal dynamics, since the dispersion properties of natural waves in a medium a much greater extent determine their behavior in comparison with different types of nonlinear mechanisms, at least in the vast majority of cases. It is shown that the analysis of such dynamics is significantly simplified by the transition to a moving coordinate system.

In the fourth chapter, we consider the effect of anomalous energy extraction from a beam of charged particles due to the occurrence of mutually synchronized deceleration of the wave and the beam particles captured by the field under conditions of a noticeable level of wave energy absorption in the system.

It is shown that the account of nonlinearity in dissipation mechanisms, as a rule, reduces its average value.

The similarity of dissipative instabilities and superradiance is discussed in the fifth chapter, in particular, on the example of radiation from a short electron beam moving in plasma. Superradiance, the basis of which is the interaction between particles or oscillators by means of a field radiated by each of them, in its classical representation is determined by the processes of their spatial and/or phase synchronization, which is enhanced when their mobility is taken into account.

In the sixth chapter, the processes of excitation by electron beams of electromagnetic waves of different polarization in magnetically active waveguides are studied. Low-density plasma is taken into account in traditional equations that describe the generation of oscillations in gyrotrons; the influence on the nature of the processes of the finite radius of rotation of the beam electrons is discussed.

The seventh chapter explains the emergence of a cascade of modulation instabilities near the threshold of their development, forming self-similar structures by narrowing the spectra of each separate process and creating the conditions for the development of a new, larger-scale one. At the same time, increasingly large-scale modulations (envelopes) of the main structure appear. The narrow spectra of each instability of the cascade form a self-similar spatial structure clearly observed on each scale.

The eighth chapter presents the phenomena of the formation of waves and their envelopes of large amplitude during the development of modulation instability of intense wave motion. The nature and frequency of the emergence of gravitational waves of anomalous amplitude on the surface of the ocean are discussed.

The ninth chapter makes it possible to compare the Silin and Zakharov models of the modulation instability of Langmuir waves, respectively, in cold and non-isothermal plasmas. It is shown that in the developed instability regime, the fraction of energy transferred to ions does not exceed 5–6 % of the initial field energy, the ion velocity distribution is close to Maxwellian, which allows us to speak about their temperature.

In the tenth chapter, structural-phase transitions in a thin layer of convection of liquid or gas are considered. A state function is presented, and the characteristic time of each next structural – phase transition increases, and changes in the state function decrease.

The second part of the book includes annexes to the discussed issues, allowing you to understand the formalisms for the effects under consideration. Nevertheless, some topics in the second part are of independent interest, for example, the nature of distributed defects in a solid body, the estimation of the number of defects by the spectral characteristics of the spatial structure,

self-similar nanostructures on the surface of graphite, and a new understanding of the mechanism of the Mössbauer effect.

Very often, the pioneering works of talented scientists who turned to a physical phenomenon reveal only one, as a rule qualitative aspect of the phenomenon. At the same time, real physical mechanisms that already quantitatively determine the process, are remain unseen and usually clarified later as a result of attracting the attention of the scientific community to this effect or phenomenon. For example, the nonlinear damping of intense Langmuir waves, which led to its heating, was often explained by the Landau damping in the emerging collapsing caverns of plasma density, which apparently takes place only to some extent.

However, multiple scattering by numerous caverns-field inhomogeneities, arising from instability is the decisive mechanism for the transfer of field energy to ions and their further thermalization is multiple scattering by numerous caverns-field inhomogeneities arising from instability (for more details, see Section 21). Waves of anomalous amplitude under specific conditions, which are presented as permanently existing and which unpredictably occur under these conditions as an autowaves, that is soliton-like perturbations with variable amplitude in nonequilibrium media, are actually very definitely generated by modulation instability. In its turn, it forms a wave (or envelope) of anomalous amplitude due to the forced interference of the modes of the instability spectrum under the influence of wave motion. The nature of the Mossbauer effect can also be quite simply explained by the characteristics of the radiation of atoms with excited nucleus, which are oscillating in potential wells of the crystal structure.

Such topics of given research in annexes as the wake field and self-modulation of an electron bunch moving in a plasma, abnormal oscillations of the reflection coefficient of the electromagnetic wave from the plasma surface and a number of others can be of interest for readers.

Extra edition of this book in English made it possible to correct the errors and add explanations of some of the issues raised in the discussions in the annexes at the end of the book.

PART I

Processes in nonequilibrium media

CHAPTER 1. Spontaneous and induced radiation

The features of describing the processes of spontaneous and stimulated emission of particles and waves are presented. The role of spontaneous noise in the injection of a beam of charged particles and the transition to the development of beam instability are discussed. The process of wave generation by current, which is the result of the interaction of other waves, is considered; it is shown that this phenomenon is in the nature of spontaneous emission. Using the expression for the intensity of such radiation, the nonlinear terms of the equation that describes the processes of induced interaction can be obtained. Thus, a simple connection between expressions for spontaneous and induced emission of particles and waves is shown.

SECTION 1.

TWO-LEVEL SYSTEM

In the most general case, particle radiation can be either spontaneous and independent of external influence, or stimulated and imposed by an intense external field. In nonequilibrium systems and media all these phenomena acquire collective properties. The connection of stimulated or induced radiation with similar spontaneous processes was discovered and described in the work by A. Einstein [1-1] and experimentally confirmed by R. Ladenburg (see links in the review paper [1-2]).

Let us consider a particle that has an eigen-field. If this field or its part does not propagate independently of the particle and accompany the particle, then there is no radiation. The work of the field on the particle in this case will be zero. However, if during translational particle motion (for example, at a speed of a higher velocity of the waves of the medium [1-3] – [1-5]) or oscillatory particle motion (dipole) we shall consider the field of a particle, then under certain conditions there will be a part that will be capable to spread in the medium independently.

The work of this part of the field on the particle will not be zero and will lead to its inhibition or to a decrease in the amplitude of the oscillations, respectively, which is a sign of the presence of radiation of the field energy by the particle [1-6].

It is also important to note that the value of the work of the particle self-field on its intrinsic current is always sign-defined and describes only the

radiation process. By the way, this sign-definiteness is one of the characteristic signs of spontaneous processes.

Another characteristic feature of spontaneous emission is the fact that its sources are independent and the radiation process is not depends on a wave at given frequency that exists in a medium or system (see, for example, [1–7]. The induced radiation is due to the fact that an external field in the entire interaction space modulates the movement of particles of the medium. In this case, radiation (or absorption) of many particles located at different points in space occurs in phase with this field.

Ch. H. Townes drew attention to this fact in his Nobel lecture: “... the energy radiated by molecular systems has the same field distribution and the same frequency as the inducing radiation, and, therefore, a constant (possibly zero) phase difference” [1-8].

Such radiation and particle absorption synchronized by an external field leads to a sharp increase in the efficiency of interaction between particles and the field. We shall note right away that the presence of processes that violate the phase matching of the external field and the particle motion imposed by this field can weaken the effectiveness of such an interaction. The cause of the induced (stimulated) radiation, as it turned out, is the presence of population inversion (a positively defined difference of particles at higher and lower energy levels) [1-1]. According to A. Einstein, if there is radiation at the transition frequency $\varepsilon_2 - \varepsilon_1 = \hbar\omega_2$, the description of the simplest one-dimensional two-level system is:

$$\partial n_2 / \partial t = -(u_{21} + w_{21} \cdot N_k) \cdot n_2 + w_{12} \cdot N_k \cdot n_1, \quad (1.1)$$

$$\partial n_1 / \partial t = -w_{12} \cdot N_k \cdot n_1 + (u_{21} + w_{21} \cdot N_k) \cdot n_2, \quad (1.2)$$

along with this, the total number of particles in the first and second levels is constant $n_1 + n_2 = Const$, u_{21} , is the rate of change in the number of quanta of the second excited level due to spontaneous radiation processes. The rate of change in the number of quanta (particles) at these levels is due to the induced processes of radiation $w_{21} \cdot N_k \cdot n_2$ and absorption $w_{12} \cdot N_k \cdot n_1$. Here N_k – is the number of radiation quanta (spectral density) at the transition frequency, for which the equation takes the following form:

$$\frac{\partial N_k}{\partial t} = (u_{21} + w_{21} \cdot N_k) \cdot n_2 - (w_{12} \cdot N_k) \cdot n_1. \quad (1.3)$$

In statistical equilibrium at temperature T, derivatives are $\partial n_i / \partial t = 0$ and $n_i = const \cdot \exp\{-\varepsilon_i / kT\}$, in this case ε_i is the energy of particles in the i -th state. In case of statistical equilibrium, the number of radiation quanta $N_k = N_{k0}$ shall be valid for the radiation intensity, where the right-hand side is determined by the Planck formula

$$N_{k0} = \frac{1}{\exp\{\hbar\omega / kT\} - 1}, \quad (1.4)$$

and when calculating the integrated intensity, the summation is carried out over the wave numbers, while $\omega = \omega(\vec{k})$ and expression (1.4) retains its form regardless of the dimension of the problem.

For equation (1.3) to remain valid in the state of statistical equilibrium, it is necessary that the expression

$$N_{k0} = \frac{u_{21}}{w_{12} \exp\{\hbar\omega / kT\} - w_{21}} \quad (1.5)$$

shall coincide with Planck's formula (1.4). In other words, the number of radiation quanta take the following form for the coefficients

$$u_{21} = w_{12} = w_{21}. \quad (1.6)$$

Let us note that in a 3D case, the relation between the coefficients u_{21} and w_{21} can be represented as it follows

$$\frac{u_{21}}{w_{21}} = g = \frac{A_{21}}{\hbar\omega \cdot B_{21}} = \frac{2\omega^2}{\pi c^3} \quad (1.6a)$$

where A_{21} and B_{21} – are corresponding Einstein coefficients. The dimension of this ratio is time per unit volume, since we are talking about the spectral density of quanta. For yellow light, the numerical value is $g \approx 0.25$, whereas for violet $g \approx 0.6$ is at the edge of the visible spectrum.

Using the obtained relations, equation (1.3) can be represented as

$$\frac{\partial N_k}{\partial t} = \Sigma + \frac{\partial \Sigma}{\partial(\hbar\omega)} N_k \cdot \hbar\omega, \quad (1.7)$$

where $u_{21} \cdot (n_2 - n_1) = u_{21} \cdot [n(\varepsilon_2) - n(\varepsilon_1)] = \frac{\partial \Sigma}{\partial(\varepsilon)} \cdot \hbar\omega = \frac{\partial \Sigma}{\partial(\hbar\omega)} \cdot \hbar\omega$, $\varepsilon_2 = \varepsilon_1 + \hbar\omega$, and $\Sigma = u_{21} \cdot n_2 = u_{21} \cdot n(\varepsilon_2)$.

It is useful to introduce the notion of population inversion $\mu = (n_2 - n_1)$. If the initial values of $n_2(0) \gg N_k(0), n_1(0)$, and $\mu > 0$, then spontaneous processes can be neglected. In this case

$$\frac{\partial \mu}{\partial t} = -2u_{21} \cdot \mu \cdot N_k = -2\gamma \cdot N_k. \quad (1.8)$$

Let us pay attention to the fact that only taking into account the induced processes, it is possible to detect instability during a significant inversion of the level populations – a rapid increase of the number of field quanta N_k at the initial stage $\propto \exp\{\gamma \cdot t\}$ with an increment equal to γ , when changes in the inversion can be neglected (see annex I).

References to section 1

- 1-1. Einstein A. Quantentheorie der Strahlung. // Mitteilungen d. Phys. Ges. Zurich, 1916. Nr. 18; Phys. Zs. 1917. Nr. 18, P. 121.
- 1-2. Ladenburg R. Reviews of Modern Phys. 1933. – N. 4. – P. 243–260.
- 1-3. Ginzburg V. L. On the nature of spontaneous radiation // UFN, 1983. – V. 140. – No. 4. – P. 687–698 (in Russian).
- 1-4. Ginzburg V. L. Radiation of uniformly moving sources (the Vavilov-Cherenkov effect, transition radiation and some other phenomena) // UFN, 1996. – V. 166. – № 10. – S. 1033–1042 (in Russian).
- 1-5. Ginzburg V. L. Several remarks on the radiation of charges and multipoles moving uniformly in a medium // UFN, 2002. – V. 172 – No. 2. – S. 373–376 (in Russian).
- 1-6. Landau L. D., Livshits E. M. Electrodynamics of continuous media. – M. : GIFML, 1959. – 532 p.
- 1-7. Zagorodny A. G., Kuklin V. M. Features of radiation in nonequilibrium media / Problems of theoretical physics. Scientific works / V. A. Buts, A. G. Zagorodny, V. E. Zakharov, V. I. Karas, V. M. Kuklin, A. V. Tur, S. P. Fomin, N. F. Shulga, V. V. Yanovsky; ed. V. M. Kuklin. – Kh. : KhNU named after V. N. Karazin, 2014. – Issue. 1. – 532s. Pp. 13–81 (Series "Problems of Theoretical and Mathematical Physics"; under the general editorship of A. G. Zagorodny, N. F. Shulga. in Russian).
- 1-8. Townes Ch. H. Production of Coherent Radiation by Atoms and Molecules, IEEE Spectrum – 2 (2), – 30 (1965).

SECTION 2.

SPONTANEOUS AND INDUCED RADIATION OF ELECTRON BEAM PARTICLES IN PLASMA

Let us consider the process of spontaneous emission of plasma (Langmuir) waves by a single electron moving with speed in the direction of the OZ axis. For simplicity, we restrict ourselves to the one-dimensional case [2-1] (see also [2-2]). Let us imagine the electron charge density in the following form

$$\rho = -e \cdot \delta(v \cdot t - z + s). \quad (2.1)$$

In this one-dimensional representation, beam particles emit and absorb quanta of longitudinal (Langmuir) waves – plasmons whose energy is equal to $\hbar\omega(k)$. Let us determine the number of longitudinal wave quanta emitted per unit time in the interval of wave numbers dk in cases of spontaneous and induced processes $n_m u_{mn} dk$ and $n_m w_{mn} N_k dk$, respectively.

In this case, particles emitting a plasmon pass from state m to state n . In the same wavelength range, let us similarly determine the plasmon absorption rate as $n_n w_{nm} N_k dk$, where n_m is the number of particles in the state m , and N_k is the number of field quanta, u_{mn} , w_{mn} , w_{nm} are the coefficients in A. Einstein equations for this case. The equations that describe the change in the number of particles at the upper and lower energy levels have a form similar to (1.1) and (1.2):

$$\partial n_m / \partial t = -(u_{mn} + w_{mn} \cdot N_k) \cdot n_m + w_{nm} \cdot N_k \cdot n_n, \quad (2.2)$$

$$\partial n_n / \partial t = -w_{nm} \cdot N_k \cdot n_n + (u_{mn} + w_{mn} \cdot N_k) \cdot n_m. \quad (2.3)$$

In thermal equilibrium, obviously $n_m / n_n = \exp\{\hbar\omega(k) / T\}$, the number of emitted and absorbed field quanta is equal (the Boltzmann constant will be assumed equal to unity here and below), and the Planck formula $N_{k0} = [\exp\{\hbar\omega(k) / T\} - 1]^{-1}$ is valid for the number of field quanta, which also leads to the relation $u_{mn} = w_{nm} = w_{mn}$. Thus, in the nonequilibrium case, in order to describe the dynamics of the number of plasmons, we shall obtain the equation

$$dN_k / dt = u_{mn} \cdot n_m \{(1 - n_n / n_m) \cdot N_k + 1\}. \quad (2.4)$$

Let us note that a change in the energy density of plasmons $dE_k / dt = \hbar\omega(k) \cdot u_{mn} \cdot n_m$ in the absence of other mechanisms of radiation and absorption of their energy, in addition to spontaneous and induced radiation of beam particles, is equal to the loss of its energy per unit time $w(k)$. With this in mind, equation (2.4) takes the form:

$$dE_k / dt = w(k) \cdot \{(1 - n_n / n_m) \cdot N_k + 1\}. \quad (2.5)$$

The change in the momentum of particles upon plasmon radiation is, $m \cdot (v_m - v_n) = \hbar k$ whence it follows $v_m = v_n + \hbar k / m$, which is also the case if the velocity interval, where the particle distribution function changes significantly, exceeds $\hbar k / m$, then

$$n_n / n_m = f(v_m - \hbar k / m) / f(v_m) \approx 1 - (\hbar k / m) \cdot df(v_m) / f(v_m) dt. \quad (2.6)$$

and equation (2.5) takes the form (see annex II)

$$dE_k / dt = 2\pi^2 e^2 [\omega^2(k) / k^2] \cdot \{f_b[\alpha(k) / k] + E_k \cdot (k / \alpha(k) \cdot m) \cdot \partial f_b(v) / \partial v|_{v=\omega(k)/k}\} - \delta_D E_k, \quad (2.7)$$

where $\gamma_L = \frac{2\pi^2 e^2 \omega^2}{mk^2} \partial f_b(v) / \partial v|_{v=\omega(k)/k}$ is the linear increment of the beam-plasma instability in the absence of plasmon energy loss, δ_D is the damping decrement in the plasma in the absence of a particle beam.

By the way, the equality of the coefficients $u_{mm} = w_{mm} = w_{mm}$, as well as the dependence of the term responsible for the induced processes on N_k , allows us to present expression (2.7) in a more general form

$$dN_k / dt = \Sigma_m + \{\Sigma_m - \Sigma_n\} N_k = \Sigma_m + \frac{\partial \Sigma_m}{\partial(\hbar\omega)} E_k, \quad (2.8)$$

where Σ_m is the change in the number of quanta of radiation energy $E_k = \hbar\omega \cdot N_k$ due to spontaneous processes per unit time, and the transition $\Sigma_m \rightarrow \Sigma_n$ corresponds to quantum radiation $\hbar\omega$, i.e.

$$\Sigma_m - \Sigma_n = \Sigma(\varepsilon_m) - \Sigma(\varepsilon_n) = \frac{\partial \Sigma_m}{\partial \varepsilon} \hbar\omega = \frac{\partial \Sigma_m}{\partial(\hbar\omega)} \hbar\omega. \quad (2.9)$$

where $\Sigma_m = \Sigma(\varepsilon_m) = \Sigma(\varepsilon_n + \hbar\omega)$.

Cases of describing spontaneous and induced radiation are considered in more detail in the review [2-3]. Let us consider the noise level, that is, the intensity of plasma turbulence in a non-dissipative medium. In plasma without a beam, the intensity of plasma turbulence (fluctuations) is determined by $E_k \propto T_e$. When a beam is injected below the instability threshold (or in spectral regions where instability does not develop), the noise level can increase significantly, for example, if the beam temperature is comparable to or higher than the plasma temperature.

Indeed, for the Maxwellian velocity distribution function of electrons $f_{0b} = [n_{b0} / \sqrt{\pi} v_{Tb}] \cdot \exp\{-(v - v_{0b})^2 / v_{Tb}^2\}$, under stationary conditions, we shall find that the noise intensity can reach order values (see annex II)

$$E_k = \frac{\omega(k)}{\omega(k) - kv_{0b}} \cdot T_b, \quad (2.10)$$

due to spontaneous radiation of the beam in the region of high phase velocities $\omega(k) > kv_{0b}$ ($\gamma_L < 0$) even under conditions of negligible energy losses ($\delta_D \rightarrow 0$).

In the region of low phase velocities $\omega(k) < kv_{0b}$ (in this case $\gamma_L > 0$), the growth of fluctuations can be restrained only by dissipative processes ($\delta_D > \gamma_L$) in the plasma

$$E_k = \gamma_L \cdot \omega(k) \cdot T_b / (kv_{0b} - \omega)(\delta_D - \gamma_L). \quad (2.11)$$

When approaching the instability threshold (determined from the condition $\delta_D = \gamma_L$), the level of spectral density of oscillations rapidly and explosively

increases. This, in particular, improves the starting conditions for the development of instability. The abnormal growth of fluctuations in this case is similar to the well-known phenomenon of critical opalescence when the system parameters approach the instability threshold – the region of phase transition.

A significant increase in noise in the system during beam injection in wide spectral ranges, even outside the instability region, was discovered as far back as the first experiments on plasma-beam interaction [2-4 – 2-5].

It should be noted that an increase in the number of quanta of the spontaneous field per unit time in the interaction volume in the quantum case or an increase of the field energy in the classical descriptions have some features that distinguish them from the case of an energy increase of the induced field during the development of instability. First of all, the spontaneous fields of individual oscillators or beam particles (if they are uniformly distributed and in the absence of external synchronization mechanisms) differ in phase, which, generally speaking, at least at the initial moment, is random, that is, spontaneous emission is uniformly distributed and not phased emitters are incoherent.

The change in the energy of spontaneous emission per unit time is proportional to the number of emitters. The field of spontaneous emission grows linearly, but starting from some moment, the grouping of emitters may turn out to be such that the induced radiation can intercept the initiative. This growth of induced radiation occurs exponentially and that part of the field is formed in which the coherence fraction is high, that is, the phases of many individual emitters are slightly different from each other.

In this case the change in the field energy per unit time is proportional to the square of the number of synchronized oscillators. Moreover, such synchronization occurs under the influence of the emitted wave and is controlled by it. A certain and constantly growing level of the spontaneous component of radiation, which has the character of increasing noise, should also be taken into account, especially in the regimes of long pulses of corpuscular and wave pumping.

If in the absence of dissipative processes, a quantity $\partial f_b(v) / \partial v |_{v=\omega(k)/k} > 0$ is possible, instability can develop, which is an

exponential increase with the increment $\gamma_L = \frac{2\pi^2 e^2 \omega}{mk^2} \partial f_b(v) / \partial v |_{v=\omega(k)/k}$

of the wave with frequency ω and wave number k , that is, the wave field is presented as $E(t) \cdot \exp\{-i\omega t + ikx\}$ by only one mode in the spectrum. The implementation of such a single-mode regime is possible taking into account a special selection of initial conditions. In this case, an increasing part of the beam particles, which velocities are not equal to the phase velocity $v_F = \omega/k$ of the wave but are close enough (i.e., so-called non-resonant particles), are trapped by the wave in its potential well.

The equations, describing the nonlinear dynamics of the wave excited by a particle beam (here of electrons), in the absence of energy absorption in the medium, have the form (see annex II):

$$\partial A / \partial \tau = 8\pi \cdot \int_{-1/2}^{1/2} d\zeta_{p0} \int_{-\eta}^{\eta} d\eta_0 \eta_0 \exp\{-2\pi i \xi\}, \quad (2.12)$$

$$2\pi \cdot d^2 \xi / d\tau^2 = 2\pi \cdot d\eta / d\tau = -\text{Re}[A \cdot \exp\{2\pi i \xi\}], \quad (2.13)$$

where $\omega_{be} = (4\pi e^2 n_{b0} / m_{e0})^{1/2}$ is the plasma frequency of the electron beam, and $\omega_{pe} = (4\pi e^2 n_{e0} / m_{e0})^{1/2}$ is the Langmuir frequency of the plasma (here, $e, m_{e0}, n_{b0}, n_{e0}$ is the charge, rest mass of the electron, and the unperturbed density of the beam and plasma), $2\pi \xi_0 = kz_0 - \omega t$ and $\eta_0 = (kv - \omega_{pe}) / 2\pi\gamma$. Here, the position of each particle in the beam is determined by the value ξ , and the velocity is defined by the quantity η . The integration in (2.12) is carried out over the initial values of the coordinate and velocity of the particles, i.e., $\xi_0 = \xi(t=0)$ and $\eta_0 = \eta(t=0)$. Moreover, to simplify the description, let us assume that the derivative of the velocity distribution function in the vicinity of the phase velocity of the wave is $\partial f_b(v) / \partial v|_{v=\omega(k)/k}$ and it is proportional to the velocity [2-5].

We can estimate the average oscillation frequency Ω_{TR} of trapped particles in the potential well of the wave $\Omega_{TR} = \sqrt{ekE / m_{e0}}$. As a result of such oscillatory motion of the captured particles, the sign of the derivative of the distribution function in the vicinity of the phase velocity of the wave changes [2-7 – 2-8]. Such a change in the sign of the derivative can lead to an oscillatory change in the direction of the process, i.e. to a sequential change in the radiation of field quanta to their absorption and vice versa.

Let us note that the change in sign of the derivative of the distribution function is due to the dynamics of the beam particles in the wave field, which is represented by the second equation of the system (2.13). This process takes into account the nonlocality of the processes of interaction between the beam particles and the wave.

It is useful to introduce into consideration the parameter Ω_{TR} / γ_L that, during instability, gradually increases from the initial values of much smaller units. When this parameter reaches the value of the order of unit, the instability saturates [2-9]. Subsequently, an energy exchange takes place between the wave and trapped particles [2-6] with characteristic time $\Omega_{TR}^{-1} \approx \gamma_L^{-1}$. Due to the mixing of particles in the potential well of the wave, oscillations of the wave intensity rapidly decay.

References to section 2

2-1. Andronov A. A. On the issue of attenuation and growth of plasma waves // *Izv. Universities. Radiophysics*, 1961. – Vol. 4. – No. 5. – P. 861–866 (in Russian).

2-2. Kondratenko A. N., Kuklin V. M. *Fundamentals of Plasma Electronics*. – M. : Energoatomizdat, 1988. – 320 p (in Russian).

2-3. Kuzelev M/ V/, Rukhadze A. A. Spontaneous and stimulated emission of an electron, an electron bunch and an electron beam in plasma // *UFN*, 2008. – V. 178. – No. 10. – P. 1025–1055.

2-4. Interaction of an electron beam with plasma / I. F. Kharchenko, Ya. B. Fainberg, R. M. Nikolaev, E.A. Kornilov, E. A. Lutsenko, N. S. Pedenko. // *ZhETF*, 1960. – V. 38. V. 3. – S. 685–692 (in Russian).

2-5. Demirkhanov R. A., Gevorkov A. K., Popov A. F. Interaction of a beam of charged particles with a plasma // *ZhTF*, 1960. – V. 30. – N. 3. – P. 315–319 (in Russian).

2-6. To the nonlinear theory of excitation of a monochromatic plasma wave by an electron beam / I. N. Onishchenko A. R. Linetsky, N. G. Matsiborko, V. D. Shapiro, V. I. Shevchenko // *JETP Letters*, 1070. – Vol. 12. – N 8. – P. 407–410 (in Russian).

2-7. Mazitov R. K., On the damping of plasma waves, *Zh. app. mat. and theor. physical* 1965. – No. 1. – P. 27–31 (in Russian).

2-8. O’Neil Th. Collisionless damping of non-linear plasma oiscillation // *Phys. Fluids*. 1965. – V. 8. – N. 12. – P. 2255–2264 (in Russian).

2-9. Shpiro V. D. and Shevchenko V. I., Wave-particle interaction in nonequilibrium media, *Izv. Universities. Radiophysics*. 1976 – V. 19. – No. 5–6. – P. 787–791 (in Russian).

SECTION 3.

SPONTANEOUS AND INDUCED EFFECTS

WITHIN THE FRAME OF THE THREE-WAVE INTERACTION

In the case of multiwave interaction induced processes are very diverse in contrast to the wave-particle systems, one of which was discussed in the previous section. For definiteness, let us consider the interaction in a nonisothermal plasma of three sound waves whose frequencies and wave numbers are comparable (for the first time, such a “decay” process was considered in [3-1]). At the same time, let us digress from the notions of compact wave packets and random changes in their phases [3-2, 3-3]. Let two waves with frequencies ω_2 and ω_3 propagating in a nonlinear

medium excite a nonlinear current \tilde{j}_{23} capable of fulfilling the conditions of space-time synchronism¹

$$\omega_1 \approx \omega_2 + \omega_3 \quad \text{and} \quad \vec{k}_1 = \vec{k}_2 + \vec{k}_3, \quad (3.1)$$

of emitting quanta of the field of a natural wave of a medium (eigenmode) at a frequency ω_1 .

If we take into account the action of waves with frequencies ω_2, ω_3 and neglect the effect of the field of the first wave with frequency ω_1 on this nonlinear current \tilde{j}_{23} , then such a process of emission of field quanta $\hbar\omega_1$ could be considered spontaneous. However, if the field of the first wave, for example, accumulates in the interaction space and its amplitude becomes significant, the effect of this field on the nonlinear current \tilde{j}_{23} will no longer be neglected.

In this case, we can talk about the interaction of three waves, moreover, the phase synchronization of the modes and the formation of a coherent field takes place with the self-consistent participation of all interacting waves.

At the frequency of the first wave, the character of energy exchange, accurate to the fourth order of smallness, is determined from the amplitudes of the interacting waves by the relation

$$(\tilde{j}_{23} + \tilde{j}_1^{(3)})(\tilde{E}_1^* + \tilde{E}_{23}^*) \approx \tilde{j}_{23} \cdot \tilde{E}_{23}^* + \tilde{j}_{23} \cdot \tilde{E}_1^* + \tilde{j}_1^{(3)} \tilde{E}_1^*, \quad (3.2)$$

where, for the field strength at the frequency ω_1 , the first $\tilde{E}_1^{(1)}$ and second \tilde{E}_{23}^* order quantities are retained, and for the currents, the second \tilde{j}_{23} and third $\tilde{j}_1^{(3)}$ order magnitudes in wave amplitudes are retained.

The first term on the right-hand side of (3.2) is responsible for the processes of interaction between the current \tilde{j}_{23} and the field $\tilde{E}_{23} = \tilde{E}_{23}(\tilde{j}_{23})$ formed by this current at combination frequencies. The origin of the current \tilde{j}_{23} is due to the nonlinear interaction of oscillations at frequencies ω_2 and ω_3 . These processes under the conditions of space-time synchronism (3.1) can lead to the generation of radiation at the frequency of the first wave, and this generation with respect to this wave has the characteristic features of a spontaneous process, as it is shown below. The second term (3.2) can be considered responsible for the processes of interaction of three waves at once. The last term determines the induced processes of radiation and absorption of field quanta at the frequency ω_1 of the first wave. If the real part of this expression is nonzero, then induced radiation or absorption of field quanta at a frequency ω_1 is possible.

¹ Here, the case of the synthesis of two waves, that is, the process opposite to decay.

The second term (3.2) dominates in the well-studied processes of three-wave interaction, and the role of the third term is reduced only to corrections to the slow phases and partly the wave amplitudes (see, for example, [3-4, 3-5]).

In case of a multi-wave interaction, violations of the coherence of radiation as well as the interaction efficiency are possible, because these phenomena are determined by the dispersion that generates phase mismatches of the spatiotemporal synchronism. It is not uncommon for a multiwave interaction to have a phase mismatch Δ between the frequencies of the waves participating in the interaction. Moreover, the first of relations (3.1) takes the form

$$\omega_1 - \omega_2 - \omega_3 = \Delta_{-1,2,3} = \Delta. \quad (3.3)$$

Without taking into account self-interaction (the term is proportional to $\propto N_1^2$), the equation for the number of quanta at a frequency ω_1 can be formally written (see annex III) in the following form (the possibility of such a presentation was indicated before in the report [3-6])

$$dN_1 / dt = \Sigma + \frac{1}{\hbar\omega} \{j_{23} E^*_{1} + j^*_{23} E_1\} + \frac{\partial \Sigma}{\partial(\hbar\omega)} W_1, \quad (3.4)$$

where

$$\Sigma = \alpha \frac{8}{3\hbar} \left(\frac{e}{m_i v_s} \right)^2 \frac{W_2 W_3}{\omega_2 \omega_3}, \quad \frac{\partial \Sigma}{\partial(\hbar\omega_1)} W_1 = \frac{8}{3\hbar^2} \left(\frac{e}{m_i v_s} \right)^2 \alpha \frac{W_1}{\omega_1} \left(\frac{W_2}{\omega_2} + \frac{W_3}{\omega_3} \right), \quad (3.5)$$

and define

$$\frac{\partial \Sigma}{\partial(\hbar\omega_1)} = \alpha \frac{8}{3\hbar} \frac{e^2 [(W_2 + \hbar\omega_2)(W_3 + \hbar\omega_3) - W_2 W_3] / \hbar\omega_1}{(m_i v_s)^2} \frac{1}{\omega_2 \omega_3} = \alpha \frac{8}{3\hbar} \frac{e^2}{(m_i v_s)^2} \left(\frac{W_2}{\omega_2} + \frac{W_3}{\omega_3} \right) \frac{1}{\hbar\omega_1}. \quad (3.6)$$

The presence of sufficiently wide spectra can lead to the following equations

$$\frac{\partial N_k}{\partial t} = \alpha \cdot w \sum_{k'} N_{k'} N_{k-k'} + w \left\{ \frac{\alpha'}{2} N_k^2 + \alpha N_k \sum_{k'} [N_{k'} + N_{k-k'}] \right\}, \quad (3.7)$$

$$N_k \frac{\partial \phi_k}{\partial t} = \frac{w}{2} \sum_{k'} N_{k'} N_{k-k'} + \frac{w}{2} \left\{ \frac{1}{2} N_k^2 + N_k \sum_{k'} [N_{k'} + N_{k-k'}] \right\}. \quad (3.8)$$

The terms, corresponding to the three-wave interaction are excluded here. It occurs due to averaging over turbulent pulsations. Without taking into account self-interaction (see annex III for more on this), equation (3.7) takes the form

$$\frac{\partial N_k}{\partial t} = \Sigma_k + \hbar\omega_k N_k \frac{\partial}{\partial(\hbar\omega_k)} \Sigma_k, \quad (3.9)$$

where

$$\Sigma_k = w \cdot \alpha \sum_{k'} N_{k'} N_{k-k'}, \quad w = 8e^2 \hbar / 3(m_i v_s)^2, \quad (3.10)$$

$$\hbar\omega_k N_k \frac{\partial}{\partial(\hbar\omega_k)} \Sigma_k = \alpha \cdot w \cdot N_k \sum_{k'} [N_{k'} + N_{k-k'}].$$

It is important to note that in equation (3.4), the relation between the expression for spontaneous emission (the first term of the right-hand side) and the expression for the induced processes of radiation and absorption (the third term of the right-hand side) coincides in form and meaning with the corresponding expressions in the equations (1.7) and (2.8).

It should be noted that the first terms (3.7) and (3.8) are of the same order as the last terms of these equations. This sometimes gives reason to consider the physical mechanisms for which they are responsible, of the same type, which is far from the case.

In addition, the generation of oscillations at a frequency ω_1 , determined by the first terms on the right-hand side of equations (3.7) and (3.8), can be significant and it has no obvious signs of noise, and you can see a certain similarity of the discussed phenomenon to radiation from a beam modulated at a certain frequency. The description of radiation processes in case of wave packets in representation (3.9) is similar to the description of spontaneous and induced radiation in case of active media (1.7) and in case of particle – wave interactions (2.8).

It is important to note that the system under consideration (see, for example, equation (3.9)) is close to and slightly above the threshold for the generation of induced radiation, which is discussed in the next chapter. This promises, with the correct consideration of the inverse effect of radiation on turbulence, the emergence of new effects and phenomena. In accordance with the ideas developed in the reviews by V. L. Ginzburg [1-3] – [1-5], when discussing the nature of spontaneous emission in the description of classical systems, quantum effects were not involved above, which nevertheless did not affect [3- 3] the generality of consideration.

References to section 3

3-1. Sagdeev R. Z., Oraevskii V. N. On the stability of steady-state longitudinal plasma oscillations // ZhTF, 1962, V. 32. – N. 7, – pp. 1291–1299 (in Russian).

3-2. Kirichok A. V., Kuklin V. M. Theory of Some Nonlinear Processes in Plasma in Terms of Spontaneous and Stimulated Radiation // Phys. Scripta, 2010, v. 82. N 11. – P. 35–41.

3-3. Zagorodny A. G., Kuklin V. M. Features of radiation in nonequilibrium media / Problems of theoretical physics. Scientific works / V. A. Buts, A. G. Zagorodny, V. E. Zakharov, V. I. Karas, V. M. Kuklin, A. V. Tur, S. P. Fomin, N. F. Shulga, V. V. Yanovsky; ed. no. V. M. Kuklin. – Kh. : V. N. Karazin Kharkiv National University, 2014. – Issue. 1. – 532 p. pp. 13–81 (Series "Problems of Theoretical and Mathematical Physics"; under the general editorship of A. G. Zagorodny, N. F. Shulga in Russian).

3-4. Oraevskii V. N., Wilhelmsson H., Kogan E. Ya., Pavlenko V. P. On the stabilization of explosive instabilities by nonlinear frequency shift // *Physica Scripta*, 1973. V. 7. – P. 217–221 (in Russian).

3-5. Weiland J. Influence of nonlinear frequency Shifts and effective nonlinear dissipation on explosive Instabilities // *Physica Scripta*, 1973. – V. 9. – P. 343–349.

3-6. Kirichok A. V., Kuklin V. M., Zagorodny A. G. A Theory of Some Nonlinear Processes in Plasma in Terms of the Spontaneous and Induced Radiation // *Modern Problem of Theoretical and Mathematical Physics: Proc. Bogolubov Kyiv Conference, Kyiv, Ukraine, 15–18 Sept. 2009.*

SECTION 4. SEMI-CLASSICAL MODEL

In the framework of the semiclassical model (see annex V), let us show that the nature of the process of excitation of electromagnetic waves in a resonator or in a waveguide filled with a medium representing a two-level system of dipoles depends on the relation of the Rabi frequency and the line width of the wave packet. If there is a significant population inversion or strong fields, the line width can be neglected.

In this case, the field energy density is high. In this mode, we can observe noticeable nutations of population inversions with different frequencies along the waveguide length corresponding to local Rabi frequencies, the interference of which determines the oscillatory behavior of the wave field amplitude. At low levels of electric field intensity or small values of population inversion, the behavior of a two-level system is described by balanced equations; it becomes monotonic, population inversion tends to zero, and the characteristic time of a field change increases.

In his famous work [4-1] R. Dicke considered the interaction of oscillators or emitters that are close to each other; he believed that they are actually combined into one quasiparticle, which contains several oscillators or emitters. Let us draw attention to the fact that in the quantum case we do not mean the phase synchronization of the oscillators, as in the classical analysis; it is about increasing the probability of radiation, which in fact leads to the same result.

In this case, their wave functions overlap and the probability of spontaneous emission of this quasiparticle increases in comparison with the probability of emission of individual oscillators or emitters² [4-2]. However, if the oscillators or emitters are located in space, the overlap of their wave functions becomes either weak or generally imperceptible. In most existing lasers, the density of active

² The radiation from a bunch of particles, whose dimension is noticeably smaller than the wavelength, is coherent in the quantum and classical description.

particles is such that the distances between them are very significant and the overlapping of wave functions should not obviously be expected³.

How do the electrons of active atoms interact in lasers? Their interaction is due to electromagnetic radiation fields. In the quantum case, when the phases of the oscillator and the field are not defined, and only the relative orientation of the radiating dipole and the electric field is indicated, that is, only the projections of the dipole moment on the direction of the electric field are known, the role of the Rabi frequency can become determining. Many authors note that the Rabi frequency determines the oscillatory nature of the change in the population inversion of a system of radiating dipoles (nutations), which have main and excited energy levels and, generally speaking, are proportional to the probability of induced radiation and absorption of field quanta [4-4, 4-5].

In this case, the medium of the emitters can be considered as quantum mechanical, and the field is considered in the classical representation. The system of one-dimensional equations of the semiclassical theory (see annex V) for the amplitudes of perturbations of the electric field E , and polarization P , which describe the excitation of electromagnetic waves in a two-level active medium, can be represented in the following form:

$$\frac{\partial^2 E}{\partial t^2} + \delta \frac{\partial E}{\partial t} - c^2 \frac{\partial^2 E}{\partial x^2} = -4\pi \frac{\partial^2 P}{\partial t^2} \quad (4.1)$$

$$\frac{\partial^2 P}{\partial t^2} + \gamma_{12} \frac{\partial P}{\partial t} + \omega^2 \cdot P = -\frac{2\omega |d_{ab}|^2}{\hbar} \mu E, \quad (4.2)$$

to which you need to add the equation for the population inversion slowly varying over time

$$\frac{\partial \mu}{\partial t} = \frac{2}{\hbar \omega} \langle E \frac{\partial P}{\partial t} \rangle, \quad (4.3)$$

where the transition frequency ω between the levels corresponds to the field frequency, we shall neglect the relaxation of the inversion due to external reasons, δ is the decrement of field absorption in the medium, d_{ab} is the matrix element of the dipole moment (more precisely, its projection onto the direction of the electric field), the population difference per unit volume is $\mu = n \cdot (\rho_a - \rho_b)$, ρ_a and ρ_b are the relative population levels in the absence of a field, γ_{12} is the width of the spectral line, and n is the density of the

³ At low temperatures in semiconductors there are few free electrons and there is no overlap of their wave functions. In this case, their distribution is actually Maxwellian [4-3] and their temperature is approximately equal to the temperature of the atomic system, which corresponds to the classical description. It should be mentioned that the Fermi distribution, that is, the quantum representation, is possible only if the wave functions of the electrons overlap, which can be observed in metals, where the number of free electrons is comparable to the number of atoms.

dipoles of the active medium. Here, the line width is inversely proportional to the lifetime of states, which is due to relaxation processes.

Shortened equations. Let the fields be represented as

$$E = [E(t) \cdot \exp\{-i\omega t\} + E^*(t) \cdot \exp\{i\omega t\}] \quad (4.4)$$

$$P = [P(t) \cdot \exp\{-i\omega t\} + P^*(t) \cdot \exp\{i\omega t\}] \quad (4.5)$$

Then, the number of field quanta is equal to

$$\langle E^2 \rangle / 4\pi\hbar\omega = 2 |E|^2 / 4\pi\hbar\omega = N. \quad (4.6)$$

Also, for slowly varying amplitudes, the equations are as it follows

$$\frac{\partial E(t)}{\partial t} + \delta \cdot E(t) = 2i\pi\omega P(t) \quad (4.7)$$

$$\frac{\partial P(t)}{\partial t} + \gamma_{12} P(t) = \frac{|d_{ab}|^2}{i\hbar} \mu E \quad (4.8)$$

$$\frac{\partial \mu}{\partial t} = \frac{2i}{\hbar} [E(t)P^*(t) - E^*(t)P(t)]. \quad (4.9)$$

From equations (4.7) and (4.9) follows the law of conservation of energy

$$\frac{\partial N}{\partial t} + 2\delta N + \frac{\partial \mu}{2\partial t} = 0 \quad (4.10)$$

Balance equations. If the conditions are fulfilled $\gamma_{12} \gg \partial P / P \partial t$ (as it will be clear from further consideration), the oscillatory nature (nutations) of the population inversions can be neglected and the system of equations (4.7) – (4.10) can be written in a form similar to that obtained in [4-6]. This is a simplified version of the balanced (speed) equations of a two-level system in the presence of an electric field without taking into account spontaneous radiation

$$\frac{\partial \mu}{\partial t} = -\frac{8\pi\omega |d_{ab}|^2}{\hbar\gamma_{12}} \mu N, \quad (4.11)$$

$$\frac{\partial N}{\partial t} + 2\delta N = \frac{4\pi\omega |d_{ab}|^2}{\hbar\gamma_{12}} \mu N, \quad (4.12)$$

where $\Omega_N = 4\sqrt{\pi\omega |d_{ab}|^2 N / \hbar}$ is the Rabi frequency corresponding to the density of the number of field quanta N , and τ_N is the characteristic process time, determined from the relation $\tau_N^{-1} = \Omega_N^2 / \gamma_{12}$.

Let us note that the transition to equations (4.11) and (4.12) is similar to the transition to the case of a noticeable spectral field width, when the width

of the spectral line is greater than the inverse characteristic time of the change in the amplitude of perturbations [4–7, 4–8].

We shall use the notation $\mu / \mu_0 = M$, and immediately note that the changes in the population inversion will be determined by the choice μ_0 and the initial conditions $\Omega_0 = |d_{ab}| \cdot |E_0| / \hbar = |d_{ab}| \cdot [4\pi\omega \cdot \mu_0 / \hbar]^{1/2}$, which represents the Rabi frequency corresponding to the value of the electric field amplitude $|E_0| = [4\pi\hbar\omega\mu_0]^{1/2}$, $E = E(t) / [4\pi\hbar\omega\mu_0]^{1/2}$, $P = 4\pi\omega P(t) / \Omega_0 [4\pi\hbar\omega\mu_0]^{1/2}$, $\tau = \Omega_0 t$, $\Gamma_{12} = \gamma_{12} / \Omega_0$, $\Theta = \delta / \Omega_0$.

Excitation of a resonator with an active medium. In order to solve the problem of field interaction in a limited system (resonator or waveguide), one should use the local character of population inversion and, correspondingly, polarization, determining these quantities in separate spatial sectors. The electromagnetic field in this case can be represented in the waveguide in the form of a standing wave, which is due to the effects of reflection of the field from the boundaries of the system. In the case of radiation from a waveguide when $\delta \neq 0$, one should choose the field dependence in each of the spatial sectors $1 < j < S$ in the form of a relative number of quanta

$$|E_j(\tau = 0)|^2 = 2 \frac{1}{S} \cdot |E(\tau = 0)|^2 \cdot \text{Sin}^2 \left\{ 2\pi \frac{j}{S} + \alpha \right\} \quad (4.13)$$

where α is the almost constant phase associated with δ . Obviously, $\sum_j 2 \frac{1}{S} \text{Sin}^2 \left\{ 2\pi \frac{j}{S} + \alpha \right\} = m$ is in the case considered below, when a countable number m of waves fit along the length of the waveguide or resonator $b = m \lambda$. The total (relative) number of field quanta can be written as

$$N(\tau) = \sum_{j=1}^S \langle E_j(\tau) \rangle^2 \quad (4.14)$$

Generally speaking, $\delta \approx \frac{c}{4\pi} \langle E \rangle^2 (x=0) / \left(\frac{\langle |E|^2 \rangle}{4\pi} b \right)$, where $b = m \lambda$ is the waveguide length. It is easy to see that $\langle E \rangle^2 (x=0) = 2 \langle E^2 \rangle^2 \text{Sin}^2 \alpha$ and $\delta \approx 2c(\text{Sin}^2 \alpha) / b$, where c is the group velocity of the wave outside the waveguide.

The system of equations (4.7) – (4.10) in this case is transformed as it follows. For local variables E_j , P_j and M_j such equations are valid

$$\frac{\partial P_j}{\partial \tau} + \Gamma_{12} P_j = -i M_j E_j, \quad (4.15)$$

$$\frac{\partial M_j}{\partial \tau} = \frac{i}{2} [E_j P_j^* - E_j^* P_j], \quad (4.16)$$

where $E_j(\tau) = \left(\sqrt{\frac{2}{S}}\right) \cdot |E(\tau)| \cdot \text{Sin}\left\{2\pi \frac{j}{S} + \alpha\right\}$, $\frac{1}{2} \sum_{j=1}^S (M_j + M_j^*) = M$.

For the number of field quanta, we shall write the equation (conservation law, consequence of equations (4.7) and (4.9))

$$\frac{\partial M}{2\partial \tau} + \frac{\partial N(\tau)}{\partial \tau} + 2\Theta N(\tau) = 0. \quad (4.17)$$

It should be noted that the case $\gamma_{12} \gg \Omega = |d_{ab}| |E(t)| / \hbar$ or $\gamma_{12} \gg [4\pi\omega]^{1/2} |d_{ab}| \mu / \hbar^{1/2}$ corresponds to low levels of electric field intensity or small values of population inversion. On the contrary, under strong reverse inequalities, the line width can be neglected, and in this case the radiation intensities and population inversions are very significant. These remarks can be illustrated if we consider field excitation in a cavity without absorption.

Let us examine the solutions of system (4.15), (4.16), (4.17), using the following notations

$$N(\tau) = \frac{1}{S} \sum N_j(\tau), \quad M(\tau) = \frac{1}{S} \sum M_j(\tau), \quad E_j(\tau) = \sqrt{2N(\tau)} \cdot \text{Sin}\left(2\pi \frac{j}{S}\right). \quad (4.18)$$

Under the conditions $N(0) = 0.001$, $M(0) = 1$, $S = 100$, $\Gamma_{12} = 0$, $\Theta = 0$, the calculation results are identical [4–9, 4–10] under conditions $\Gamma_{12} = 0$ at the corresponding scales indicated above (see Fig. 4.1 and Fig. 4.2). An increase of the line width from the system $\Gamma_{12} > 0$ in the absence of energy output results in smoothing out of the field oscillations and the average population inversion in the waveguide volume (see Fig. 4.1 and Fig. 4.2.)

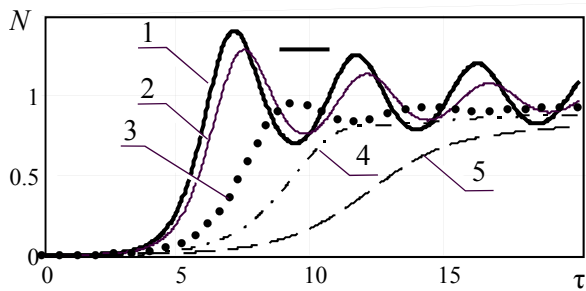


Fig. 4.1. Behavior of field intensity versus time for values 1 - $\Gamma_{12} = 0$;
2 - $\Gamma_{12} = 0.1$; 3 - $\Gamma_{12} = 0.5$;
4 - $\Gamma_{12} = 0.9$; 5 - $\Gamma_{12} = 1.9$
in the absence of energy output ($\Theta = 0$)

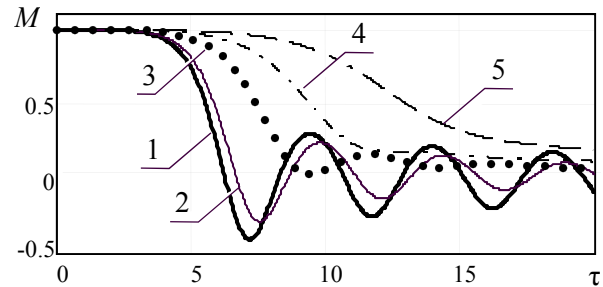


Fig. 4.2. The behavior of the average population inversion versus time for values 1 - $\Gamma_{12} = 0$; 2 - $\Gamma_{12} = 0.1$;
3 - $\Gamma_{12} = 0.5$; 4 - $\Gamma_{12} = 0.9$; 5 - $\Gamma_{12} = 1.9$
in the absence of energy output ($\Theta = 0$)

In all these cases, the inversion changes over time in an oscillatory manner or monotonically (with a large line width) tends to zero. The distribution of M along the waveguide length (by sectors j) at the moments of the onset of the first maximum N , the first minimum in the absence of energy output has the form (see Fig. 4.3 – Fig. 4.5).

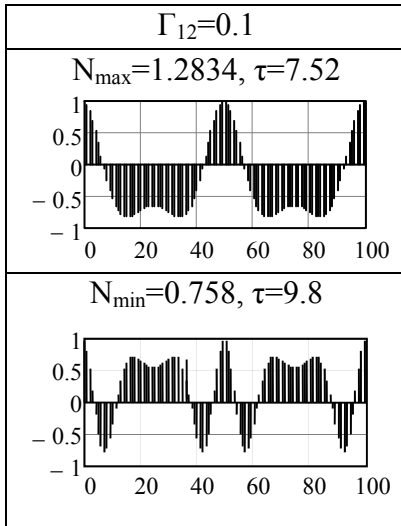


Fig. 4.3. The distribution of M by sectors at the moments of the occurrence of the first maximum and the first minimum N with different line widths $\Gamma_{12} = 0.1$ and in the absence of energy output ($\Theta = 0$)

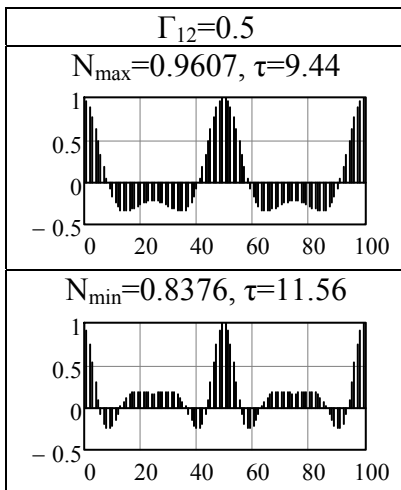


Fig. 4.4. The distribution of M by sectors at the moments of the occurrence of the first maximum and the first minimum N with a line width $\Gamma_{12} = 0.5$ and in the absence of energy output ($\Theta = 0$)

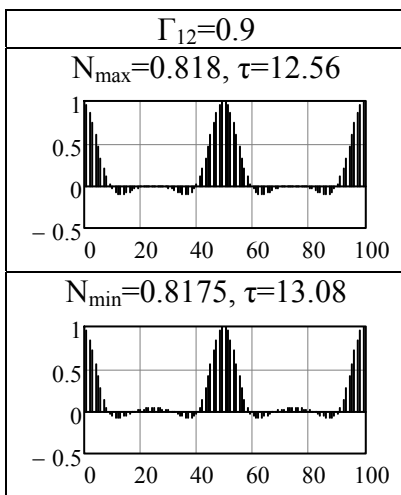


Fig. 4.5. The distribution of M by sectors at the moments of the occurrence of the first maximum and the first minimum N with a line width $\Gamma_{12} = 0.9$ and in the absence of energy output ($\Theta = 0$)

References to section 4

4-1. Dicke R. H. Coherence in spontaneous radiation processes // *Phys. Rev.* 1954. – V. 93. – P. 99.

4-2. Andreev A. V, Emelyanov V. I, Il'inskiy Yu. A. "Collective spontaneous emission (Dicke superradiance)" *UFN* 1980. – 131. – P. 653–694 (in Russian).

4-3. Bass F. G., Gurevich Yu. G. Hot electrons and strong electromagnetic waves in the plasma of semiconductors and gas discharge – Nauka, M. 1975. – 400 p. (in Russian).

4-4. Davydov A. S. Quantum Mechanics. Fizmatgiz. 1963 . – 748 p. (in Russian).

4-5. Allen L., Eberly J. Optical resonance and two-level atoms. Wiley-Interscience Publication John Wiley and Sons. New York – London – Sydney – Toronto. 1975. – 222 p.

4-6. Einstein A. Quantentheorie der Strahlung // *Mitteilungen d. Phys. Ges. Zurich*, Nr. 1916. – 18, (1916); *Phys. Zs.* 1917. – Nr. 18. – P. 121.

4-7. Valeo E. J. and Olerman C. R. Model of Parametric Excitation by an Imperfect Pump. *Phys. Rev. Lett.* 1973. V. 30. – N 21. – P. 1035–1038.

4-8. Thomson J. J. and Karush J. I. Effect of finite-bandwidth Driver on the Parametrical Instability. *The Physics of Fluids*, 1974. – V. 17. – N 8, – P, 1608–1613.

4.9. Kuklin V. M. Energy exchange between the field and the active medium of the waveguide/V. M. Kuklin, E. V. Poklonskiy. // *East European Journal of Physics* 2019. – V. 6. – N 3 – P. 46–53.

4.10. Kostenko V. V. Kuklin V. M., Poklonskiy V. M. On generation of a wave package in a waveguide, filled active medium / *VANT*, 2020. – N 3 (127).

CHAPTER 2. Spontaneous vs induced radiation

It is shown that near the detected new threshold of induced radiation, competition between spontaneous and stimulated processes leads to the occurrence of pulses of induced radiation, the intensity of which can be comparable or greater than the intensity of spontaneous radiation of the system. In this case, the population inversion can be many orders of magnitude less than the total number of states. It is shown that there are the conditions when regimes of periodic changes in the luminosity of such sources with different periods and amplitudes are possible. An external low-frequency wave in the system under the conditions of competition between spontaneous and forced radiation processes is considered, which leads to the development of the so-called turbulent-wave instability.

There are physical processes when spontaneous emission should not be neglected. This is due to the fact that spontaneous processes are able to reduce the inversion and they are absorbers with respect to the generation of induced radiation.

SECTION 5.

NEW THRESHOLD OF INDUCED RADIATION

If, based on the results of studies of the correlation of fluctuations in laser radiation [5-1], we assume that the fraction of the coherent component is large in the induced radiation, then we can detect the threshold for the appearance of such radiation due to the existence of spontaneous processes at a certain critical value of population inversion [5-2]. A specific feature of this threshold of induced radiation is that in the absence of field energy absorption mechanisms, it corresponds to the initial population inversion equal to the square root of the total number of states⁴.

On the other hand, taking into account the values of the initial inversion in the vicinity of this threshold, it is not difficult to see a change in the nature of the process. When this threshold is exceeded, the number of emitted quanta begins to grow exponentially over time. Moreover, such exponential growth is not observed below the threshold. That is, the excess of the detected threshold by the initial inversion leads to an exponential increase in the number of quanta. At a qualitative level it can be assumed that the terms on the right-hand sides of equations (1.1) – (1.3) are proportional N_k to the induced processes, as well

⁴ The intensity of spontaneous emission, not synchronized (randomly distributed) over the phases of the oscillators, is known to be proportional to their number. The intensity of coherent stimulated emission is proportional to the square of the number of oscillators.

as the number of quanta written there. It is rational to imagine $N_k = N_k^{(incoh)} + N_k^{(coh)}$ where $N_k^{(incoh)}$ and $N_k^{(coh)}$ are, respectively, the number of quanta of spontaneous and induced radiation. Then a qualitative (i.e. simplified) description model can be written in the form [5-2]

$$\partial n_2 / \partial t = +w_{12} \cdot N_k^{(coh)} \cdot n_1 - (g \cdot w_{21} + w_{21} \cdot N_k^{(coh)}) \cdot n_2, \quad (5.1)$$

$$\partial n_1 / \partial t = -w_{12} \cdot N_k^{(coh)} \cdot n_1 + (g \cdot w_{21} + w_{21} \cdot N_k^{(coh)}) \cdot n_2, \quad (5.2)$$

$$\partial N_k^{(incoh)} / \partial t = u_{21} \cdot n_2, \quad (5.3)$$

$$\partial N_k^{(coh)} / \partial t = w_{21} \cdot N_k^{(coh)} \cdot n_2 - w_{12} \cdot N_k^{(coh)} \cdot n_1. \quad (5.4)$$

That is, generally speaking, we shall consider two models of description - traditional and qualitative - modified⁵

Traditional system of equations

$$\partial M_1 / \partial T = -N_0 - 2M_1 \cdot N_1 \quad (5.5)$$

$$\partial N_1 / \partial T = (N_0 / 2) + M_1 \cdot N_1 - \theta \cdot N_1$$

Qualitative system of equations with the separation of quanta by their origin

$$\partial M / \partial T = -N_0 - 2M \cdot N_c$$

$$\partial N_{inc} / \partial T = (N_0 / 2) - \theta \cdot N_{inc}; \quad (5.6)$$

$$\partial N_c / \partial T = M \cdot N_c - \theta \cdot N_c,$$

where $N_{inc} = N_k^{(incoh)} / \mu_0$, $N_c = N_k^{(coh)} / \mu_0$, $M = \mu / \mu_0$, $M = M_1 = \mu / \mu_0$, $T = w_{21} \cdot \mu_0 \cdot t = \mu_0 \cdot \tau$, $N_1 = N_k / \mu_0$, the only free parameter that is convenient for analysis is $N_0 = g \cdot N / \mu_0^2$. For the comparison to be correct, let us assume that the total number of real states is $N = n_1 + n_2 = 10^{12}$ and a threshold inversion $\mu_{0th} = \sqrt{N} = 10^6$. Let us evaluate the transition to a single time scale according to the relation $T = \tau \cdot \mu_0$, where T is the time in each individual case. The initial values are defined as it follows $M(T=0) = M_1(T=0) = 1$, $N_{inc}(T=0) = N_{inc} / \mu_0 = 3 \cdot 10^4 / \mu_0$, $N_c(T=0) = N_c / \mu_0 = 3 \cdot 10^4 / \mu_0$, $N_1(T=0) = N_k / \mu_0 = 3 \cdot 10^4 / \mu_0$, as well.

The absorption of field energy will be taken into account by the value $\theta = 2\delta_D / w_{21}\mu_0$. The change in the nature of the process for the traditional system (5.5) is shown in Fig. 5.1, which reflects the dynamics of the development of the process for cases of parameter change $N_0 \in (30 \div 0.01)$.

⁵ Already A. Poincare noted that "mainly equations should teach us what can and should be changed in them."

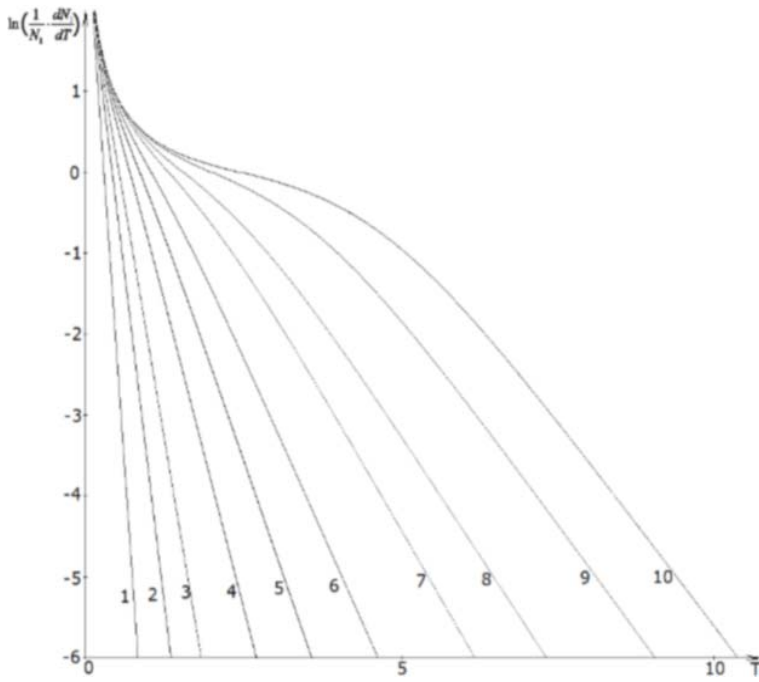


Fig. 5.1. The behavior of the quantity $\ln\{dN_1 / N_1 dT\}$ versus time for the parameter value:

$$N_0 = (n_1 + n_2) / (n_2 - n_1)^2 :$$

1- $N_0=30$; 2- $N_0=10$;
 3- $N_0=5$; 4- $N_0=2$; 5- $N_0=1$;
 6- $N_0=0.5$; 7- $N_0=0.2$;
 8- $N_0=0.1$; 9- $N_0=0.03$;
 10- $N_0=0.01$

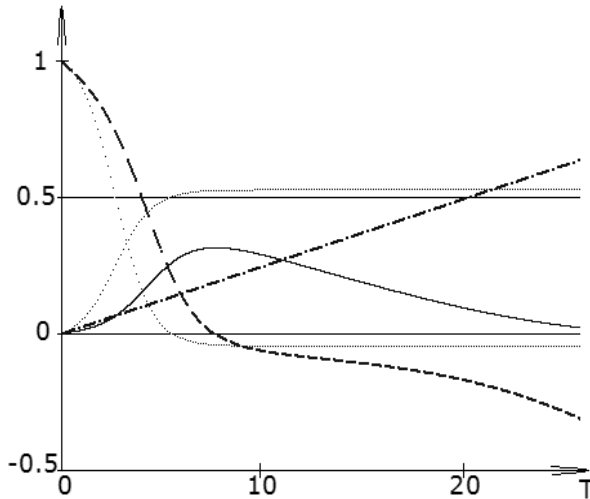


Fig. 5.2. The behavior of the quantities M_1 and N_1 points); M (dashed lines) corresponding to the traditional system N_1 and N_{nc} (solid and dash-dotted lines, respectively) in the absence of absorption ($\Theta = 0$) and for $N_0 = N / \mu_0^2 = 0.05$

The traditional idea of the instability threshold meets the requirement of positivity of the right-hand side of the third equation of system (5.6) $M > \theta$ or, what is the same

$$\mu > \mu_{TH1} = \delta_D / w_{21} \tag{5.7}$$

We should also (see Fig. 5.1) pay attention to changes in the number of quanta upon crossing the threshold [5-2]

$$n_2 - n_1 = \mu_{TH2} \approx (2N)^{1/2} = [2(n_2 + n_1)]^{1/2} \tag{5.8}$$

Indeed, when the threshold (5.8) is exceeded, it can be seen that the magnitude $\ln(dN / N dT)$ (ordinate axis of Fig. 5.1) becomes more and more gentle, that is, the number of quanta grows, and this growth acquires a clear exponential character with distance from the threshold (5.8). Let us discuss the conditions under which it makes sense near the threshold of induced radiation (5.8) to use a qualitative system of equations (5.6).

In the framework of the classical description, the intensities of spontaneous emission of particle-oscillators whose phases are randomly distributed and added up, because the intensity of spontaneous emission is equal to the sum of the intensities of the radiation of individual particle-oscillators in an excited state or at a higher energy level. In the case of induced, actually coherent radiation, the field strength is so significant that it synchronizes both emitting and absorbing particle oscillators, therefore it depends on the sign of population inversion $\mu = n_2 - n_1$ whether this induced field will increase or decrease, and the characteristic time of this process is inversely proportional to μ .

However, if there is no such induced coherent field, then the oscillator particles in the excited state will be emitted spontaneously, because they are not synchronized.

In the traditional model (5.5), there is a term $\mu \cdot N_k$ that is responsible for the induced processes of excitation and absorption. But this term does not have physical meaning below the threshold (5.8), because in this case there is no an intense induced field that can synchronize the radiation of many particles in the system.

In a stationary state, the radiation intensity of the source will be determined only by spontaneous radiation $\delta \cdot N_k^{(incoh)} \propto g \cdot N/2$, which leads to a decrease in inversion.

However, when the threshold (5.8) is exceeded, the term $\mu \cdot N_k$ in the right-hand sides of the equations plays an important role, providing a description of the induced processes at $\mu > \mu_{TH2}$. Near the threshold (5.8) it is rational to use precisely a qualitative system of equations, then the intensity of spontaneous emission in a unit volume is determined by $\delta \cdot N_k^{(incoh)} \simeq g \cdot N/2$, but the energy flux density of the induced radiation is $\delta \cdot N_k^{(coh)}$.

Figure 5.2 shows the dynamics of the radiation process both in the case of a description by means of the traditional model and in the case of a qualitative description near the threshold (5.8). At large values of the initial inversion, induced radiation appears. In this case, the regime of exponential growth in a number of quanta is more and more clearly distinguished. In the absence of absorption of quantum energy, according to the qualitative description (5.6), after a decrease in the pulse amplitude of the induced radiation, the number of spontaneous emission quanta continues to increase. In the traditional model (5.5), absorption processes limit the growth of the total number of quanta and the radiation level reaches its stationary value.

However, comparing the dynamics of the processes, it can be understood that after decreasing the amplitude of the pulse of the induced radiation, the main contribution to the total number of quanta is made only by spontaneous emission. That is, at times greater than the pulse duration of the induced radiation, spontaneous incoherent radiation dominates.

It should be noted that in case of a fixed final level of loss or absorption of quantum energy, the pulse size of the induced radiation remains almost unchanged even with a significant increase in the level of population inversion (Fig. 5.3b). Thus, if the formation of the leading edge of the induced radiation pulse is determined by the initial level of inversion, then largely the duration of its trailing edge is determined by the levels of quantum energy loss in the system [5-3].

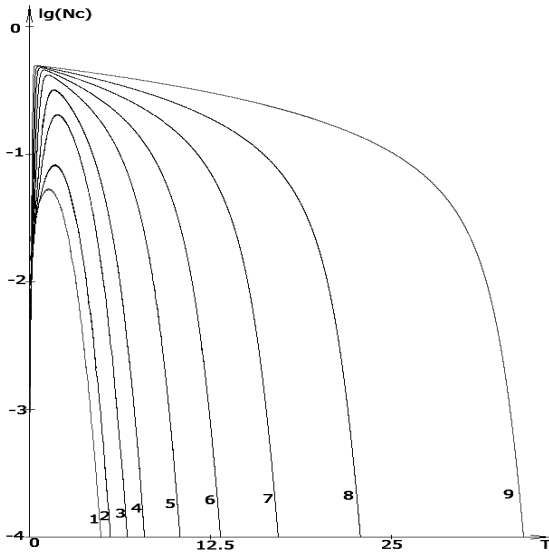


Fig. 5.3a. Form of the coherent pulse in the absence of absorption ($\theta=0$) for inversion value $s \mu_0 = \sqrt{2} \cdot 10^6$; $2 \cdot 10^6$; $\sqrt{10} \cdot 10^6$; $\sqrt{20} \cdot 10^6$; $\sqrt{50} \cdot 10^6$; 10^7 ; $\sqrt{2} \cdot 10^7$; $2 \cdot 10^7$; $\sqrt{10} \cdot 10^7$

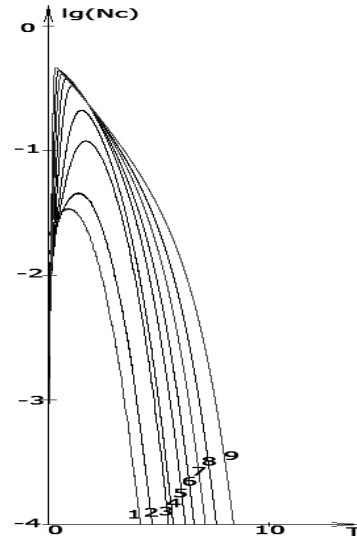


Fig. 5.3b. Form of the coherent pulse in an absorbing medium ($2\delta = 4 \cdot 10^5$) for inversion values $\mu_0 = \sqrt{2} \cdot 10^6$; $2 \cdot 10^6$; $\sqrt{10} \cdot 10^6$; $\sqrt{20} \cdot 10^6$; $\sqrt{50} \cdot 10^6$; 10^7 ; $\sqrt{2} \cdot 10^7$; $2 \cdot 10^7$; $\sqrt{10} \cdot 10^7$.

The threshold of induced radiation discussed in this work corresponds to the case when spontaneous emission randomly distributed over phases is comparable to induced radiation. Exceeding a threshold that is extremely low (for example, at $N = n_1 + n_2 = 10^{12}$, threshold inversion $n_2 - n_1 = \mu_{0th} = \sqrt{N} = 10^6$, and relative inversion $(n_2 - n_1) / (n_2 + n_1) \approx 10^{-6}$) leads to the occurrence of pulses of induced radiation, which is largely coherent. Moreover, the intensity of the pulses is comparable to the intensity of spontaneous emission.

These are the results of the analysis that let us expect that this mechanism could be one of the reasons for the formation of coherent pulses of approximately the same duration under cosmic conditions in the atmospheres of stars. Let us discuss the possibility of such processes below.

References to section 5

5-1. Brown H. R., Twiss R. Q. Interferometry of the intensity fluctuations in light. I. Basic theory: the correlation between photons in coherent beams of radiation"// Proc of the Royal Society of London. 1957. – V. A 242 (1230). – P. 300–324;

Interferometry of the intensity fluctuations in light. II. An experimental test of the theory for partially coherent light // *Ibid* 1958. – V. A 243 (1234). – P. 291–319.

5-2. Zagorodny A. G., Kuklin V. M. To realization conditions of maser radiation // *High-power pulsed electrophysics. International conference XIV Khariton's topical scientific readings. Digest of technical papers* – Sarov: FSUE RFNC-VNIIEF, 2013. – pp. 38–43.

5-3. Kirichok A. V., Kuklin V. M., Mischin A. V., Pryjmak A. V., Zagorodny A. G. On the formation of pulses of coherent radiation in weakly inverted media / *VANT*, 2013, N. 4 (86). – series “Plasma Electronics and New Methods of Acceleration” issue 8. – P. 267–271.

SECTION 6. PERIODIC CHANGES IN THE LUMINOSITY OF QUANTUM SOURCES

Let us consider the radiation source and select in it the layer, where the medium, capable of generating periodic radiation pulses, is located. For example, such a layer in stars can be localized in the region of the photosphere. In some cases, there may be several layers. It is possible to simulate the active zone of this layer by a two-level quantum system, and the populations of these two levels will be considered approximately equal. With very insignificant excess of the upper level population (the population inversion is positive in this case), in addition to spontaneous emission, the generation of induced radiation is possible, the threshold of which was found in [6-1, 6-2]. Given a sufficient thickness of the overlying layers due to the effects of scattering radiation emanating from the active zone of the two-level system in them, the emission spectrum of a completely black body can be formed [6-3].

In addition, let us assume the existence of strong convective flows from layers closer to the hot region of the source, which are capable of introducing a certain fraction of excited atoms of this active substance into the active zone. That is, such convective flows are able to increase the inversion in the active zone. One can be convinced that the intensity of the induced radiation of a given spectral line, described by a two-level system, can significantly exceed not only the spontaneous intensity of atoms of a given substance, but also the spontaneous emission of the entire spherical source as a whole.

Let us discuss the possibility of generating periodic pulses of induced radiation in a heated gas with a fraction of active particles in two states (two-level system). It is important that in some active zone of the radiation source, the number of active particles at two energy levels is approximately equal, and the population inversion is much less than the total number of particles.

Under these conditions, the intensity of the induced radiation is comparable to the intensity of spontaneous emission. It is assumed that in the active zone, which

is transparent to radiation at the frequency of the energy transition, active particles with the excited state from the underlying dense layers enter due to convection. That is, in the medium there is a source of inverted (excited) active particles.

Let us consider the conditions for the approximate equality of the number of states at two working levels [6-4, 6-5], that is, if the threshold is exceeded (5.8). In addition, we assume that the system is close to the threshold (5.7). Equations (5.1) and (5.2) can be written in the following form

$$\partial n_2 / \partial \tau = -g \cdot n_2 - \mu \cdot N_k + \frac{\nu}{w_{21}} n_1 \quad (6.1)$$

$$\partial n_1 / \partial \tau = +g \cdot n_2 + \mu \cdot N_k - \frac{\nu}{w_{21}} n_1, \quad (6.2)$$

or otherwise

$$\partial \mu / \partial \tau = [(\nu - u_{21}) / w_{21}] \cdot n_1 - 2\mu \cdot N_k, \quad (6.3)$$

where ν is the effective frequency of collisions with fast electrons of the medium, which provides a transition from the lower energy level of the quantum system to the upper energy level. In this case, $\nu \approx u_{21}$, $T / t = X / x = w_{21} \cdot \mu_0$ and we can introduce the value $[(\nu - u_{21}) / w_{21}] n_1 = \mu_0^2 I_0$.

The equations of system (5.6) can be represented in the form

$$\partial M / \partial T = I_0 - 2M \cdot N_c, \quad (6.4)$$

$$\partial N_{inc} / \partial T = N_0 / 2 - \theta \cdot N_{inc}, \quad (6.5)$$

$$\partial N_c / \partial T = M \cdot N_c - \theta \cdot N_c. \quad (6.6)$$

Let us also assume that the thresholds (5.7) and (5.8) $\mu_{TH2} \approx \mu_{TH1} = 2\delta / w_{21}$ are close to each other. In this case, damped relaxation oscillations will bring the system to the stationary state $N_{cst} \approx -1 + I_0 / 2\theta$ and $M_{st} = \theta$. The radiation flux density in this case reaches the value $\theta \cdot N_{cst} + \theta \cdot N_{incst} = (I_0 - 2\theta) / 2 + N_0 / 2 \geq N_0 / 2$.

However, in the presence of an external source of inversion which is proportional to K , its value will be greater than the stationary value. When the equilibrium conditions for the processes of collisional excitation by free electrons of the main gas of active atoms and their radiative relaxation are satisfied ($I_0 = 0$), then

$$\partial M / \partial T = K \cdot M - 2M \cdot N_c + I_0, \quad (6.7)$$

One of the possible mechanisms for supporting inversion in a system may be its transfer from other internal layers of the radiation source

$$-V \cdot \partial M / \partial X \approx V \frac{M}{L} = KM > 0, \quad (6.8)$$

where $-V \cdot \nabla M \approx V \cdot M \cdot L^{-1} = V \cdot M / (l \cdot w_{21} \cdot \mu_0)$ is responsible for convective transfer of inversion from the denser underlying source layers. Equations (6.5) –

(6.7) are similar to Statz-DeMars equations [6-6], which describe relaxation oscillations with the establishment of a stationary state with a negative first term on the right-hand side of (6.7).

It is the inversion flux into the region of the active medium that can lead to a change in the nature of oscillations: from relaxation to periodic oscillations. In this case, the occurrence of periodic pulses of induced radiation in the selected normalization against the background of the average radiation flux can be observed

$$\theta \cdot N_{cst} + \theta \cdot N_{incst} = (\Gamma \theta + N_0) / 2, \quad (6.9)$$

When $I_0 > 0$ the collisional excitation is large, the induced radiation is monotonic in nature; however, in the case $I_0 < 0$ there is no induced emission. That is, the generation of periodic pulses reveals itself only under conditions of equilibrium of the processes of collisional excitation by free electrons of the main gas of active atoms and their radiative relaxation, mainly due to spontaneous emission $I_0 = 0$. In this case, if there is a pulse, the integrated radiation intensity can increase several times.

It should be noted that the authors of [6-4, 6-5] observed the phenomenon only under the condition of equilibrium $I_0 = 0$ and also in the case of proximity of the generation thresholds (5.7) and (5.8) (see annex VI).

Note that the system of equations (6.6) and (6.7) for large values of the line width γ_{12} and conditions $K = I_0 = 0$ can be obtained from the system of equations (4.7) – (4.10) of the semiclassical model (see Section 4), and the relation $w_{21} = \Omega_0^2 / \mu_0 \cdot \gamma_{12}$ is valid, whence it follows $T = \Omega_0^2 t / \gamma_{12}$.

You can make of one-parameter system of equations [6-6]:

$$\frac{\partial M_2}{\partial \tau} = K_2 \cdot M_2 - 2M_2 \cdot N_2, \quad (6.10)$$

$$\frac{\partial N_2}{\partial \tau} = M_2 \cdot N_2 - 2N_2, \quad (6.11)$$

where $\tau = \delta \cdot t$, $M_2 = \frac{\mu}{\mu_0} \frac{\Omega_0^2}{\delta \cdot \gamma_{12}}$, $N_2 = \frac{\langle E^2 \rangle}{4\pi\hbar\omega} \frac{\Omega_0^2}{\delta \cdot \gamma_{12}}$, $\Omega_0 = |d_{ab}| \cdot [4\pi\omega \cdot \mu_0 / \hbar]^{1/2}$,

γ_{12} – is the spectral line width, $K_2 = K \cdot w_{21} \cdot \mu_0 / \delta = 2K \cdot (\Omega_0^2 / \delta \gamma_{12}) = 2K / \theta$.

These equations describe the generation of induced radiation with a number of quanta per unit volume $N_c = N_k^{(coh)}$, which is periodic pulses with some constant component. In addition, there is a spontaneous incoherent component of the same source, the relative number of quanta of which is equal to $N_{inc} = N_k^{(incoh)} / \mu_0$, described, for example, by equation (5.5). A significant part of the radiation of a quantum source is induced radiation, which is almost monochromatic.

However, if the quantum source is surrounded by a sufficiently extended atmosphere, as it is noted in [5–3] due to multiple scattering the radiation characteristics will approach the radiation characteristics of an absolute black body. The total relative number of radiation quanta per unit volume is equal to $N = N_{inc} + N_c$, and in spontaneous emission not only the radiation of a quantum source, but all types of radiation of a similar nature should be taken into account. It is important to note that despite the extremely small population inversion, the intensity of the induced radiation may greatly exceed the spontaneous intensity.

System (6.10) – (6.11) has a singular point $(2, K_2 / 2)$ and a stationary solution $M_2 = 2, N_2 = K_2 / 2$. In case of small deviations M_2, N_2 from the singular point, the system can be linearized and then the equation for the phase trajectory is: $K_2(M_2 - 2)^2 + 8(N_2 - K_2 / 2)^2 = Const$. The phase trajectory turns out to be a closed line, which indicates the presence of stable periodic solutions.

Figures 6.1–6.3 show M_2, N_2 time dependences and phase trajectories for different cases of removal from the critical point at $K_2 = 20$.

The initial values for M_2 were set constant $M_2(0) = 2$; the choice of the curve was controlled by removing the initial value $N_2(0)$ from its critical value of 10.

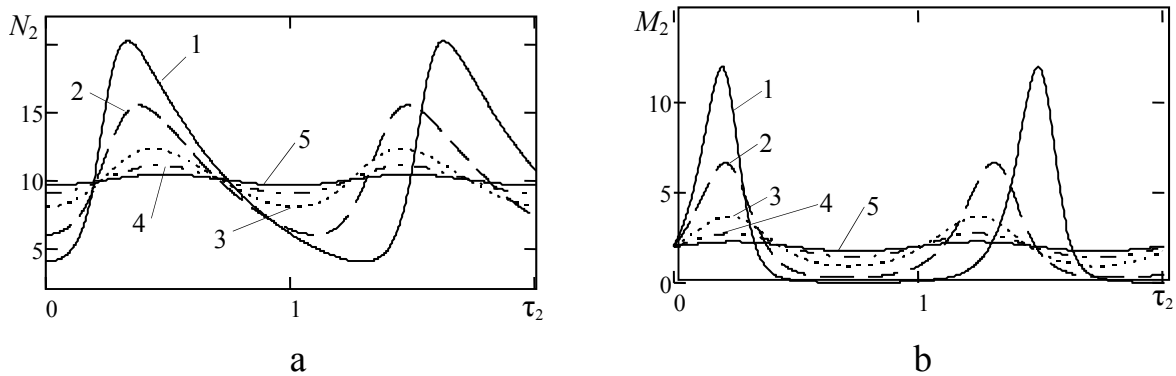


Fig. 6.1. a). The behavior of the relative magnitude of the density of quanta N_2 as a function of time b) The behavior of the relative density of the inversion of populations M_2 as a function of time τ_2 , at 1 - $N_2(0) = 4$, 2 - $N_2(0) = 6$, 3 - $N_2(0) = 8$, 4 - $N_2(0) = 9$, 5 - $N_2(0) = 9.6$

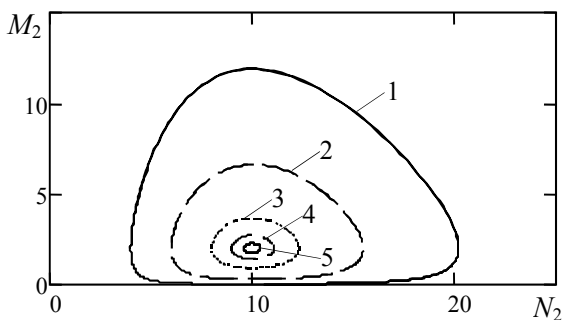


Fig. 6.2. Phase diagrams (M_2, N_2) for the system of equations (6.10) – (6.11), when choosing the initial conditions in the form for 1 - $N_2(0) = 4$, 2 - $N_2(0) = 6$, 3 - $N_2(0) = 8$, 4 - $N_2(0) = 9$, 5 - $N_2(0) = 9.6$

For purposes of clarity, Table 6.1. presents the minimum number of quanta $N_{2\min}$ (constant component in the induced radiation), the maximum number of quanta $N_{2\max}$, the average value of the number of quanta N_{2av} , the amplitude of oscillations $N_{2\max} - N_{2\min}$, and the period of oscillations T_2 . It should be noted that the average value of the relative number of quanta N_{2av} depends only on the choice of the position of the center of the diagram – its critical value $K_2 / 2$.

Table 6.1

Calculation	$N_{2\min}$	$N_{2\max}$	N_{2av}	$N_{2\max} - N_{2\min}$	T_2
1	4	20,188	10	16,188	1,289
2	6	15,474	10	9,474	1,0964
3	8	12,308	10	4,308	1,0147
4	9	11,071	10	2,071	0,9984
5	9,635	10,374	10	0,739	0,9941

The graph of the change in the number of quanta N_2 has the form of a sinusoid for phase trajectories near the critical point (calculation 4 and 5). For phase trajectories far from the critical point (calculations 1 and 2), the change graph N_2 takes the form of a saw: a sharp increase and a slow decrease. A similar behavior is characteristic of the luminosity of Cepheid stars, where thermonuclear fusion has reached its limit element, i.e. iron: significant sawtooth oscillations of the luminosity of stars, Cepheus deltas and small sinusoidal oscillations of the North Star.

The solutions (6.10) – (6.11) can be given in variables adopted in astrophysics, for example, the relation between the apparent magnitude m and luminosity L (using the known distance to the star in parsec d); $m = M_{lsun} + 5 \lg(d / 10) - 2.5 \lg(L)$ is the ratio between the absolute magnitude M_l (visible magnitude from a distance of 10 parsecs) and the visible magnitude m , i.e. $M_l = m - 5 \lg(d / 10)$.

The solutions of equations (6.10) – (6.11) are presented in Fig. 6.3 and 6.4. Here the change in the magnitude of the star of the Cepheus delta [6-8] and the Polar star [6-9] is depicted (for details see annex VI). The ordinate shows the values of the apparent magnitude; the abscissa shows time in fractions of the period of change in the brightness of the star.

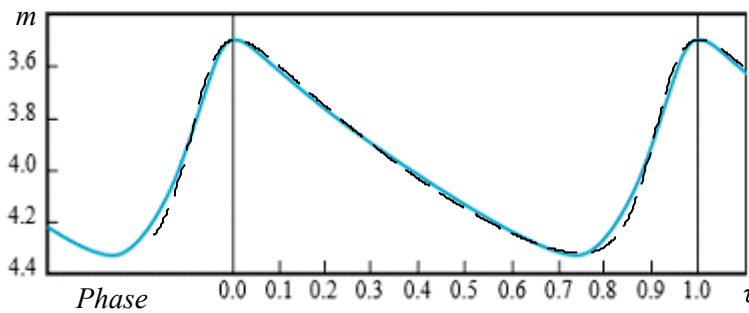


Figure 6.3. Change in the stellar magnitude of the star of the Cepheus delta with time. (solid curve – obtained in the 1930s by N.F. Florey using a visual photometer) see, for example, [6-10] and the solution of the equations of system (6.10) - (6.11) in the same variables, when selecting the level of spontaneous emission and scale (dotted line)

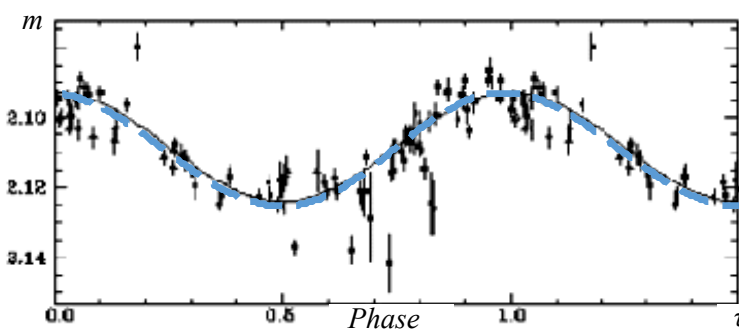


Fig. 6.4. The time change⁶ in the magnitude of the North Star (solid curve) and the solution of the equations of the system (6.10), (6.11) in the same variables when choosing the level of spontaneous emission and scales (dotted line).

References to section 6

6-1. Zagorodny A. G., Kuklin V. M. To realization conditions of maser radiation // High-power pulsed electrophysics. International conference XIV Khariton's topical scientific readings. Digest of technical papers – Саров: ФГУП «РФЯЦ-ВНИИЭФ», 2013. – С. 38–43.

6-2. Kirichok A. V., Kuklin V. M., Mischin A. V., Pryjmak A. V., Zagorodny A. G. On the formation of pulses of coherent radiation in weakly inverted media/ VANT, 2013, N. 4 (86). – series “Plasma Electronics and New Methods of Acceleration” issue 8. – P. 267–271. 6–3. P. B. Pikelner. Atmospheres of stars <http://www.astronet.ru/db/msg/1179555>

6-4. Kirichok A. V., Kuklin V. M., Zagorodny A. G. On the nature of sources of pulsating radiation in weakly inverted media / Problems of Atomic Science and Technology, 2015. – N 4 – P. 9–11.

6-5. Kirichok A. V., Kuklin V. M., Zagorodny A. G. On the nature of periodically pulsating radiation sources / arXiv preprint arXiv / 1610.04628v1 [quant-ph] – 2016.

⁶ The trivial solution of system (6.10) – (6.11) $M_2 = 2, N_2 = K_2 / 2$ is at the same time the so-called special solution (see Steklov V., Butz V.) in the vicinity of which even small perturbations can lead to a jump from one phase trajectory to another. Apparently, the changes in the luminosity period of the Polar Star are due to this unstable state near the point $M_2 = 2, N_2 = K_2 / 2$.

6-6. Stutz C. L., DeMars G. Quantum Electronics. N.Y.: Columbia Univ. Press, 1960. – 530 p.

6-7. Kostenko V. V., Kuklin V. M., Poklonskiy E. V. On the periodic change of the luminosity of the cosmic sources with an active medium / East Eur. J. Phys. **2**. 48-56 (2020) DOI:10.26565/2312-4334-2020-2-03

6-8. Jim Kaler, Stars and stars of the week. University of Illinois. <http://stars.astro.illinois.edu/sow/deltacep.html>

6-9. Jim Kaler, Stars and stars of the week. University of Illinois. <http://stars.astro.illinois.edu/sow/polaris.html>

6.10. Samus, N. N. & Durlevich, O. V. (April 2011), GCVS – General Catalog of Variable Stars, Institute of Astronomy of Russian Academy of Sciences and Sternberg State Astronomical Institute of the Moscow State University <http://heasarc.gsfc.nasa.gov/W3Browse/all/gcvs.html>.

SECTION 7.

TURBULENT-WAVE INSTABILITY

Turbulent-wave instability is the interaction of a slow (in comparison with the characteristic time of turbulent pulsations) wave of finite amplitude $\psi = A \exp [i(Kx - \Omega t)]$ with a turbulent medium, the pulsations of which are maintained by a constantly acting source in the absence of a wave near the threshold for the development of instability (i.e., the process of growth of turbulent energy). In order to describe such a phenomenon in various physical realizations, there is a universal system of equations presented in [7-1, 7-2].

Studies of the turbulent-wave interaction in a stratified fluid with a shear flow located near the stability boundary (that is, at $Ri_0 \geq Ri_{cr}$, where $Ri_{cr} \equiv N^2/U_0'^2$ is the critical Richardson number close to 1/4, $N^2 = g \cdot \rho_0^{-1} \rho_0'(z)$ is the Brunt-Väisälä frequency (buoyancy frequency), $\vec{U} = (U_0(z), 0, 0)$ is the rate of fluid flow) in the presence of an internal wave were undertaken in a number of works [7-3, 7-4].

As shown in these works, an internal wave can change the values of the velocity shift and lead to the development of small-scale turbulence, which, due to positive feedback with the internal wave, leads to the so-called turbulent-wave instability. A particular problem in describing the interaction of an external wave and its initiated turbulence is the calculation of the coefficients of this interaction.

One of the main methods for describing turbulence is the method of statistical moments, based on the representation of hydrodynamic quantities as a sum of averaged and random components.

After substituting these quantities into hydrodynamic equations and then averaging over the ensemble of realizations, an infinite system of equations for statistical moments is obtained, where the main task is to close this system.

For developed turbulence, closure schemes are usually used, according to which turbulent flows (second-order statistical moments) are assumed to be proportional to the gradients of the corresponding averaged quantities (for example, velocity U_i), in particular, the turbulent momentum flow in uniform isotropic turbulence is assumed to be

$$-(u_i u_j) = \nu_T \left(\frac{\partial U_i}{\partial x_j} + \frac{\partial U_j}{\partial x_i} \right) - \frac{2}{3} \delta_{ij} E, \quad (7.1)$$

where E is the energy of turbulence and u_i is the speed of turbulent pulsations, ν_T is the coefficient of turbulent viscosity, for the determination of which additional physical considerations are required.

Earlier, A. N. Kolmogorov suggested that molecular transfer is negligible compared with turbulent one; he determined the form $\nu_T \sim L\sqrt{E}$, where the scale of turbulence L in the general case is a flow functional (turbulence energy), that is, ν_T depends only on the kinetic energy E and the characteristic scale of turbulence L . For turbulence, near the threshold of instability, these assumptions (or at least the second one) may not be valid. A system of equations relating the amplitude of the internal wave and the energy of turbulence was obtained in [7-3, 7-4], where the coupling coefficients were calculated on the basis of the Kolmogorov hypothesis, which led to the solutions that are not physically interpreted in all areas of variation of the studied variables. Therefore, it made sense to formulate another hypothesis (see [7-2]), *on the basis of which turbulent flows can be found: near the instability threshold, between the pulsations of individual quantities (density, pressure, velocity, etc.) the ratio are kept the same as at the initial stage of the process, which generates and enhances turbulence.*

That is, the correlations between the values are imposed by processes that have generated turbulence and intensify it. Let us note that such an approach is constructive for other problems, in particular, for a more correct description of transport in plasma-like media and it was used in a number of works. The application of the proposed closure model when allocating zero and first harmonics of its space-time distribution in the energy density of turbulence E is as it follows $E = W_0 + W_1 \exp[i(K_0 x - \Omega_0 t)]$; let us obtain the following system of nonlinear equations (see annex VII):

$$\begin{aligned} \frac{\partial W_0}{\partial \tau} &= -\bar{\varepsilon}_0 W_0 + \alpha \operatorname{Im}(AW_1^*) - \lambda \operatorname{Re}(AW_1^*) + \bar{q} \\ \frac{\partial W_1}{\partial \tau} &= -\bar{\varepsilon}_0 W_1 + i\alpha AW_0 + \lambda AW_0, \\ \frac{\partial A}{\partial \tau} &= -\mu W_1, \end{aligned} \quad (7.2)$$

where A , Ω , K are the amplitude, frequency, and wave number of the internal wave, W_1 is the variable component (having a spatio-temporal dependence

proportional to $\exp\{i(Kx - \Omega t)\}$, and W_0 is the average value of the energy of small-scale pulsations, $\bar{\varepsilon}_0 \propto (Ri_0 - Ri_{cr})$ is the value which characterizes the deviation from the turbulence growth threshold and \bar{q} determines the effect on system of external fluctuations, α , λ , μ are the parameters that determine the relation between the shear flow and the amplitude of the internal wave.

One can find a similar mechanism for the interaction of a wave with turbulence in the case of nonisothermal plasma in the presence of a low-density electron beam. Let the system be near the threshold of instability, which could lead to an increase in Langmuir oscillations. Nevertheless, the level of turbulent pulsations, in the absence of a wave near the instability threshold, is quite significant.

A mechanism that can lead to the development of such instability and enhance Langmuir turbulence can be an ion-sound wave of finite amplitude, with the frequency and wave number of the ion-sound wave being much less than the corresponding values of the Langmuir oscillations.

It turns out (see [7-1]) that in this case as well, the system of equations describing the interaction of the ion-sound wave and the energy density of the wave turbulence energy can be written in the same form on the corresponding space and time scales (7.2). Thus, we can assume that the system of equations (7.2) is universal, at least for the description of the interaction of the wave and turbulence in a medium near the stability threshold (see annex VII).

The analysis of the equations showed that there is a range of parameter values α , and β when there is a nonexponential simultaneous increase of the wave amplitude and turbulence energy caused by their nonlinear interaction due to a constantly acting source of turbulent pulsation energy. The mutual amplification of the wave and turbulence takes place at finite times of the order of $\tau_{ampl} \sim 10|\bar{\varepsilon}_0|^{-1}$. As a result of the development of instability, the wave provokes the appearance of spatially distinguished structures – regions of growth of turbulent pulsations. The initial value is $W_0(\tau=0) = q/\varepsilon_0$.

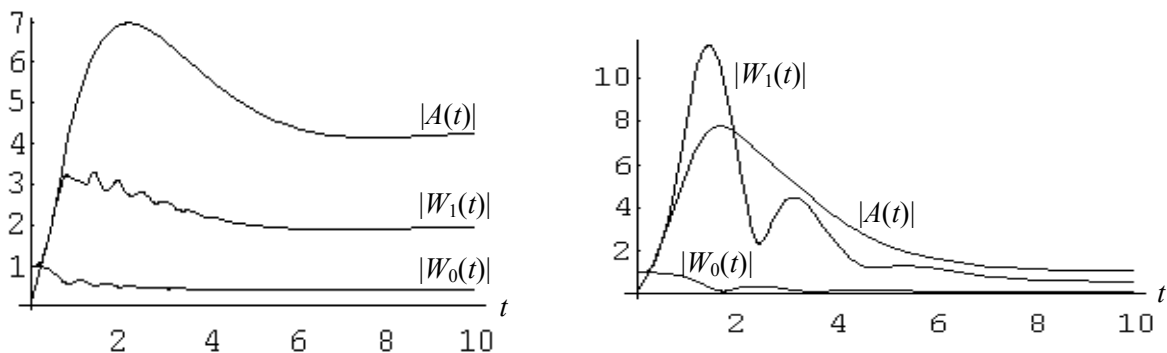


Fig. 7.1. The results of the solution of the system of equations (7.2) for the case $\bar{\varepsilon}_0 = \bar{q} = 1$, a) $\alpha = 5$, $\lambda = 0.1$, $\mu = 1$; b) $\alpha = 5$, $\lambda = 0.1$, $\mu = 0.1$

On the other hand, the presence of a turbulent medium near the instability threshold leads to an increase in the wave amplitude, which will make it possible to use this phenomenon to diagnose critical zones where catastrophic processes are very likely. Since the conclusion of turbulent-wave instability presented in annex VII is based on the equations of classical physics, it can be expected that the application of this approach [7-2] will allow describing a lot of phenomena.⁷

It is important to note that the development of the instability process occurs mainly due to the energy stored in turbulent pulsations, which is anomalously high near the instability threshold (similar to how it occurs during critical opalescence). Turbulence, in its turn, is directly related to temperature. The excitation of instability, which is already a macroscopic and large-scale perturbation, and the maintenance of this perturbation due to the energy of a microscopic turbulent state (which is perceived as a heated region with a large level of fluctuations), can sometimes be presented as a direct transfer of fluctuation (or thermal) energy to macroscopic movement.

References to section 7

7-1. Kirichok A. V., Korsunsky S. V., Kuklin V. M. An example of turbulent-wave instability in plasma // Reports of the Academy of Sciences of Ukraine, 1994. – № 11 – P. 85–89 (in Russian).

7-2. Kirichok A. V., Kuklin V. M., Panchenko I. P., Moiseev S. S. Wave–Turbulence Instability in Nonequilibrium Hydrodynamics Systems // Physics and Chemistry of the Earth. Part A. 1999. – № 6. – P. 539–541.

7-3. Chimonas G. The stability of a coupled wave–turbulence system in a parallel shear flow. – Bound.–Layer Meteor., 1972. – V. 2. – P. 444–452.

7-4. Fua D., Chimonas G., Einaudi F., Zeman O. An analysis of wave–turbulence interaction. – J. Atmos. Sci., 1982. – V. 39. – N. 11. – P. 2450–2463.

⁷ The energy of the synchronous growth of the wave amplitude and local disturbance of turbulence is drawn from the total energy of turbulence. Therefore, after the passage of the wave and the local growth of turbulent pulsations, the level of turbulence decreases. Small perturbations can only diagnose the nature of the distribution of the turbulent zone. When the initial amplitude of the wave is exceeded, it is capable of transforming from a diagnostic wave into an initiating one, provoking a noticeable emission of turbulent energy. This phenomenon attracted the interest of the military, who in the 1980s perhaps not wishing to cause disaster tested seismological weapons (geophysical bombs) near seismically active zones.

CHAPTER 3. Spatial and temporary dynamics of some types of instability

The spatiotemporal dynamics of the development of certain types of interaction of waves and disturbances is considered; however, their nonlinearity was neglected. It is important to note that the nonlinearity of waves usually does not affect the nature of the spatiotemporal dynamics, which allows us to restrict ourselves to linear equations for waves, taking into account only their connection. It is shown that the transition to a moving reference frame of reference makes it easier to describe the processes of generation and amplification of oscillations, and also simplifies the determination of the conditions for the development of convective and absolute instability.

SECTION 8.

SPATIAL AND TEMPORARY DYNAMICS OF THREE-WAVE INSTABILITY

Let us discuss the development in space and time of the decay instability, which was investigated in Section 3. Generally speaking, in the one-dimensional case, the interaction of three waves satisfies the conditions $\omega_0 \approx \omega_1 + \omega_2$ and $k_0 \approx k_1 + k_2$, and the development of the process can be understood by considering the energy conservation law $\Delta E_0 \approx \Delta E_1 + \Delta E_2$, where there is the change in the energy of the i th wave ΔE_i . Imagining $\Delta E_i = \hbar \omega_i \cdot \Delta N_i$ where ΔN_i is the change in the number of quanta of the i -th wave, we again come⁸ to the ratio $\omega_0 \approx \omega_1 + \omega_2$, and this necessarily leads to $\Delta N_0 = \Delta N_1 = \Delta N_2$.

In the absence of energy absorption, wave decay ω_0 is periodically replaced by wave synthesis $\omega_1 + \omega_2$, however, when energy absorption in the system is taken into account, such a frequency of energy exchange is violated. Below we are going to consider the decay process of a high-frequency wave of large amplitude with a frequency ω_0 and a wave number k_0 under the conditions of absorption of one of the excited waves.

If waves with a frequency ω_i and wavenumbers k_i are eigenwaves of a medium, under certain conditions it is possible to decay the main wave of large amplitude, which obeys the conditions of spatial synchronism $k_0 = k_1 + k_2$, then an approximate expression is valid for frequencies $\omega_0 \approx \omega_1 + \omega_2$. Subject to the condition of temporary synchronism $\omega_0 = \omega_1 + \omega_2$, the relation $k_0 \approx k_1 + k_2$ can also approximately written for wave vectors. In the first case, this refers to the generation of oscillations (ω_i, k_i) , in the second one their amplification

⁸ Interactions of this type were first obtained in [8-1].

is discussed. Indeed, in the first case of spatial synchronism, the detuning $\Delta\omega = \omega_0 - \omega_1 - \omega_2$ can have an imaginary part, which corresponds to an increase (or decrease) in the amplitudes of coupled waves $\propto \exp\{\text{Im } \Delta\omega \cdot t\}$, where $\text{Im } \Delta\omega$ is the (temporal) increment (or decrement) of the instability. That is, this corresponds to the process of generating two waves. In the second case, the wave frequencies can be written as $k_0 - k_1 - k_2 = \Delta k$, only the amplitude grows along the coordinates $\propto \exp\{\text{Im } \Delta k \cdot x\}$, where $\text{Im } \Delta k$ is the spatial increment (or decrement) of the process.

However, this representation is simplified. In fact, these processes should be considered differently in their spatio-temporal dynamics. Generally speaking, wave instabilities (ω_0, k_0) , are represented as the excitation of a spectrum of waves that obey only approximate space-time synchronism

$$k_0 - k_1 - k_2 - \Delta k = 0, \quad \omega_0 - \omega_1 - \omega_2 - \Delta\omega = 0, \quad (8.1)$$

where $(\Delta\omega, \Delta k)$; they respond slowly varying in time and in space envelope.

In other words, it is useful to use equations for the two waves connected by conditions (8.1)

$$\begin{aligned} \frac{\partial A_1}{\partial t} + v_1 \frac{\partial A_1}{\partial x} + \delta_1 A_1 &= \alpha_1 A_2 \\ \frac{\partial A_2}{\partial t} + v_2 \frac{\partial A_2}{\partial x} + \delta_2 A_2 &= \alpha_2 A_1 \end{aligned} \quad (8.2)$$

where A_i ; v_i ; δ_i are the amplitude, group velocity and decrement of absorption of that i -th wave respectively, $\alpha_i = \alpha_i(A_0)$ are the coupling coefficients between the waves, which in this case are proportional to the amplitude of the main unstable wave A_0 .

In order to simplify the calculations, let us assume below that the fast wave ($v_1 > v_2$) practically does not decay ($\delta_1 \ll \delta_2$). Such a process was studied by numerical methods in the works by L. M. Gorbunov in 1972–1977, where the regime change was clearly shown when taking into account the attenuation of one of the waves. However, a constructive analytical representation of the nature of such an instability is possible.

It is convenient to carry out further consideration in a moving frame of reference V with respect to the laboratory frame of reference $(\xi = x - Vt, t)$, in this case $v_2 < V < v_1$. It turns out that in this range of speeds for a certain value of the velocity of the reference frame V , one can find a regime where the wave packet – the envelope of oscillations in this reference frame – will not be shifted as a whole in space. Such an instability is called **absolute**. Let us note that if in this reference frame the wave packet moves (drifts) in space – such an instability in this reference frame is called **convective**.

The question of the nature of instability has been actively studied by many authors, an extensive bibliography of their works is given in books [8-2, 8-3]. The most informative description of the nature of instability is given in the book [8-4]. Unfortunately, sometimes such descriptions are rather cumbersome, as the authors look into detail too much. Therefore, it is rational to switch to a moving coordinate system, the speed of which allows finding the absolute instability regime, which was done in [8-5].

It is clear that the same instability in one frame of reference can turn out to be absolute, and in all other systems it will be convective – drift one. For perturbations form $\sim \exp\{-i\Omega t + i\mathbf{K}\xi\}$ in a moving reference frame, the dispersion equation can be written as

$$D(\Omega, \mathbf{K}) = (\Omega - \mathbf{K}v_1 + \mathbf{K}V)(\Omega + \mathbf{K}V - \mathbf{K}v_2 + i\delta_2) + \alpha_1\alpha_2. \quad (8.3)$$

To determine the value Ω , corresponding to the development of absolute instability, it is necessary to solve the equations together (see annex VIII)

$$D(\Omega, \mathbf{K}) = 0, \quad (8.4)$$

$$\frac{\partial D(\Omega, \mathbf{K})}{\partial \mathbf{K}} = 0, \quad (8.5)$$

that is, this condition for the development of instability, in which the group velocity of propagation of the envelope of the oscillations is zero

$$V_g = -\left[\frac{\partial D(\Omega, \mathbf{K})}{\partial \mathbf{K}}\right] / \left[\frac{\partial D(\Omega, \mathbf{K})}{\partial \Omega}\right] = 0. \quad (8.6)$$

Solving equations (8.4) and (8.5) together, we shall obtain получим

$$\Omega_{ab} = \frac{i\sqrt{\alpha_1\alpha_2}}{v_1 - v_2} \{2[(v_1 - V)(V - v_2)]^{1/2} - \theta(v_1 - V)\}, \quad (8.7)$$

$$\mathbf{K}_{ab} = \frac{\Omega_{ab}(2V - v_1 - v_2) - i\delta_2(v_1 - V)}{2(v_1 - V)(V - v_2)}, \quad (8.8)$$

where $\theta = \delta_2 / (\alpha_1\alpha_2)^{1/2} = \delta_2 / \gamma_0$ is the ratio of the absorption decrement in the absence of instability ($\gamma_0 = 0$) to the maximum possible increment of nondissipative instability ($\delta_2 = 0$).

The parameter θ as it will be seen from what follows, is decisive for the description of the nature of the so-called *dissipative instabilities* in media with a finite level of losses. Obviously, the absolute instability will develop only at high critical speeds критической V_{cr}

$$V > V_{cr} = (v_1 + 4\theta^2 v_2) / (1 + 4\theta^2), \quad (8.9)$$

The largest time increment as a function of speed is not difficult to determine from expression (8.7)

$$(\text{Im } \Omega_{ab})_{\max} = \sqrt{\alpha_1\alpha_2} \cdot \{(4 + \theta^2)^{1/2} - \theta\} / 2, \quad (8.10)$$

it is achieved at drift speed

$$V_T = \frac{v_1 + v_2}{2} + \theta \frac{v_1 - v_2}{2(4 + \theta^2)^{1/2}}. \quad (8.11)$$

It is important to note that in such a case $\text{Im}K_{ab}=0$. That is, the shape of a packet moving at a speed V_T will not change. For other values of the velocity of the reference system $V_{cr} < V < v_1$, growth at a fixed point in the wave amplitudes will be suppressed by the drift of the wave packet.

In other words, the envelope of the wave packet as a whole does not shift in space only in the reference frame, which moves with speed V_T .

At a lower or greater speed V of the reference system $v_1 < V_{cr} < V < v_2$ in the interval in the region near a fixed point ξ , one can also observe an increase in the amplitude of the packet. However, due to the demolition of this package as a whole, this growth will not be so significant.

As shown in [8–5], the maximum amplitude of the packet grows in time with a time increment (8.10) and quickly drifts with speed V_T to the boundaries of the system, after which a much smaller field amplitude is established. Nevertheless, it can be determined. The spatial increment of the process as a function of drift velocity will be equal to

$$\text{Im} K(V) = \text{Im} \Omega_{ab}(V) / V, \quad (8.12)$$

and it is achieved as a result of the balance of processes of growth and energy transfer. The greatest gain corresponds to speed

$$V_L = \frac{4v_1v_2 + \theta^2v_1^2}{(v_1 + v_2)^2 + \theta^2v_1^2} \left[\frac{v_1 + v_2}{2} + \theta v_1 \frac{v_1 - v_2}{2} (4v_1v_2 + \theta^2v_1^2)^{-1/2} \right]. \quad (8.13)$$

In the absence of energy loss ($\theta = 0$) for the optimal drift velocity and the largest spatial increment, we shall obtain the known expressions

$$V_L = \frac{2v_1v_2}{v_1 + v_2}, \quad \text{Im} K = \sqrt{\frac{\alpha_1\alpha_2}{v_1v_2}}. \quad (8.14)$$

If the instability is dissipative, and the absorption level is large enough $\theta^2 \frac{v_1}{v_2} \gg 1$, then for the optimal drift velocity and the greatest spatial increment in such a dissipative regime, estimates are

$$V_L \approx \frac{v_1}{1 + \theta^{-2}}, \quad \text{Im} K \approx \frac{\sqrt{\alpha_1\alpha_2}}{v_1\theta}. \quad (8.15)$$

Thus, over time $\tau_T \approx L/V_T$, the field amplitude increases at the system boundary by a factor of $\exp\{(\text{Im} \Omega_{ab})_{\max} \cdot \tau_T\}$. Then, over time $\tau_L \approx L/V_L > \tau_T$,

a stationary state is established with a significantly lower amplitude value $\exp\{\text{Im } \Omega_{ab} |_{V=V_L} \cdot \tau_L\}$.

References to section 8

8-1. Manley J. M., Rowe H. E., Some general properties of nonlinear elements, pt 1 – General energy relations, "Proc. IRE", 1956. – V. 44. – № 7. – P. 904.

8-2. Plasma Electrodynamics / A. I. Akhiezer et al. Edited by A. I. Akhiezer. M. – 1974. – 719 p.

8-3. Kuzelev M. V, Rukhadze A. A. Electrodynamics of dense electron beams in plasma. – M. : Nauka, 1990. – 336 p.

8-4. Fedorchenko A. M., Kotsarenko N. Ya. Absolute and convective instability in plasma and solids M. Nauka 1981. – 176 p.

8-5. Kuklin V. M. On the influence of dissipative processes on the space-time dynamics of instability in a plasma. // Radio engineering and electronics. 1987. – T. 32. – B. 2. – C. 432–434 (in Russian).

SECTION 9.

SPATIAL-TEMPORAL DYNAMICS OF A BEAM-PLASMA INSTABILITY

The development of kinetic instability. Let us consider the spatiotemporal dynamics of the processes discussed in previous chapters.

In Section 2, the particles of the electron beam whose mean and thermal velocities are equal to v_{0b}, v_{Tb} respectively, and the unperturbed density is n_{b0} , excited Langmuir oscillations in the plasma with frequency is ω_{pe} and wave number is $k \approx \omega_{pe} / v_{0b}$, that is, the electric field of which can be represented as $E(t, x) \cdot \exp\{-i\omega t + ikx\}$. Far from the excitation condition of such a (kinetic) beam instability ($\gamma_L > \delta_D$), which is accomplished when the condition is

$$v_{Tb} / v_{0b} > (n_{b0} / n_{p0})^{1/3}, \quad (9.1)$$

the induced emission of the beam electrons dominates and the equations for a slowly changing wave field $E(t, x)$ can be represented as (see, for example, [9-1, 9-2])

$$\frac{\partial E}{\partial t} + v_g \frac{\partial E}{\partial x} - \gamma_L E = 0, \quad (9.2)$$

where $v_g = \partial \omega / \partial k \approx 2v_{Tp}^2 / v_{0b}$ is the group velocity of Langmuir oscillations, $v_{Tp} = \sqrt{T_p / m}$ is the thermal velocity of plasma electrons,

$\gamma_L = \frac{2\pi^2 e^2 \omega}{m k^2} \partial f_b(v) / \partial v |_{v=\omega(k)/k}$ (see Section 2). Let us choose the boundary and initial conditions in the simplest form $E(t=0, x) = E(t, x=0) = E_{in}$, then the solution (9.2) will be

$$E(t, x) = E_{in} \cdot \{1 + \Theta(t - x/v_g) [\exp(\gamma_L \frac{x}{v_g} - \gamma_L t) - 1] \cdot \exp\{\gamma_L t\}. \quad (9.3)$$

Thus, for $t > x_0/v_g$, for $x < x_0$, where x_0 is a fixed point in the instability zone, the field amplitude $E(t, x)$ does not change, that is, a stationary state is established. It is easy to see that in space this amplitude increases from the boundary of the system according to the law $\propto \exp\{\gamma_L x/v_g\}$. Therefore, it is possible to define a quantity $\gamma_L/v_g = -\text{Im}k > 0$ as a spatial increment. In the region $x > x_0$, field growth occurs $\gamma_L = \text{Im} \omega > 0$ only in time in accordance with a time increment.

The development of hydrodynamic instability. In case of violation of condition (9.1), that is, with a slight spread of the beam electrons in velocities, the regime of hydrodynamic beam instability is accomplished. In this case, the perturbations in the beam are perturbations of the density and average-hydrodynamic velocity of the particles.

When waves or perturbations interact in a beam (stream) of charged particles (in most cases these are electrons) with waves in a resting plasma, it should be borne in mind that such two-wave hydrodynamic instability occur for waves of different signs of energy. Indeed, slow waves in the beam (whose phase velocity is less than the average flow velocity) are waves of negative energy, that is, an increase in their amplitude decreases the total energy of the particle beam (see, for example, [9-3, 9-4], also look (10.3)). It can be shown [9-2] that unstable perturbations in the beam will be perturbations of negative energy. The equation for the envelope of the oscillation field in the system “non-relativistic electron beam – plasma” in the case of quasihydrodynamic equations describing the effects of absorption of wave energy in the plasma takes the following form

$$\{(\frac{\partial}{\partial t} + v_0 \frac{\partial}{\partial x})^2 (\frac{\partial}{\partial t} + v_g \frac{\partial}{\partial x} + \delta) - i\gamma_0^3\} A_i = 0, \quad (9.4)$$

The corresponding dispersion equation for perturbations of the form $\sim \exp\{-i\Omega t + iK \xi\}$ in a reference frame that moves with speed V with respect to the laboratory reference frame can be represented as

$$D(\Omega, K) = (\Omega - Kv_0 + KV)^2 (\Omega + KV - Kv_g + i\delta) - \gamma_0^3 = 0, \quad (9.5)$$

where v_g and δ are the group velocity and damping decrement of the Langmuir plasma oscillations in the absence of an electron beam,

$\gamma_0^3 = \omega_{be} \omega_{pe}^2 / 2$ is the expression determining the increment in the absence of dissipation, $\omega_{pe} = \sqrt{4\pi e^2 n_{e0} / m_{e0}}$, $\omega_{be} = \sqrt{4\pi e^2 n_{b0} / m_{e0}}$ are the Langmuir plasma and electron beam frequencies, n_{e0} and n_{b0} are the unperturbed plasma and beam densities, and e, m_{e0} are the electron charge and rest mass

In order to determine the value Ω corresponding to the development of absolute instability in a moving frame of reference ($\xi = x - Vt, t$), in this case $v_g < V < v_0$, it is necessary to solve equations (9.5) and (9.5) consistently (see annex IX). Let us rewrite (9.5) in the form

$$D_1 = (y - z)^2 (y + \alpha_1 z + i\Gamma) + 1 = 0, \quad (9.6)$$

where the notation $y = \frac{K}{\gamma_0} [(v_0 - V)^2 (V - v_g)]^{1/3}$, $z = \frac{\Omega}{\gamma_0} \alpha_1^{-1/3}$, $\alpha_1 = \frac{v_0 - V}{V - v_g}$,

$\Gamma = \frac{\delta \cdot \alpha_1^{2/3}}{\gamma_0}$ is used. Solving equations $D_1 = 0$ and $\partial D_1 / \partial y = 0$ together, we find,

following [9-2], the corresponding instabilities of the value $z = z_2$ and $y = y_2$:

$$z_2 = -(1 + \alpha)^{-1} \cdot \{i\Gamma + \frac{3}{2^{5/2}} (1 - i\sqrt{3})\}, \quad (9.7)$$

$$y_2 = (1 + \alpha)^{-1} \cdot \{-i\Gamma - \frac{(1 - 2\alpha)(1 - i\sqrt{3})}{2^{5/2}}\}. \quad (9.8)$$

In the absence of absorption ($\Gamma = 0$), the envelope at a fixed point in the moving reference frame grows incrementally

$$\text{Im } \Omega = \frac{\sqrt{3}}{2} \gamma_0 \cdot f(\alpha), \quad (9.9)$$

where $f(\alpha) = 3\alpha^{1/3} / 2^{2/3} (1 + \alpha)$ provided that the greatest value of this function is $f(1/2) = 1$.

In the laboratory coordinate system, the envelope with the maximum increment $(\text{Im } \Omega)_{MAX} = \gamma_0 \sqrt{3} / 2$ moves with speed $V_T = \frac{2}{3} v_0 + v_g$. In addition, it is important to note that in this case $\text{Im } z_2 = 0$, that follows from the expression (9.6). That is, in the frame of reference that moves at a speed V_T relative to the laboratory frame, the wave packet as a whole does not shift.

In the absence of energy absorption in the plasma, the amplification of oscillations is most effective for the envelope, the drift velocity of which in the laboratory reference system is equal to $V = V_L = (3v_0 v_g) / (2v_g + v_0)$. The maximum spatial increment in this case is

$$(\text{Im } K)_{MAX} = (\sqrt{3} / 2) \gamma_0 (v_0^2 v_g)^{-1/3} \quad (9.10)$$

When absorption is taken into account, absolute instability is developed in a moving reference frame whose velocity V is in the range

$$v_g < V_{cr} < V < v_0 \tag{9.11}$$

where $V_{cr} = (2^{5/2}\theta \cdot v_0 + 3^{9/4}v_g) / (2^{5/2}\theta + 3^{9/4})$. With an increase in the absorption level $\theta = \delta / \gamma_0$, the velocity range (9.11) shifts to its upper boundary. That is, in the regimes of dissipative instability, the oscillation envelope moves with a speed slightly lower than the velocity of the beam particles. The maxima of the temporal increment $(\text{Im}\Omega)_{MAX}$ and spatial increment $(\text{Im}K)_{MAX}$ are determined respectively using the equations

$$2\alpha + \frac{2^{5/3}}{3^{1/2}}\theta\alpha^{2/3} - 1 = 0, \quad 2\alpha \frac{v_g}{v_0} + \frac{2^{5/3}}{3^{1/2}}\theta\alpha^{2/3} - 1 = 0. \tag{9.12}$$

The maximum achievable amplification of the oscillations along the length L neglecting the effects of reflection of the order $\exp\{(\text{Im}K)_{MAX}L\}$, and the time of the transition process until the stationary distribution of the field amplitude in the system is established L/V_L .

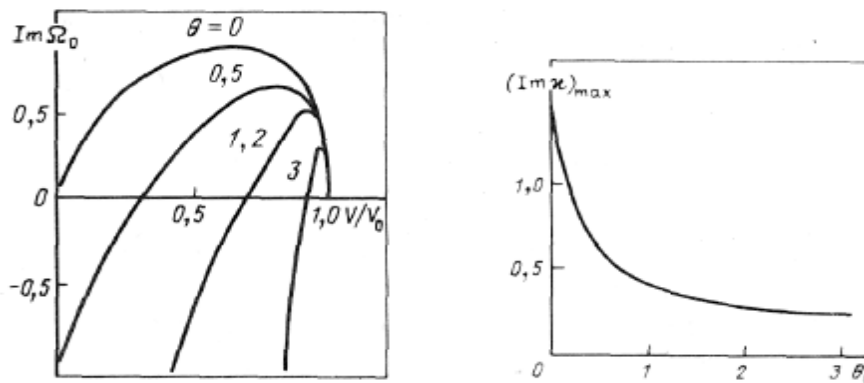


Fig. 9.1. Time increment as a function of drift velocity (right).
The dependence of the spatial increment of amplification of oscillations as a function of absorption level (left) [9-2]

References to section 9

9-1. Kuklin V. M. On the influence of dissipative processes on the space-time dynamics of instability in a plasma // Radio engineering and electronics. 1987. – V. 32. – B. 2. – P. 432–434 (in Russian).

9-2. Fundamentals of Plasma Electronics / A. N. Kondratenko, V. M. Kuklin. – Moscow : Energoatomizdat, 1988 – 320 p. (in Russian).

9-3. Kadomtsev B. B., Mikhailovsky A. B., Timofeev A. V. Waves of negative energy in dispersive media. JETP 1964. – V. 47. – AT 6. – P. 2266–2268 (in Russian).

9-4. Briggs R. Two-beam instability. Advances in Plasma Physics. V. 3–4 / A. Simon, W.B.Thompson NY 1969–1971.

CHAPTER 4. Dissipative instability

The nature of the development of dissipative instabilities of charged particle beams in a medium is considered. In this case, the damping decrement in the absence of a particle beam exceeds the maximum increment of the beam instability, which occurs in the medium without dissipation or other losses of RF energy. Under the conditions of the development of dissipative instabilities, one can find the regimes of the most efficient energy extraction from the beam particles and, accordingly, the largest energy flux from the system to the loss channels. It is shown that this effect of anomalous energy extraction from the beam is achieved due to the synchronism between particles captured by the field and the wave decelerating under conditions of such instability. It is noted that in the nonrelativistic case this effect will be preserved for multimode instability modes. It is noted that the inclusion of nonlinearity in the mechanisms of energy loss in a medium usually reduces the absorption decrements in the absence of a beam. Such a process can lead to a change in the nature of instability, translating it into a reactive mode. The case of taking into account dissipative processes directly in the beam of charged particles is also considered, which corresponds to the case of negative dissipation, in which the field growth can be significant.

SECTION 10.

DISSIPATIVE BEAM INSTABILITY

Abnormal beam energy loss. In real systems, there are several channels for the loss of oscillation energy resonantly excited by a monoenergetic beam of charged particles (the beam velocity is close to the phase velocity of the eigenwave of the system). The use of such monoenergetic beams in traditional and plasma electronics [10-1] is extremely effective. The nonlinear theory of the interaction of such beams with a plasma-like medium under the conditions of a relatively small level of dissipation and insignificant energy losses has been studied quite well [10-1 – 10-6]. Let us consider below systems with a high level of energy absorption.

The parameter Θ in this case corresponds to the ratio of $\delta_D(\omega, k)$, which is the decrement of oscillation damping in the absence of a nonequilibrium element (beam), to $\gamma(\omega, k)|_{\delta=0}$ which here is the maximum increment of nondissipative instability (i.e., in the absence of losses), that in this case is equal to $(\sqrt{3}/2)(\omega_b/\omega_0)^{2/3}\omega_0$; in this case ω_0 is the frequency of the waveguide eigenwave, and $\omega_b = (4\pi e^2 n_{b0}/m_{e0})^{1/2}$ is the plasma frequency electron beam

(here e, m_{e0}, n_{e0} are charge, electron mass and unperturbed beam density),
 $\omega_b \ll \omega_0$

$$\Theta = \delta_D |_{n_{b0}=0} / \gamma(\omega, k) |_{\delta=0}. \quad (10.1)$$

The modes where $\Theta > 1$ are of interest in this case; here the greatest energy flow from the system to the loss channel is achieved. It was in the analysis of such dissipative instability regimes that the phenomenon of anomalously large energy losses of beam particles was discovered [10–7]. $\Theta = (\delta_D / \omega_0)(\omega_0 / \omega_b)^{2/3}$ is a fair expression for Θ . The increment of dissipative instability at $\Theta > 1$ is equal to

$$\text{Im}\omega = \omega_b(\omega_0 / \delta_D)^{1/2} / \sqrt{2}. \quad (10.2)$$

We can make sure that the energy of perturbations in the system is negative, that is, the presence of perturbations leads to a decrease in the total energy of the medium – beam of charged particles system.

Let us consider disturbances in the medium and disturbances in the beam (i.e., disturbances in its density and velocity). We can see that at values $\Theta > 1$, the energy of perturbations in the beam exceeds the energy of perturbations in the medium through which its particles propagate. The total energy density of the system can be written as

$$W = W_0 + \delta W \approx \frac{1}{2} n_{b0} m_{e0} v_0^2 - \frac{1}{16} |E|^2 \Theta^{3/2}, \quad (10.3)$$

that is, the energy density is less than the energy density of the unperturbed system and continues to decrease with an increase of amplitude of the electric field of the perturbation $|E|$. It can be shown that, at large values Θ , the increment decreases by a factor of time $\sqrt{\Theta}$, and the field amplitude which is achieved is smaller by a factor Θ in comparison with the non-dissipative case.

The one-parameter system of nonlinear equations, which describe the relaxation of a monoenergetic beam of charged particles in a dissipative medium, can be represented in the form

$$\partial A / \partial \tau = -\Theta A + \int_{-1/2}^{1/2} d\xi_0 \cdot \exp\{-2\pi i \xi\} \quad (10.4)$$

$$2\pi \cdot d^2 \xi / d\tau^2 = -\text{Re}[A \cdot \exp\{2\pi i \xi\}] \quad (10.5)$$

where $\tau = t(2\gamma/3^{1/2})$, $A = eEk / m_e(2\gamma/3^{1/2})^2$, $2\pi\xi = kz - \omega \cdot t$, $\Theta = \delta |_{\gamma=0} / \gamma |_{\delta=0}$

In this case, the law of conservation of energy takes the form

$$\frac{d}{d\tau} \left(\frac{|A|^2}{2} + 2\pi \int_{-1/2}^{1/2} d\xi_0 \frac{d\xi}{d\tau} \right) = -\Theta \cdot |A|^2. \quad (10.6)$$

The limitation of the growth of the field amplitude, as in the case of reactive instability (see [10-5]), is due to the capture of part of the beam particles by the wave. Oscillations of the trapped particles of the beam (whose frequency increases with an increase of the field amplitude) lead to a phase mismatch between the wave and the beam, and the increase in the wave amplitude is replaced by the regime of energy exchange between the beam and the wave. The dependence of the amplitude $|A|$ versus time τ and increase in beam losses for values $\Theta = 0; 3$ are presented in Fig. 10.1.

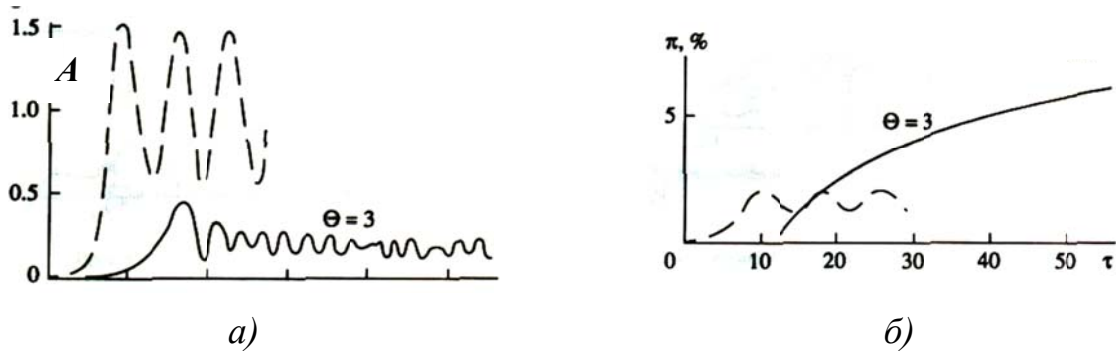


Fig. 10.1. Dependence of the amplitude of oscillations (a), the energy loss of the beam π (%) (b) on time. Dotted curves correspond to the case $\Theta = 0$

The energy loss of the beam in the dissipative mode is several times greater if to compare with the case of nondissipative (reactive) instability. By changing a single parameter Θ of the problem, it is possible to obtain [10-7, 10-8] the dependences of the maximum achievable amplitudes $|A|_{max}$, increment $\text{Im}\omega$, and relative rate of energy output π (%), shown in Fig. 10.2.

The phase velocity of a wave at large values in such a system decreases over time and the average velocity of the beam particles trapped by the wave also synchronously decreases. Considering the behavior of the beam particles [10-7, 10-9], we are convinced that the wave with trapped particles is a long-lived formation, which explains the effect of an anomalously large energy take-off from the beam (see Fig. 10.3).

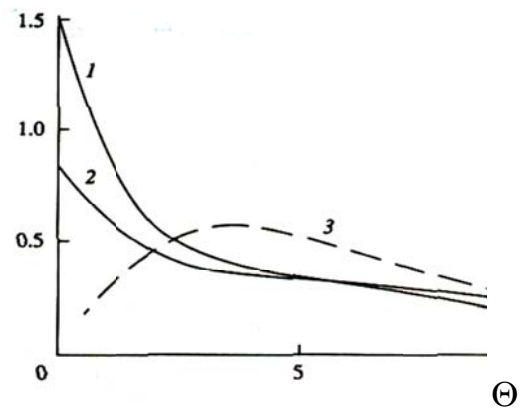


Fig. 10.2. The maximum amplitude of oscillations is $|A|_{max}$ (1), the increment $\partial \ln\{|A|/|A_0|\} / \partial t$ is (2) and the relative rate of beam energy loss is the rate of energy output from the system $\propto \Theta |A|^2$ - (3) as a function of the parameter Θ

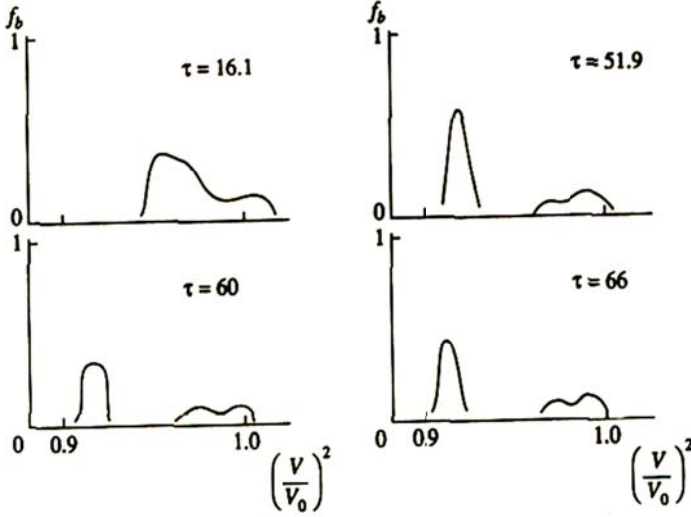


Fig. 10.3. The evolution of the velocity distribution function of particle particles $f_b(V)$

The results obtained are valid for a relatively narrow spectral width of the initial perturbation, when an instability mode close to single-mode is achieved.

Multiwave modes. In the multiwave mode, effective capture of particles into a potential oscillation well is possible only with sufficient synchronization of the spectrum of excited oscillations with a decelerating beam. With increasing absorption or removal of energy from the system, the average velocity of the beam particles and the group velocity of the excited wave packet synchronize both at the linear stage of instability (see Section 3) and in the nonlinear mode [10–10], which at least in the nonrelativistic case allows achieving a noticeable energy extraction from the beam.

The equations for the real amplitude and phase of the spectrum mode can be written as

$$\frac{1}{p} \frac{\partial A_{0p}}{\partial \tau} + \Theta \frac{A_{0p}}{p} = -R_{0p} \int_{-1/2}^{1/2} (1 + V_b / V_{b0}) \text{Sin}\{2\pi p \zeta - \varphi_{0p}\} \cdot d\zeta_0, \quad (10.7)$$

$$\frac{\partial \varphi_{0p}}{\partial \tau} + \Delta_p = R_{0p} \frac{p}{A_{0p}} \int_{-1/2}^{1/2} (1 + V / V_0) \text{Cos}\{2\pi p \zeta - \varphi_{0p}\} \cdot d\zeta_0. \quad (10.8)$$

The equations of motion of particles simulating a beam can be represented as

$$\frac{d\zeta}{d\tau} = V_b, \quad (10.9)$$

$$\frac{dV_b}{d\tau} = \frac{1}{2\pi} \left(\frac{1}{\gamma_b^3}\right) \sum_{p>0} \frac{|A_{op}|}{p} \text{Sin}\{2\pi p \zeta - \varphi_{op}\}, \quad (10.10)$$

moreover

$$V_b(0) = V_b|_{\tau=0} = 0, \quad \gamma_b = \gamma_b(\tau) = [1 - V_{0b}^2 (1 + \frac{V_b}{V_{0b}})^2 / c^2]^{-1/2},$$

$$C = \frac{1}{2\pi p_0} \left(\frac{\omega_{pe}}{\delta}\right) \frac{1}{\beta_{b0}}, \quad \beta_{b0} = (1 - \gamma_{b0}^{-2})^{1/2}.$$

The integral of the system of equations (10.7) – (10.10) is

$$\sum_{p>0} \frac{p^2 + p_0^2}{8\pi p^2} \left\{ \frac{|A_{0p}|^2}{p^2} - 2\Theta \cdot \int_0^\tau d\tau' \frac{|A_{0p}(\tau')|^2}{p^2} \right\} + 2\pi C^2 \gamma_{b0}^3 \left(\frac{\delta}{\omega_{pe}}\right) \cdot G \int_{-1/2}^{1/2} (\gamma_b - \gamma_{b0}) \cdot d\zeta_0 = \text{Const.} \quad (10.11)$$

It is easy to see that the integral (9.12) is the law of conservation of energy in the "relativistic electron beam – plasma" system. It can be shown (see Fig. 10.4) that at $\theta \approx 0.5$ a non-relativistic beam and the energy extraction rate are the highest, although this is not so pronounced as in the case of a single-mode regime [10-10].

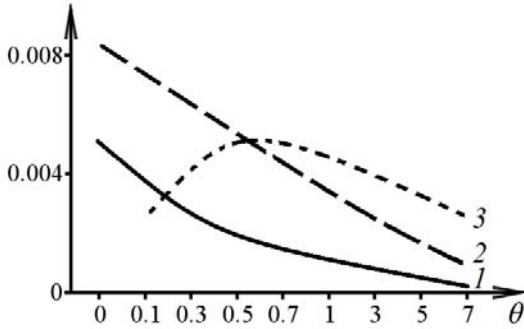


Fig. 10.4. Values as a function of absorption Θ for a weakly relativistic beam $\gamma_{b0} = 1.6$

(1 – $a_{0\max}$, 2 – divided by 4

$$\delta(\Theta) / \omega_{pe} \approx \frac{\delta}{\omega_{pe}} \cdot \left\{ 1 + \left(\frac{3}{2}\right)^{1/2} \Theta \right\}^{-1},$$

$$3 - \sum_{p>0} \left(\frac{p^2 + p_0^2}{8\pi p^2} \cdot 2\Theta \cdot \sum_0^\tau \frac{A_{0p}^2}{p^2} \partial\tau \right)$$

multiplied by the 30)

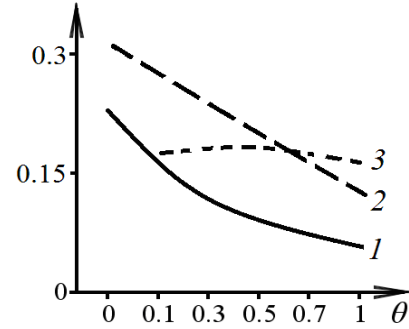


Fig. 10.5. Values as a function of absorption Θ for a strongly relativistic beam $\gamma_{b0} = 10$

(1 – $a_{0\max}$, 2 – magnitude multiplied by 10

$$\delta(\Theta) / \omega_{pe} \approx \frac{\delta}{\omega_{pe}} \cdot \left\{ 1 + \left(\frac{3}{2}\right)^{1/2} \Theta \right\}^{-1},$$

$$3 - \text{divided by 3} \\ \sum_{p>0} \left(\frac{p^2 + p_0^2}{8\pi p^2} \cdot 2\Theta \cdot \sum_0^\tau \frac{A_{0p}^2}{p^2} \partial\tau \right)$$

Spectrum characteristics. It is possible to determine the characteristics of the spectrum in the interval from τ_{MIN} (when the first maximum of the energy density of the oscillation spectrum of the beam is reached) to $\tau_{MAX} = 50-60$. Fig. 10.6 and fig. 10.7 present the average change in frequency with respect to the frequency of the main wave

$$\langle \Delta \omega_{pe} \rangle = \left\langle \frac{\delta}{\omega_{pe}} \frac{d\varphi_0}{d\tau} \right\rangle = \frac{1}{\tau_{MAX} - \tau_{MIN}} \int_{\tau_{MIN}}^{\tau_{MAX}} d\tau \cdot \left\{ \frac{\delta}{\omega_{pe}} \frac{d\varphi_0}{d\tau} \right\} \quad (10.12)$$

and the relative standard deviation of the frequency value from its average value (spectrum width)

$$[\langle (\Delta \omega_{pe} - \langle \Delta \omega_{pe} \rangle)^2 \rangle]^{1/2} = \left[\frac{1}{\tau_{MAX} - \tau_{MIN}} \int_{\tau_{MIN}}^{\tau_{MAX}} d\tau \cdot \left\{ \left(\frac{\delta}{\omega_{pe}} \frac{d\varphi_0}{d\tau} \right) - \left\langle \frac{\delta}{\omega_{pe}} \frac{d\varphi_0}{d\tau} \right\rangle \right\}^2 \right]^{1/2} \quad (10.13)$$

for different values of the absorption level in cases of weakly relativistic and relativistic electron beams

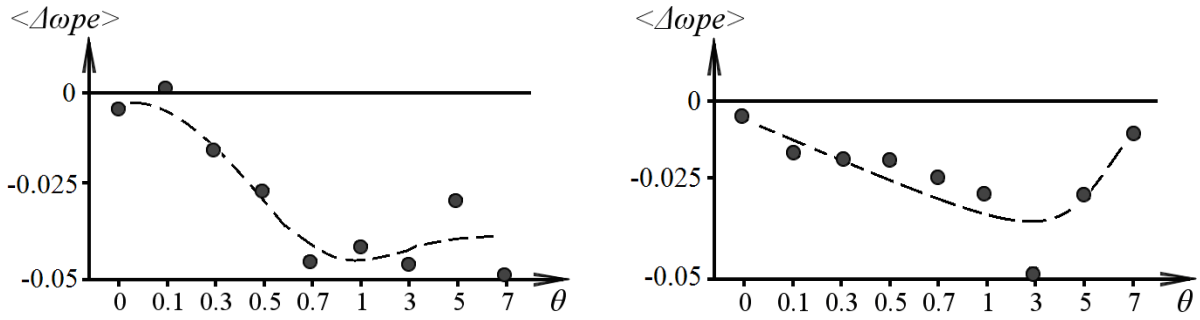


Fig. 10.6. The average value $\langle \Delta \omega_{pe} \rangle$ as a function of absorption Θ for a weakly relativistic beam $\gamma_{b0} = 1.6$ (left) and a relativistic beam $\gamma_{b0} = 10$ (right)

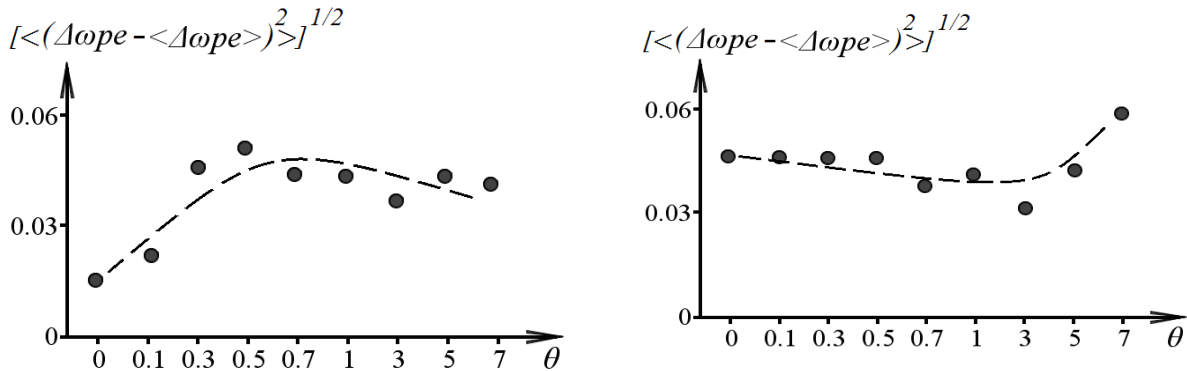


Fig. 10.7. Standard deviation $[\langle (\Delta \omega_{pe} - \langle \Delta \omega_{pe} \rangle)^2 \rangle]^{1/2}$ as a function of absorption Θ for a weakly relativistic beam $\gamma_{b0} = 1.6$ (left) and a relativistic beam $\gamma_{b0} = 10$ (right)

Understanding of the frequency shift and spectrum width allows predicting the nature of the processes in the system. In particular, with a sufficiently wide spectral width, some instabilities whose increment is less than the spectral width do not develop.

References to section 10

- 10-1. Fainberg Ya. B. Plasma electronics. Ukr. physical journal, 1978, V. 23. – No. 11. – P. 1885–1901; Some questions of plasma electronics. Plasma physics. 1985. –V. 11. – N. 11. – P. 1398–1410 (in Russian).
- 10-2. Rabinovich M. S., Rukhadze A. A. Principles of relativistic plasma electronics // Plasma Phys. 1976. – V. 2. – Issue 5. – P. 715–722 (in Russian).
- 10-3. O’Neil T. M., Winfrey J. H., Malmberg J. H. Nonlinear interaction of a small cold beam and plasma // Phys. Fluids. 1971. – V. 14. – N 6. – P. 1204–1212.
- 10.4. O’Neil T. M., Winfrey J. H. Nonlinear interaction of a small cold beam and plasma. Part II // Phys. Fluids. 1972. – V. 15. – N 8. – P. 1514–1522.

10-5. Shapiro V. D., Shevchenko V. I. Wave – particle interaction in nonequilibrium media. *Izv. Universities Radiophysics*, 1976. – T. 19. – No. 5–6. – P. 787–791 (in Russian).

10-6. Kuzelev M. V., Rukhadze A. A. *Electrodynamics of dense electron beams in plasma*. – M. : Science. Ch. ed. phys.-mat. lit. 1990. – 336 p. (in Russian).

10-7. Kondratenko A. N., Kuklin V. M. *Fundamentals of Plasma Electronics*. – M. : Energoatomizdat, 1988. – 320 p. (in Russian)

10-8. Kondratenko, A. N., Kuklin, V. M., and Tkachenko, V. I., Nonlinear theory of beam instability in collisional plasma, *Izv. universities. Radiophysics*, 1978. – T. 21. – No. 10. – P. 1535–1537 (in Russian)

10-9. Kondratenko A. N., Kuklin V. M., Tkachenko V. I. On the anomalous level of beam energy loss during the development of dissipative beam instability // *Ukrainian Physical Journal* 1979. – V. 24. – № 4. – P. 559–561 (in Russian).

10-10. Zagorodny A. G., Kirichok A. V., Kuklin V. M., Priymak A. V. Modulation of the integral field of multimode beam instabilities in plasma // *East Eur. J. Phys.* 2014. – V. 1. – No. 2. – P. 53–66 (in Russian).

SECTION 11. BEAM INSTABILITY IN NONLINEAR AND NEGATIVE DISSIPATIONS

Development of beam instability in hot plasma. In plasma with a Maxwellian electron velocity distribution, the energy of the Langmuir wave excited by the beam is absorbed by the plasma electrons, and the linear decrement of this absorption (Landau absorption) is

$$\delta_k = \sqrt{\pi/8}(\omega_{pe}\omega^3/k^3v_{Te}^3)\exp\{-\omega^2/k^2v_{Te}^2\}, \quad (11.1)$$

where v_{Te} is the thermal velocity of the plasma electrons. The equations describing the nonlinear dynamics of the wave excited by the beam (cf. (2.12), (2.13)) have the form [11-1]:

$$\partial A / \partial \tau = \int_{-1/2}^{1/2} d\xi_{b0} \cdot \exp\{-2\pi i \xi_b\} - 8\pi \cdot \Theta \int_{-1/2}^{1/2} d\xi_{p0} \int_{-\eta}^{\eta} d\eta_0 \eta_0 \exp\{-2\pi i \xi_p\}, \quad (11.2)$$

$$2\pi \cdot d^2 \xi_{b,p} / d\tau^2 = -\text{Re}[A \cdot \exp\{2\pi i \xi_{b,p}\}], \quad (11.3)$$

where $\Theta = \delta_k / \gamma$, δ_k is the Landau damping decrement for Langmuir oscillations, $\gamma = \gamma|_{\Theta=0} = \sqrt{3}(\omega_{e0}\omega_{b0}^2/2)^{1/3}/2$ in this case is the increment of hydrodynamic beam instability in the absence of absorption ($\Theta=0$), $\omega_b = (4\pi e^2 n_{b0}/m_{e0})^{1/2}$ is the Langmuir frequency of the electron beam, and $\omega_{pe} = (4\pi e^2 n_{e0}/m_{e0})^{1/2}$ is the Langmuir plasma frequency, ($e, m_{e0}, n_{b0}, n_{e0}$ are

the charge, electron rest mass, and undisturbed beam and plasma density); $2\pi\xi_{b,p0} = kx_{b,p0} - \omega t$ and $\eta_{b,p0} = (kv_{b,p0} - \omega_{pe})/2\pi\gamma$, in this case the index b corresponds to beam particles, and the index e corresponds to plasma particles.

In the nonlinear regime of the development of beam instability, the field amplitude of the excited wave experiences modulation, and large-scale modulation is caused by oscillations in the potential well of the quasiparticle (i.e. captured beam particles). The regime of energy exchange between the trapped particles of the beam and the wave is accomplished. Since at the initial moment

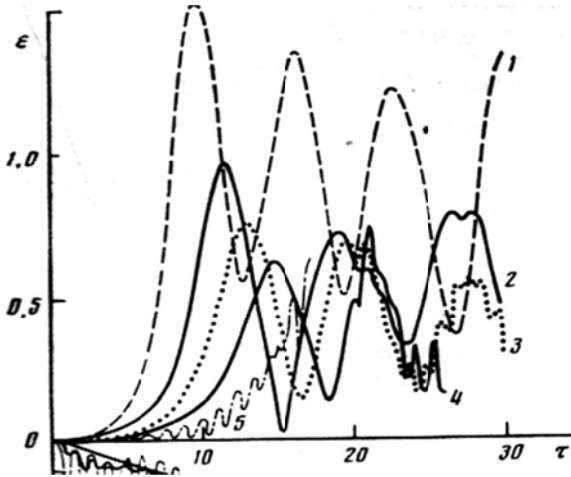


Fig. 11.1. The structure of the field of the envelope of oscillations at
 1. $\Theta = 0$; 2. $\Theta = 3$; 3. $\Theta = 5$;
 4. $\Theta = 7$; 5. $\Theta = 10$

the beam is assumed to be monoenergetic, this quasiparticle is quite compact, and accordingly, the modulation depth is large.

Plasma electrons near the resonance $v = \omega/k$ are also trapped by the wave field. For parameter values Θ , which are appreciably greater than unity, the plasma electrons captured by the wave field also form a more diffuse and denser quasiparticle, whose movement in the wave field leads to small-scale and relatively shallow wave modulation. Moreover, this modulation is superimposed on deeper and relatively

slower changes in the wave amplitude due to the motion of the captured beam particles in the potential wave well. In this regime, an energy exchange between the formed quasiparticle and the wave also takes place, while the average absorption of wave energy by plasma particles during these oscillations decreases. Thus, we can assume that Θ_{eff} (the effective value of the parameter Θ) is somewhat reduced. Beam instability passes from a dissipative regime to a more reactive regime, which corresponds to lower values Θ_{eff} .

Change in the nature of beam instability with the excitation of surface waves in plasma with a blurred boundary. When a surface wave is excited by an external source, its field amplitude increases, and the fraction of its energy absorbed in the plasma resonance region, which is located on the diffuse plasma boundary, also decreases [11-2, 11-3].

Suppose, at first, the regime of dissipative instability was realized with large values of the parameter Θ , which here also corresponds to the ratio δ_L – the damping decrement in the absence of a nonequilibrium element (i.e., the beam) $\gamma(\omega, k)|_{\delta=0}$ – to the maximum increment of the nondissipative

instability. In the process of instability development, a decrease Θ and, accordingly, a change in the instability mode occurs [11-2]. For more details see annex XII.

The “wave – trapped particle” structure in a weakly ionized gas flow.

In flows, it is also possible to implement the “negative friction” regime, when the flow is a weakly ionized medium, the particle velocity of which is quite high.

The electronic component of this stream is capable of exciting oscillations in the waveguide system through which it is transported. Significant friction of the electrons decelerating by the wave on neutral (its density is much higher) and the ionic components of the flow leads to the restoration of the velocity of the electronic component. Thus, long-term synchronism between the electrons of the flow and the wave is achieved. In addition, such “negative friction” leads to their spatial grouping. The equations describing the process of electron excitation of a weakly ionized stream of natural oscillations of the medium can be represented in the form [10-4]

$$\partial A / \partial \tau = \int_{-1/2}^{1/2} d\xi_0 \cdot \exp\{-2\pi i \xi\}, \quad (11.4)$$

$$2\pi(d^2 \xi / d\tau^2 + \Theta_1 d\xi / d\tau) = -\text{Re}[A \cdot \exp\{2\pi i \xi\}], \quad (11.5)$$

where $\alpha^{1/3} = (2\gamma|_{v=0} / \sqrt{3}) / \omega_{pe}$, $2\pi\xi = kz - \omega_{pe}t$, $\eta = (kv - \omega_{pe}) / \alpha^{1/3} \omega_{pe}$, $A = kE\alpha^{1/3} / 4\pi en_{b0}$, $\Theta_1 = v / \alpha^{1/3} \omega_{pe}$ up to a numerical factor, the ratio of the collision frequency of the flow electrons with the neutral (or ionic) component of the flow to the increment of beam instability in the absence of friction between the flow components. The solution of the one-parameter system of equations in this case is illustrated in Fig. 11.2. The oscillatory increase in the field amplitude is replaced by a monotonic increase even at parameter $\Theta_1 > 0,5$.

The behavior of the beam electrons on the phase plane is shown in Fig. 11.3. A rapid increase in the field amplitude leads to the grouping of the beam captured by the field electrons into dense bunches, the volume of which in ordinary space decreases. A quasiparticle is formed, which is located in the phase of the field, which

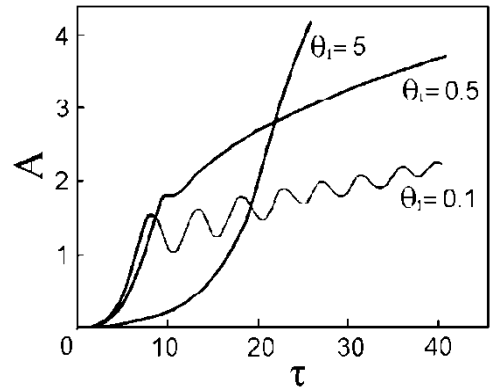


Fig. 11.2. The dependence of the amplitude of wave A on time for various values of the parameter Θ_1

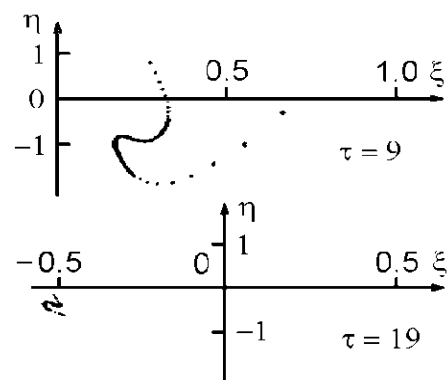


Fig. 11.3. Behavior of beam electrons in the phase plane for different time instants with parameter value $\Theta_1 = 0,5$

contributes to the selection of energy from the electrons by the wave. On the other hand, friction against heavy particles of the flow leads to a restoration of the electron velocity. Since friction is proportional to the velocity difference of the components of the flow, the electrons are slightly behind the main flow (that is, the so-called slip mode occurs).

The process of implementing the regime with "negative friction" dramatically increases the efficiency of excitation of oscillations, the amplitude of which can be many times greater than the values obtained from the conditions of particle capture by the wave. Such a phenomenon can lead to additional ionization of the flow, which is, for example, of interest for MHD devices for energy conversion.

References to section 11

11-1. Kuklin V. M., Panchenko I. P., Sevidov S. M. On the nonlinear theory of hydrodynamic beam instability in high-temperature plasma // Radio engineering and electronics. 1986. – V. 31. – No. 3. – P. 611–614 (in Russian).

11-2. Instability of the relativistic electron beam – semi-finite plasma system. // Auth: Peneva J. Kh., Kondratenko A. N., Kuklin V. M., Tkachenko V. I. // *Bolg. Phys. Journal*. 1977. – V. 4. – Number 3. – P. 308–317 (in Russian).

11-3. Kondratenko A., N. Kuklin V. M., Tkachenko V. I., Peneva I. Ch. On the change of beam instability nature in the plasma waveguide with diffuse boundaries. Conf. on Surface waves in plasma. Blagoevgrad Bulg., Sept. 28 – Oct. 3 1981. Inv. talk and contr. papers. Sofia, 1983. – P. 325–327.

11-4. Excitation of plasma waves by means of weakly ionized monoenergetic particle beam. // Auth.: Kondratenko A. N., Kruscha J., Kuklin V. M., Tkachenko V. I., Vorobjov V. M. // *Beit, Plasmaphysics*, 1983. – V. 23. – N 6. – P. 615–620.

CHAPTER 5. Superradiation modes

A self-consistent interaction of a bunch of monoenergetic charged particles – a short beam of electrons, propagating in a plasma, are considered. It is shown that the macroscopic dielectric constant in the volume of the beam is negative, that is, the particles of the beam are attracted instead of repulsing. However, the developing instability process, which corresponds to the superradiation regime, leads to intense spatial modulation of the beam density and the formation of a wake field behind the beam. For short bunches, the size of which is less than the wavelength of the wake field, a self-profiling mode is possible when fields are formed in a separate region of the medium, the intensity of which corresponds to the radiation of all particles as if they were collected in one point. The similarity of dissipative instability processes and superradiation modes for particles of a moving bunch and a system of oscillators whose centers are at rest is shown.

SECTION 12.

FORMATION OF THE THIN STRUCTURE OF ELECTRON BUNCHES INJECTED IN PLASMA

Below, let us practically consider monoenergetic bunches of charged particles moving with velocity V_0 , whose longitudinal size a does not exceed $(V_0 / \omega_0)(\omega_b / \omega_0)^{-2/3}$ (where $\omega_0 = \omega_{pe} = (4\pi e^2 n_{po} / m_{e0})^{1/2}$ is the Langmuir plasma frequency and n_{po} is the unperturbed plasma density and $\omega_b = (4\pi e^2 n_{b0} / m_{e0})^{1/2}$ is the plasma frequency electron beam n_{b0} is the unperturbed beam density) so that the energy of plasma oscillations is not accumulated in their volume. Plasma oscillations excited by a short bunch of charged particles lag behind him, forming the so-called wake trace.

An example of negative macroscopic permittivity [12-1]. The effect of the reversal of Coulomb forces in the volume of a single monoenergetic bunch is due to the fact that when integrating over the wave numbers of the fields in the rest frame of the bunch ($\xi = z - v_0 t, t$) created by each of the bunch particles and depending on the dielectric constant $\varepsilon(\omega, k) \equiv \varepsilon(0, k) = 1 - (\omega_{pe} / kv)^2$, the contribution of large-scale density perturbations (small values of the wave number k) exceeds the contribution of small-scale ones. For example, in the one-dimensional case, choosing the distribution function of particles of an unmodulated bunch in the form $f(\xi, v) = (N / a\sqrt{\pi}) \exp(-\xi^2 / a^2) \cdot \delta(v - v_0)$, for the field strength we shall get the expression

$$E(\xi) = 2i |e| N \int dk \cdot \exp \{ ik\xi - k^2 a^2 / 4 \} [k \cdot \varepsilon(0, kv_0)]^{-1} \approx$$

$$\approx 4\sqrt{\pi} \cdot |e| \cdot N \cdot \xi \exp \{ -\xi^2 / a^2 \} / a \cdot \varepsilon_{eff}, \quad (12.1)$$

where $\varepsilon_{eff} = -\omega_{pe}^2 a^2 / 2v_0^2 < 0$ is the value of effective dielectric constant. It can be found [12-1] that in the three-dimensional case, for a bunch of such dimensions, the macroscopic permittivity in its volume is also negative. That is, in the case of a moving monoenergetic electron bunch, its particles do not experience repulsion, but attraction. In contrast to the case of electromagnetic radiation generation, when a generating bunch, which is a source of energy, experienced both focusing and defocusing forces, the excitation of longitudinal waves in the plasma simultaneously led to radial [12-2] – [12-4] and longitudinal [12-1], [12-5] – [12-9] focusing. The superradiation process under these conditions, which is similar to beam dissipative instability (about this similarity, see below) generates fields inside the bunch that exceed in $k^2 a^2 > 1$ times the focusing effect of the reversed Coulomb field, but does not allow the beam to expand in the longitudinal and transverse directions.

Indeed, at first glance, the intrinsic fields of the bunch, the longitudinal dimensions of which exceed the length of the emitted Langmuir wave, should lead to compression of the bunch as a whole. However, instability develops in the volume of the bunch, which, due to the spatial grouping of its particles, sharply enhances the wake radiation both outside and inside the bunch. Therefore, the dynamics of a monoenergetic electron bunch is determined precisely by the development of the discussed instability. The first attempts to describe self-consistently the interaction of particles of a short bunch with the field of their own radiation, apparently, were presented in [12-7, 12-8].

This channel of energy loss (i.e., wake radiation) has a noticeable effect on the development of disturbances in the volume of the bunch and, in general, on the formation of its fine structure. The equations describing the nonlinear dynamics of an electron bunch in the one-dimensional case propagating through a dense plasma are as it follows (see annex XV)

$$\frac{d\xi}{d\tau} = v, \quad \frac{dv}{d\tau} = E(\xi), \quad (12.2)$$

$$E(\xi) = -\frac{2}{N} \sum_{\alpha}^N f_{\alpha} \cos [2\pi g_{\alpha} (\xi - \xi_{\alpha})] \Theta(\xi_{\alpha} - \xi), \quad (12.3)$$

where $2\pi\xi = K_0(z - V_0 t)$, $v = K_0(V - V_0) / 2\pi\gamma_L$, $\gamma_L^2 = e^2 K_0 M / m_e$, $g = (1 + \Delta v)^{-1}$, $\Delta = 2\pi\gamma_L / K_0 V_0$, $\tau = \gamma_L t$ and M is the total number of particles in the bunch $E = eK_0 E / 2\pi m_e \gamma_L^2$, E is the electric field strength, f_{α} is the statistical weight of a large particle which models the beam.

The amplitude of the radiation field of a bunch, the size of which is small compared to the wake (plasma) wavelength $2\pi(V_0 / \omega_{pe})$, decreases monotonically over time. If the initial longitudinal size of the bunch a is considerably

greater than $2\pi(V_0/\omega_{pe})$, then the initial radiation amplitude is small and the macroscopic dielectric constant of the plasma for such a bunch is negative, so it can be expected that it will be compressed as a whole.

However, in the process of rapidly developing instability of a dissipative type (since the effective decrement of oscillation damping in a bunch δ_D can be defined as the ratio of the energy flux of the oscillations leaving the bunch to the total oscillation energy in its volume $\delta_D = V_0/a$, and a parameter $\Theta = \delta_D / \gamma |_{\delta=0} = (V_0/a \cdot \omega_0)(\omega_b/\omega_0)^{-2/3} > 1$) a structure with spatial period $2\pi(V_0/\omega_{pe})$ is formed in the volume of the bunch. The occurrence of such a fine structure of the bunch is accompanied by an increase in the amplitude of the wake trace. At the nonlinear stage of the process, particles are captured by the field of increasing oscillations, phase mixing occurs, the fine structure of the bunch is destroyed, and the amplitude of its wake trace decreases.

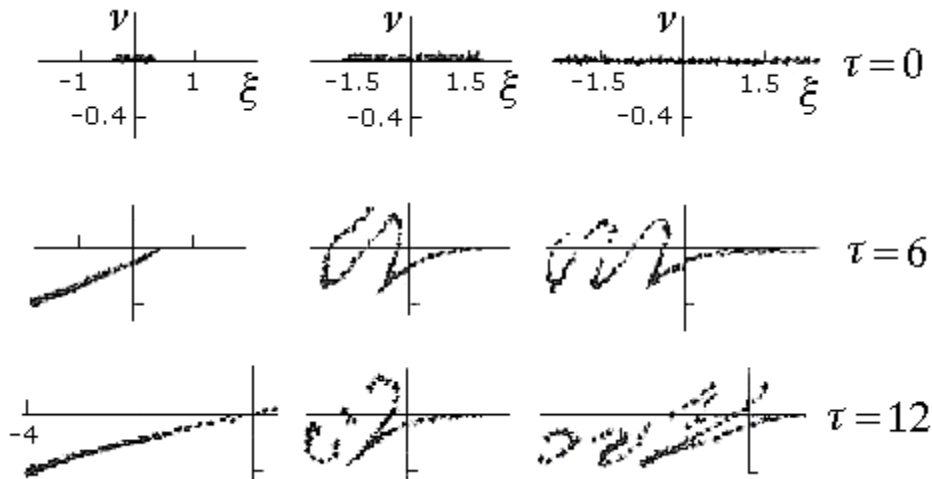


Fig. 12.1. Behavior of particles of short beams of different lengths ($K_0 a = 0.6\pi$, (2) 6π , (3) 10π) with the same number of particles on the phase plane (ξ, ν).

Let us note that in the case of extended bunches with the same fixed number of particles $(a\omega_{pe}/2\pi V_0) > 1$, the largest radiation amplitude achieved during the instability weakly depends on the initial longitudinal size of the bunch, which allows considering it (amplitude) as maximum possible and approximately equal to unity at the selected problem scales. Let us pay attention to the fact that if all the particles were collected to a point, then the amplitude of the wake field would be equal to two, which is easy to see from relation (12.3). That is, the degree of radiation coherence is 25 %.

Therefore, to some extent the usage of charged particles for the acceleration in the wake field of single electron bunches is not critical with respect to their longitudinal size [12-9, 12-10]. Some time later incoherent radiation is the same after the destruction of the structure.

As shown by experimental studies and numerical experiments conducted at the NSC KIPT, a sequence of clumps, which is not too big, also can synchronize its dynamics, which increases its stability and coherence length. Then the bunch particles are captured by the field, the periodicity of the structure, and, consequently, the coherence of the radiation are violated.

It can be shown that for three-dimensional clusters of charged particles of the same sign moving in a plasma, the longitudinal dimensions a_{\parallel} of which

$$2\pi(V_0 / \omega_0) < a_{\parallel} \ll 2\pi(V_0 / \omega_0)(\omega_b / \omega_0)^{-2/3}, \quad (12.4)$$

focusing forces appear in their volumes, compressing the bunches as a whole in the transverse direction (the dielectric constant of the medium is negative for them [12-11, 12-12]) The radiation of such bunches is also amplified during the development of instabilities that form the fine structure of the bunches [12-13] – [12-16].

Clusters Usually, the occurrence of a spatial structure increases the energy flux into the loss channels, which reaches its maximum at the moment of the largest amplitude of this structure. However, there may be cases when the structure – a cluster of only a few charged particles remains stable [12-17, 12-18] and forms a minimal energy flow during the relaxation of the system. Let us construct a cluster of moving charged particles, and the first of them – the leader, let us place at the origin of coordinates. We arrange a particle having the same velocity at the point where the electric field of the leader is zero or the potential is minimal.

By placing each subsequent particle at the minimum of the potential of the field created by the particles located in front, we can build a cluster whose stability is very high, and the initial velocities in the cluster rest system are zero

$$\xi = 0, \quad K_0 \xi_n = - \sum_{m=2}^n a \sin(1 / \sqrt{m}). \quad (12.5)$$

The forces exerted by the radiation field on each particle of such a cluster are the same and equal to the braking force of an individual particle. Let us mention that a similar structure (a cluster) can be built in a three-dimensional case. The amplitude of the electric radiation field behind the cluster, the number of particles of which is equal to M , is \sqrt{M} times the amplitude of the radiation field of a single particle. Thus, the radiation intensity of such a cluster of M particles is minimal and proportional to M . In the previously discussed cases, the radiation of coherent structures was proportional to M^2 with a numerical factor, which is less than unity, determining the degree of coherence of the structure [12-18]. The cluster size is determined by the stability of the particles located in its tail, and the particle binding energy for sufficiently large m is proportional $1 / \sqrt{m}$, that is, it rapidly decreases with the number m of the particle counted from the leader of the cluster.

Self-profiling of a short bunch of electrons moving in plasma. The problems of obtaining the largest amplitude of the wake field behind an electron bunch arose in connection with the analysis of the possibility of the usage of

high-energy and high-current short electron beams – bunches moving in plasma to accelerate ions [12-19, 12-20]. Despite the fact that the bunches, whose initial sizes is much smaller than the radiation wavelengths, are unstable in the one-dimensional and three-dimensional cases (see, for example, [12-8, 12-21]) with a certain preliminary profiling of the particle density and velocity, one could hope significant wake fields, comparable to the field of a bunch, the particles of which are collected in a very small area of space [12-21 – 12-24]. If the goal was to ensure the stability of the bunch, then it was preferable to use longer clusters, which made it possible to obtain significant field values both inside such a short beam and in their wake radiation [12-13 – 12-16, 12-25, 12-26 .].

The wake field behind the radiating particle in the system of its rest moving with speed v is $\text{Cos}[k\zeta] = \text{Cos}[k(x - vt)]$. In cold plasma, the group velocity of Langmuir oscillations with a frequency ω_{pe} is equal to zero, therefore, if we go to the laboratory reference frame, the field amplitude at each point will change as $\text{Cos}[\omega_{pe}t] = \text{Cos}[kvt]$. It is important to note that this is one and the same field, only in different reference frames. If the speeds of each particle are different, then these cosine waves will have different values of the wave number $k = \omega_{pe} / v$.

Moreover, if the configuration of the bunch particles in space does not change, the general field of its wake field will be represented as the interference of individual fields of emitted particles already having a velocity spread. Along with this, in the laboratory reference system, this field represents the interference of oscillations with a different phase. There are configurations and a corresponding spread in the velocities of the particles of the bunch of emitters, which make it possible to achieve a small spread in the phases of the fields in separate, sufficiently extended areas of the laboratory reference frame. Such profiling of the bunch in terms of velocity and density was proposed to be specially created to achieve the maximum value of the wake field [12-25], at least in certain regions of the plasma space. It is clear that in the rest system of the bunch as a whole there was the field maximum region moving in the opposite direction at approximately the same speed [12-10].

Let us show below that such profiling occurs spontaneously in the beam volume. In the rest frame (where the beam as a whole is at rest), a field maximum lags behind the beam at the same, but opposite speed. That is, in the laboratory frame of reference this area remains localized. The modes of excitation of the wake field, which are achieved in case of short bunches, whose size is less than the length of the wake wave, are of great interest for this issue.

From the calculation results⁹ it follows that for bunches the longitudinal size of which is smaller, but nevertheless comparable to the wavelength, the

⁹ The program that implements the mathematical model of the problem was created using JCUDA technology. [12-28].

phenomenon of self-profiling of the bunch is detected, the radiation efficiency of which in a certain region behind the bunch reaches a value field strength E in selected units, equals 2 (as if all the beam particles were collected at one point in space).

Indeed, for bunches whose length exceeds several wavelengths of the emitted waves, the value of the field amplitude in this normalization is always less or of the order of unity [12-10]. In the case of a bunch, where all particles are assembled to a point, the amplitude of the wake field in the selected representation (12.2) – (12.3) turns out to be two times larger and reaches its absolute maximum – a value of 2 [12-27]. Consider a bunch with the size of 0.5 wavelength. It turns out that it is generally inhibited, forming the characteristic triangular distribution of particles in the configuration and phase spaces (see Fig. 12.2 and Fig. 12.3.)

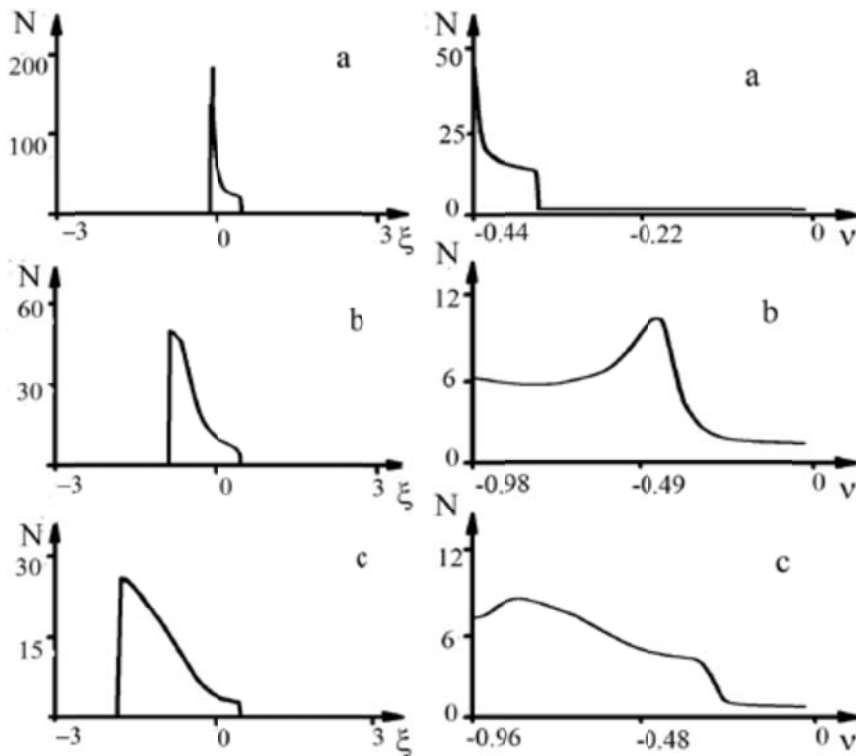


Fig. 12.2. Particle distribution in space ξ (left), particle velocity distribution v (right), a). $\tau = 1$; b). $\tau = 2$; c). $\tau = 3$.

It is the formation of such triangular distributions, similar to the initial profiling bunch in [12-25, 12-27] that leads to interference of the fields of the studied particles in a certain region of space, which moves away from the beam in its rest system with a speed in the units of measurement chosen by us

$$\left\langle \frac{d\xi}{d\tau} \right\rangle = \frac{K_0 V_0 t}{2\pi\gamma_L t} = \frac{1}{\Delta}, \tag{12.6}$$

It can be seen (see Fig. 12.3) that the region of the absolute maximum of the field shifts with the velocity of the bunch in the opposite direction from it. Moreover, the beam is located on the right side of the figure in the vicinity of the point $\xi = 0$. Moreover, in the laboratory reference system, this region of the field maximum does not move.

Some distortions of the field region are associated with a small change in the beam profile in this time interval. This model qualitatively describes the process of the dynamics of a bunch and its radiation, however, it makes it easy to detect the effect of beam self-profiling. The achievements as a result of such self-profiling (in a region that exceeds the initial size of the bunch by more than an order) of magnitude are significant wake field amplitudes almost equal to the maximum possible value of the radiation field of the bunch, particles of which are collected in a very small area.

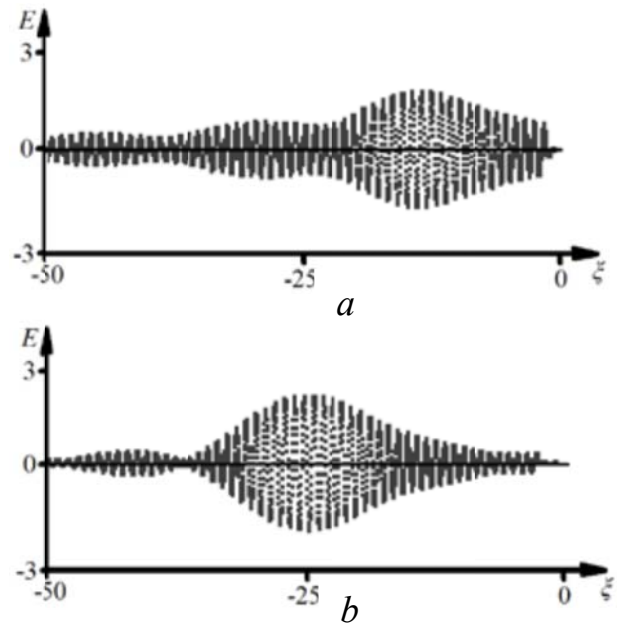


Fig. 12.3. View of the radiation field E in the reference frame of the beam as a whole at time points a) $\tau = 2$ and b) $\tau = 3$

References to section 12

12-1. Kondratenko A. N., Kuklin V. M., Repalov N. S. Evolution of a bunch of charged particles in the field of its own radiation. Ukr. Phys. Journal 1982. – T. 27.– № 8. – P. 1159–1164 (in Russian).

12.2. Krasovitskiy V. B. Nonlinear radial self-focusing of an electron beam in plasma // JETP Letters, 1969. – No. 9. – P. 679–684 (in Russian).

12.3. Dorofeenko V. G., Krasovitskiy V. B. Self-focusing of a modulated electron beam in a plasma. // Ukr. Phys. Journal, 1984. – V. 29. – No. 3. – P. 395–405 (in Russian).

12-4. Krasovitskiy V. B. Self-focusing of relativistic electron bunches in a plasma. – Kharkov, Folio, 2000. – 196 p.

12-5. Grishin V. K., Shaposhnikova E. N. Stability of a charged beam of short duration in a plasma waveguide. // Plasma Physics. 1982. – V. 8. – N. 2. – S. 287–292 (in Russian).

12-6. Gladkiy A. M., Kovalenko V. P., Yusmanov P. N. Properties of plasma waves excited by electron bunches // Letters ZhETF, 1976. – No. 24. – P. 533–542 (in Russian).

12-7. Kuklin V. M., Panchenko I. P., Sevidov S. M. Evolution of a short beam of charged particles and reversal of Coulomb forces in plasma. Sat.

"Problems of Nuclear Physics and Cosmic Rays", Ed. KhSU, 1983. – N. 19. – P. 97–100 (in Russian).

12-8. Kuklin V. M., One-dimensional moving bunches of charged particles in plasma. Ukr. Phys. Journal 1986. – V. 31. – No. 6. – P. 853–857 (in Russian).

12-9. Kuklin V. M., Moiseev S. S., Panchenko I. P. On the issue of transportation and radiation of short one-dimensional bunches of charged particles in plasma // Preprint № 1314, Space Research Institute. Moscow, 1987. – 15 p. (in Russian).

12-10. Kirichok A. V., Kuklin V. M., Mishin A. V., Priymak A. V. 1D model of a bunch of charged particles moving in plasma // Physical foundations of instrument engineering. 2013. – T. 2. – No. 3. – P. 80–93 (in Russian).

12-11. Alterkop B. A., Zheksemin S. R., Rukhlin V. G., Tarakanov V. P. Two-dimensional dynamics of a compensated electron bunch in a dense plasma // Preprint of the Institute of High Temperatures of the Academy of Sciences of the USSR, 1986. – N 6–193. – P. 35–45 (in Russian).

12-12. Kuklin V. M., Moiseev S. S., Panchenko I. P. 3-D short Beam Dynamics // Moscow. Reprint of Institute of Space Research, N 1619, 1989. – 11 p.

12-13. Batishchev O. V., Karas' V. I., Sigov Yu. S. and Fainberg Ya. B. 2.5 Dimensional computer simulation of relativistic bunch propagation in tenuous and dense plasmas // Plasma Physics Reports, 1994. – V. 20. – P. 583–586 (in Russian).

12-14. Balakirev V. A., Sotnikov G. V., Fainberg Ya. B. Modulation of relativistic electron bunches in plasma // Plasma Physics, 1996. – V. 22. – No. 2. – P. 165–169 (in Russian).

12-15. Balakirev V. A., Karas' I. V., Karas' V. I., Levchenko V. D., Bornatici M. Charged particle (CP) acceleration by an intense wake-field (WF) excited in plasma by either laser pulse (LP) or relativistic electron bunch (REB) // Issues of atomic energy and technique. Plasma electronics and new methods of acceleration (3), 2003. – No 4. – P. 29–32 (in Russian).

12-16. Onishenko N. I., Sotnikov G. V. Theoretical studies of the resonator concept of dielectric wakefield accelerator // Issue of Atomic Science and Techniques. Topical: Plasma Electronics and New Methods of Acceleration (3), 2006. – № 5. – C. 203–207 (in Russian).

12-17. Evidence for an alignment effect in the motion of surface ion clusters through solids // Auth.: Gemmell D. S., Remillieux J. et al. Phys. Rev. Letter. 1975. – V. 34. – N. 22. – P. 1420–1424.

12-18. On the theory of cluster systems in plasma-like media. // Auth.: Kondratenko A. N., Kuklin V. M., Panchenko I. P., Sevidov S. M. Izv. Universities, Physics, 1987. – No. 5 – P. 83–87 (in Russian).

12-19. P. Chen, J. M. Dawson, R. W. Huff and T. Katsouleas. Acceleration of electrons by the interaction of a bunched electron beam with plasma // Phys Rev. Lett., 1985. – V. 54. – P. 693–696.

12-20. T. Katsouleas Physical Mechanisms in the plasma wake-field accelerator // Phys.Rev. A., 1986. – V. 33. – P. 2056–2064.

12-21. Kuklin V. M., Panchenko I. P., Khakimov F. Kh. Multiwave processes in plasma. – Dushanbe, Donish, 1999. – 175 p. (in Russian).

12-22. Bane, K. L. F., P. Chen and P. B. Wilson, "On Collinear wakefield acceleration", IEEE Transactions on Nuclear Science 1985. – V. 32. – №. 5. – P. 3524.

12-23. Chen, P. et al., "Energy Transfer in the Plasma Wake-Field Accelerator", Physical Review Letters 1986. – V. 56. – N. 12. – P. 1252.

12-24. Laziev, E., V. Tsakanov and S. Vahanyan, "Electromagnetic wave generation with high transformation ratio by intense charged particle bunches", in EPAC (IEEE, 1988), – P. 523.

12-25. Lawson, J. D., Particle Acceleration Mechanisms: Possibilities and Limitations, Phys. 1989, V. 158. – N. 2. – P. 303–313.

12-26. Balakirev V. A., Karbushev N. I., Ostrovsky A. O., Tkach Yu. V. Theory of Cherenkov's Amplifiers and Generators on Relativistic Beams. – 1993. – Kiev: Naukova Dumka, 1993. – 208 p. (in Russian).

12-27. Kirichok A. V., Kuklin V. M., Mischin A. V., Pryimak A. V. Modeling of superradiation processes driven by an ultra-short bunch of charged particles moving through a plasma// Problems of Atomic Science and Technology, 2015. – N 4. – series "Plasma Electronics and New Methods of Acceleration" – p. 255–257.

12-28. Gushchin I. V., Kuklin V. M., Mishin O. V., Priymak O. V. Model of physical processes due of CUDA technology. – Kh. : KhNU imeni V. N. Karazin, 2017. – 116 p. (in Ukrainian).

SECTION 13.

DISSIPATIVE INSTABILITIES AND SUPERRADIANCE MODES

Electron beam in a longitudinally bounded system. In plasma, the dynamics of an electron beam, the longitudinal size of which is b , and the unperturbed velocity is V_0 , can be described by the following system of equations in its simplest one-dimensional case:

$$\partial E / \partial \tau = -\theta \cdot E + N^{-1} \cdot \sum_{i=1}^N \text{Cos} \{2\pi \xi_i + \varphi\}, \quad (13.1)$$

$$\partial \varphi / \partial \tau = -N^{-1} \cdot \sum_{i=1}^N \text{Sin} \{2\pi \xi_i + \varphi\}, \quad (13.2)$$

$$\begin{aligned} 2\pi \cdot d^2 \xi_j / d\tau^2 = & \\ & E \cdot \text{Cos} \{2\pi \xi_j + \varphi\}, \\ = -\{ & (N \cdot \theta)^{-1} \sum_{i=1}^N \cos [2\pi g_i (\xi_j - \xi_i)] \cdot U (\xi_i - \xi_j), \end{aligned} \quad (13.3)$$

where $2\pi\xi = kz - \omega t$, $\tau = t \cdot \gamma$, $\omega_{pe,b}^2 = 4\pi e^2 n_{0e,b} / m_e$, e, m_e are the charge and mass of the electron, $n_{0e,b}$ are plasma and beam densities, δ_D is the effective damping decrement of oscillations that can be defined as the ratio of the energy flux of the oscillations, leaving the beam volume to the total oscillation energy in its volume¹⁰ $\delta_D = V_0 / a$, $\theta = \delta_D / \gamma|_{\delta=0} = (V_0 / b \cdot \omega_{pe})(\omega_{be} / \omega_{pe})^{-2/3}$, $\gamma^3 = (n_{0b} / 2n_{0e}) \cdot \omega_{pe}^3$, $M = n_{pb} \cdot b$ is the total number of particles in the beam, $g_i = (1 + (v - v_0) / v_0)^{-1} = (1 + V \omega_{pe} / \gamma)^{-1}$ which is easily determined from the equation $2\pi d\xi / d\tau = k(v - v_0) / \gamma = V$. Here $U(x) = 1; x \geq 0$ and $U(x) = 0; x < 0$. The parameter $\theta = \delta_D / \gamma$ corresponds to the ratio of the damping decrement δ_D in the absence of a nonequilibrium element (here, the beam) to the maximum increment of nondissipative instability (i.e., in the absence of losses) γ .

For clarity, we switched from integration over the initial states of particles to the usual summation of their contributions to the field. The upper term in the right-hand side of (13.3) should be used to describe the beam; the integral field of which $E \cdot \text{Cos}\{2\pi\xi_j + \varphi\}$ can accumulate in its volume. The lower term on the right-hand side of (13.3) describes the total field of particles of a sufficiently short beam at large values θ . Let us note that the lower term on the right-hand side of (13.3), generally speaking, determines the total spontaneous emission of the Langmuir wave with the frequency ω_{pe} of all beam particles.

The integrated field $E \cdot \exp\{2\pi i \xi_j + i\varphi\}$ can be formed due to the initial perturbation or it occurs when the RF energy is accumulated in a sufficiently extended beam in the cavity or waveguide. In this case, the beam particles do not directly interact with each other and are associated only with the wave field. Generally speaking, such a field is usually considered in problems of generation and amplification of induced radiation. For small θ , that is, for an extended beam, this field accumulates in its volume and in many cases the lower term (13.3) can be neglected if the number of particles in the beam description is very large.

For large values $\theta \gg 1$, if initially there was not any an integral field in the system (not a waveguide, but an open system), equations (13.1) and (13.2) together with equation (13.3), where the upper term on the right-hand side is held, are no longer applicable. In this case, the interaction of the particles with each other is significant (the particles that are in front in the direction of motion act on the particles following them, but not vice versa). When particles are grouped in a beam and their phase synchronization arises at the same time, the formation of the so-called superradiance is possible; it is described only by equation (13.3), where the lower expression should be kept on the right side. If the beam is short enough, the energy of the field in time $b / V_0 < \gamma^{-1}$ (i.e., $\theta > 1$) is carried out

¹⁰ See, a representation of such an absorption, for example, in Annex I, expression (I.6).

from the volume of the bunch. In this case, the field in the beam volume is determined only by the second – lower term of equation (13.3).

The field growth is due to the independent grouping of particles and an increase in the coherence of their radiation, which forms the field of superradiance. In [13-1, 13-2], it was noted that for the same values $\theta > 1$, the increment of the superradiation process of a beam limited in the direction of motion of the beam is comparable to the increment of dissipative beam instability $\gamma_D \approx \omega_{pb}(\omega_{pe}/\delta_D)^{1/2} = \omega_{pb}(kb)^{1/2}$, the energy loss in which is determined by the transfer of energy from the beam volume.

That is, spatial modulation of particles, similar in both cases, led to phase synchronization of particles and, accordingly, to increased radiation coherence. The amplitude limitation in the cases under discussion was due to the capture of particles in the wave field, which corresponded to the equality of the oscillation frequency of the captured particles in the potential wave well increment $\Omega = \sqrt{ekE/m} \approx \gamma_D$.

The maximum value of the field amplitude, arising during the development of instability for beams whose length is several times longer than Langmuir wavelength, is equal and depends only on the total number of particles $E_{\max} \approx 2\pi eM$ [13-3].

It is not difficult to see that the maximum radiation intensity in the superradiation mode for beams whose length is several times the length of the Langmuir wave reaches values $P_{\text{sup}} = v \cdot E_{\max}^2 / 4\pi = \frac{\pi e^2 v}{4} M^2 \propto M^2$, i.e., it is proportional to the square of the number of all particles in the bunch $M = n_0 \cdot b$. Let us note that the intensity of spontaneous emission of the same (but still homogeneous, not modulated) beam-bunch of particles is

$$P_{\text{spont}} = v \cdot E_{\text{spont}}^2 / 4\pi = \pi e^2 v M \propto M, \quad (13.4)$$

and is proportional to the total number of particles.

Thus, superradiance is the result of the self-synchronization of emitters, the spontaneous field of which at the initial moment was incoherent (due to interference of the individual fields of each oscillator, in particular, due to random phase spread). It is important to emphasize that the field intensity in the case of the development of dissipative beam instability in a resonator or waveguide at a dissipation level determined as $\theta = c/\gamma_0 b$ and the intensity of superradiance of a particle bunch of particles, the longitudinal dimensions of which are b almost equal to the same density, coincide. Beam instability increments are almost equal to $\gamma_D^2 \approx \gamma_0^3 / \delta_D = \gamma_0^2 / \theta$ (where $\gamma_0 = \gamma|_{\delta_D=0}$).

A system of oscillators whose centers are fixed in radiation field.

The issues of oscillator emission in electronics have been actively discussed, starting from [13-4, 13-5]. An important circumstance is the synchronization conditions by the eigenfields of the radiation of the system of oscillators in the superradiance mode. It turns out that only when the nonlinearity of the oscillators is taken into account, it becomes possible to ensure the synchronization of the phases of the field and the oscillator [13-6] (see also [13-7]). Let us consider an oscillator whose charge (electron) moves along the OX axis, i.e. $x(t) = i \cdot a \cdot \exp\{-i\omega t + i\psi\}$, while $\text{Re } x = a \cdot \sin(\omega t - \psi)$, where $\vec{r} = (x(t), 0, z_0)$. In this case, the velocity and current can be written as $dx/dt = a \cdot \omega \cdot \exp\{-i\omega t + i\psi\}$ and $J_x = -e \cdot dx/dt = -e \cdot a \cdot \omega \cdot \exp\{-i\omega t + i\psi\}$.

The equation describing the field excitation by the oscillator current takes the form

$$\frac{\partial^2 E_x}{\partial z^2} - \frac{1}{c^2} \frac{\partial^2 D_x}{\partial t^2} = \frac{4\pi}{c^2} \frac{\partial J_x}{\partial t} = \frac{4\pi}{c^2} \cdot e \cdot a \cdot \omega^2 \cdot i \cdot \exp\{-i\omega t + i\psi\} \cdot \delta(z - z_0). \quad (13.5)$$

The dielectric constant of the medium in the absence of oscillators is set equal to unity $\epsilon_0 = 1$. Let us seek a solution for the amplitude of the electric field in the form $\vec{E} = (E \cdot \exp\{-i\omega t + ikz\}, 0, 0)$, that is $E_x = E \cdot \exp\{-i\omega t + ikz\}$, assuming a slow change in the complex amplitude $E_x(t, z)$:

$$\left| \frac{1}{E_x(t, z)} \frac{\partial}{\partial t} E_x(t, z) \right| \ll \omega, \quad \left| \frac{1}{E_x(t, z)} \frac{\partial}{\partial z} E_x(t, z) \right| \ll k. \quad (13.6)$$

Generally speaking, the field excited in the system of oscillators consists of the sum of all the fields of individual oscillators.

The field of the waveguide or resonator. However, the resonator or waveguide can form the field in such a way that the form of the field will not depend on the radiation of individual oscillators. Note that such a field, generally speaking, should consist of traveling waves in two directions ($k > 0$)

$$E_x = E_+ \cdot \exp\{-i\omega t + ikz\} + E_- \cdot \exp\{-i\omega t - ikz\}, \quad (13.7)$$

where the slowly varying complex wave amplitude has the form $E_{\pm} = |E_{\pm}| \cdot \exp\{i\varphi_{\pm}\}$. The interaction of oscillators with these fields can be described by the equation

$$2i\omega_0 \left(\frac{\partial E_{\pm}}{\partial t} + \delta_D \right) = -e\omega^2 \frac{4\pi n_0}{N \cdot 2i} \int a_s dz \cdot \exp\{i\psi_s \mp ikz\} \cdot \delta(z - z_s), \quad (13.8)$$

where added δ_D is the decrement of wave absorption in the absence of sources, $A_j = a_j \exp(i\psi_j)$.

Let us represent the equations of motion in the form

$$\frac{d}{dt} \frac{v_i}{\sqrt{1 - \frac{|v_i|^2}{c^2}}} + \omega^2 x_i = -\frac{e}{m} E_x(z_i, t), \quad (13.9)$$

where $x_i(t) = i \cdot a_i \cdot \exp\{-i\omega t + i\psi\} = iA \cdot \exp\{-i\omega t\}$,

$$v_i = \omega \cdot a_i \cdot \exp\{-i\omega t + i\psi\} = \omega A \cdot \exp\{-i\omega t\}.$$

Using the following notation

$$\frac{e |E(t)| \exp\{i\varphi\}}{m \gamma_0 \omega_0 a_0} = E(t), \quad \gamma_0 t = \tau_0, \quad \gamma_0^2 = \pi e^2 n_0 / m = \omega_{pe}^2 / 4, \quad A_j = a_j / a_0,$$

$kz_j = 2\pi Z_j$, $\theta = c / \gamma_0 b = \delta / \gamma_0$, $\alpha = \frac{3\omega}{4\gamma_0} (k_0 a_0)^2$ takes into account the weak dependence of the relativistic particle mass on speed. Let us write (13.8) and (13.9) in the form

$$\frac{\partial}{\partial \tau_0} E_{\pm} + \theta \cdot E_{\pm} = \frac{1}{N} \sum_{j=1}^N A_j \cdot \exp i\{\mp 2\pi Z_j\}, \quad (13.10)$$

$$\frac{d}{d\tau_0} A_j - i\alpha (A_j | A_j|^2) = -\frac{1}{2} [E_+ \cdot \exp i\{2\pi Z_j\} + E_- \cdot \exp i\{-2\pi Z_j\}]. \quad (13.11)$$

You can get the law of conservation of energy in the form

$$\left(\frac{\partial}{\partial \tau_0} + 2\theta\right) \{|E_+|^2 + |E_-|^2\} = 2 \frac{\partial}{\partial \tau_0} \sum_{j=1}^N |A_j|^2, \quad (13.12)$$

Let us determine the total radiation field of the oscillators in the same variables and in the same volume (see annex XVII)

$$E_x(Z, \tau_0) = \frac{2}{N\theta} \sum_{s=1}^N A_s \left(e^{i2\pi(Z-Z_s)} \cdot \theta(Z-Z_s) + e^{-i2\pi(Z-Z_s)} \cdot \theta(Z_s-Z) \right). \quad (13.14)$$

Taking into account the resonator field and the total field of individual oscillators (13-15), system (13-10) –(13-11) can be written as

$$\frac{\partial}{\partial \tau_0} E_{\pm} + \theta \cdot E_{\pm} = \frac{1}{N} \sum_{j=1}^N A_j \cdot \exp i\{\mp 2\pi Z_j\}, \quad (13.15)$$

$$\frac{d}{d\tau_0} A_j - i\alpha A_j^3 = -\frac{1}{2} [E_+ \cdot \exp i\{2\pi Z_j\} + E_- \cdot \exp i\{-2\pi Z_j\}] - \frac{1}{2} E_x(Z, \tau_0). \quad (13.16)$$

Dissipative instability regime. Let us consider the dissipative instability regime below. If there is no distinguished radiation direction, with a sufficiently large amount of radiation loss, the decrement of which can be determined from the condition $\delta_D > \partial E / E \partial t$

$$\delta_D = \left(\int_S c \langle E \rangle^2 / 4\pi \right) \cdot dS / \int_V (\langle E \rangle^2 / 4\pi) \cdot dV \approx c / b, \quad (13.17)$$

here $b = n\lambda = 2\pi cn / \omega$, at the same time, without violating generality, the restriction to one wavelength can be taken in calculations.

Equation (13.10) in this case takes the form

$$E_{\pm} = \frac{1}{N\theta} \sum_{j=1}^N A_j \cdot \exp i\{\mp 2\pi Z_j\}, \quad (13.18)$$

and the equation of motion (13.11) does not change, but can be represented as it follows

$$\frac{d}{d\tau} A_j - i\alpha(A_j | A_j|^2) = -\frac{1}{2} E(Z_j) = -\frac{1}{N} \sum_{i=1}^N A_i \text{Cos}\{2\pi(Z_j - Z_i)\} \quad (13.19)$$

where the time scale is changed $\tau \rightarrow \tau/\theta$ and the equation for the field can be written as

$$E(Z_j) = E_+ \cdot \exp i\{2\pi Z_j\} + E_- \cdot \exp i\{-2\pi Z_j\} = \frac{2}{N\theta} \sum_{i=1}^N A_i \text{Cos}\{2\pi(Z_j - Z_i)\} \quad (13.20)$$

The energy conservation law in this case takes the form

$$\sum_{j=1}^N \frac{d |A_j|^2}{d\tau} = -\text{Re} \sum_{j=1}^N E(Z_j) A_j^*, \quad (13.21)$$

let us note that in this case $\{|E_+|^2 + |E_-|^2\} = -\text{Re} \sum_{j=1}^N E(Z_j) A_j^*$.

In this case, the field $E(Z_j)$ is the field of induced radiation. It is not difficult to see the nature of the formation of coherence of particle radiation under the action of a waveguide or resonator field. Neglecting relativistic corrections, the equation for the oscillator phase ψ_s can be written as

$$\partial \psi_s / \partial t = -(e |E| / m\omega a_0) \cdot \text{Sin}(\varphi - \psi_s) = -(\Omega / n_h) \cdot \text{Sin}(\varphi - \psi_s), \quad (13.22)$$

where $ea_0 |E| \omega / m\omega^2 a_0^2 = 2d |E| / n_h \hbar = \Omega / n_h$, $n_h \gg 1$ is the oscillator energy expressed by the number of field quanta.

For oscillators in the quantum case $n_h = 1$, and Ω is the Rabi frequency. Obviously, the coordination time - synchronization of the phase of the oscillator with the phase of the field (in the place where the particle is located) n_h / Ω is of the same order of magnitude for all oscillators in volume. Let us recall that the reciprocal of the Rabi frequency Ω^{-1} in quantum mechanics is proportional to the probability of induced radiation [13-8, 13-9]. This is the difference between the oscillators of the classical and quantum systems, where in the latter case the intensities of the spontaneous radiation fields are many orders of magnitude lower than the intensities of the induced radiation.

The intensity of the fluctuations of the spontaneous field is proportional to the number of particles, and the intensity of the induced field is proportional to the square of the number of emitting particles. With a large number of particles, the difference in the intensities of spontaneous and induced radiation is significant. But when modeling, the number of particles cannot be so large and the intensity of spontaneous emission – fluctuations can be great, which does not correspond to physical reality. In addition, classical oscillators are capable of emitting a large number of field quanta, because for them $n_h \gg 1$, therefore, care should be paid to the results of modeling spontaneous emission, fluctuations, and superradiation modes of classical systems.

If you go to the time scale $\tau = \gamma_0 t \rightarrow \gamma t = \gamma_0^2 b t / c = \gamma_0 t / \theta$, then the variables will look like $\frac{e |E(t)| \exp\{i\varphi\}}{m\gamma\omega a_0} = E(t)$, $\gamma t = \tau$, $\gamma^2 = \pi e^2 M / mc$,

$A_j = a_j / a_0$, $kz_j = 2\pi Z_j$, $\alpha = \frac{3\omega}{4\gamma} (k_0 a_0)^2$ and the dissipative excitation regime can be described by the equation

$$\frac{d}{d\tau} A_j - i\alpha (A_j | A_j|^2) = -\frac{1}{2} E(Z_j) = -\frac{1}{N} \sum_{i=1}^N A_i \text{Cos}\{2\pi(Z_j - Z_i)\}, \quad (13.23)$$

and for the field the expression is

$$E(Z) = [E_+ \cdot \exp i\{2\pi Z\} + E_- \cdot \exp i\{-2\pi Z\}] = \frac{2}{N} \sum_{i=1}^N A_i \text{Cos}\{2\pi(Z - Z_i)\}, \quad (13.24)$$

here, the time scale is slightly different $\tau_1 = \gamma t$; increment also changed, n_0 is the particle density per unit volume, $M = b \cdot n_0$, b – is the length of the space under consideration in the longitudinal direction (here, generally speaking, also $b = n\lambda = 2\pi cn / \omega$). The law of conservation of energy takes the form

$$\sum_{j=1}^N \frac{d |A_j|^2}{d\tau} = -\text{Re} \sum_{j=1}^N E(Z_j) A_j^*, \quad (13.25)$$

where summation over j is equivalent to summation over the space of the core.

It can be shown that when $\theta \gg 1$ solutions (13.10) – (13.11) for $[E_+ \cdot \exp i\{2\pi Z_j\} + E_- \cdot \exp i\{-2\pi Z_j\}] \rightarrow [E_+ \cdot \exp i\{2\pi Z_j\} + E_- \cdot \exp i\{-2\pi Z_j\}] / \theta$ and $\tau \rightarrow \tau / \theta$ coincide with the solutions of system (13-23) – (13-24).

Superradiation mode. In the absence of a resonator field, only equation (13.16) remains in the form

$$\frac{d}{d\tau_0} A_j - i\alpha A_j^3 = -\frac{1}{2} E_x(Z, \tau_0), \quad (13.26)$$

where for $E_x(Z, \tau_0)$ the expression (13.14) is valid for the field. However, passing to the time scale of the corresponding dissipative regime (13.23) – (13.24) $\tau \rightarrow \tau/\theta$, we shall rewrite equation (13-26) in the form

$$\frac{d}{d\tau} A_j - i\alpha A_j^3 = -\frac{1}{2} E_{Dx}(Z, \tau_0), \quad (13.27)$$

where

$$E_{Dx}(Z, \tau_0) = E_x(Z, \tau_0)/\theta = \frac{2}{N} \sum_{s=1}^N A_s \left(e^{i2\pi(Z-Z_s)} \cdot \theta(Z-Z_s) + e^{-i2\pi(Z-Z_s)} \cdot \theta(Z_s-Z) \right). \quad (13.28)$$

Let us consider the field excitation in the resonator whose size b is equal to the wavelength (without loss of generality, the results are generalized to the case of several wavelengths), the group radiation speed is C , and the effective field attenuation decrement is equal to $\delta_d = c/b$.

In the dissipative mode, when the increment of the process is equal to $\gamma = \gamma_0^2 / \delta_d = \gamma_0 / \theta$, in this case $\delta_d = \frac{c}{b} > \gamma_0 = \sqrt{\pi e^2 n_0 / m}$, equations (13.19) and (13.20) describe the process of excitation of such a resonator field $E(Z_j)$ by the oscillators $A_s(\tau=0) = A_{s0} = 1$ located along the length b in the dissipative mode (Fig. 13.1 a). If there is no waveguide field, the same oscillators also located along the same length b can generate a field E_{Dx} (13.28) in the superradiation mode (Fig. 13.1. b). The increments of these two types of generation and the maximum field amplitudes are similar.

It is of interest to compare the excited field with a field of another type, which the same particles could generate (shown in dashed line in Fig. 13.1).

It is curious that in all cases the superradiance field would turn out to be larger than the resonator field. You should also pay attention to the fact that the maximum value of the superradiance field is two times less than the most possible value of the field if all particles were at one point in space (Fig. 13.1 b). That is, the degree of coherence of superradiance, as well as in the cases discussed in section 12 and above in this section, is approximately 25%. However, at lower α , maximum value of the superradiance field and degrees of the coherence decreases and, when $\alpha = 0$, there is no field excitation.

Let us note that a small number of particles give rise to noticeable oscillations of the initial field; therefore, the generation processes, especially in the superradiation mode, do not need an initiating field. However, the use of such a field, even slightly exceeding the fluctuation (spontaneous), nevertheless leads to a noticeable acceleration of the process, at least in the classical case.

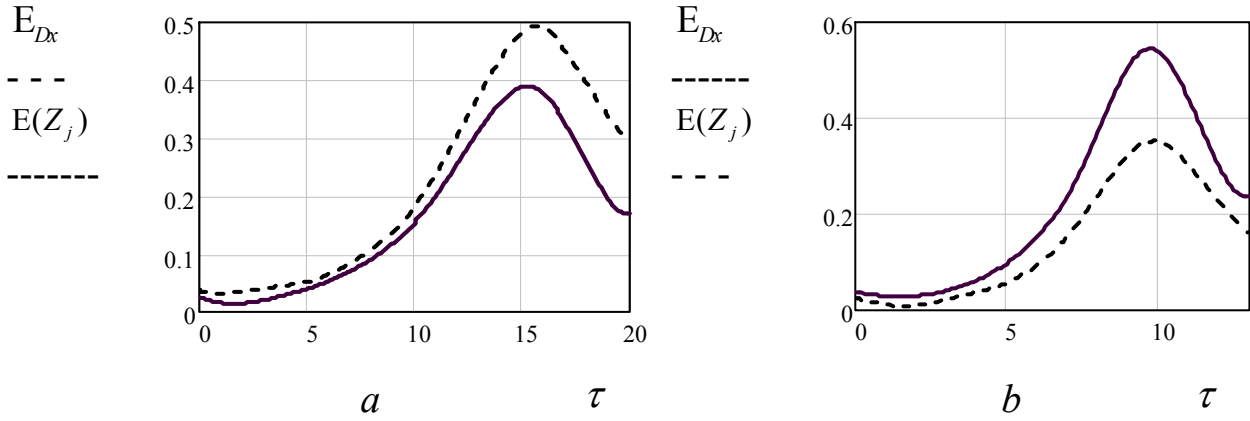


Fig. 13.1. a). The dependence of the maximum amplitude of the resonator field $E(Z_j)$ (13.20) in volume on time (solid line) and the estimate of the total field E_{Dx} (13.28) that these particles could generate (dotted line); b) the time dependence of the maximum amplitude of the superradiance field E_{Dx} (13.28) in the bulk of the bunch (solid line) and the estimate of the resonator field $E(Z_j)$ (13.20), which could generate the same particles (dotted line)

The growth of the field in the superradiance regime occurs from the level of fluctuations (i.e., from the level of spontaneous emission), the intensity of which is proportional to $1/\sqrt{N}$, where N is the number of particles. In real conditions, N is large and the initial field intensity in the superradiance regime is very low. But in the example above $N = 3600$, and only with weak relativism of $\alpha \ll 1$, it is necessary to use an external field.

Dissipative regime in a quantum system. We are interested in the case of a large level of radiation loss ($\Theta > 1$). From equation (4.7) – (4.10) of section 4 for $\delta_D > \tilde{\gamma}_0 = \Omega_0 / \sqrt{2} = 2 |d_{ab}| \cdot |E_\mu| / \hbar$

$$\frac{\partial M}{\partial \tau} = -N, \quad (13.29)$$

$$\frac{\partial N}{\partial \tau} = M \cdot N, \quad (13.30)$$

where $M = \mu / \mu_0$, $N = 4(\delta_D^2 / \tilde{\gamma}_0^2) \cdot (N / \mu_0)$, $N \ll \langle E^2 \rangle / 4\pi\hbar\omega$. The increment of such instability is equal to $\gamma = \tilde{\gamma}_0^2 / \delta_D \gg \gamma_{12}$, that is, it significantly exceeds the natural line width, and the role of the dissipative increment γ_0 is taken by the Rabi frequency $\Omega_0 = 2 |d_{ab}| |E_\mu| / \hbar$, where $\langle E^2 \rangle_\mu = 2 |E_\mu|^2 = [4\pi\hbar\omega\mu_0]$. Along the length of the system, as in Section 4, let us arrange the sectors

$$N_j(\tau = 0) = 2 \cdot N(\tau = 0) \cdot \text{Sin}^2 \left\{ 2\pi \frac{j}{S} + \alpha \right\}, \quad (13.31)$$

where

$$N(\tau) = \frac{1}{S} \sum_{j=1}^S N_j(\tau), \quad (13.32)$$

Equations (13.29) – (13.30) for sectors have the form:

$$\frac{\partial M_j}{\partial \tau} = -N_j, \quad (13.33)$$

$$\frac{\partial N_j}{\partial \tau} = M_j \cdot N_j, \quad (13.34)$$

where

$$M(\tau) = \frac{1}{S} \sum_{j=1}^S M_j(\tau), \quad (13.35)$$

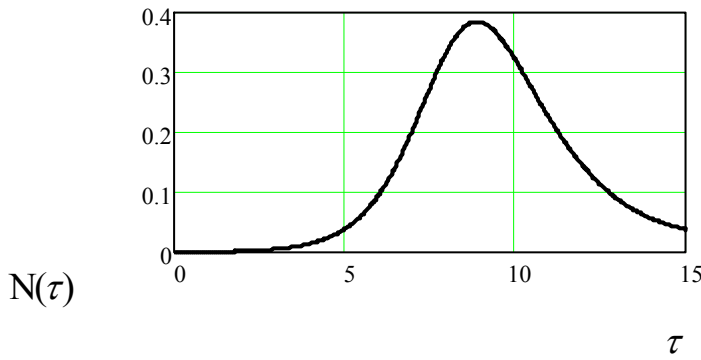


Figure 13.2. The behavior of the number of quanta $N(\tau)$ in the cavity volume over time.

$$N(\tau = 0) = 1/3600, \quad M(\tau = 0) = M_j(\tau = 0) = 1, \\ S = 100, \quad b = 2\pi c / \omega$$

Superradiance regime in the quantum case. Let us consider the behavior of quantum emitters, the dimensions of which are much smaller than the length of the emitted wave, and the wave functions of which do not overlap and their interaction is determined only by the electromagnetic field. As in Section 4, we present the inversion and polarization for each emitter $\bar{\mu} = (\rho_{aa} - \rho_{bb})$ and \bar{p} , as well as the electric

field $E + E^* = A(t) \cdot \exp\{-i\omega t\} + A^*(t) \cdot \exp\{i\omega t\}$. An equation similar to (4.1) for a field which is generated by each emitter, takes the form

$$\frac{\partial^2 E}{\partial t^2} - c^2 \frac{\partial^2 E}{\partial z^2} = 4\pi\omega^2 \cdot \bar{p} \cdot e^{-i\omega t} \cdot \delta(z_0), \quad (13.36)$$

whence we define

$$A(z, t) = \frac{i \cdot 2\pi \cdot \omega \cdot N}{c} \cdot \frac{1}{N} \sum_s \bar{p}(z_s, t) \cdot e^{ik|z-z_s|}. \quad (13.37)$$

Using the notation $P_j = P(z_j, \tau)$, $M_j = M(z_j, \tau)$, $\mu_{01} = \mu_j(\tau = 0)$,

$$t = \tau / \gamma, \quad |E|^2 = 4\pi\hbar\omega N, \quad |2A|^2 = 2 \cdot \frac{|d_{ba}|}{\gamma \cdot \hbar} |E|^2, \quad \gamma = \frac{2\pi \cdot \omega \cdot |d_{ba}|^2 \cdot \mu_{01} \cdot n_0 \cdot b}{\hbar c}$$

$$z = \frac{2\pi}{k} Z, \quad \mu = \mu_{01} \cdot N, \quad \bar{p} = |d_{ab}| \cdot \mu_0 \cdot P, \quad \Gamma_{12} = \frac{\gamma_{12}}{\gamma}, \quad n_0 \cdot b = N, \quad \text{write down}$$

the system of equations, describing the generation mode of a quantum system, similar to superradiance (see annex XXVIII)

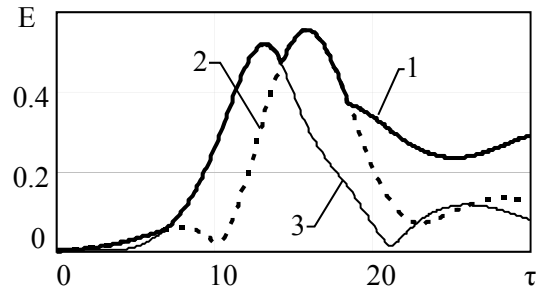
$$\frac{d}{dt} M_j = -2 \cdot [P_j^* A_j + P_j A_j^*], \quad (13.38)$$

$$\frac{d}{dt} P_j = M_j \cdot A_j, \quad (13.39)$$

where

$$A(Z, \tau) = \frac{1}{N} \sum_s P(Z_s, \tau) \cdot e^{i2\pi|Z-Z_s|}. \quad (13.40)$$

For 4000 emitters distributed at the wavelength, at $P_j(\tau = 0) = P_0 \exp(i\varphi)$, φ is a random variable $\varphi \in (0 \div 2\pi)$, $P_0 = 0.1$, $M(\tau = 0) = 1$, $\Gamma_{12} = 0$, we obtain the following results of the numerical solution. In fig. 13.3, the time dependences of the field amplitude to the left, to the right of the system and the maximum inside the emitter and the average inversion of the system are presented. The field strength has two approximately equal maxima at times $\tau = 13.2$ ($E = 0.52$) and $\tau = 15.8$ ($E = 0.555$). The first maximum is at the right edge of the system ($Z = 1$), the second is at the left ($Z = 0$). These two values of the field strength maxima in this normalization in Fig. 13.3 correspond to values $|E|^2 = |2A|^2$ equal to 0.27 and 0.31, respectively.



Puc. 13.3. Dependence of the field amplitude on time, 1 – $\max_Z(E(Z, \tau))$, 2 – $E(Z = 0, \tau)$, 3 – $E(Z = 1, \tau)$

We draw attention to the fact that the increment γ of the superradiance process is equal to the increment of the dissipative instability $\tilde{\gamma}_0^2 / \delta_D$ considered above in the quantum model at the same values of the Rabi frequency and decrement δ_D

$$\gamma = \frac{2\pi \cdot \omega \cdot |d_{ba}|^2 \cdot \mu_{01} \cdot n_0 \cdot b}{\hbar c} = \frac{\tilde{\gamma}_0^2}{\delta_D} = \frac{\Omega_0^2}{2\delta_D},$$

and the value of the electric field strength $E = 2|A|$ in the accepted normalization is related to the value used above N (see the notation after formula (13.30))

$$|2E|^2 = |2A|^2 = 4 \frac{\delta_D^2 |d_{ba}|^2 |E_\mu|^2 |E|^2}{\Omega_0^4 \hbar^2 \cdot 2\pi \hbar \omega \mu_0} = 2 \frac{\delta_D^2 N}{\Omega_0^2 \mu_0} = 4 \frac{\delta_D^2}{\tilde{\gamma}_0^2 \mu_0} N = N,$$

which makes it possible to compare the efficiency of excitation of oscillations in the case of dissipative instability and in the superradiance regime.

Thus, in the quantum model, the dissipative instability and the superradiance regime are characterized by the same process increments, and the values of the achieved generation intensity turn out to be comparable.

In the case of dissipative instabilities in waveguides, the initial amplitude of the integral field is given, while during generation in the superradiance regime, the field grows from the fluctuation (spontaneous) level. With a large number of emitters, this level is very small and the development time of the process becomes very long. Therefore, usually some external initiating field is used to speed up the process.

References to section 13

13-1. Kuklin V. M. The role of deduction and dissipation of energy in the formation of spacious non-linear structures in non-important middles / V. M. Kuklin // UFZh. Look around. – 2004. – V. 1. – № 1. – P. 49–81 (in Ukrainian).

13-2. Zagorodny A. G., Kuklin V. M. Features of radiation in nonequilibrium media. in the book. Problems of theoretical physics. Scientific works / V. A. Buts and others; edit. V. M. Kuklin. – Kh. : KhNU, 2014. – Issue. 1. – P. 13–82 (in Ruuaian).

13-3. Kirichok A. V., Kuklin V. M., Mischin A. V., Pryimak A. V. Modeling of superradiation processes driven by an ultra-short bunch of charged particles moving through plasma/ Problems of Atomic Science and Technology, 2015 N 4. – series “Plasma Electronics and New Methods of Acceleration” P.255–257.

13-4. Gaponov A. V. Instability of a system of excited oscillators with respect to electromagnetic excitations ZhETP 1960. V. 39. – N. 2. – P. 326–321 (in Russian).

13.5. Gaponov A. V., Petelin M. I., Yulpatov V. K. Induced emission of excited classical oscillators and its use in high-frequency electronics. Izv. Universities. Radiophysics 1967. V. 10, – No. 9–10. p. 1414–1433.

13-6. Il'inskii Yu. A., Maslova N. S. Classical analog of superradiance in a system of interacting nonlinear oscillators // Zh. Eksp. Teor. Fiz. – 1988. – Vol. 91. – No. 1. – P. 171–174 (in Russian).

13-7. Kuklin V. M., Litvinov D. N., Sporov V. E. Superradiance of stationary oscillators // Problem of Atomic science and technology. Ser. Plasma Electronics and new methods of acceleration. Issue 10. – N. 4 (116). – 2018. – P. 217–220.

13-8. Davydov A. S. Quantum Mechanics Fizmatgiz. 1963. – 748 p. (in Russian).

13-9. Allen L., Eberly J. Optical resonance and two-level atoms. Witey-Interscicitce Publication John Witty and Sons. New York – London – Sydney – Toronto. 1975. – 222 p.

CHAPTER 6.

Cyclotron instability of particle flows

The excitation of TE and TM electromagnetic waves in magnetoactive waveguides is considered. The low-density plasma is taken into account in the traditional equations of the gyrotron, and the change in the operating point and the generation level in this case is shown. It is noted that the laws of energy conservation corresponding to elementary processes under the conditions of anomalous and normal Doppler are also satisfied for more complex beam systems with stimulated emission of the considered waves of different polarization. The finite Larmor radius, which is comparable with the characteristic transverse inhomogeneity of the wave field, is taken into account, in particular for the case of the anomalous Doppler effect in a plasma waveguide.

SECTION 14.

EXCITATION OF TE WAVES BY A BEAM OF CHARGED PARTICLES

Generally speaking, there are several approaches to the theoretical description of nonlinear modes of excitation of oscillations by electron beams moving in an external magnetic field, or so-called oscillator beams – rotating electrons.

As a rule, in most works, the Larmor radius of rotation of these electrons is small, smaller than the characteristic size of the transverse field inhomogeneity, and less or on the order of the beam thickness (moreover, the beam electrons fairly uniformly fill a plane or cylindrical layer).

The scientific school of A. V. Gaponov in the USSR developed methods for describing the excitation of natural oscillations of waveguides in the presence of an external magnetic field by an electron beam [14-1, 14-2], which helped to develop many (vacuum) instruments and devices.

Then, it became necessary to study the processes of excitation by beams of charged particles (usually electrons) of cyclotron oscillations of plasma, for its further heating, mainly for the purposes of controlled thermonuclear fusion. This led to a whole series of works which were published by Kharkov scientists (see, for example, [14-3 – 14-5]). These papers were devoted to the nonlinear theory of wave excitation in a magnetically active plasma medium (and waveguides) by charged particle beams, in particular, with finite values of the Larmor radius [14-6, 14-7]. In these works it was also shown that the laws of conservation of elementary effects of anomalous and normal Doppler are also satisfied for more complex beam systems with stimulated emission.

Similar original descriptions of nonlinear processes of excitation of oscillations by beams of charged particles, where the main attention was paid to

taking into account already relativistic effects and the limitations of complex resonant systems, were also considered by the authors [14-8 – 14-12].

The field of an electromagnetic wave in a cylindrical waveguide is not difficult to obtain from the equations

$$[\nabla, \vec{E}] = -\frac{1}{c} \frac{\partial \vec{H}}{\partial t}, \quad [\nabla, \vec{H}] = \frac{1}{c} \frac{\partial \vec{D}}{\partial t} + \frac{4\pi}{c} \vec{J}, \quad (14.1)$$

where \vec{J} is the current of a beam of electrons that are in a constant magnetic field $\vec{B}_0 = (0, 0, B_0)$. The dispersion relation determining the relationship of the wave vector $\vec{k} = (\vec{k}_\perp, k_z)$ with the frequency ω for perturbations in the form $\exp\{-i(\omega t - k_z z - \vec{r}_\perp \cdot \vec{k}_\perp)\}$ can be written as

$$D(\omega, \vec{k}) \equiv (k_z^2 + k_\perp^2 - \omega^2 / c^2) / (k_z^2 - \omega^2 / c^2) = 0. \quad (14.2)$$

In the absence of a particle beam, for the field of the TE wave, which does not have a component of the electric vector in the direction of propagation in a smooth cylindrical waveguide of radius r_W , the expressions are

$$B_z = b(z, t) J_m(k_\perp r) \exp(-i\omega t + ik_z z + im\theta), \quad (14.3)$$

$$(B_\theta, E_r) = \left\{ -\frac{k_z m}{r k_\perp^2}, -\frac{\omega m}{c r k_\perp^2} \right\} b(z, t) J_m(k_\perp r) \exp(-i\omega t + ik_z z + im\theta), \quad (14.4)$$

$$(B_r, E_\theta) = \{ik_z / k_\perp, -i\omega / c k_\perp\} b(z, t) J'_m(k_\perp r) \exp(-i\omega t + im\theta), \quad (14.5)$$

where the cylindrical coordinate system (r, θ, z) is used; b is the complex amplitude of the wave, m is an integer, $J_m(x)$ and $J'_m(x) = dJ_m(x)/dx$ is the Bessel function and its derivative. Usually, in order to describe the field in a waveguide, many authors use an auxiliary membrane function $\Psi_s = -i(c/\omega)J_m(k_\perp r)$ which satisfies the relation $(\Delta_\perp + k_\perp^2)\Psi_s = 0$ and boundary conditions $\frac{\partial \Psi_s}{\partial n} \Big|_s = \frac{\partial \Psi_s}{\partial r} \Big|_{r=0} = 0$.

Similarly, it can be stated that the field component E_θ vanishes at the boundary of the waveguide, which determines the values of the transverse wave number $k_\perp = k_{ms} = x_{ms} / r_W$, and x_{ms} – s root of the equation $dJ_m(x) / dx = 0$.

The electron beam occupies a cylindrical layer in the section of the waveguide. For definiteness, let us consider it to be sufficiently thin, assuming that all centers of Larmor rotation of electrons are at the same distance from the axis of the waveguide.

In order to go to a coordinate system which center coincides with the center of rotation of an individual electron in the beam (see annex XVIII), that is (R, Φ, z) , one can use the following relations (see, for example, [14-4, 14-13]):

$$\begin{aligned}
b_z &= B_z \\
b_\Phi &= B_\theta \sin(\Phi - \theta) + B_r \cos(\Phi - \theta) \\
b_R &= -B_\theta \cos(\Phi - \theta) + B_r \sin(\Phi - \theta) \\
e_R &= -E_\theta \cos(\Phi - \theta) + E_r \sin(\Phi - \theta) \\
e_\Phi &= E_\theta \cos(\Phi - \theta) + E_r \sin(\Phi - \theta)
\end{aligned} \tag{14.6}$$

Using the values of (14.3) and (14.5), we shall find the values of the components of the electromagnetic field in the coordinate system with the center of rotation of an individual electron

$$\begin{aligned}
(b_z, b_\Phi, e_R) &= b \sum_q J_q(k_{ms} r_c) J_{m+q}(k_{ms} r_B) \exp(-i\omega t + im\Phi + iq\Phi_c + i\pi m/2) \times \\
&\times \left(1, -\frac{k_z m}{r k_{ms}^2}, -\omega \frac{m+q}{k_{ms} c r} \right),
\end{aligned} \tag{14.7}$$

$$\begin{aligned}
(b_R, e_\Phi) &= b \sum_q J_q(k_{ms} r_c) J'_{m+q}(k_{ms} r_B) \exp(-i\omega t + ik_z z + im\Phi + iq\Phi_c + i\pi m/2) \times \\
&\times \left[ik_z / k_{ms}, -\frac{i\omega}{k_{ms} c} \right].
\end{aligned} \tag{14.8}$$

In this case $\Phi_c = \Phi_{c0} + \omega_B \cdot t$, $\Phi = \Phi_0 + \omega_B \cdot t$, where Φ_{c0} , Φ_0 are the slowly changing phases, which store information about the initial position of the beam particle (see annex XVII) $z = z_0 + v_z \cdot t$. In the case of resonance of the beam particles with the wave $\omega - k_z v_z \approx n\omega_B$, where $\omega_B = eB_0/m_e c$ is the electron cyclotron frequency, the relation holds $m + q = n$ and in the expressions (14.7) and (14.8), only the resonance terms can be retained:

$$(b_z, b_\Phi, e_R) = b \cdot J_{n-m}(k_{ms} r_c) J_n(a) \exp(2i\pi\zeta) \left[1, -\frac{k_z m}{r k_{ms}^2}, -\omega \frac{m+q}{k_{ms} c r} \right], \tag{14.9}$$

$$(b_R, e_\Phi) = b J_{n-m}(k_{ms} r_c) J'_n(a) \exp(2i\pi\zeta) \left[\frac{ik_z}{k_{ms}}, -\frac{i\omega}{k_{ms} c} \right], \tag{14.10}$$

where $\zeta = \frac{1}{2\pi} \left(-\omega t + n\omega_B t + m\Phi_0 + (n-m)\Phi_{c0} + \frac{\pi m}{2} \right)$, $a = k_{ms} r_B$, $r_B = v_\Phi / \omega_B$

is Larmor radius of the beam particle. It can be shown that the equation for the wave field takes the form

$$\begin{aligned}
&\omega D(\omega, \vec{k}) b + i \left[\frac{\partial D(\omega, \vec{k})}{\partial \omega} \frac{\partial b}{\partial t} - \frac{\partial D(\omega, \vec{k})}{\partial k} \frac{\partial b}{\partial z} \right] = \\
&= 4i \left[r_w^2 b^* J_m^2(x_{ms}) \left(1 - \frac{m^2}{x_{ms}^2} \right) \right]^{-1} \int_0^{r_w} r dr \int_0^{2\pi} d\theta \vec{J} \vec{E}^*,
\end{aligned} \tag{14.11}$$

where there is the group velocity of oscillation $v_g = \frac{\partial D(\omega, \vec{k})}{\partial k} / \frac{\partial D(\omega, \vec{k})}{\partial \omega}$, detuning is $\Delta = \text{Re}\{D(\omega, \vec{k}) / \gamma_e \frac{\partial D(\omega, \vec{k})}{\partial \omega}\}$, and $\Theta = \text{Im}\{D(\omega, \vec{k}) / \gamma_e \frac{\partial D(\omega, \vec{k})}{\partial \omega}\}$ is the decrement of wave attenuation in the absence of a beam, normalized to the process increment γ_e .

In a homogeneous extended waveguide, equation (14.11) is simplified and can be represented as

$$\left[\frac{d}{d\tau} - i\Delta + \Theta \right] E_e \exp\{i\varphi_e\} = \frac{i}{N} \sum_{j=1}^N a_j \cdot J'_n(a_j) \cdot \exp(-2\pi i \zeta_j) \quad (14.12)$$

where $E_e \exp\{i\varphi_e\} = e \cdot b \cdot J_{n-m}(k_{ms} \cdot r_c) / m_e \cdot c \cdot \gamma_e$, N is the number of particles simulating the beam. The equations of motion for the particles of the beam can be represented as it follows:

$$v_\Phi \frac{d\Phi_c}{dt} = \frac{e}{m_e} \left[e_R - \frac{v_z}{c} b_\Phi + \frac{v_\Phi}{c} b_z \right] = v_\Phi \frac{eb}{mc\omega_B} J_{n-m}(k_{ms}r_c) J_n(a) \exp(2i\pi\zeta) \times \left[\left(\omega_B - \omega \frac{n}{a^2} \right) + \frac{nv_z k_z}{a^2} \right], \quad (14.13)$$

$$\frac{dv_\Phi}{dt} = -\frac{e}{m_e} \left[e_\Phi + \frac{v_z}{c} b_R \right] = i \frac{e(\omega - k_z v_z) b}{mck_{ms}} J_{n-m}(k_{ms}r_c) J'_n(a) \exp(2i\pi\zeta), \quad (14.14)$$

$$\frac{dv_z}{dt} = -\frac{e}{m_e} \left[-\frac{v_\Phi}{c} b_R \right] = \frac{iek_z v_\Phi b}{mck_{ms}} = J_{n-m}(k_{ms}r_c) J'_n(a) \exp(2i\pi\zeta). \quad (14.15)$$

If to come to dimensionless quantities and use the value of the integral phase ζ , the system of equations for real variables can be written as (see, for example, [14-7])

$$\frac{dE_e}{d\tau} + \theta_e \cdot E_e = N^{-1} \cdot \sum_{j=1}^N a_j \cdot J'_n(a_j) \cdot \text{Sin}(2\pi\zeta + \varphi_e), \quad (14.16)$$

$$\frac{d\varphi_e}{d\tau} - \Delta_e = (E_e N)^{-1} \cdot \sum_{j=1}^N a_j \cdot J'_n(a_j) \cdot \text{Cos}(2\pi\zeta_j + \varphi_e). \quad (14.17)$$

The equations of motion of electrons in the field of this wave in the presence of a constant magnetic field are as it follows

$$2\pi \frac{d\zeta_i}{d\tau} = \eta_i + nE_e \cdot J_n(a_i) \cdot \left\{ 1 - \frac{n^2}{a_i^2} \right\} \cdot \text{Cos}(2\pi\zeta_i + \varphi_e), \quad (14.18)$$

$$d\eta_i / d\tau = -R_e \cdot E_e \cdot a_i \cdot J'_n(a_i) \cdot \text{Sin}(2\pi\zeta_i + \varphi_e), \quad (14.19)$$

$$da_i / d\tau = -n \cdot E_e \cdot J'_n(a_i) \cdot \text{Sin}(2\pi\zeta_i + \varphi_e), \quad (14.20)$$

where $\tau = \gamma_e t$,

$$\gamma_e^2 = 4e^2 \cdot \omega_B \cdot N_{b0} \cdot [m_e \cdot c \cdot k_{ms}^2 \cdot r_w \cdot J_m^2(x_{ms}) \cdot (1 - m^2 / x_{ms}^2) \cdot D_\omega]^{-1} \cdot J_{m-n}^2(k_{ms} \cdot r_C),$$

$$D_\omega = \partial D / \partial \omega = \partial \{ [\omega^2 - (k_z^2 + k_{ms}^2) c^2] / [\omega^2 - k_z^2 c^2] \} / \partial \omega |_{D=0},$$

$$R_e = k_z^2 \cdot \omega_B / k_{ms}^2 \cdot \gamma_e, \quad E_e = e \cdot b \cdot J_{m+n}(k_{ms} \cdot r_C) / m_e \cdot c \cdot \gamma_e,$$

$\eta = (k_z \cdot v_z - \omega + n \cdot \omega_B) / \gamma_e$, $a = k_{ms} r_B = k_{ms} v_\Phi / \omega_B$, $\omega_B = eB / m_e c$, N_{b0} is the number of particles of the unperturbed beam per unit length. Here b is the wave amplitude.

However, the modes under discussion describe the interaction of an integral, common field with particles, and the particles themselves do not directly interact with each other.

The situation changes if it is necessary to summarize the radiation fields of each particle, with that particles can interact with each other due to the influence of radiated fields. This process refers to the **mode of superradiation of the oscillator system**.

The case of radiation of an individual particle (from the total number equal to N) should be considered somewhat differently. The equation for the field emitted by an individual particle $B_j = e \cdot b_j \cdot J_{m+n}(k_{ms} \cdot r_C) / m_e \cdot c \cdot \gamma_e$, can be written as

$$v_g \frac{\partial B_j}{\partial z} = i \frac{a_j}{N} J'_n(a_j) \exp\{-2\pi i \zeta_j\} \exp\{-ik_z z_j\} \cdot \delta(z - z_j), \quad (14.21)$$

or

$$\frac{\partial B_j}{\partial z} = \lambda \cdot \delta(z - z_j)$$

where $\lambda = i \frac{a_j}{N v_g} J'_n(a_j) \exp\{-2\pi i \zeta'_j\} \exp\{-ik_z z_j\}$, solution of which, generally

speaking, is $B_j = C + \lambda \cdot \theta(z - z_j)$, where C is a constant that should be determined.

Since for the wave emitted by the oscillator the equation $D(\omega, k) = 0$ is true,

whose roots are $k_{z,2} = \pm \text{Re} D(1 + i \text{Im} D / \text{Re} D) \approx \pm (\frac{\omega^2}{c^2} - k_\perp^2)^{1/2} (1 + i0)$, then for the

wave, propagating in the direction $z > z_j$, the wave number is $k_z = k_{z1} > 0$ and

constant value C should be chosen equal to zero in order to avoid unlimited

growth of the field at infinity. For a wave, propagating in the direction

$\xi = \frac{k_z z}{2\pi} < \xi_j = \frac{k_z z_j}{2\pi}$, the wave number is $k_z = k_{z2} < 0$, and constant value should

be chosen equal to $-\lambda$ for the same reason. The field amplitude in this case is

$$B_j(\xi) = i \frac{a_j}{N v_g} J'_n(a_j) \exp\{-2\pi i \zeta_j\} [\exp\{2\pi i(\xi - \xi_j)\} \cdot U(\xi - \xi_j) + \exp\{-2\pi i(\xi - \xi_j)\} \cdot U(\xi_j - \xi)] \quad (14.22)$$

where $U(z)=1$ at $z \geq 0$ and $U(z)=0$ at $z < 0$. Let us draw attention to the fact that the direction of the intensity vector of the longitudinal component of the magnetic field in this case does not depend on the direction of wave propagation. This is due to the suppression of the intrinsic magnetic field of a rotating electron by radiation of waves in both directions.

Obviously, the equation for the field of the system of oscillators can be written as

$$B(\xi) = i \frac{1}{2N\mathcal{G}} \sum_{j=1}^N a_j J'_n(a_j) \exp\{-2\pi i \zeta_j\} [\exp\{2\pi i(\xi - \xi_j)\} \cdot U(\xi - \xi_j) + \exp\{-2\pi i(\xi - \xi_j)\} \cdot U(\xi_j - \xi)] \quad (14.23)$$

where $\mathcal{G} = 2V_g N_{ob} / M = 2v_g / d \cdot \gamma_e$ is the ratio of the maximum increment δ to the decrement of attenuation due to radiation from the ends of the system $2v_g / d$.

It is important to note that in such designations the ratio of the wave energy at the length of the system $\xi_M = 2\pi k_z d$ to the particle energy is proportional to the value $\int_0^{\xi_M} |B(\xi)|^2 d\xi / \frac{1}{N} \sum_{i=1}^N a_{i0}^2$, and since the ratio of the energy radiated from the system to the total field energy during the time $1/\delta$ in the system is equal to \mathcal{G} , the efficiency of the system (if a unit of time is chosen $1/\delta$) proportional to the value $\frac{\mathcal{G}}{\xi_M} \int_0^{\xi_M} |B(\xi)|^2 d\xi / \frac{1}{N} \sum_{i=1}^N a_{i0}^2$. The equations of motion are then transformed as it follows

$$\left(\frac{n}{\delta}\right) v_\Phi \frac{d\Phi_c}{dt} = \left(\frac{n}{\delta}\right) \frac{e}{m_e} \operatorname{Re} \left[e_R - \frac{v_z}{c} b_\Phi + \frac{v_\Phi}{c} b_z \right] = \left(\frac{n}{\delta}\right) \frac{v_\Phi e}{mc\omega_B} J_{n-m}(k_{ms} r_c) \left[\left(\omega_B - \omega \frac{n}{a^2} \right) + \frac{nv_z k_z}{a^2} \right] J_n(a) \times \\ \times \operatorname{Re} b \exp(2i\pi\zeta) = mv_\Phi \left(1 - \frac{n^2}{a^2} \right) J_n(a_i) \operatorname{Re} \exp(2i\pi\zeta_i) \cdot B(\xi_i);$$

$$\left(\frac{k_{ms}}{\omega_B \delta}\right) \frac{dv_{\Phi i}}{dt} = \frac{da_i}{d\tau} = -\left(\frac{k_{ms}}{\omega_B \delta}\right) \frac{e}{m_e} \left[e_\Phi + \frac{v_z}{c} b_R \right] = \left(\frac{k_{ms}}{\omega_B \delta}\right) \frac{e(\omega - k_z v_z)}{m_e c k_{ms}} J_{n-m}(k_{ms} r_c) J'_n(a_i) \operatorname{Re} i b \exp(2i\pi\zeta'_i) = \\ = n \left[\frac{e}{\delta m_e c} J_{n-m}(k_{ms} r_c) \right] J'_n(a_i) \operatorname{Re} i \exp(2i\pi\zeta_i) b = n J'_n(a_i) \operatorname{Re} i \exp(2i\pi\zeta_i) \cdot B(\xi_i);$$

$$\frac{k_z}{\delta^2} \frac{dv_{zi}}{dt} = -\frac{k_z}{\delta^2} \frac{e}{m_e} \left[-\frac{v_\Phi}{c} b_R \right] = \frac{k_z}{\delta^2} \frac{ie k_z v_{\Phi i}}{m_e c k_{ms}} J_{n-m}(k_{ms} r_c) J'_n(a_i) \operatorname{Re} i b \exp(2i\pi\zeta_i) = \\ = a_i \left(\frac{k_z^2 \omega_B}{k_{ms}^2 \delta} \right) \left[\frac{e}{m_e c \delta} J_{n-m}(k_{ms} r_c) \right] J'_n(a_i) \operatorname{Re} i b \exp(2i\pi\zeta_i) = a_i R \cdot J'_n(a_i) \operatorname{Re} i \exp(2i\pi\zeta_i) \cdot B(\xi_i);$$

Using the representation $B(\xi_i)$, in order to change the phase $n \frac{d\Phi_{ci}}{d\tau}$, we shall obtain the expression

$$n \frac{d\Phi_{ci}}{d\tau} = -\frac{n}{\vartheta} \left(1 - \frac{n^2}{a^2}\right) J_n(a_i) \frac{1}{2N} \sum_{j=1}^N a_j J'_n(a_j) [\text{Sin}\{2\pi(\zeta_{i+} - \zeta_{j+})\} \cdot U(\zeta_{i+} - \zeta_{j+}) + \text{Sin}\{2\pi(\zeta_{i-} - \zeta_{j-})\} \cdot U(\zeta_{j-} - \zeta_{i-})]$$

Similarly, we can write the equation for $2\pi\zeta_i$ and other equations of the system describing the process of superradiance

$$2\pi \frac{d\zeta_i}{d\tau} = \eta_i - n \cdot J_n(a_i) \cdot \left\{1 - \frac{n^2}{a_i^2}\right\} \frac{1}{2N\vartheta} \sum_{j=1}^N a_j J'_n(a_j) [\text{Sin}\{2\pi(\zeta_i - \zeta_j) + 2\pi(\xi_i - \xi_j)\} \cdot U(\xi_i - \xi_j) + \text{Sin}\{2\pi(\zeta_i - \zeta_j) - 2\pi(\xi_i - \xi_j)\} \cdot U(\xi_j - \xi_i)], \quad (14.24)$$

$$da_i / d\tau = -n \cdot J'_n(a_i) \cdot \frac{1}{2N\vartheta} \sum_{j=1}^N a_j J'_n(a_j) [\text{Cos}\{2\pi\zeta_i - \zeta_j\} + 2\pi(\xi_i - \xi_j)\} \cdot U(\xi_i - \xi_j) + \text{Cos}\{2\pi\zeta_i - \zeta_j\} - 2\pi(\xi_i - \xi_j)\} \cdot U(\xi_j - \xi_i)], \quad (14.25)$$

$$d\eta_i / d\tau = -R_e \cdot a_i \cdot J'_n(a_i) \frac{1}{2N\vartheta} \sum_{j=1}^N a_j J'_n(a_j) [\text{Cos}\{2\pi(\zeta_i - \zeta_j) + 2\pi(\xi_i - \xi_j)\} \cdot U(\xi_i - \xi_j) + \text{Cos}\{2\pi(\zeta_i - \zeta_j) - 2\pi(\xi_i - \xi_j)\} \cdot U(\xi_j - \xi_i)]. \quad (14.26)$$

Equations (14.16) – (14.20) can be transformed (for more details see annex XIII) into the well-known Gaponov equations, which were usually used to describe phenomena in a vacuum waveguide.

Let us note that a detailed analysis of the behavior of particles and the field in the gyrotron was also performed in [14-11]. The authors [14-12] were also interested in the problems of gyrotron excitation. However, when certain gyrotron power is exceeded, gas evolution from the structural elements and its ionization led to the appearance of a relatively low density plasma, where the Langmuir plasma frequency remained much lower than the operating frequency ($\omega > \omega_{pe} = \sqrt{4\pi e^2 n_p / m_{e0}}$). The direct inclusion of plasma in the procedure for obtaining the Gaponov equations was difficult, therefore, an analog of the above system of equations (14.16) – (14.20) was used; it was obtained taking into account the influence of low-density plasma. The difficulty associated with the inability to separate waves of different polarization in magnetoactive plasma was circumvented by using a small parameter of their coupling

$$g = \left(\omega^2 \varepsilon_{xy} / c^2 k_{\perp}^2\right) = \omega^2 \varepsilon_2 / c^2 k_{\perp}^2 \ll 1,$$

where $\varepsilon_{xy} \equiv \varepsilon_{\perp} = \varepsilon_2 = i\omega_{pe}^2 \omega_B / \omega(\omega^2 - \omega_B^2)$ is the transverse component of the dielectric constant of cold magnetic plasma. In addition, the ratio of the

longitudinal and transverse components of the wave vector was small. Below let us consider the account of the influence of low-density plasma in the traditional form [14-1] of the gyrotron equations carried out in [14-15]. Let us also discuss the efficiency of generating a gyrotron in the presence of plasma in its volume [14-16]. In this case the system of equations takes the following form (see annex XVIII)

$$\frac{d^2 F}{d\xi_G^2} + i \frac{\partial}{\partial \tau_P} + \gamma'_G{}^2 F = -I_P (1 + g) \langle \vec{A}^{*n} \rangle, \quad (14.27)$$

$$\frac{d\vec{A}}{d\xi_G} + i \left[\Delta + |\vec{A}|^2 - 1 \right] \vec{A} = -i(1 + g) F^* \vec{A}^{*n-1}, \quad (14.28)$$

where
$$I_P = \frac{64eI_0 n^3}{m_{e0} c^3} \frac{\beta_{z0}}{\beta_{\perp 0}^{2(4-n)}} \left(\frac{n^n}{2^n n!} \right)^2 \frac{J_{n-m}^2(k'_{ms} r_c)}{J_m^2(x'_{ms}) x_{ms}'^2 + J_m^2(x'_{ms}) (x_{ms}'^2 - m^2)},$$

$I_0 = N_{b0} e v_{z0}$ is initial normalized longitudinal beam current,

$$\Delta = \frac{2(\omega - n\omega_{B0})}{n\omega_{B0}\beta_{\perp 0}^2}, \quad \vec{A} = \frac{\vec{a}}{a_0}, \quad \vec{a} = a \exp\left\{ \frac{2\pi i \zeta}{n} \right\}, \quad \Omega_B = eB_0 / m_e c = \omega_B (1 - \beta_{\perp 0}^2 - \beta_{z0}^2)^{-1/2},$$

$$a_0 = a(\xi_G = 0), \quad \xi_G = \frac{\beta_{\perp 0}^2 \omega_{B0} z}{2v_z}, \quad \sigma = \frac{v_{z0}}{v_z}, \quad \gamma'_G{}^2 = 4v_z^2 \frac{\varepsilon_1 \omega^2 / c^2 - k_{ms}'^2}{(\beta_{\perp 0}^2 \omega_{B0})^2},$$

$$F = 4 \frac{n^2 a_0^{n-2} e b \exp(i\varphi) J_{n-m}(k'_{ms} r_c)}{2^n n! c m_{e0} \beta_{\perp 0}^2 \omega_{B0}}, \quad \tau_P = \rho_P^2 c^2 / 2\omega G, \quad G = \frac{(\omega^2 - \Omega_B^2)^2 + \omega_{pe}^2 \Omega_B^2}{(\omega^2 - \Omega_B^2)^2},$$

the averaging procedure has the form $\langle A^{*n} \rangle = \frac{1}{N} \sum_{j=1}^N \left(\frac{a_j}{a_{j0}} \right)^n \exp(-2i\pi\zeta_j)$.

It can be shown that the account of the presence of plasma results in a slight increase in the radiated power (see Fig. 14.1). The upper curve corresponds to the presence of a low-density plasma in the volume of the waveguide; the lower curve corresponds to the case of a vacuum waveguide.

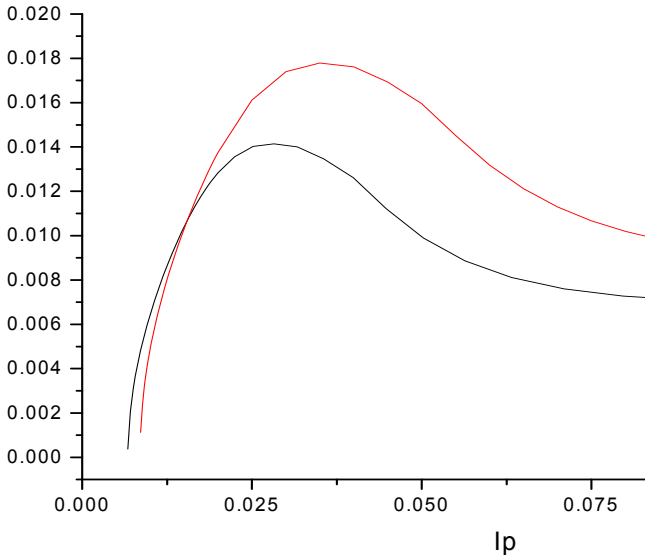


Fig. 14.1. The dependence of the power radiated from the waveguide (in relative units) on the normalized current I_P at $\beta_z(\tau=0) = v_{z0} / c = 0,24$, $\beta_{\perp}(\tau=0) = v_{\Phi} / c = 0,336$, $\omega_B / \omega = 1.062$, $z_{out} = 12$, $\Delta = 0,6$, $\omega_{pe} / \omega = 0,1$ [14-16]

Similarly, we can write equations describing the process of superradiance in the gyrotron system. The equations of motion for a spatial problem can be represented as

$$2\pi \frac{d\zeta_i}{dz} = \frac{(n\omega_{B0} - \omega)}{v_z} + \frac{n\omega_{B0}}{v_z} [\beta_{\perp 0}^2 - \beta_{\perp}^2] + \frac{ne}{mcv_z} \left(1 - \frac{n^2}{a_i^2}\right) J_{n-m}(k_{ms}r_c) J_n(a_i) \operatorname{Re} b \exp(2i\pi\zeta_i) =$$

$$= \frac{(n\omega_{B0} - \omega)}{v_z} + \frac{n\omega_{B0}}{v_z} [\beta_{\perp 0}^2 - \beta_{\perp}^2] + \frac{n\delta}{v_z} \left(1 - \frac{n^2}{a_i^2}\right) J_n(a_i) \operatorname{Re} \exp(2i\pi\zeta_i) \cdot B;$$

$$\frac{da}{dz} = \frac{en}{mcv_z} J_{n-m}(k_{ms}r_c) J'_n(a) \operatorname{Re} i b \exp(2i\pi\zeta) = \frac{\delta n}{v_z} J'_n(a) \operatorname{Re} i \exp(2i\pi\zeta) \cdot B.$$

Here let us not take into account the change in a very slow longitudinal velocity in phase relations. The origin of the first terms is easy to understand, noting that $\omega_{B0} \approx \frac{eB}{m_e c} (1 - \beta_{\perp 0}^2 / 2)$, then $\omega_B \approx \omega_{B0} [1 + (\beta_{\perp 0}^2 - \beta_{\perp}^2) / 2]$.

Assuming the arguments of the Bessel functions to be small $J_n(x) \approx (x/2)^n \frac{1}{n!}$; $J'_n(x) = \frac{1}{x} (x/2)^n$, let us transform the previous equations as it follows

$$\frac{d(\zeta_i/n)}{d\xi_G} = i\Delta + i(|A|^2 - 1) - G \frac{(|A_i|/2)^{n-1}}{N} \sum_{j=1}^N \left(\frac{|A_j|}{2}\right)^n \cdot \operatorname{Sin}\{2\pi(\zeta_i - \zeta_j) + 2\pi(\xi_i - \xi_j)\} \cdot U(\xi - \xi_j), \quad (14.29)$$

$$\frac{d|A_i|}{d\xi_G} = -G \frac{(|A_i|/2)^{n-1}}{N} \sum_{j=1}^N \left(\frac{|A_j|}{2}\right)^n \operatorname{Cos}\{2\pi(\zeta_i - \zeta_j) + 2\pi(\xi - \xi_j)\} \cdot U(\xi - \xi_j), \quad (14.30)$$

where the following values are used: $\omega_b^2 = 4\pi e^2 N_{0b} / S m_e$ is the volume-average Langmuir particle frequency of the beam, $S = \pi r_W^2$ is the waveguide cross section, $Z = \xi_G = \omega_B \delta^2 \beta_{\perp 0}^2 z / 2v_z$, $\Delta = \frac{2(\omega - n\omega_{B0})}{n\omega_{B0} \cdot \beta_{\perp 0}^2}$, $\beta_{\perp}^2 = (v_{\perp} / c)^2$,

$$G = \frac{\omega_b^2 n V \cdot J_{m-n}^2(k_{ms}r_c) a_0^{2n-1}}{4\pi \beta_{\perp 0}^2 \cdot c^2 \cdot J_m^2(x_{ms}) \cdot (x_{ms}^2 - m^2) \cdot D_k}, \quad A_i = a_i \cdot \exp\{i\zeta_{i+} / n\}.$$

These two equations can be written in a complex form

$$\frac{dA_i}{d\xi_G} = i\Delta + i(|A|^2 - 1) \{A_i - GA_i \frac{(|A_i|/2)^{n-2}}{N} \sum_{j=1}^N \left(\frac{|A_j|}{2}\right)^n \exp\{2\pi(\zeta_i - \zeta_j) + 2\pi(\xi - \xi_j)\} \cdot U(\xi - \xi_j)\}. \quad (14.31)$$

References to section 14

14-1. Gaponov A. V., Petelin M. I. and Yulpatov V. K. The induced radiation of excited classical oscillators and its use in high-frequency electronics. "Radiophysics and Quantum Electronics", 1967. – Vol. 10. – P. 794–813 (in Russian).

14-2. Flyagin V. A., Gaponov A. V., Petelin M. I. and Yulpatov V. K. The Gyrotron. // IEEE Transactions on microwave theory and techniques, 1977. – Vol. MTT-25. – No. 6. – P. 514–521.

14-3. Panchenko I. P., Sotnikov. V. I. Nonlinear theory of excitation of monochromatic waves by an electron beam in plasma placed in a magnetic field // Sov. Plasma Physics 1976. – V. 2 – N. 6. – P. 945–952 (in Russian).

14-4. Aburdzhania Kh. D., Kitsenko A. B., Pankratov I. M. Nonlinear stage of interaction of a flow of charged particles with plasma in a magnetic field // Sov. Plasma Physics. 1978. – T. 4, – B. 1. – P. 227–234 (in Russian).

14-5. Balakirev V. A., Karbushev N. I., Ostrovsky A. O., Tkach Yu. V. Theory of Cherenkov's Amplifiers and Generators on Relativistic Beams. – 1993. – Kiev: Naukova Dumka, 1993. – 208 p. (in Russian).

14-6. Kondratenko A. N., Krusha J., Kuklin V. M. On the features of the development of beam-plasma instability under conditions of the anomalous Doppler effect. // Beitr. Plasmaphys. 1979. – V. 19. – N 4. – R. 201–209.

14-7. Kuklina O. V., Kuklin V. M. On the mechanisms of saturation of cyclotron instabilities of an electron beam in waveguides // Electromagnetic phenomena. 2001. – V. 2. – No. 4 (8). – P. 490–497 (in Russian).

14-8. Ginzburg N. S. Nonlinear theory of amplification and generation based on the anomalous Doppler effect. "Radiophysics and Quantum Electronics", 1979. – V. 22. – No. 4, – P. 470–479 (in Russian).

14-9. Granatstein V. L. and Alexeff I. High-Power Microwave Source. Boston, Arlech House. – 1987.

14-10. K. R. Chu, A. T. Lin. Gain and Bandwidth of the Gyro-TWT and CARM Amplifiers. IEEE Transactions on Plasma Science. 1988. – Vol. 16. – No 2. – P. 90–104.

14-11. Kuzelev M. V., Rukhadze A. A. Electrodynamics of dense electron beams in plasma. Moscow: Nauka, 1990. – 336 p. (in Russian).

14-12. Superradiance of electrons in a magnetic field and a nonrelativistic gyrotron / A. G. Zagorodniy, P. I. Fomin, A. P. Fomina // Dop. NAS of Ukraine. 2004, No. 4, – p. 75–80; Fomin P. I., Fomina A. P. Dicke Superradiance on Landau Levels / Problems of Atomic Science and Technology, 2001. N 6. – P. 45–48 (in Russian).

14-13. Edgcombe C. J., Gyrotron Oscillators: Their Principles and Practice. London, U.K.: Taylor & Francic. – 1993.

14-14. Ginzburg N. S., Zavolsky N. A., Nusinovich G. S. Gyrotron Dynamics with Nonfixed Longitudinal RF Field Structure. Radiotekhnika and Elektronika 1987. – V. 5. – P. 1031–1039 (in Russian).

14-15. Kuklin V. M. Report / PST EV N 978763, NATO Science Programm Cooperative Science & Technology Sub-Programme, Hamburg – 2002.

14-16. Influence of low-density Plasma on Gyrotron Operation / V. M. Kuklin, S. Yu. Puzyrkov, K. Schunemann, G. I. Zaginaylov // UPhJ. – 2006. – V. 51, № 4. – P. 358–366.

SECTION 15.

EQUATIONS, THAT DESCRIBE EXCITATION OF TM WAVES

Let us obtain a system of nonlinear equations that describes the excitation by an electron beam of a TM wave in a cylindrical smooth metal waveguide of radius r_W . The dispersion equation, which describes the dependence of the wave frequency ω on the longitudinal and transverse wave numbers k_z and k_\perp , accordingly, has the form (14.2). The components of the TM waves electromagnetic field can be represented as:

$$E_z = h(z, t) J_m(k_\perp r) \exp(-i\omega t + ik_z z + im\theta), \quad (15.1)$$

$$(E_\theta, B_r) = \left\{ \frac{m}{(1 - \omega^2 / c^2 k_z^2) k_z r}, -\frac{\omega m}{(1 - \omega^2 / c^2 k_z^2) c r k_z^2} \right\} \cdot$$

$$\cdot h(z, t) J_m(k_\perp r) \exp(-i\omega t + ik_z z + im\theta),$$

$$(E_r, B_\theta) = \left\{ -ik_\perp / (1 - \omega^2 / c^2 k_z^2) k_z, -i\omega k_\perp / (1 - \omega^2 / c^2 k_z^2) c k_z^2 \right\} \cdot$$

$$\cdot h(z, t) J'_m(k_\perp r) \exp(-i\omega t + ik_z z + im\theta), \quad (15.3)$$

where h is the complex amplitude of the wave, whereas other notations are the same. The transverse wave number $k_\perp = k_{ms} = x_{ms} / r_W$ is determined from the requirement that the tangential field components vanish at the boundary of the waveguide, and x_{ms} is the s -root of the equation $J_m(x_{ms}) = 0$.

Let, just as in the previous case, an electron beam occupy a cylindrical layer in the section of the waveguide, with all centers of Larmor electron rotation being at the same distance from the axis of the waveguide. When passing to a coordinate system the center of which coincides with the center of rotation of an individual electron in the beam, we use relations (14.6), where b_z and B_z should be replaced by e_z and E_z , respectively. The values of the components of the electromagnetic field in the coordinate system of the rotation of a single electron have the form:

$$(e_z, e_\Phi, b_R) = h \sum_q J_q(k_{ms} r_c) J_{m+q}(k_{ms} r_B) \exp(-i\omega t + ik_z z + im\Phi + iq\Phi_c + i\pi m / 2) \times$$

$$\times (1, (m+q) / (1 - \omega^2 / c^2 k_z^2) r_B k_z, -\omega(m+q) / (1 - \omega^2 / c^2 k_z^2) k_z^2 c r_B), \quad (15.4)$$

$$(e_R, b_\Phi) = h \sum_q J_q(k_{ms} r_c) J'_{m+q}(k_{ms} r_B) \exp(-i\omega t + ik_z z + im\Phi + iq\Phi_c + i\pi m/2) \times \quad (15.5)$$

$$\times \left[-ik_{ms} / (1 - \omega^2 / c^2 k_z^2) k_z, -ik_{ms} \omega / (1 - \omega^2 / c^2 k_z^2) k_z^2 c \right].$$

Since $\Phi_c = \Phi_{c0} + \omega_B \cdot t$, $\Phi = \Phi_0 + \omega_B \cdot t$, $z = z_0 + v_z \cdot t$, then in the case of resonance of the beam particles with the wave $\omega - k_z v_z \approx n\omega_B$, the relation $m + q = n$ is satisfied in both expressions (15.3) and (15.4), as in the previous section, we hold only the resonant terms:

$$(e_z, e_\Phi, b_R) = h \cdot J_{n-m}(k_{ms} r_c) J_n(a) \exp(2i\pi\zeta) \left[1, \frac{n}{(1 - \omega^2 / c^2 k_z^2) r_B k_z}, -\frac{\omega \cdot n}{(1 - \omega^2 / c^2 k_z^2) k_z^2 c r_B} \right], \quad (15.6)$$

$$(e_R, b_\Phi) = J_{n-m}(k_{ms} r_c) J'_n(a) \exp(2i\pi\zeta) \left[-\frac{ik_{ms}}{(1 - \omega^2 / c^2 k_z^2) k_z}, -\frac{ik_{ms} \omega}{(1 - \omega^2 / c^2 k_z^2) k_z^2 c} b \right], \quad (15.7)$$

where the notation from the previous section is used. It can be shown that the equation for the wave field takes the form

$$\omega D(\omega, \vec{k}) h + i \left[\frac{\partial D(\omega, \vec{k})}{\partial \omega} \frac{\partial h}{\partial t} - \frac{\partial D(\omega, \vec{k})}{\partial k} \frac{\partial h}{\partial z} \right] = \quad (15.8)$$

$$= 4i \left[r_w^2 h^* J_m^2(x_{ms}) \right]^{-1} \int_0^{r_w} r dr \int_0^{2\pi} d\theta \vec{J} \vec{E}^*,$$

group vibration velocity is $v_g = \frac{\partial D(\omega, \vec{k})}{\partial k} / \frac{\partial D(\omega, \vec{k})}{\partial \omega}$, detuning is

$\Delta = \text{Re} \{ D(\omega, \vec{k}) / \gamma_e \frac{\partial D(\omega, \vec{k})}{\partial \omega} \}$ and decrement of wave attenuation in the absence

of a beam is $\Theta = \text{Im} \{ D(\omega, \vec{k}) / \gamma_e \frac{\partial D(\omega, \vec{k})}{\partial \omega} \}$.

In a homogeneous extended waveguide, equation (15.8) is simplified and can be represented as

$$\left[\frac{d}{d\tau} - i\Delta + \Theta \right] E_h \exp\{i\varphi_h\} = \frac{1}{N} \sum_{j=1}^N J_n(a_j) \cdot \exp(-2\pi i \zeta_j) \quad (15.9)$$

where N is the number of particles, simulating the beam. Passing to dimensionless quantities and using the value of the integral phase ζ , the system of equations for real variables can be written in the following form (see, for example, [14-7, 15-2]):

$$\frac{dE_h}{d\tau} + \Theta \cdot E_h = N^{-1} \cdot \sum_{j=1}^N a_j \cdot J_n(a_j) \cdot \text{Cos}(2\pi\zeta + \varphi_h), \quad (15.10)$$

$$\frac{d\varphi_h}{d\tau} - \Delta = -(E_h N)^{-1} \cdot \sum_{j=1}^N J_n(a_j) \cdot \text{Sin}(2\pi\zeta_j + \varphi_h). \quad (15.11)$$

The equations of motion of electrons in the field of this wave in the presence of a constant magnetic field are as it follows

$$2\pi \frac{d\zeta_i}{d\tau} = \eta_i + nE_h \cdot J'_n(a_i) \cdot \text{Sin}(2\pi\zeta_i + \varphi_h) \quad (15.12)$$

$$d\eta_i / d\tau = -R_h \cdot E_h \cdot J_n(a_i) \cdot \text{Cos}(2\pi\zeta_i + \varphi_h), \quad (15.13)$$

$$da_i / d\tau = -(n/a) \cdot E_h \cdot J_n(a_i) \cdot \text{Cos}(2\pi\zeta_i + \varphi_h), \quad (15.14)$$

where $\tau = \gamma_h t$, $\gamma_h^2 = 4e^2 \cdot \omega_B \cdot N_{b0} \cdot [m_e \cdot c^2 \cdot r_w \cdot J_m^2(x_{ms}) \cdot D_\omega]^{-1} \cdot (k_{ms}^2 / k_z^2 \omega_B) \cdot J_{m-n}^2(k_{ms} \cdot r_C)$,

$$D_\omega = \partial D / \partial \omega = \partial \{ [\omega^2 - (k_z^2 + k_{ms}^2) c^2] / [\omega^2 - k_z^2 c^2] \} / \partial \omega |_{D=0}, \quad R_h = k_z^2 \cdot \omega_B / k_{ms}^2 \cdot \gamma_h,$$

$$E_h = e \cdot h \cdot J_{m+n}(k_{ms} \cdot r_C) \cdot (k_{ms}^2 / k_z \omega_B) / m_e \cdot \gamma_h, \quad \eta = (k_z \cdot v_z - \omega + n \cdot \omega_B) / \gamma_h,$$

$a = k_{ms} r_B = k_{ms} v_\Phi / \omega_B$, $\omega_B = eB / m_e c$, N_{b0} is the number of particles of the unperturbed beam per unit length. Here h is the wave amplitude.

It turns out that for linear oscillators that do not move in the direction of wave propagation, under the following conditions: $n=1$, $\theta=0$, $\Delta=0$, $\Phi \rightarrow -\Phi$, $\psi \leftrightarrow 2\pi\zeta + \pi/2$, $R \rightarrow 0$ at small a_i ($J_1(a_i)_{a_i \rightarrow 0} \rightarrow a_i/2$, $J_0(a_i)_{a_i \rightarrow 0} \rightarrow 1$, $J'_1(a_i)_{a_i \rightarrow 0} \rightarrow 1/2$) and using known ratios $\text{Sin} \alpha = -\text{Cos}(\alpha + \pi/2)$, $\text{Cos} \alpha = +\text{Sin}(\alpha + \pi/2)$ the systems of equations for TE and TM waves (14.16) – (14.20) and (15.10) – (15.14) practically coincide (For the integrals of the systems of equations, see annex XIX).

Excitation of a longitudinal wave in a magnetically active plasma waveguide. Let us note that in case of substitution $\varphi_h \rightarrow \varphi_h + \pi/2$, equations (15.10) – (15.16) are reduced to the same system of equations considered in [15-1, 15-2], which describes the excitation of a longitudinal wave in a plasma waveguide, where the dispersion equation takes the form

$$D(\omega, \vec{k}) = k_i k_j \varepsilon_{ij}(\omega, \vec{k}), \quad (15.15)$$

where there is the dielectric constant tensor of cold plasma

$$\varepsilon_{ij}(\omega, \vec{k}) = \begin{pmatrix} \varepsilon_{11} & \varepsilon_{12} & 0 \\ \varepsilon_{21} & \varepsilon_{22} & 0 \\ 0 & 0 & \varepsilon_{33} \end{pmatrix} \quad \text{and its components} \quad \varepsilon_{11} = \varepsilon_{22} = 1 - \frac{\omega_{pe}^2}{\omega^2 - \omega_B^2},$$

$$\varepsilon_{33} = \varepsilon_3 = 1 - \frac{\omega_{pe}^2}{\omega^2}, \quad \varepsilon_{12} = -\varepsilon_{21} = i\varepsilon_2 = i\omega_{pe}^2 \omega_B / \omega(\omega^2 - \omega_B^2).$$

In this case, the expressions for dimensionless variables and parameters are slightly different:

$$\gamma_h = \omega_{b0} \left[\frac{\omega_B k_z^2}{k_{ms}^2} \frac{\partial D}{\partial \omega} \Big|_{D=0} \right]^{1/2}, \quad E_h = \frac{e k_{ms}^2 \Phi}{m_{e0} \omega_B \gamma_h}, \quad \Phi \text{ is the amplitude of the}$$

longitudinal wave potential. In [15-2], (see also [15-3, 15-4]) for the conditions

of the anomalous Doppler effect, that is $n=-1$, the dependences of the amplitude and phase of the field, the average beam velocity $\bar{\eta}$, of the average scatter on time Δa for values $R = 1, 0; 0, 05$ are found. For small $R = 0, 05$, the process is delayed, when the field maximum is reached, when the transverse velocities of almost all beam particles reach the values $v_{\Phi} = \omega_B x_{-11} / k_{ms}$, where x_{-11} is the first root of the equation $J_{-1}(x_{-11})=0$. That is, as it turned out, the transverse inhomogeneity of the field, the characteristic size of which is comparable with the value of the Larmor radius significantly affects the dynamics of instability.

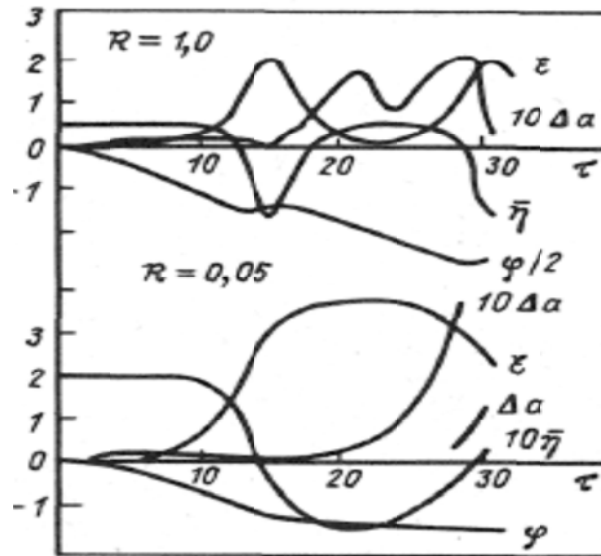


Fig. 15.1. The amplitude and phase of the field, the average beam velocity $\bar{\eta}$, and the average time spread Δa for the values $R = 1, 0; 0, 05$ [15-2]

References to section 15

15-1. Aburdzhania Kh. D., Kitsenko A. B., Pankratov I. M. Nonlinear stage of interaction of a flow of charged particles with plasma in a magnetic field // Sov. Plasma Physics. 1978. – V. 4.– B. 1. – P. 227–234 (in Russian).

15-2. Kondratenko A. N., Krusha J., Kuklin V. M. On the features of the development of beam-plasma instability under conditions of the anomalous Doppler effect // Beitr. Plasmaphys. 1979. – Vol. 19. – N 4. – p. 201–209 (in Russian).

15-3. Ginzburg N. S. Nonlinear theory of amplification and generation based on the anomalous Doppler effect. Radiophysics and Quantum Electronics, 1979. – V. 22. – No. 4. – P. 470–479 (in Russian).

15-4. Kondratenko A. N., Kuklin V. M. Fundamentals of Plasma Electronics. – M.: Energoatomizdat, 1988 – 320 p. (in Russian).

CHAPTER 7.

Modulation instability and self-similar structures

The development of modulation instability of a wave of finite amplitude under conditions of a high level of absorption of wave energy in the medium is considered. A modified S-theory is used to describe these modes; it takes into account the resonant interactions of disturbances with the main wave and the interactions of these disturbances. It is shown that in these modes, the appearance of long-lived states of a modulated wave with linear spectra is possible, which are the cause of the development of the following instability cascades. As a result, a self-similar spatial wave structure can be formed at different scales, which was confirmed by the results of numerical modeling.

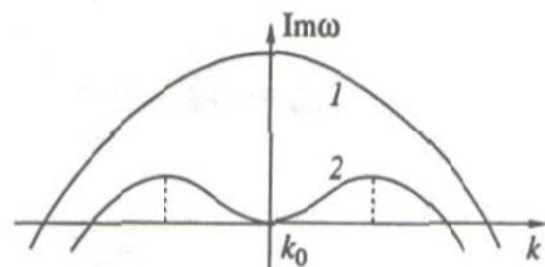
SECTION 16.

MODULATION INSTABILITY

The authors of [16-1 – 16-4] found that periodic waves of finite amplitude in media with the most common form of local cubic nonlinearity are unstable in case of excitation of two side spectra of stimulated perturbations, respectively, with a larger and shorter wavelength. The development of such an instability results in amplitude and phase modulation of the initial wave. Subsequently this determined the name of this type of instability – modulation [16-5]. In multidimensional cases, in addition to modulation instabilities, self-focusing processes are also possible [16-6].

A remarkable property of modulation instability near the threshold turned out to be its ability to create self-similar structures [16-7, 16-8]. Indeed, under the conditions of a balance between the mechanisms of generation of the main wave and the levels of absorption of wave energy, the development of modulation instability leads to the formation of stationary self-similar structures, the spatial scales and intensity of which are due to nonlinear resonant interaction between the main wave and the excited side satellites wave and the excited side satellites.

*Fig. 16.1. Increment of the main wave (periodic structure),
2 - increment of modulation instability of an already developed main wave (periodic structure)*



The interaction of the disturbance pairs ($k = k_0 \pm \Delta k$) arising as a result of the instability associated with the resonant conditions, is weakened under these conditions; they interact to a greater extent with the main wave, and their effect

on the main wave is integral. That is why we can assume that such a system near the threshold of modulation instability can be defined as quasilinear [16-9].

In [16-8, 16-10], two main features of modulation instabilities in media and systems with a high level of energy absorption were noted. Firstly, in the mode of saturation of modulation instability, narrow spectra of lateral disturbances are formed as a result of the mode competition mechanisms discussed below, and in the limit of large times, the developed spatial structure acquires a characteristic linear spectrum. Secondly, it was theoretically predicted that the formation of a line spectrum facilitates the fulfillment of conditions for the next, already secondary modulation instability, which is developed in the framework of such scenario [16-11]. Moreover, the wave (or structure) modulated as a result of the development of primary modulation instability should undergo modulation due to secondary instability, but on a much larger scale [16-11, 16-12].

The results of numerical studies of such a multimode system qualitatively confirmed the assumptions made by the authors of [16-11] and their theoretical conclusions about the appearance of a multifractal structure of perturbations. In addition, it was found that in the mode of saturation of instability, the integrated energy of the spectrum stabilizes, which indicates the formation of a long-lived quasi-stable physical state [16-13], and there remains noticeably less energy of the main wave.

The evolution of instabilities near the threshold can be traced using the modified S-theory [16-10, 16-14], which allows considering in detail the evolution of individual spectrum modes¹¹.

Let us consider the instability of a monochromatic wave

$$A(x, t) \cdot \exp \{i\omega t - ikx\} \quad (16.1)$$

in a wave medium with weak dispersion and local cubic nonlinearity, where $A(x, t)$ is its slowly varying complex amplitude. In general, if the dispersion of a system is known

$$\omega = \omega_0 + \beta \cdot \vec{k}^2 + \alpha \cdot |A|^2, \quad (16.2)$$

then the equation for changing the complex amplitude A can be written as

$$\frac{\partial}{\partial t} A = i\omega_0 A - i\beta \frac{\partial^2}{\partial \vec{r}^2} A + i\alpha A |A|^2, \quad (16.3)$$

or in the one-dimensional case

$$\frac{\partial}{\partial t} A = i\omega_0 A - i\beta \frac{\partial^2}{\partial x^2} A + i\alpha A |A|^2 \quad (16.4)$$

¹¹ In a number of works of the group by Zakharov V. E and Lvov V.S. (see the detailed review [16-15] and the book [16-16]), relying on the inclusion of only two interaction diagrams, namely $2\omega_0 = \omega(k) + \omega(-k)$, $\alpha(k) + \alpha(-k) = \alpha(k') + \alpha(-k')$, where ω_0 is the frequency of the main wave, authors formulated approaches to describe the nonlinear stage of modulation instability, which subsequently received name of S-theory.

A similar dispersion is characteristic of Langmuir waves in plasma and oscillations in a plasma waveguide in the corresponding normalization

$$\omega = \omega_0 + \bar{k}^2 - |A|^2. \quad (16.5)$$

Lighthill criterion [16-1] is accomplished in this case

$$(\partial^2 \omega / \partial k^2)^{-1} \cdot \partial \omega(|A|^2) / \partial |A|^2 < 0, \quad (16.6)$$

according to which the wave (modulation) is unstable in the direction of its propagation.¹²

Below let us consider the case of a balanced source and sink (distributed output, absorption, or dissipation) of wave energy. The Lighthill equation, describing the slow evolution of the envelope of oscillations under these conditions takes the form

$$\frac{\partial A}{\partial t} = -\delta A - i \frac{\partial^2 A}{\partial x^2} - iA|A|^2 + g, \quad (16.7)$$

where δ is the absorption decrement and g is the external source of wave energy. The amplitude $A(t, x)$ of oscillations slowly varying with time can be represented as

$$\begin{aligned} A &= u_0(t) \exp\{i\phi_{k_0}(t) - ik_0x\} + \sum_{n \neq 0} u_n(t) \exp\{i\phi_{k_n}(t) - ik_nx\} = \\ &= \{u_0(t) + \sum_{n \neq 0} u_n(t) \exp[i(\phi_{k_n} - \phi_{k_0}) - i(k_n - k_0)x]\} \exp\{i\phi_{k_0}(t) - ik_0x\}. \end{aligned} \quad (16.8)$$

That is, instability is considered as the excitation of the perturbation spectrum $\sum_{n \neq 0} u_n(t) \cdot \exp\{i\phi_{k_n}(t)\} \cdot \exp\{i\omega_0 t - ik_nx\}$, where $u_n(t) \cdot \exp\{i\phi_{k_n}(t)\}$ is the slowly varying complex amplitude of the n-th mode of the spectrum. The real field is a modulated wave at a frequency ω_0 .

Therefore, in order to restore the form of the wave field, expression (16.8) should be multiplied by $\exp\{i\omega_0 t\}$. Selecting the “fast” phase factor $\exp\{i\omega_0 t - ik_0x\}$ corresponding to the main wave, in this case we shall obtain the oscillation field as the product

$$A = \exp\{i\omega_0 t - ik_0x\} \cdot \{u_0 \exp[i\phi_{k_0}] + \sum_{n \neq 0} u_n \exp[i\phi_{k_n} - i(k_n - k_0)x]\}, \quad (16.9)$$

where $\exp\{i\omega_0 t - ik_0x\}$ is the rapidly changing phase.

Often, a slightly different type of field representation is used, highlighting the full phase of the main wave $\exp\{i\omega_0 t - ik_0x + i\phi_{k_0}\}$

$$A = \exp\{i\omega_0 t - ik_0x + i\phi_{k_0}\} \cdot \{u_0 + \sum_{n \neq 0} u_n \exp[i(\phi_{k_n} - \phi_{k_0}) - i(k_n - k_0)x]\}. \quad (16.10)$$

¹² Generally speaking, if $\partial \alpha(|A|^2) / \partial |A|^2 < 0$, then self-focusing effects are possible [16-17].

In the case of modulation instability of a monochromatic wave of large amplitude, we are talking only about one wave, which is characterized by the phase $v_f = \omega/k$ and the group $v_g = \partial\omega/\partial k$ velocities. In a reference frame moving with a group velocity of a wave the equation, which describes the behavior of the envelope of the wave field that occurs when a wave is modulated with an initial complex amplitude u_0 at small perturbation amplitudes $|u_k| \ll |u_0|$ takes the form

$$\frac{\partial u_{k_{1,2}}}{\partial \tau} + \delta u_{k_{1,2}} + i \frac{\partial^2 u_{k_{1,2}}}{\partial \zeta^2} + i \{ [u_{k_{1,2}} |u_0|^2 + u_{k_{2,1}}^* u_0^2] \} = 0, \quad (16.11)$$

where δ is the absorption decrement at selected time scales τ and coordinates ζ . It is not difficult to see that the interaction of two perturbations u_{k_1} and $u_{k_2}^*$ occurs with the drag stream proportional to $|u_0|^2$ and the second harmonic of the wave which is proportional to $|u_0|^2$.

The last term on the right-hand side of (16.11) in braces shows that the spatial modes¹³ with wave vectors satisfying the spatiotemporal synchronism $2k_0 = k_1 + k_2$, (where $k_1 = k_0 + K$, $k_2 = k_0 - K$, $k_0 \gg |K|$.) interact most effectively, at least at the stage of modulation instability, which is linear in perturbations ($|u_0| \gg |u_{k_{1,2}}|$).

Let us write a system of interacting modes and obtain the equation for $u_{k_2}^*$ using the complex conjugate equation (16.11), where we substitute the indices

$$\frac{\partial u_{k_1}}{\partial t} + \delta u_{k_{1,2}} + i \frac{\partial^2 u_{k_1}}{\partial \zeta^2} + i \{ [u_{k_1} |u_0|^2 + u_{k_2}^* u_0^2] \} = 0, \quad (16.12)$$

$$\frac{\partial u_{k_2}^*}{\partial t} + \delta u_{k_2}^* - i \frac{\partial^2 u_{k_2}^*}{\partial \zeta^2} - i \{ [u_{k_2}^* |u_0|^2 + u_{k_1} u_0^2] \} = 0. \quad (16.13)$$

Assuming the dependence on time and coordinate in the form $\exp \{-i\Omega \tau + iK \zeta\}$, we can represent the dispersion equation of the process

$$D(\Omega, K) = (\Omega + i\delta + K^2 - |u_0|^2)(\Omega + i\delta - K^2 + |u_0|^2) + |A_0|^4 = 0, \quad (16.14)$$

whence we can see that the absolute instability in the reference frame, which moves with a group wave velocity relative to the laboratory one, has an increment equal to

¹³ It is important to note that disturbances with wave numbers k_1 and k_2 are not the waves of the system, that is, they are not able to exist in this medium independently without the support of a wave with a wave number k_0 .

$$\text{Im } \Omega = -\delta + \sqrt{K^4 - 2K^2 |u_0|^2}, \quad (16.15)$$

with the maximum increment

$$(\text{Im } \Omega)_{MAX} = -\delta + |u_0|^2,$$

disturbances grow, their wave number is $K^2 = K_0^2 = |u_0|^2$.

The width of the spectrum determines the localization of this modulation. The value $(K_0 - \delta) = 2\pi / L$ corresponds to the modulation localization region L . The position of the maximum increment determines the average spatial period T of the modulation, that is $K_0 = 2\pi / T$.

Instability threshold is not difficult to determine

$$|u_0|_{thr} = \delta^{1/2}. \quad (16.16)$$

Let us write the envelope (modulation) of the field in the form

$$a = \{u_0 \exp[i\phi_0] + \sum_{n \neq 0} u_n \exp[i\phi_n - iK_n \xi]\}, \quad (16.17)$$

where $\phi_{k_n} \equiv \phi_n(K_n)$, $u_k \equiv u_n(K_n)$, and for the wave vector in the region of linear instability, the expression is $K_n^2 = 1 + \left(\frac{2|n| - N}{N}\right) \sqrt{1 - \delta}$.

Taking into account the terms, which are non-linear in amplitude perturbations, the equations for the fundamental mode and the modes of unstable spectra can be represented as it follows

$$\frac{d\phi_0}{dt} = -u_0^2 - 2 \sum_{m>0}^N (u_m^2 + u_{-m}^2) - 2 \sum_{m>0}^N u_m u_{-m} \cos \Phi_m, \quad (16.18)$$

$$u_0 = -g \left\{ -\delta - 2 \sum_{m>0}^N u_m u_{-m} \sin \Phi_m \right\}^{-1}, \quad (16.19)$$

$$\frac{du_n}{dt} = \left\{ -\delta + u_0^2 \frac{u_{-n}}{u_n} \sin \Phi_n \right\} u_n, \quad (16.20)$$

$$\frac{d\phi_n}{dt} = K_n^2 - u_0^2 \frac{u_{-n}}{u_n} \cos \Phi_n - 2 \left[u_0^2 + \sum_{m>0}^N (u_m^2 + u_{-m}^2) - \frac{1}{2} u_n^2 \right]. \quad (16.21)$$

Origins of instability. At the beginning of the development of the process, when all phases of the initial perturbations are randomly distributed (and especially near the instability threshold), the rate of change of the mode amplitudes is much lower than the rate of change of their phases. Therefore, we can assume that the left side of equation (16.21) is always small. Thus, we can find the value of a steady or stable phase Φ_n^* for each pair of disturbances, interacting with the main wave, which is determined from the expression.

$$\cos(\Phi_n^*) \approx (2K_m^2 - 2u_0^2) / u_0^2 \left[\frac{u_{-m}}{u_m} + \frac{u_m}{u_{-m}} \right].$$

From equation (15.23) it follows that for $\delta = 0$ stable phases of growing modes are in the interval $0 < \Phi_n^* < \pi$, the maximum increment corresponds to the value $\Phi_n^* = \pi / 2$. When $K_m > u_0$, we have $\Phi_n^* < \pi / 2$, and when $K_m < u_0$, on the contrary $\Phi_n^* > \pi / 2$. As the absorption level δ increases, the interval Φ_n^* narrows. Actually, upon reaching this stable phase value $\Phi_n \rightarrow \Phi_n^*$, the growth of perturbations begins.

The consideration of the most effective interactions that occur only between spectrum-symmetric modes with respect to pumping ($k_s + k_{-s} = k_n + k_{-n}$) according to the modified S-theory leads to the following equations

$$\frac{dv_s}{dt} = v_s \left\{ -\delta + u_0^2 \frac{v_{-s}}{v_s} \sin \Phi_s + 2 \frac{v_{-s}}{v_s} \sum_{n \neq s}^N u_n u_{-n} \sin \Psi_{sn} \right\}, \quad (16.22)$$

$$\frac{d\phi_s}{dt} = K_s^2 - 2(u_0^2 + \frac{3}{2}v_s^2 + 2 \sum_{n \neq s}^N u_n^2) - u_0^2 \frac{v_{-s}}{v_s} \cos \Phi_s - 2 \frac{v_{-s}}{v_s} \sum_{n \neq s}^N u_n u_{-n} \cos \Psi_{sn}, \quad (16.23)$$

to which the first two equations of the system (16.21) – (16.24) should be added. The notation $\Psi_{sn} = \Phi_s - \Phi_n$ is used above. Here, for the convenience of analysis, we used the notation of the amplitudes of the spectrum modes $v_s \equiv u_s$ with wave numbers k_s . In the developed instability stage, this system of equations can describe not only the processes of energy exchange between spectrum modes, but also the development of a cascade of modulation instabilities, the result of which may be the formation of a fractal disturbance spectrum.

Modeling a process at high absorption levels. The numerical solution of the above system of differential equations (16.21) – (16.24) demonstrates the excitation of the instability spectrum on both sides of the main wave [16-9]. As the instability spectrum is excited, modulation of the fundamental mode is observed. Below there are the results of numerical modeling carried out at different levels of suprathreshold $1 - \delta$, considered as the degree of distance from the instability threshold (15.16). The number of modes N is taken equal to 100. At the level of suprathreshold $u_{00} - \delta = 0,2$, or, which is the same, the decrement of absorption is $\delta = 0,8$ (because $u_{00} = u_0(t=0) = 1$), the experimental result is as it follows.

At the initial values, one main mode is observed, and as a result of nonlinear interaction, a slow but accelerating growth of the instability spectrum begins. The amplitudes of the instability modes are small at this stage; therefore, they have no significant effect on the main wave.

Moreover, the level of spectral imperfection of the structure $D = \frac{2}{u_0^2} \sum_{m>0} u_m^2$ and the level of spectrum intensity $I_s = 2 \sum_{m>0} u_m^2$, are small, and the intensity of the main wave $I_0 = u_0^2$ is close to unity.

Then, the time derivative of the amplitudes of the instability spectrum of the instability spectrum reaches its maximum, a spectrum of excited modes is quickly formed, which reach values sufficient to effectively affect the main wave (Fig. 16.2 – 16.3). At this stage, the spectrum is wide, the amplitude of the excited modes is 1–5 % of the amplitude of the fundamental, but their interaction leads to deviations of the form of the fundamental wave by 15–20 % of the regular sinusoidal shape. In this process, there is an increase in the level of defectiveness D .

At the next stage of the development of process ($t > 100$), a narrowing of the spectrum of modulation instability is observed with a simultaneous increase in the amplitude of the excited modes (Fig. 16.4). The derivative of the extreme modes of the spectrum takes a negative value, the maximum of the spectrum shifts toward the main mode. Further, the rate of change of the amplitude of the excited modes decreases, and the system reaches a quasistable state. An increase in the amplitude of the excited modes leads to a more noticeable effect on the fundamental wave (Fig. 16.5).

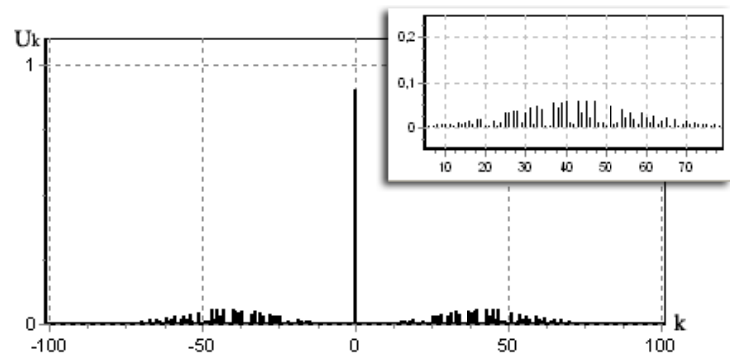


Fig. 16.2. Excitation of a wide spectrum of instability ($t \approx 50$, $\delta = 0,8$)

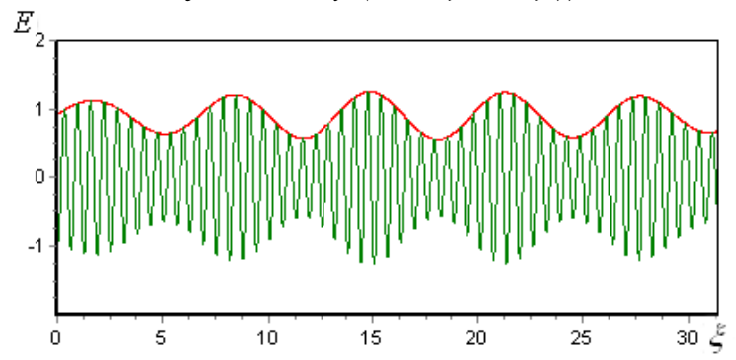


Fig. 16.3. The fundamental wave modulated by the modes of the excited spectrum ($t \approx 50$, $\delta = 0,8$)

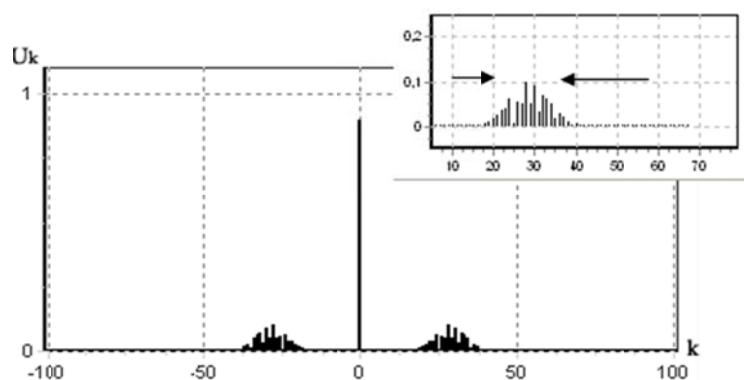


Fig. 16.4. Instability spectrum at the final stage of development ($t \approx 300$, $\delta = 0,8$)

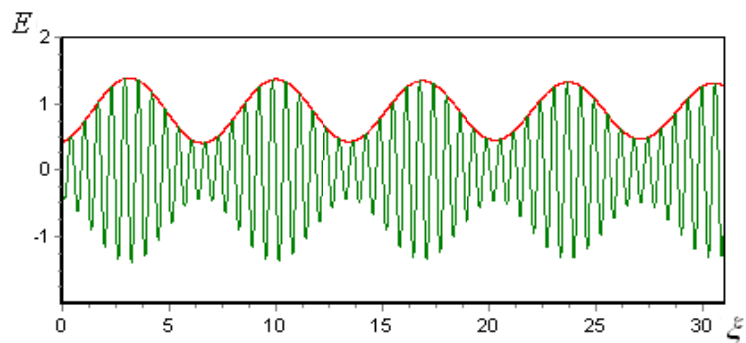


Fig. 16.5. View of the main wave at the final stage of development of the instability spectrum ($t \approx 300$, $\delta = 0,8$)

Integral and local characteristics of the process of instability. Let us consider in detail the process of spectrum formation and the transition of the system to the quasilinear stage in terms of mode intensity. As it can be seen from Fig. 16.6 and 16.7, the intensity of the fundamental mode at the initial stages of the process noticeably decreases and approaches the value δ when $t \approx 100$. The levels of suprathreshold $(1-\delta)$ limit the intensity of the main mode from below. During a decrease in the intensity of the fundamental mode, the intensity of the spectrum of excited modes begins to increase, also approaching the upper boundary, the value of which depends on the parameter δ .

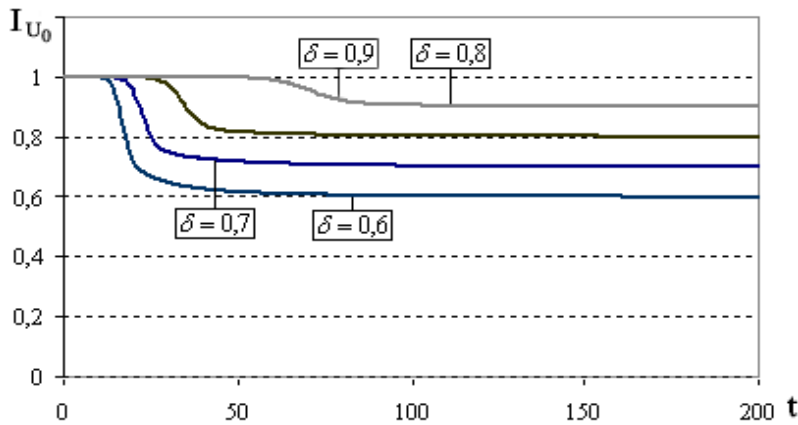


Fig. 16.6.
Intensity of the
fundamental mode
 $I_0 = u_0^2$
at the linear stage
of the process

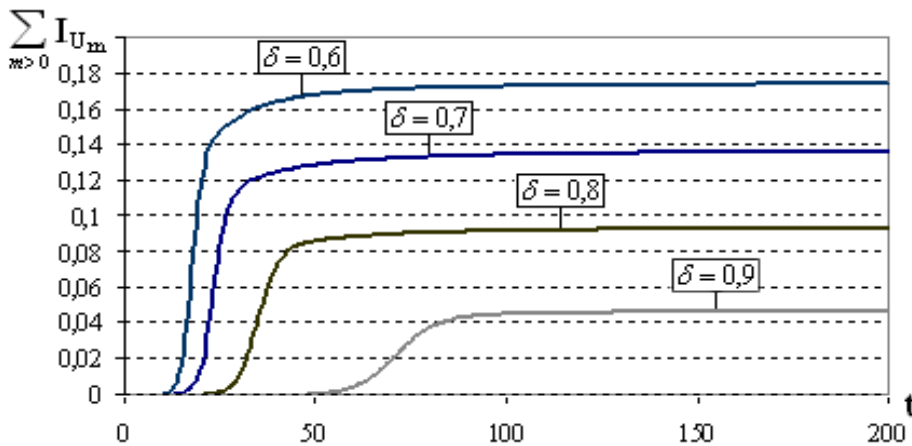


Fig. 16.7. Total
intensity of the
spectrum of the
excited modes
 $I_s = 2 \sum_{m>0} u_m^2$
at the linear stage
of the process

In this case, total intensity does not exceed unity (Fig. 16.8), and with the development of instability it decreases, being limited from below to values that depend on the parameter δ .

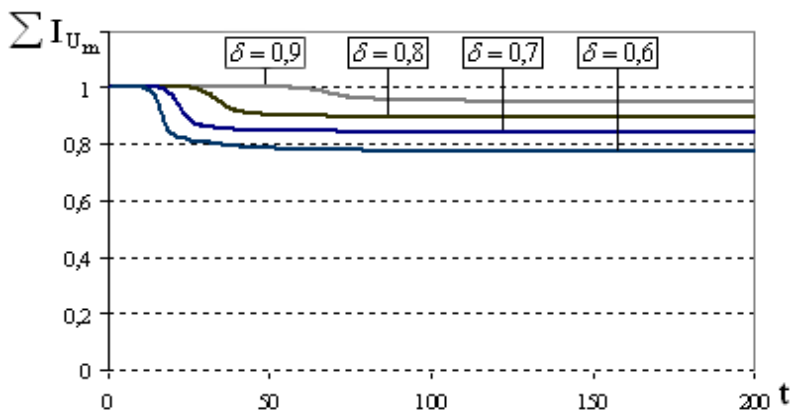


Fig. 16.8.
Total intensity
of the structure

References to section 16

16-1. Lighthill M. J. Contribution to the theory of waves in nonlinear dispersive system // *J. Inst. Math. Appl.* 1965. – Vol. 1. – No. 2. – P. 269–306.

16-2. Silin V. P. Parametric resonance in plasma // *JETP*. 1965. – Vol. 48. – No. 6. – P. 1679–1691 (in Russian).

16-3. Zakharov V. E. Stability of nonlinear waves in dispersive media // *J. Teor. Prikl. Fiz.*, – 1966. – Vol. 51. – P. 668–671 (in Russian).

16-4. Benjamin T. B., Feir J. E. The disintegration of wave trains on deep water // *J. Fluid Mech.* 1967. – Vol. 27. – P. 417–430.

16-5. Zakharov V. E. The Instability of Waves in Nonlinear Dispersive Media // *Sov. Phys. JETP*. 1967. – Vol. 24. – P. 740 (in Russian).

16-6. Askaryan G. A. Self-focusing effect // *UFN*. 1973. – Issue. 10. – N. 111. – P. 249–260.

16-7. Kuklin V. M. The role of deduction and dissipation of energy in the formation of spacious non-linear structures in non-important middles / V. M. Kuklin // *UFZh. Look around.* – 2004. – V. 1. – № 1. – P. 49–81 (in Ukrainian).

16-8. Kuklin V. M. The self-similar Structures Formation in Modulation unstable Media // *Electromagnetic Phenomena*. 2004. – V. 4. – N. 1 (in Russian).

16-9. Belkin E. V., Kirichok A. V., Kuklin V. M., Priymak A. V. Anomalous waves in a modulation unstable wave field // *East Eur. J. Phys.* 2014. – V. 1. – N. 2. – P. 4–39.

16-10. Belkin E. V., Kirichok A. V., Kuklin V. M. On interference in multimode modes of modulation instabilities // *Problems of Atomic Science and Technology (VANT) Issue “Plasma electronics and new acceleration methods*. 2008. – No. 4 (6). – P. 222–227 (in Russian).

16-11. Kuklina O. V., Kirichok A. V., Kuklin V. M. The dynamics of the formation of self-similar structures in nonlinear wave dissipative media with a non-decay spectrum // *The Journal of Kharkiv National University, physical series “Nuclei, Particles, Fields”*. 2001. – No. 541. – Iss. 4 (16). – P. 73–76.

16-12. Kuklin V. M., Kirichok A. V., Kuklina O. V. On the mechanisms of formation of self-similar structures in a nonequilibrium continuous medium // *Problems of Atomic Science and Technology. (VANT). Ser. Plasma electronics and new acceleration methods*. 2000. – No. 1. – P. 222–224 (in Russian).

16-13. Belkin E. V., Gushchin I. V. Analysis of a numerical model of modulation instability of a wave of finite amplitude in a nonlinear medium // *Bulletin of KhNU by V. N. Karazina. Ser. Mathematical modeling. Information technologies. Automated control systems*. 2008 – No. 809 (9). – P. 20–31 (in Russian).

16-14. Belkin E. V., Kirichok A. V., Kuklin V. M. Development of modulation instabilities in media with damping and forcing / *High-Power pulsed*

electrophysics. International conference XIV Khariton's topical scientific readings. Digest of technical papers - Sarov, Russia: FGUP «RFYATS-VNIIEF». 2013. – P. 14–20 (in Russian).

16-15. Zakharov V. E., Lvov V. S., Starobinets S. S. Turbulence of spin waves beyond the threshold of their parametric excitation // Phys. 1974. – V. 114. – No. 4. – P. 609–654 (in Russian).

16-16. Lvov V. S. Nonlinear spin waves. – M. : Science. Ch. ed. phys-mat. lit., 1987. – 272 p. (in Russian).

16-17. Karpman V. I. Nonlinear waves in dispersive media. – Moscow: Nauka, 1973. – 175 p. (in Russian).

SECTION 17. FORMATION OF A SELF-SIMILAR FIELD STRUCTURE

A numerical analysis of the model showed that near the instability threshold (16.16), i.e. when $\delta \leq 1$, the intensity of the fundamental mode at the initial stages of the process noticeably decreases and approaches the value δ when $t \approx 100$. As the amplitude of the main mode decreases, the spectrum of excited modes begins to grow, also approaching the upper boundary, the value of which depends on the parameter δ . The modes of the spectrum do not directly interact with each other (or this interaction is very small); they interact only with the main wave.

Such a quasilinear instability stage manifests itself under conditions, when the integral characteristics of the process practically do not change. In the

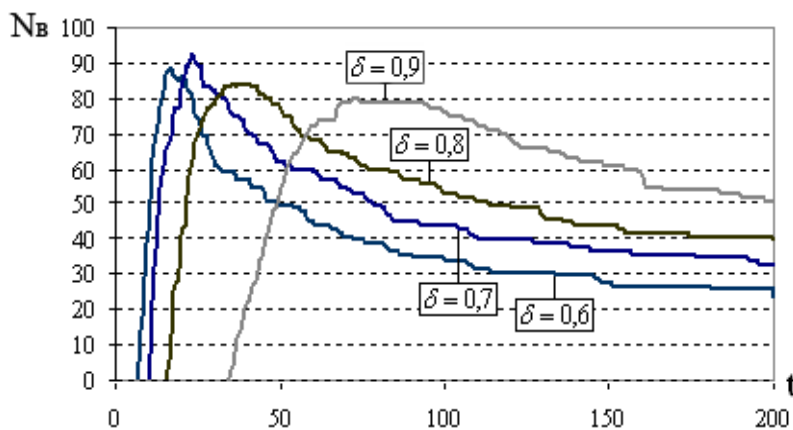


Fig. 17.1. Change in the number of excited modes of the instability spectrum N_B

developed stage of instability, the changes in the amplitudes of the spectrum modes sharply decrease.

The constant value of the total intensity of the system of spectrum modes, with a slow change in its internal structure at the quasilinear stage of the process, allows talking about the formation of a quasi-stable long-lived physical state.

It is important to note that the monotonic decrease in the number of spectrum modes that is observed at the quasilinear stage of the evolution of such a state actually corresponds to a decrease in excited degrees of freedom up to several ones (here it is the number of spectrum modes N_B , see Fig. 17.1).

The formation of long-lived quasi-stable states. In the developed instability regime, a further change in the intensity of both the wave and the spectrum does not occur. We can assume that the nonlinear, or rather the quasilinear instability stage manifests itself under conditions when the integral characteristics of the process practically do not change.

Fig. 17.1 shows that at the initial stage a set of modes is excited; it consists of more than 70 % of the modes of the initial spectrum, and the maximum number of modes is excited in the region of transition to the quasilinear stage. A mode was considered excited if its amplitude exceeded 0.1 % of the initial level of the main mode. The rate of change of the mode amplitude decreases over time, but continues to be significant. As a result of competition, the amplitude of the modes at the periphery of the spectrum decreases almost to zero, and the amplitude of a part of the modes in the center of the spectrum increases.

Thus, at the quasilinear stage, the whole spectrum narrows, the number of degrees of freedom (excited modes) decreases, that is, we can talk about a decrease in the values of characteristic quantities associated with the entropy of the system as a whole. The time derivative of the amplitudes of the peripheral modes of the spectra assumes a negative value, the spectra as a whole shift toward the wave number of the fundamental mode. Further, the rate of change in the amplitude of the excited modes decreases, and the system enters the quasilinear instability regime.

When the instability threshold is slightly exceeded, the integral indices behave similarly to the corresponding indices of the simple model, which confirms the validity of the previous assumptions concerning the possibility to neglect the interaction of modes within the spectrum when the instability threshold is slightly exceeded, and it also estimates the applicability boundary of the simple model $\delta \approx 0,7$.

The occurrence of self-similar field structures. This behavior of the instability spectrum made it possible to construct a theory of the formation of a fractal structure. Using the example of a modulation unstable wave, let us discuss the nature of the formation of a cascade of instabilities.

The modulation instability of a monochromatic wave considered in the previous section forms a new state – a modulated wave, which, as it follows from the discussion below [17-1 – 17-3], in its turn is unstable. Let us note that the modulation instability of a large amplitude wave is possible if the maximum increment (related to the monochromatic case) of the spectral line width is exceeded. In addition, the formation of narrow spectral lines of instability results in the expansion of the spatial region of modulation localization.

Let us show that as a result of secondary modulation instability, an even larger-scale modulation of the previously modulated main wave is formed.

To describe the secondary modulation instability, we can assume that the initial state of the system is a line spectrum consisting of three modes formed as a result of primary instability.

It is the formation of the line spectrum of the modulated wave upon saturation of the primary modulation instability that creates the conditions for exceeding the threshold of the secondary modulation instability.

As a result of secondary instability, spectra of unstable perturbations with wave numbers equal to $k = \pm k_2^*$ arise in the vicinity of the modes $\pm(k_2^* + \kappa)$. As before, it can be verified that the modes with $\pm(k_2^* + \kappa)$ have the same amplitude values as in absolute value. It can be shown [17-5, 17-6] that the maximum linear increment of the secondary instability is

$$\gamma_{2eff} = -\delta + [u_1^4 + 4u_{k_2^*}^4]^{1/2} \approx 2u_{k_2^*}^4 / u_1^2 \approx (u_{10}^2 - \delta)^2 / 2u_1^2, \quad (17.1)$$

where

$$\begin{aligned} \text{Sin}(\Phi_{k_2^*} - \Phi_{\kappa}) &\approx -\text{Cos} \Phi_{\kappa} = 2u_{k_2^*}^2 / [u_1^4 + 4u_{k_2^*}^4]^{1/2}, \\ \text{Sin} \Phi_{\kappa} &= -u_1^2 / [u_1^4 + 4u_{k_2^*}^4]^{1/2}, \text{ as } \Phi_{k_2^*} \approx -\pi/2. \end{aligned}$$

For the fastest growing modes at the linear stage of development of the secondary modulation instability $(k_2^* + \kappa)^2 = u_1^2 + 2u_{k_2^*}^2$ and the shift of the wave number κ relative to the wave numbers of the primary instability mode k_2^*

$$\kappa^* = k_2^* u_{k_2^*}^2 / u_1^2 = k_2^* (u_{10}^2 - \delta) / 2u_1^2. \quad (17.2)$$

It can be shown that, as a result of the development of secondary instability, its spectrum narrows. In fact, modes with wave numbers $\pm(k_2^* + \kappa^*)$ are retained in the spectrum of secondary instability. The ratio of the characteristic times of development of primary and secondary modulation instabilities

$$\tau_{1M} / \tau_{2M} = \gamma_{2eff} / \gamma_{1eff} = (u_{10}^2 - \delta) / 2u_1^2, \quad (17.3)$$

as well as the ratio of the spatial scales of the modulation of the main wave due to the consequences of the development of primary and secondary instability

$$L_{1M} / L_{2M} = (\kappa^* / k_2^*) \approx (u_{10}^2 - \delta) / 2u_1^2, \quad (17.4)$$

coincide. Thus, subsequent instability cascades form increasingly large-scale structures – modulations. Such structures are scale invariant [17-4 – 17-6].

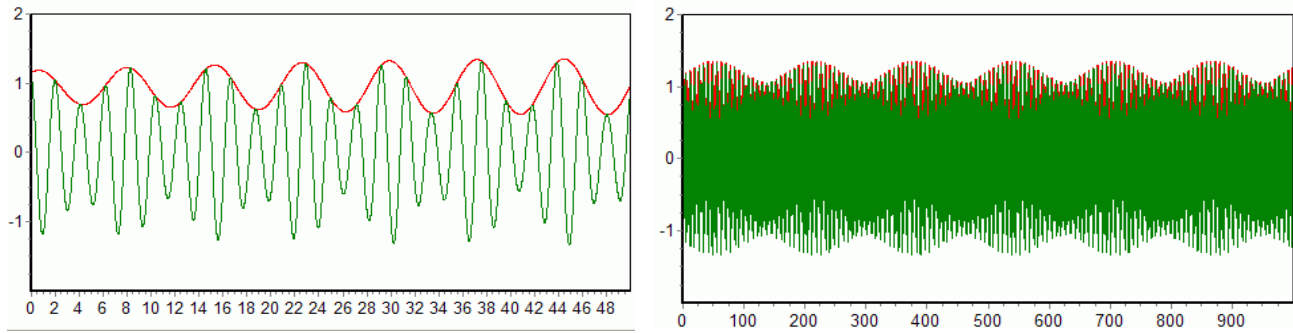


Fig. 17.2. Formation of self-similar field structures in a numerical experiment: $k_0 = 3$ is the wave number of the main wave, $K_{OPT} = 0.8$ is the wave number of the first-order envelope, and $\Delta K = 0.05$ is the wave number of the second-order envelope

Thus, the formation of a cascade of modulation near-threshold instabilities that form self-similar structures due to the narrowing of the spectra of each such separate process and the creation of conditions for the development of a new, larger-scale one is explained. In addition, narrow instability spectra of the cascade form a self-similar spatial structure that is clearly observed on each scale.

References to section 17

17-1. Modulation instability of waves supported by an external source in a medium with absorption / Belkin E. V., Kirichok A. V., Kuklin V. M. // VANT. Ser. "Plasma electronics and new acceleration methods. 2010. – No. 4 (68)). – P. 291–295 (in Russian).

17-2. Belkin E. V. The mathematical models of the modulation instability processes of waves in media with cubic nonlinearity– manuscript. / PhD–thesis by speciality 01.05.02 – mathematical modeling and computational methods. V. N. Karazin Kharkiv National University, Kharkiv, 2010 (in Russian).

17-3. Belkin E. V., Kirichok A. V., Kuklin V. M., Priymak A. V. Anomalous waves in a modulation unstable wave field // East Eur. J. Phys. 2014. – V. 1. – N. 2. – P. 4–39.

17-4. Kuklin, V. M. The role of energy absorption and dissipation in the formation of spatial nonlinear structures in nonequilibrium media, UFZh, Reviews. 2004. – V. 1. – No. 1, – P. 49–81 (in Russian).

17-5. Kuklina O. V., Kirichok A. V., Kuklin V. M. The dynamics of the formation of self-similar structures in nonlinear wave dissipative media with a non-decay spectrum // The Journal of Kharkiv National University, physical series "Nuclei, Particles, Fields". 2001. – No. 541 – Iss. 4 (16). – P. 73–76 (in Russian).

17-6. Kuklin V. M., Kirichok A. V., Kuklina O. V. On the mechanisms of formation of self-similar structures in a nonequilibrium continuous medium // Problems of Atomic Science and Technology. (VANT). – Ser. Plasma electronics and new acceleration methods. 2000. – No. 1. – P. 222–224 (in Russian).

CHAPTER 8. Modulation instability. Emergence of waves of anomalous amplitude

The development of modulation instability of wave motion far from its threshold is discussed. It is shown that instability can result in the formation of an envelope of the wave motion of anomalous amplitude. In this case, the field intensity at the maxima of the envelope can be an order of magnitude higher than the average intensity of the wave motion. The dynamics of modulation instability is analyzed in a model of practically non-decaying high-intensity ocean waves, the mechanism of formation of waves of anomalous amplitude is shown. The frequency of emergence of these waves turned out to be comparable in numerical experiments when compiling statistics both for an ensemble of many calculations and for time in one experiment with a viewing interval exceeding the lifetime of the anomalous waves. The results of calculations where the formalism of S-theory is used and direct calculations of the Lighthill-NLS equation are compared, and a qualitative agreement between these two approaches is shown.

SECTION 18.

MODULATION INSTABILITY FAR FROM THE THRESHOLD

If the instability threshold substantially exceeds $\delta \leq 0,7$, model (16.21) - (16.22), (16.25), (16.26), which takes into account the interactions between the spectrum modes ($k_S + k_{-S} = k_n + k_{-n}$), that are symmetric with respect to pumping, reveals qualitatively new effects in the process of developing the instability spectrum. This is a nonmonotonic character energy exchange between the main wave and the developing structure during modulation instability.

Let us consider the modulation of the main wave with a noticeable excess of the instability threshold. The consideration of the interactions between the modes of the excited spectrum allows examining the model in the region, which noticeably exceeds the instability threshold $\delta = 0,4$.

The calculation results are shown in fig. 18.1 – fig. 18.3. In this region of parameters, the intensity of the developed instability spectrum is higher in comparison with the region of weak overthreshold ($\delta \leq 0,7$). If the more intense spectrum affects the main wave more strongly, then the occurrence of more pronounced envelope bursts is possible.

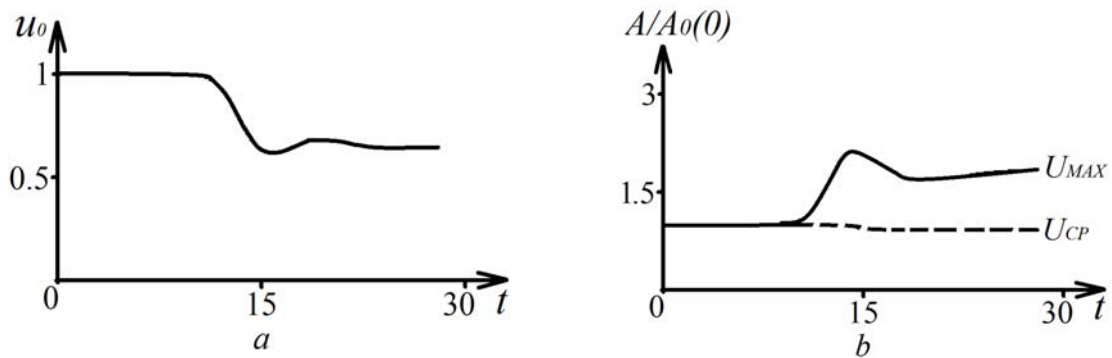


Fig. 18.1. The behavior of the amplitude of the main wave over time (a), the maximum (solid curve) and average (dashed) amplitude of the wave field envelope for the case $\delta = 0,4$, the number of modes is $N = 200$ [18-1]

When repeatedly simulating the process, it was noted that at the initial stage of the developed modulation instability, significant spikes in the amplitude of the main wave can occur. When mode spectra are excited, interference effects inevitably arise, consisting in the realization of bursts of modulation of the wave motion and in the occurrence of significant amplitudes of individual waves. The question is whether these effects are a manifestation of the random nature of mode interference or they are determined (see annex XXI).

It was noted above that the behavior of the modes of the excited spectrum is controlled by pumping, which in this case is a wave of large amplitude. In most cases, when such multimode processes occur, even if the interaction of unstable modes can be neglected, the effect of pumping on each individual mode of the instability spectrum can be large. Therefore, interference in such cases is forced, imposed by pumping. Randomness manifests itself only to the extent that the phase distribution of the modes of the instability spectrum at the initial moment was random.

Under these conditions, a narrowing of the instability spectrum can also be observed.

The dependences of the change in the energy of the mode spectrum and the energy of the fundamental wave on time in the process of instability development, shown in Fig. 18.3, are also of interest

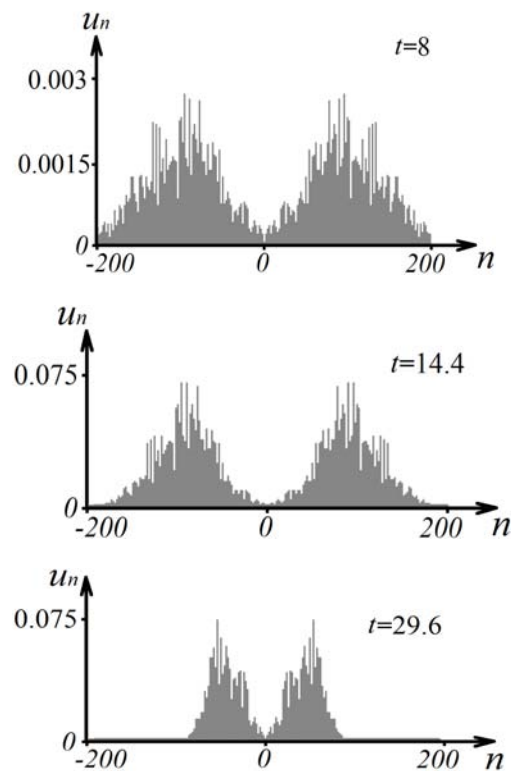


Fig. 18.2. The behavior of the instability spectrum for three time instants ($\delta = 0,4$ $N = 200$) [18-1]

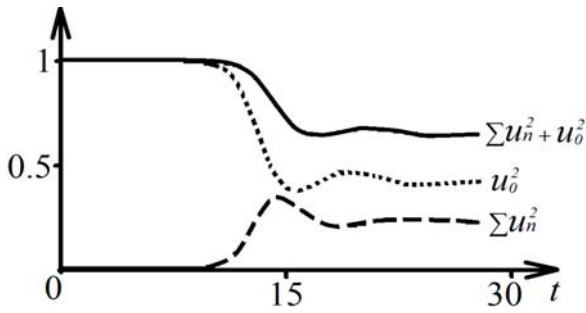


Fig. 18.3. Change in the energy of the spectrum of modes $\sim \sum_{m \neq 0} u_m^2$ and the energy of the main wave $\sim u_0^2$ and their sum over time ($\delta=0,4, N = 200$) [18-1]

Instability of a large-amplitude wave in the 2D Lighthill model [18-2]. Annex XIX discusses the excitation of mode spectra with a wave vector, which form a nonzero angle with the wave vector of the fundamental wave. The process of excitation of the two-dimensional instability spectrum (shown in Fig. 18.4) forms the instability spectrum at the initial stage of development – wide, with small ($u_k < 0,05$) mode amplitudes. In the process of development, the spectrum narrows, while the amplitude of the excited modes increases (Fig. 18.4b)

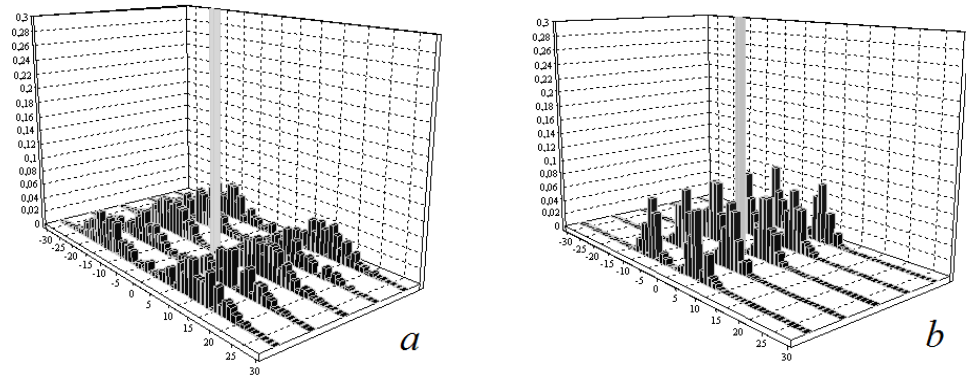


Fig. 18.4. The two-dimensional instability spectrum of a quasimonochromatic wave [18-1]

As a result of numerical modeling, three-dimensional patterns of the field envelope are obtained for the parameter values $N = 100$ and $\delta = 0,5$, at $\tau = 15$. Fig. 18.5a shows a small-scale picture of the envelope of the main wave, Fig. 18.5b illustrates bursts of the field envelope on a larger scale. Three-dimensional visualization of this wave field is presented in Fig. 18.6.

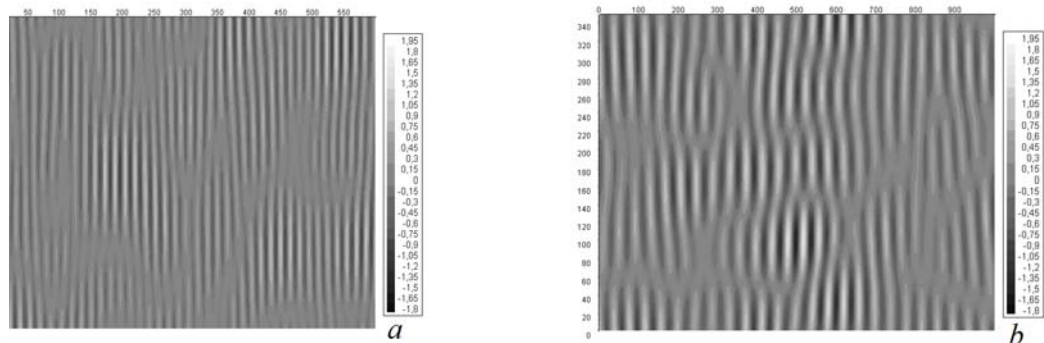


Fig. 18.5. Two-dimensional modulation of the main wave: a) small-scale representation, b) fragment [18-1]

We can make sure that taking even a small angle between wave fronts slightly increases the amplitudes of large waves, which was repeatedly noted by different authors.

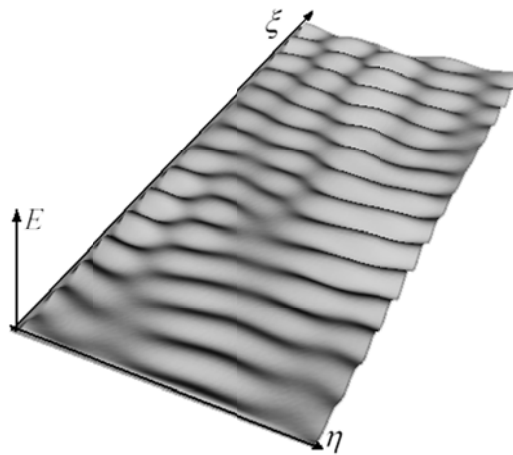


Fig. 18.6. Three-dimensional visualization of the envelope field, built on the basis of a height map (Fig. 18.5) [18-1]

Comparison of 1D Lighthill models in cases of applying S-theory (16-21) – (16.22), (16.25), (16.26) and direct calculation of equation (16.7). Near the instability threshold, the characteristics of the modulation process of the fundamental wave in two cases of applying the S-theory and the NLSE (Nonlinear Schrödinger Equation) are practically unchanged. Figure 18.7 shows the time dependences of the change in the energy of the mode spectrum $\sum_{m \neq 0} u_m^2$ and the energy of the fundamental wave u_0^2 in the process of instability development.

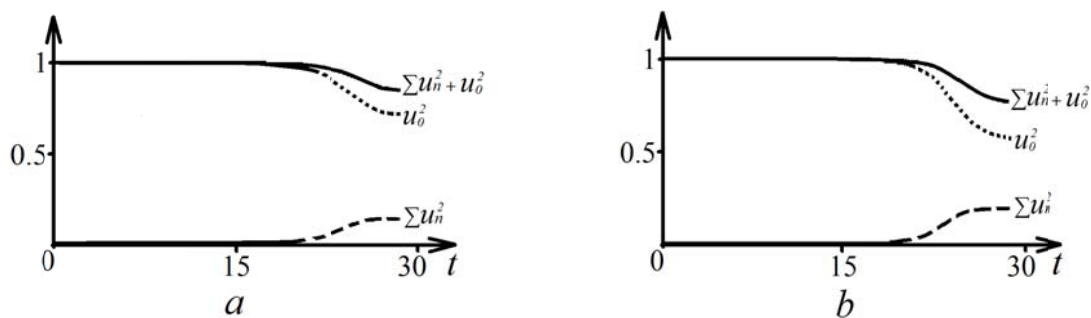


Fig. 18.7. Change in the energy of the spectrum of modes $\sum_{m \neq 0} u_m^2$ and the energy of the fundamental wave and their sum u_0^2 over time for the cases of applying S-theory (a) and NLSE (b) for $\delta = 0,7$, $N=200$ [18-1]

In case of applying S-theory (a), the average amplitude of the waves and the maximum amplitude of the wave envelope are somewhat smaller than when described by the nonlinear Lighthill-Schrödinger equation with this type of dispersion term (b). This dynamics is presented in fig. 18.8.

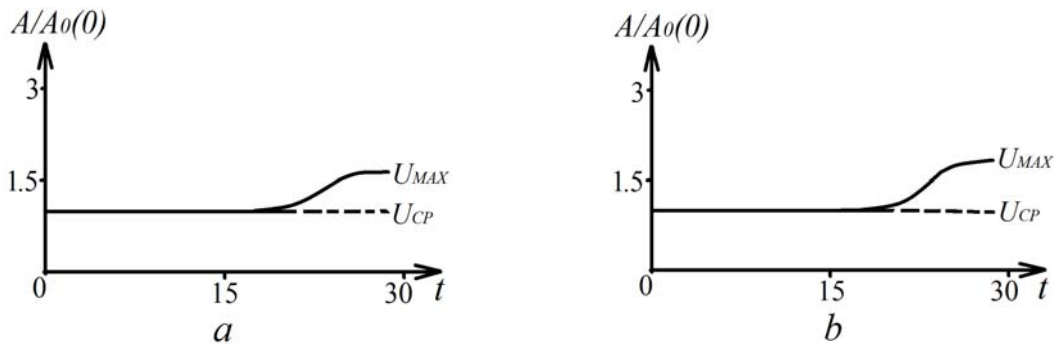


Fig. 18.8. Maximum (solid curve) and average (dashed) amplitudes of the wave field envelope for applications of the S-theory (a) and NLSE (b) for $\delta = 0,7$, $N=200$ [18-1]

Instability mode far from the threshold. Several more differences in the development of instability at low absorption levels, are far from the threshold. Thus, the characteristic time of modulation of the amplitude of the fundamental wave at the absorption level, taking into account all types of mode interactions, becomes less regular. The dependences of the energy of the mode spectrum $\sum_{m \neq 0} u_m^2$ and the energy of the fundamental wave on time u_0^2 in the process of instability development are presented in Fig. 18.9. The oscillatory nature of the energy exchange between the fundamental wave and the spectrum of unstable modes is already clearly visible.

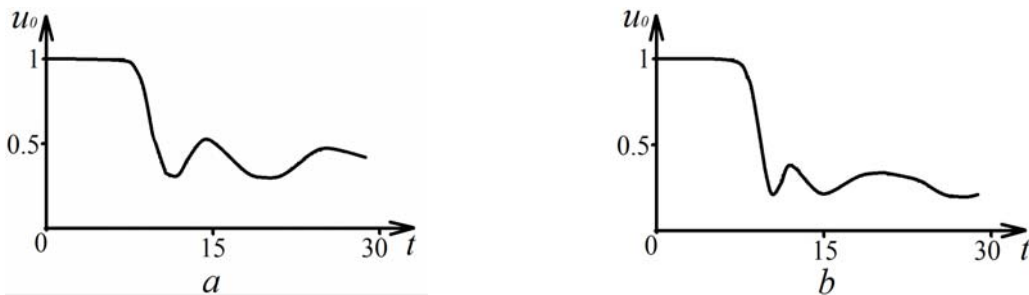


Fig. 18.9. The behavior of the amplitude of the main wave over time for cases of applying S-theory (a) and NLSE (b) for $\delta=0,1$ and $N=200$ [18-1]

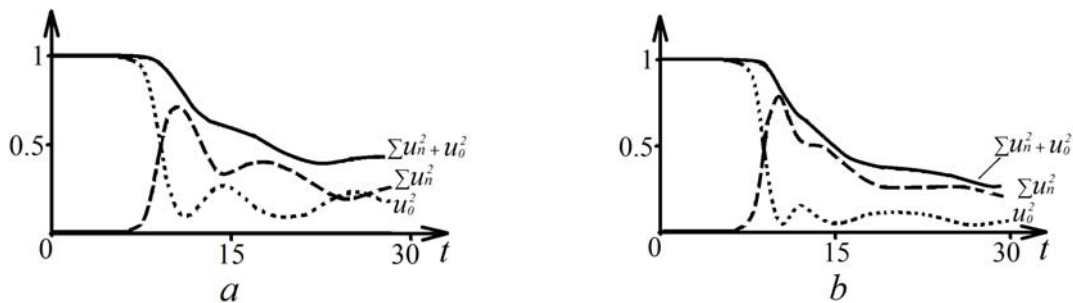


Fig. 18.10. The dependences of the energy of the mode spectrum, the energy of the fundamental wave, and their sum on time for the cases of applying S-theory (a) and NLSE (b) when $\delta=0,1$ and $N=200$ [18-1]

The envelope amplitude maxima in both cases are reached almost at the same time and are approximately equal to each other, which can be seen in Fig. 18.11. It is important to note that *the local energy density at the envelope maxima can be an order of magnitude higher than the average energy density of the modulated wave.*

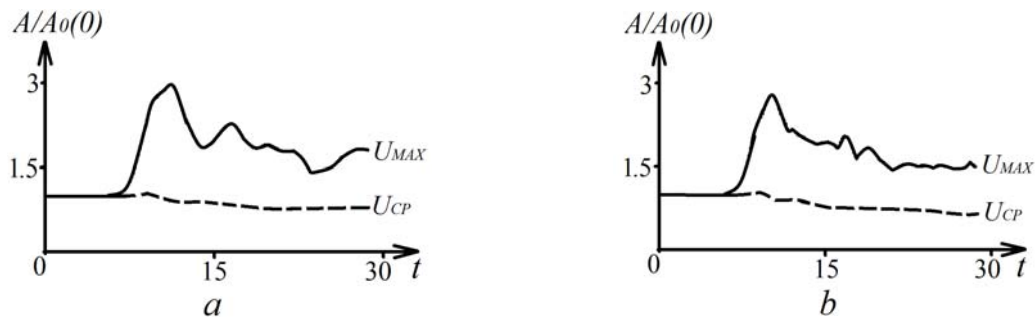


Fig. 18. 11. Maximum (solid curve) and average (dashed) amplitudes of the wave field envelope for applications of S-theory (a) and NLSE (b) when $\delta = 0,1$ and $N = 200$ [18-1]

The behavior of the instability spectrum also changes. In the case of the description in the framework of the S-theory (a), the two-humped spectrum characteristic of modulation instability narrows, while in the more general description (b) the opposite tendency to expansion is observed. The time for considering the spectrum was chosen at the process stage linear in the amplitudes of perturbations, at the moment of reaching the maximum amplitude of the wave field envelope and at the stage of developed instability (Fig. 18.12).

Under conditions of weak absorption, the energy of the spectrum of modulation instability reaches values comparable to the initial energy of a wave of finite amplitude. As we can see in fig. 18.11, at the initial stage of the nonlinear process mode, the occurrence of waves and bursts of the envelope with a very large amplitude is possible.

Subsequently, the amplitude of the main wave decreases (see Fig. 18.12) and its influence on the interference of the spectrum modes is weakened and their (bursts) amplitude significantly decreases.

The character of the modulation of the main wave in space (a fragment near a region with a maximum envelope amplitude) for the same instants of time for these two cases of instability description, is shown in Fig. 18.13. Thus, the S-theory created by the authors of [18-3, 18-4] and modified in [18-1], 18-5] allows a fairly accurate description of the initial stage of the nonlinear regime of the modulation instability process in the Lighthill – NLSE model, which provides the opportunity to quantify the maximum amplitude of the envelope of the wave field, the time of occurrence of the maximum of the envelope, and the energy concentrated in the disturbance spectrum.

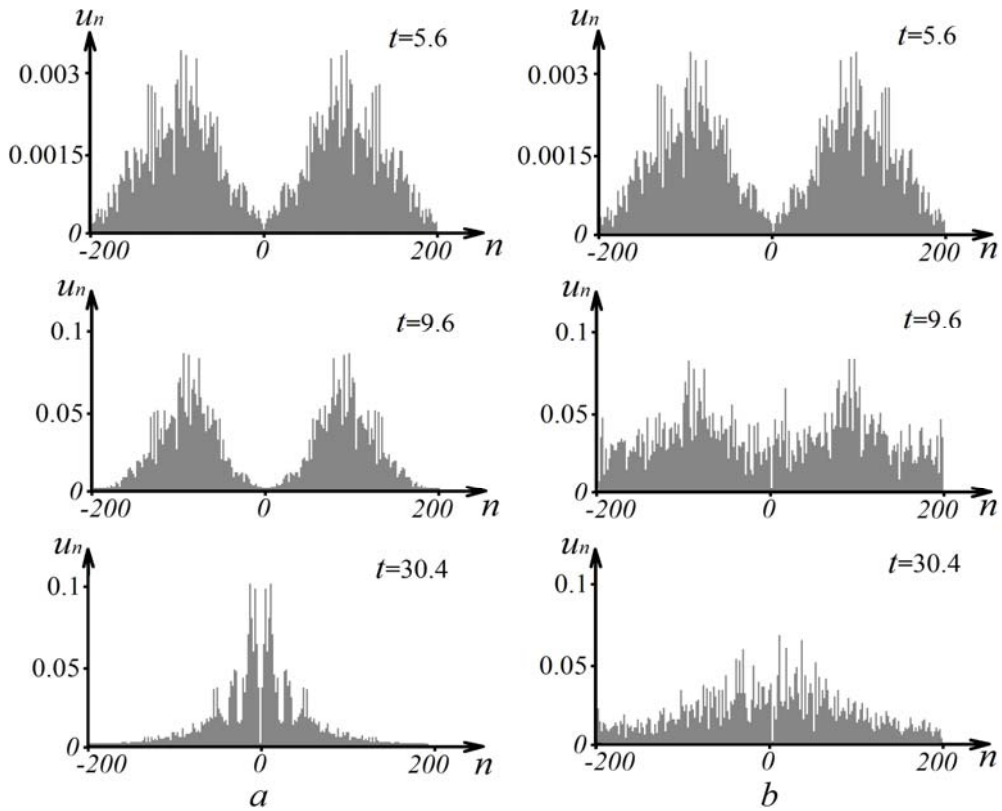


Fig. 18.12. Instability spectra for three time instants in the case of the description in the framework of S-theory (a) and for the description based on the NLSE (b) for $\delta = 0,1$ and $N = 200$ [18-1]

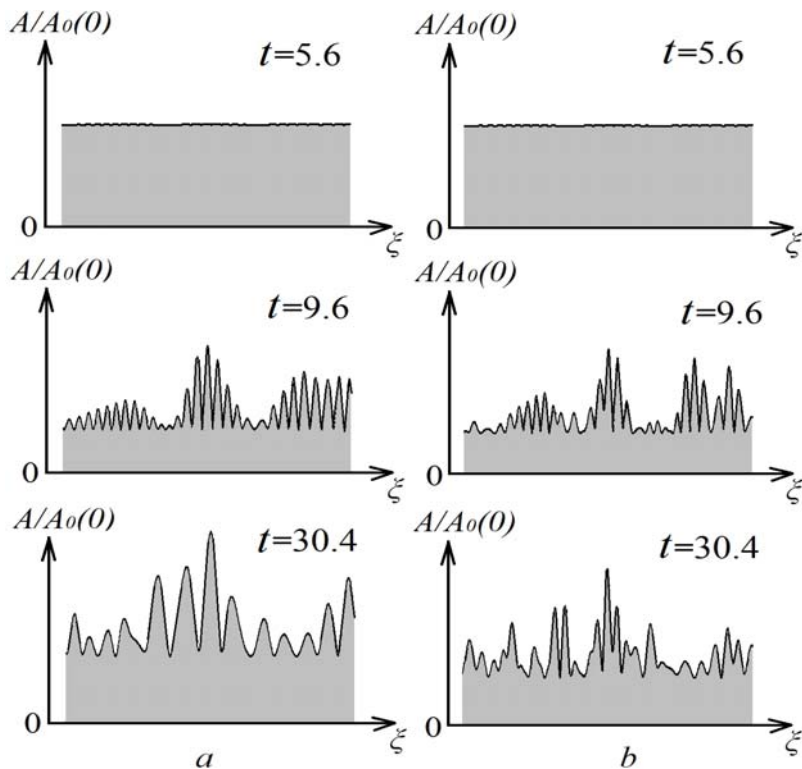


Fig. 18.13. The main wave modulation for three time instants in the case of the description in the framework of S-theory (a) and for the description based on the NLSE (b) for $\delta = 0,1$ and $N = 200$ [18-1]

It is worth paying attention to the fact that in the one-dimensional case, at low absorption levels, the maximum amplitude of the anomalous wave can be approximately three times higher than the average wave amplitude. In the two-dimensional case, for a converging wave, the maximum envelope amplitude can be noticeably larger. This can be understood if we consider the change in the width of the instability spectrum in the developed regime. Indeed, the width of the spectrum increases, which leads to a decrease in the characteristic size of the region of localization of the envelope. The expansion of the spectrum developed perturbation, while conserving the energy of the wave packet, leads to an increase in the corresponding degree of the maximum amplitude of the spatial envelope.

References to section 18

18-1. Belkin E. V., Kirichok A. V., Kuklin V. M., Priymak A. V. Anomalous waves in a modulation-unstable wave field // East Eur. J. Phys. 2014. – V. 1. – no. 2. – P. 4–39 (in Russian). (http://eejp.univer.kharkov.ua/Biblio/2014/EEJP_1_2/12p4-39.pdf)

18-2. Belkin E. V. The mathematical models of modulation instability processes of waves in media with cubic nonlinearity / Manuscript. PhD-thesis by speciality 01.05.02 – Mathematical modeling and computational methods. V. N. Karasin Kharkiv National University, Kharkiv, 2010. – 150 p. (in Russian).

18-3. Zakharov V. E., Lvov V. S., Starobinets S. S. Turbulence of spin waves beyond the threshold of their parametric excitation // UFN. – V. 114. – No. 4. – P. 609–654 (in Russian).

18-4. Lvov V. S. Nonlinear spin waves. – M. : Science. Ch. ed. phys-mat. lit. 1987. – 272 p. (in Russian).

18-5. Kuklin V. M. The self-similar Structures Formation in Modulation unstable Media // Electromagnetic Phenomena. 2004. – V. 4. – N. 1 (in Russian).

SECTION 19.

MODULATION INSTABILITY OF GRAVITATIONAL WAVES ON WATER SURFACE

For gravitational surface waves in deep water, which are of interest for shipping in areas with a high level of excitation of ocean waves, the following expression is valid for the frequency of waves of large amplitude [19-1]

$$\omega = \sqrt{g \cdot k} \cdot \{1 + |A|^2 k^2 / 2\} \quad (19.1)$$

which approximately corresponds to the Lighthill-NLS equation in the form

$$\frac{\partial}{\partial t} A = i\omega \cdot \left(1 - \frac{1}{2} |A|^2\right) \frac{\partial^2 A}{\partial x^2}, \quad (19.1a)$$

where A – is the surface deviation, W is the wave velocity, g is the acceleration of gravity.

The data of experimental observations and studies [19-2] indicate the following characteristics of such waves: the maximum steepness for stable long (gravitational) waves in deep water until they collapse (crash, are breaking) is $H/\lambda \approx 0.11 \div 0.13$, where $H = 2|A|$ is the "swing range" of the wave, that is, the distance between the upper point of the wave crest and the lower trough point of the wave, $\lambda = 2\pi/k_0$ is the wavelength. It is important to note that waves with a larger amplitude do not exist due to the collapse effect. In the absence of modulation, $|A_0|$ is the average amplitude, $\bar{H} = 2|A_0|$ is the average swing range. For anomalously large waves, their swing range (steepness) reaches $(2 \div 3) \cdot 2|A_0|$, and for the highest nondestructive waves, herewith in case of high nondestructive waves such condition must be satisfied $(2 \div 3) \frac{2|A_0|}{2\pi} k_0 < 0,11 - 0,13$.

Analyzing these data, it is easy to see that the width of the spatial spectrum of the instability under these conditions is not so small in comparison with the wavenumber of a wave of large amplitude, as in previous models.

That is why the equation for the complex slowly varying (dependence $\propto \exp\{-i\omega_0 t\} = \exp\{-igk_0 t\}$ is excluded here) field amplitude is represented as

$$\begin{aligned} \frac{\partial A_K}{\partial t} &= -\delta A_K - i(\sqrt{g(k_0 + K)} - \sqrt{gk_0}) A_K - i\sqrt{g(k_0 + K)} \frac{(k_0 + K)^2}{2} \{|A|^2 A\}_K = \\ &= -\delta A_K - i(\sqrt{g(k_0 + K)} - \sqrt{gk_0}) A_K - i\sqrt{g(k_0 + K)} \frac{(k_0 + K)^2}{2} \cdot \\ &\cdot \{A_K [2|A_0|^2 + 2 \sum_{K' \neq K, 0} |A_{K'}|^2 + |A_K|^2] + A_{-K}^* \{A_0^2 + \sum_{K \neq K, 0} A_K \cdot A_{-K}\}\}, \end{aligned} \quad (19.2)$$

In the simplest case of a plane wave front, the perturbation field is written as

$$A(\zeta, \tau) = (u_0 + \sum_{\substack{K \neq 0 \\ K > 0}} [u_K \cdot \exp\{+iK\zeta + i(\phi_K - \phi_0)\} + u_{-K} \cdot \exp\{-iK\zeta + i(\phi_{-K} - \phi_0)\}]),$$

where $A_K / A_0 = a_K = |a_K| \exp\{i\phi_K\} = u_K \exp\{i\phi_K\}$, $k_0 \xi = \zeta$, $\alpha = k_0^2 |A_0|^2$,

$\tau = t \cdot \sqrt{gk_0} \frac{k_0^2 |A_0|^2}{2}$, $K \rightarrow K/k_0$, $2\phi_0 - \phi_K - \phi_{-K} = \Phi_K$. Spectrum modes are

spaced $0 < K < 2K_{Max}$ and $-2K_{Max} < -K < 0$. $K = 0.3 \cdot \frac{i}{N}$, $i = \pm(1, 2, \dots, N)$,

$\alpha = 0.05$, $N = 100$. The initial amplitudes $u_K(\tau = 0) = 10^{-3}$ and their phases $\phi_K(\tau = 0)$ are randomly distributed in the interval from $0 - 2\pi$.

Using this representation, let us write down a system of equations describing the modulation instability of a large-amplitude gravitational surface wave under conditions of strong dispersion of deep water

$$\frac{\partial |A_K|}{\partial t} = -\delta |A_K| + \sqrt{g(k_0 + K)} \frac{(k_0 + K)^2}{2} \cdot [|A_{-K}| |A_0|^2 \sin \Phi_K + |A_{-K}| \sum_{K \neq K, 0} |A_K| \cdot |A_{-K}| \sin(\Phi_K - \Phi_K)], \quad (19.3)$$

$$\frac{\partial \phi_K}{\partial t} = -[\sqrt{g(k_0 + K)} - \sqrt{gk_0}] - \sqrt{g(k_0 + K)} \frac{(k_0 + K)^2}{2} \cdot [2|A_0|^2 + 2 \sum_{K \neq K, 0} |A_K|^2 + |A_K|^2] + \frac{|A_{-K}|}{|A_K|} |A_0|^2 \cos(\Phi_K) + \frac{|A_{-K}|}{|A_K|} \sum_{K \neq K, 0} |A_K| \cdot |A_{-K}| \cos(\Phi_K - \Phi_K). \quad (19.4)$$

For a wave of large amplitude

$$\frac{\partial |A_0|}{\partial t} + \delta |A_K| + \sqrt{gk_0} \frac{k_0^2}{2} \cdot [|A_0| \sum_{K \neq K, 0} |A_K| \cdot |A_{-K}| \sin(\Phi_K)] = G, \quad (19.5)$$

$$\frac{\partial \phi_0}{\partial t} = -\sqrt{gk_0} \frac{k_0^2}{2} \cdot [(|A_0|^2 + 2 \sum_{K \neq 0} |A_K|^2) + \sum_{K \neq 0} |A_K| \cdot |A_{-K}| \cos(\Phi_K)]. \quad (19.6)$$

The interval $0 < K < 2K_{Max}$ can be represented as a sum of N modes in a usual way, as before by introducing an interval in the space of wave numbers $\Delta K = 2K_{Max} / N$, and moving on to the use of dimensionless quantities $K_i = i \cdot \Delta K / k_0$, $i = \pm(1, 2, \dots, N)$. Finally, the system of equations describing the modulation instability of a large-amplitude wave takes the form

$$\frac{\partial u_K}{\partial \tau} = -\delta u_K + (1 + K)^{2.5} \cdot [u_{-K} \cdot u_0^2 \sin \Phi_K + 2u_{-K} \sum_{K > 0} u_K u_{-K} \sin(\Phi_K - \Phi_K)], \quad (19.7)$$

Here it is necessary to distinguish between modes with wave numbers K and K respectively, phases Φ_K and Φ_K , and also make a substitution $K \rightarrow K / k_0$

$$\frac{\partial \phi_K}{\partial \tau} = -\frac{2[\sqrt{(1+K)} - 1]}{\alpha} - (1+K)^{2.5} \cdot \{2 \sum_{K' \neq K} u_{K'}^2 + u_K^2 + \frac{u_{-K}}{u_K} \sum_{K \neq K} u_K u_{-K} \cos(\Phi_K - \Phi_K)\}, \quad (19.8)$$

In calculations, the decomposition of radical expressions shouldn't be used. The equations for the main wave can be written as

$$\frac{\partial u_0}{\partial \tau} + \delta u_0 + u_0 \sum_{K \neq K, 0} u_K u_{-K} \sin \Phi_K = G, \quad (19.9)$$

$$\frac{\partial \phi_0}{\partial \tau} = -u_0^2 - 2 \sum_{K \neq 0} u_K^2 - \sum_{K \neq 0} u_K u_{-K} \cos \Phi_K. \quad (19.10)$$

In order to analyze the swing range of the waves (that is, the distance between the upper point of the wave crest and the lower point of the trough), we single out a third of the largest ones. Let us find for each point in time in the patial interval $(\zeta \subset L = 2\pi / (\Delta K / k_0) = \pi N / K_m = \frac{\pi N}{\sqrt{2} \cdot \alpha^{1/2}}$, where $\zeta = k_o x$),

is average values of swing range $H = U_{CP}$ and average values of swing range

$H = U_{SWH}$ of the third of the largest one, as well as the largest wave swing range is $H = U_{Max}$ from the ensemble.

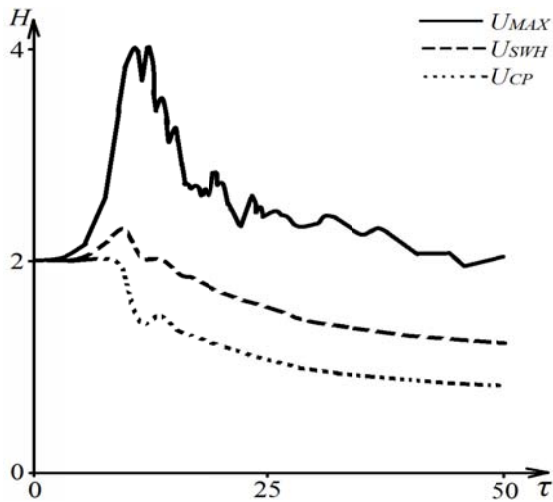


Fig. 19.1. Wave swing range (distance between the upper point of the wave crest and the lower point of the trough) as a function of time: average for all waves U_{CP} , average for the third of the largest waves U_{SWH} , maximum for each time point U_{Max} [19-3]

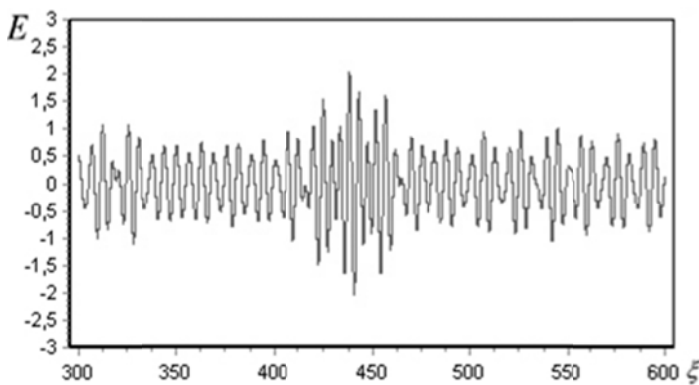


Fig. 19.2. A local wavefield surge exceeding the average amplitude of the third of the largest waves by more than 2 times ($N = 300, t = 10.2$) [19-3]

Numerical analysis of dynamics and statistical indicators using S-theory.

The calculations were performed for 600 spectrum modes; the ratio of the absorption decrement to the maximum increment was chosen equal to δ . Moreover, in order to normalize the amplitude of the main waves per unit at the initial stage of the process, the level of external pumping was chosen $G = \delta$. For the model (19.7) – (19.10), built on the basis of the S-theory, with a decrease in absorption, the quantity u_0^2 that determines the energy of the main wave decreases, and the quantity $\sum_{m \neq 0} u_m^2$ that determines the energy of the instability spectra increases.

Since the attenuation of gravitational waves on the surface of the ocean is small, it makes no sense to consider cases close to the instability threshold. Let us focus on the case when the absorption of wave energy is quite small:

let the ratio of the absorption decrement to the maximum increment be chosen at the level of 0.1 (i.e. $\delta=0,1$). The calculation results for one implementation of

the initial conditions are shown in Fig. 19.1. First of all, it should be noted that the criterion by which anomalously large waves are distinguished is of the form

$$U_{AG} > 2U_{SWH}, \quad (19.11)$$

or similar to this is ambiguous, because the largest amplitudes are observed precisely in the initial stage of development of instability, especially with final attenuation.

Nevertheless, waves of noticeably smaller amplitudes or ranges in the regime of developed instability also fall under this criterion, since there is a decrease in both medium and large wave amplitudes over time.

Fig. 19.2 shows the wave packet, i.e. the amplitude of the largest wave, which meets the criterion (19.11).

With a decrease in the absorption level δ , the processes of energy exchange between the spectrum and the main wave amplify. The shape of the spectrum is asymmetric. It can be verified that as the amplitude of the main wave decreases at the initial stage of instability, the maximum of the instability increment shifts to lower values K . In this case, since the maximum of the increment corresponds to the value of the total phase $2\phi_0 - \phi_K - \phi_{-K} = \Phi_K$ is equal to $\pi/2$, then consecutively the condensation of these phases (synchronization) near this value occurs for most modes with different values K .

The fact that the integral phases of the instability spectrum Φ_K are concentrated near $\pi/2$ creates the conditions for almost of the same type of interaction of many pairs of modes with the main wave.

This collective interaction of the spectrum modes with the fundamental wave explains the nature of the intense oscillations of the intensity of the fundamental wave and the spectrum in the initial stage of instability. Later, the spread of the integral phases increases and the energy exchange between the main wave and the spectrum weakens. Due to the fact that the phases of the individual modes ϕ_K retain a random distribution (in particular, there are no symmetries $\phi_K = \phi_{-K}$, and $\phi_K = -\phi_{-K}$), the instability spectrum forms a different interference structure synchronized with the main wave in each implementation.

Nevertheless, the intensity of the interference of the spectrum modes in the initial stage is the highest¹⁴. Considering the dynamics of the instability spectrum in the calculations carried out in this work, we can detect the phenomenon of a significant shift in relation to the spectral region of linear instability. This shift is due to a decrease in the amplitude of the main wave. In addition, it should be noted that the amplitudes of individual modes of the spectrum remain much

¹⁴ By the way, phase synchronization due to the choice of symmetric initial phases of the interacting modes of the spectrum of the modulation instability of the intense wave or the symmetrization of the equations themselves, usually led to sharpened modes. The absence of phase symmetry in pairs of interacting waves can weaken the intensity of interference bursts and shorten their lifetime.

smaller than the amplitudes of the main wave. Let us also note the asymmetry of the spectrum with respect to the fundamental wave, which is due to strong dispersion and a rather large increment of modulation instability for large amplitude waves.

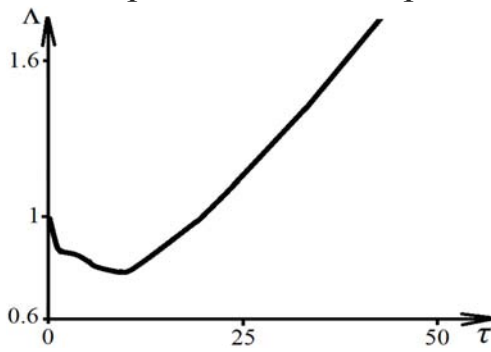


Fig. 19.3. The behavior of the relative characteristic length of the modulation $\Lambda \approx 2\pi / \Delta K$ during instability [19-3]

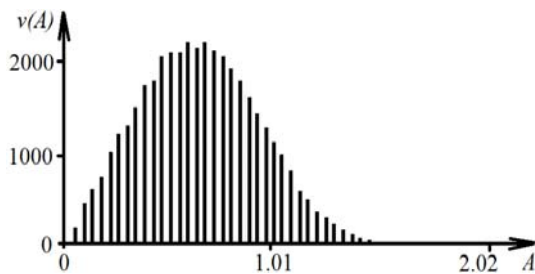


Fig. 19.4. The frequency of occurrence of waves of different amplitudes $\nu(A)$ in numerical experiments for different process realizations (under ensemble averaging conditions) at the same time $\tau \propto 10$ [19-3]

(Fig. 19.3). Due to a noticeable absorption in the system, the occurrence of waves and bursts of the envelope with a very large amplitude is possible only at the initial stage of the nonlinear process mode (for loss level $\delta = 0.1$).

With the development of the process, the amplitude of the main wave decreases and its influence on the interference of the spectrum modes is weakened. The amplitudes of large waves, even satisfying the criterion (19.11), also noticeably decrease

Thus, under conditions of a noticeable absorption of vibrational energy, the occurrence of abnormal waves of a very large amplitude is characteristic only for the initial stage of developed modulation instability. With the development of instability, the average and maximum values of waves for a given absorption level ($\delta = 0.1$) decrease noticeably (Fig. 19.1).

However, according to the accepted criterion (19.11), even under these conditions it is possible to distinguish anomalously large waves, although when

From an analysis of the spectra, it can be seen that in the developed instability regime under conditions of finite absorption, the modulation length at large times increases by almost 3.5 times. The behavior of the relative characteristic modulation length is shown in Fig. 19.3. The dynamics of two-dimensional wave processes is similar.

Thus, the number of waves along the modulation length in the initial stage of developed instability is much smaller than in the later stages of the process. Let us note that with a decrease in the absorption level in the system, this effect weakens (see below).

Analyzing the frequency of occurrence of anomalous waves in different implementations of the process, we shall find that one wave of such kind occurs among the waves, which qualitatively corresponds to known observations

$\tau \propto 30$ their amplitude is already one-and-a-half to two times less than in the most interesting case of the largest similar waves at $\tau \propto 10$. Several waves are stacked along the modulation length in the initial stage of the process, one of which in some implementations may turn out to be anomalously large. In the regime of developed instability, the number of waves along the modulation length increases by three to four times.

Comparison of 1D models in cases of applying S-theory and a more general description.

In real conditions, the absorption of energy of gravitational waves of large amplitude is very small. Therefore, it will be rational to compare two description models for a more realistic case of small absorption of ocean waves $\delta = 0.01$ and a significant amplitude of the waves $\Delta = 0.566 / N \alpha = 0.01$.

Below, let us present the results of calculations that demonstrate the development of the instability spectrum for three instants in time in the case of description in the framework of S-theory (a) and in the general case (b).

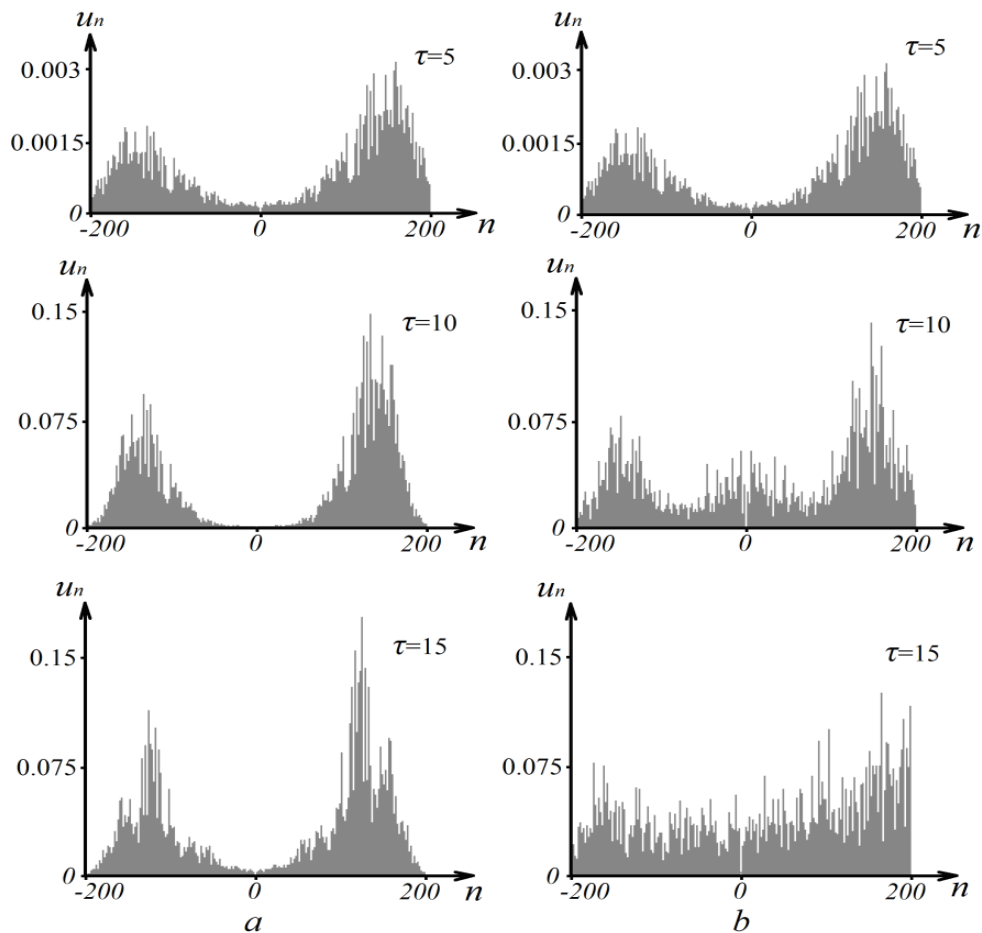


Fig. 19.5. The instability spectrum for three instants in time in the case of description in the framework of S-theory (a) and in the general case (b) [19-3]

It is easy to see the formation of a characteristic two-humped spectrum (Fig. 19.5) of modulation instability. If in the case of a description in the framework of S-theory this shape of the spectrum is preserved, then in the general

case of a description, the spectrum with the development of instability is smoothed out. Fig. 18.6 shows the nature of the change in the amplitude of the main wave in case of the S-theory description in the framework (a) and in the general case (b).

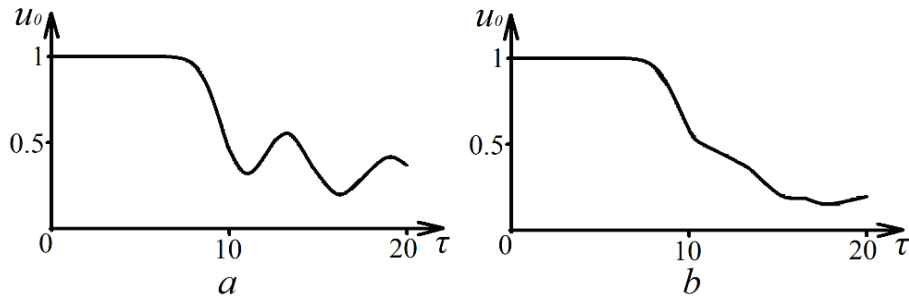


Fig. 19.6. The change in the amplitude of the main wave over time. a). when described in the framework of S-theory and b). in the general case, when all types of mode interaction in the nonlinear term of the form $\{ |A|^2 A \}$ are taken into account [19-3]

It can be seen that nonresonant interactions for which the S-theory relations are not fulfilled lead to the disruption of the oscillatory behavior of the amplitude of the main wave, which is characteristic of the resonance interaction described by the S-theory [19-4, 19-5]. The dynamics of changes in the average

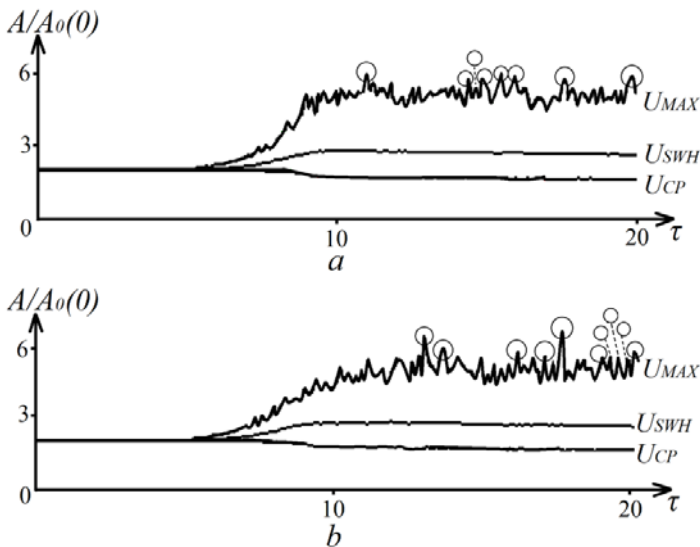


Fig. 19.7. Average amplitude U_{CP} , average amplitude of a third of the largest modes U_{SWH} , and amplitude of the largest wave U_{MAX} of the ensemble, as a function of time. The circles indicate the occurrence of waves of anomalous amplitude in the framework of S-theory (a) and in the general case (b)

amplitude U_{CP} , average amplitude of a third of the largest modes U_{SWH} and currently maximum modes U_{MAX} is shown in Fig. 19.7. The circles indicate the occurrence of waves of anomalous magnitude, which satisfy the relation (19.11), that is $U_{MAX} > 2U_{SWH}$.

Distributions of the amplitudes of the ranges H , i.e., the distances between the upper point of the wave crest and the lower point of the trough, in the developed instability regime at one moment and for the entire calculation time are shown in fig. 19.8 and fig. 19.9 when described in the framework of S-theory (a) and in the general case (b).

Waves were calculated through time instants equal to the lifetime of the anomalously large wave¹⁵. The lifetime was determined by considering the

¹⁵ Due to weak absorption, the average wave characteristics did not change.

behavior of a wave of anomalous amplitude in a given region during some necessary observation time. That is, averaged essentially over time, in contrast to the case presented in fig. 19.1, where waves with different amplitudes were estimated in numerous calculations (averaging over the ensemble of calculations).

In a numerical experiment, comparing two approaches (S-theory and direct calculation), the nature of the distribution of the ranges is similar to that discussed in [19-4, 19-5], where their number was calculated in different realizations, and the values were averaged over the ensemble of realizations. The number and distribution of the ranges of detected waves of anomalous amplitude in these two cases are presented in Table 19.1.

Attention should be paid to the presence of pronounced “tails” of distributions in both cases.

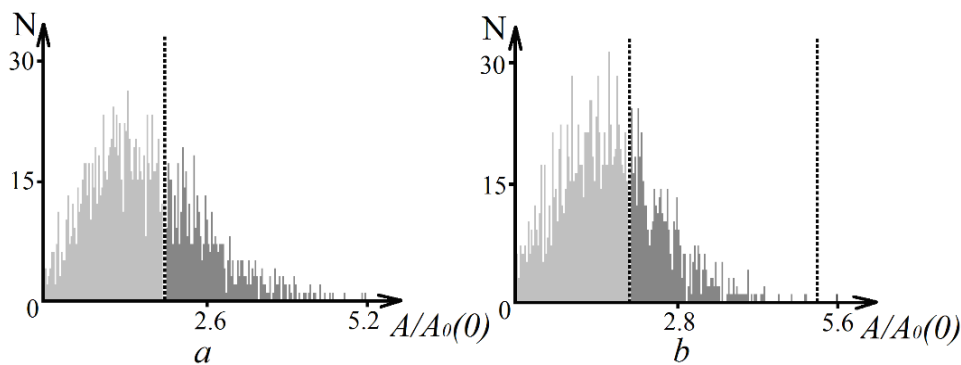


Fig. 19.8. The distribution of the amplitudes of the ranges in the observation interval at time $\tau = 20$ when described in the framework of S-theory (a) and in the general case (b). The dashed lines define the boundary between low amplitude modes and the third largest modes and a magnitude two times the average of the third largest modes [19-3]

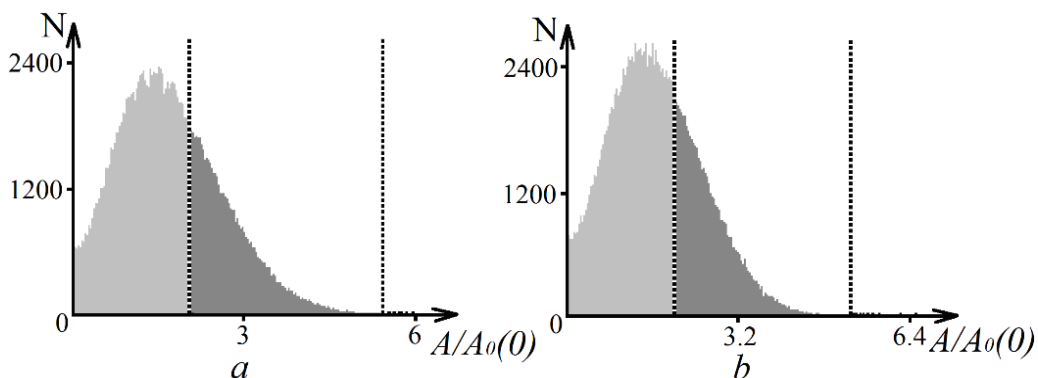


Fig. 19.9. Distribution of the amplitude of the ranges for the entire time of calculations in the observation region when described in the framework of S-theory (a) and in the general case (b), a) – total number of waves is 173526, third part of largest waves is 57842, the number of waves which are 2 times more than the average third part of the largest waves are 8, b) – the total number of waves is 176386, third part of largest waves is 58795, the waves which are 2 times more than the average third part of the largest waves are 10 [19-3]

Table 19.1

Abnormal range

$U_{MAX} / 2U_{SWH}$	S theory	General case
2-2,1	4	7
2,1-2,2	2	1
2,2-2,3	2	-
2,3-2,4	-	1
2,4-2,5	-	1
all	8	10

The source [19-3].

An analysis of observations and numerical experiments shows that anomalous waves often arise in a group of waves in the form of soliton-like formations. In this case, such waves occur precisely in the composition of groups of sufficiently large waves, and in the general case, the characteristic modulation length is shorter than when described in the framework of S-theory (see Fig. 19.10).

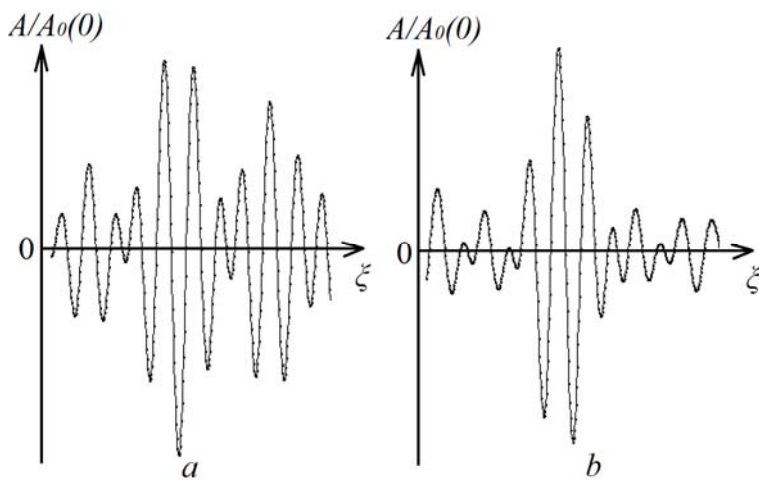


Fig.19. 10. Characteristic form of anomalous waves in the composition of wave groups when described in the framework of S-theory (a) and in the general case (b) [19-3]

In this case, such waves occur precisely in the composition of groups of sufficiently large waves, and in the general case, the characteristic modulation length is shorter than when described in the framework of S-theory (see Fig. 19.10).

Since the system under discussion can be considered almost conservative, because the mechanisms of wave energy dissipation are very weak¹⁶, the descriptions of

nonequilibrium processes under conditions of intense waves developed in [19-6 – 19-8] may turn out to be applicable to the case under consideration. However, it should be noted that the non-stationary autowave solutions found by the authors of [19-6 – 19-8], having a nature similar to solitons, receive energy from an infinite medium filled with wave motion. Therefore, the energy exchange between these disturbances and the medium was not considered. In addition, periodic breather disturbances, as shown in the experiment, are often not accomplished. However, a single short-lived breather, the Peregrin soliton [19-8], is similar to the solution shown in Fig. 19.10, which describes a single wave of anomalous amplitude.

¹⁶ Therefore, the previous consideration, where dissipative effects are significant, was carried out without the use of solution methods for conservative media used by the authors [19-6 – 19-8].

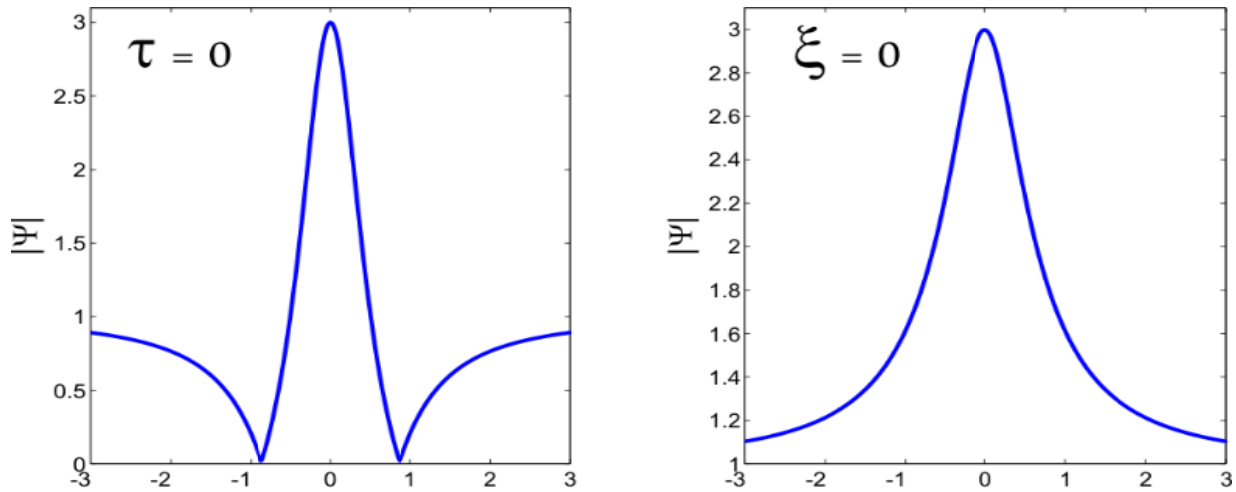


Figure 19.11. The form of a non-stationary perturbation in the form of a Peregrin soliton $\Psi = \{1 - 4(1 + 2i\tau)(1 + 4\xi^2 + 4\tau^2)^{-1}\} \exp\{i\tau\}$, in space (right) and over time (left), where Ψ satisfies equation $i\Psi_\tau + 0.5 \cdot \Psi_{\xi\xi} + |\Psi|^2 \Psi = 0$ [19.7]

A similar disturbance arises in the field of wave motion and then disappears, which corresponds to the appearance and disappearance of a short-lived anomalous wave considered above due to the interference of a packet of standing waves of the spectrum of modulation instability, moving at different speeds under the action of the main wave (see annex XXII).

It is important to note that in the one-dimensional case under discussion, the maximum amplitude of the anomalous wave (breather) is three times the average wave amplitude.

The experiment was conducted at the Technological University of Hamburg in a 15x1.5x1.6 meter tank with water for wave motion $k_0 A \approx 0.1$; the correspondence of the arising wave of anomalous amplitude (solid curve, compared fig. 19.10) with the Peregrin soliton (dashed curve) was found.

Thus, waves of anomalous amplitude under developed waves, which appear to be autowaves permanently existing and unpredictable under these conditions – soliton-like perturbations with variable amplitudes [19-6 – 19-8],

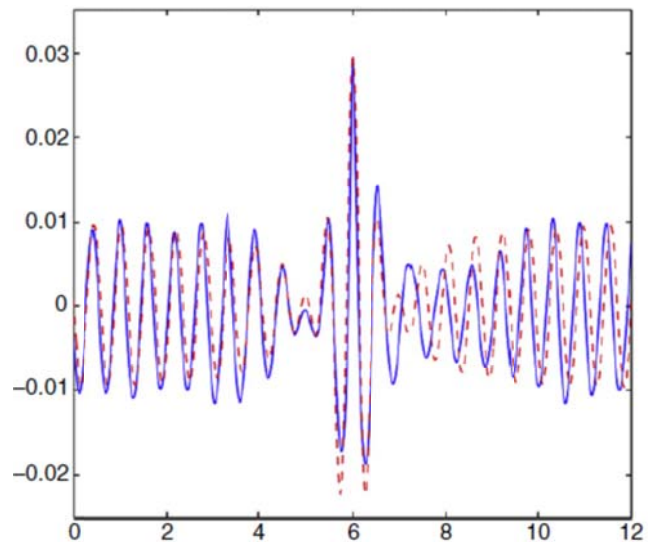


Fig. 19.12. Comparison of the experimentally observed wave of anomalous amplitude (solid curve) with the filling of the envelope, which is the Peregrin soliton (dotted line) [19-9]. The ordinate is the amplitude in meters, the abscissa is the time in seconds

are actually definitely generated by modulation instability. That forms a wave (or envelope) of anomalous amplitude due to the forced interference of the modes of the instability spectrum under the action of wave motion (see annexes XXI–XXII).

References to section 19

19-1. Karpman V. I. Nonlinear waves in dispersive media. – M. : Science. – 1973. – 175 p. (in Russian).

19.-2/ Schwartz L. W., Fenton J. D. Strongly nonlinear waves // *Ann. Rev. Fluid. Mech.* 1982. – Vol. 14. – P. 39–60

19-3. Belkin E. V., Kirichok A. V., Kuklin V. M., Priymak A. V. Anomalous waves in a modulation-unstable wave field // *East Eur. J. Phys.* 2014. – V. 1. – No. 2. – P. 4–39. (in Russian). (http://eejp.univer.kharkov.ua/Biblio/2014/EEJP_1_2/12p4-39.pdf).

19-4. Belkin E. V., Gushchin I. V. Analysis of a numerical model of modulation instability of a wave of finite amplitude in a nonlinear medium // *Bulletin of KhNU im. V. N. Karazina. – Ser. Mathematical modeling. Information technologies. Automated control systems.* 2008 – No. 809 (9). – P. 20–31 (in Russian).

19-5. Belkin E. V., Kirichok A. V. Modulation instability of waves supported by an external source in a medium with absorption // *VANT, Ser. “Plasma electronics and new acceleration methods.* 2010. – No. 4 (68). – P. 291–295 (in Russian).

19-6. E. Kuznetsov E. Solitons in parametrically unstable plasma / *Akademiia Nauk SSSR Doklady*, 236, 1977, P. 575–577 (in Russian)

19-7. Peregrine D. Water waves, nonlinear Schrodinger equations and their solutions/ *Journal of the Australian Mathematical Society Series 25* (1) (1983) 16–43.

19-8. Akhmediev N., Korneev V. Modulation instability and periodic solutions of the nonlinear Schrodinger equation / *Theoretical and Mathematical Physics* 69 (2) (1986) 1089–1093.

19-9. Chabchoub A., Hoffmann N., Akhmediev N. Rogue wave observation in a water wave tank / *Physical Review Letters* 106 (20) (2011) 204502.

5CHAPTER 9. Parametric and / or modulation Instabilities intense Langmuir oscillations in plasma

It is shown that, at least in the one-dimensional case, the description of the modulation instability of Langmuir oscillations in nonisothermal plasma by means of V.E. Zakharov equations is similar to the description of the parametric instability of these oscillations in cold plasma by the generalized V.P. Silin equations. When using the equations of quasi-hydrodynamics for electrons and the representation of ions by particles, the formation of the Maxwell distribution function of ions in both description models is shown, that is, it becomes possible to talk about their temperature. The use of a one-dimensional model $2 \div 5 \times 10^4$ ion particles for calculations, which would correspond to their number $10^{13} \div 10^{14}$ in a three-dimensional model, makes it possible to correctly describe the process of ion eating due to scattering on field inhomogeneities and Landau damping. In addition, the calculations performed will allow verification of other methods to describe such processes.

SECTION 20.

SILIN'S AND ZAKHAROV'S MODELS

Intense long-wavelength Langmuir waves in plasma are unstable. This instability leads to the excitation of the short-wavelength spectrum of Langmuir oscillations. Correct models for the description of the instability of long-wavelength Langmuir oscillations of finite amplitude were created in the fundamental works by V. P. Silin [20-1] and V. E. Zakharov [20-2], respectively, for the cases of cold (the so-called Silin model) and nonisothermal plasma (Zakharov model).

The scientific community was more interested in the effective mechanism of wave energy dissipation discovered by V. E. Zakharov – the collapse of Langmuir waves in nonisothermal plasma [20-3]. The mechanism of such attenuation of RF energy proposed in this work was due to the formation of a short-wave spectrum of Langmuir perturbations and the formation of plasma density caverns, which can be described using the Zakharov equations [20-3] obtained by means of quasi-hydrodynamic equations for electron and ionic liquids at energy density of a long-wavelength Langmuir field, which is lower than the density of thermal energy of plasma electrons.

In this case, localization regions of short-wave Langmuir oscillations arise. Plasma is ejected from these regions (caverns) under the influence of RF pressure, which can lead to the so-called collapse – narrowing and deepening of the density cavity (the so-called peaking mode).

In this case, the narrowing of the cavity should be accompanied by the attenuation of the modes of the short-wave Langmuir spectrum on electrons due to the Landau damping and “collapse” of the cavity due to the burning out of the rf field (the so-called “physical collapse”). Later, many works were devoted to the study of this extremely important phenomenon for plasma physics (see, in particular, [20-4] – [20-14]).

A similar phenomenon was also found in the Silin model, that is, in stronger fields in a cold plasma [20-15, 20-16], where, as shown below, the mechanism of field energy transfer to plasma particles turned out to be similar, although the role of Landau damping in ion heating as shown below turned out to be somewhat exaggerated.

Different definitions of instability in the Zakharov model and in Silin models are also intriguing: in Zakharov model it was modulation, and in Silin model – parametric. Processes are usually called parametric instabilities when a certain parameter of the system experiences high-frequency oscillations as in the Mathieu equation (or so-called multiplicative noise, as in the Hill equation). In this case, there may be an inverse effect of the arising disturbances on the noise source (self-consistent system). A similar instability was considered in [16-15, 16-16] – this is the so-called parallel pumping of spin waves. That is, an alternating magnetic field which is uniform in space excited spin waves in the samples, and the parameters of the equations for perturbations contained a multiplicative component. It is not difficult to see the analogy of the case discussed above with homogeneous excitation (this is the physical realization of the long-wave pump wave in the models of V. E. Zakharov and V. P. Silin) in space by the intense Langmuir field of the spectrum of small-scale Langmuir waves and ionic disturbances in the plasma in models B E. Zakharov and V. P. Silin. That is, formally, such an instability is self-consistent parametric. However, the nature of such an instability is very similar to the modulation instability process, especially since small-scale modulation of the plasma density actually appears. Therefore, the use of such definition can be considered acceptable.

Problems of description. It is known that in the hydrodynamic model accounting for Landau damping is impossible. Therefore, a phenomenological approach to representing the mechanism of this attenuation is usually applied. In addition, the quasi-hydrodynamic description, as well as the kinetic description (using equations for the particle velocity distribution functions), describes the motion of a continuous medium and operates on objects that are not particles, but small phase volumes and in the classical limit these phase volumes are arbitrarily small.¹⁷

¹⁷ According to V. E. Zakharov and his colleagues (see [20-17]), the direct simulation of the phenomena of collapse by the particle method is “the most consistent”.

This leads to a lesser inertia of the substance as if they were described by particles, to the formation of not only very small-scale and deep caverns of plasma density, but also to exacerbated regimes (collapses), which are not always adequate to physical reality.

As for the methods of description using large particles in high-dimensional models, here is another extreme. Large particles have an excessively large inertia, therefore, they are often replaced by local objects with cell regions where the averaging of internal contents occurs.

On a small scale it brings this approach closer to the hydrodynamic description, while on a large scale it retains the features of the large particle method and their averaged inertia. It is possible to increase the number of model particles in the description, decreasing the specific fraction (charge and mass) of each, although it is unlikely to be close to real physical parameters in three-dimensional space.

In one-dimensional models, some features of real processes are preserved, at least at a qualitative level. And the requirements for the number of particles in one-dimensional description models are significantly weakened, which makes it possible to correctly apply the particle method.

For example, below, for one-dimensional modeling, $2 \div 5 \times 10^4$ model-ion particles are used (which in a three-dimensional model would correspond to $10^{13} \div 10^{14}$ such objects in the volume of consideration), and these particles already correspond to individual ions in their characteristics. Therefore, the dynamics of such a number of particles simulating ions is largely adequate to the dynamics of plasma ions; moreover, the mechanisms of energy exchange between the field and particles correspond to the real interaction of ions with the spectrum of low-frequency oscillations.¹⁸

Below, let us discuss the development of instability processes in plasma of intense Langmuir oscillations in one-dimensional Silin and Zakharov models, with electrons being described only by quasi-hydrodynamic equations (taking into account the phenomenological Landau damping by electrons), and let us use a similar description or description using model particles for ions. In the latter case, hybrid models (electrons are represented by quasi-hydrodynamic equations, and ions by particles) allow us to see the formation of the Maxwellian velocity distribution of ions and evaluate the efficiency of their heating.

Equations of the Silin hybrid model. Let us first consider the case of parametric instability of an external long-wavelength Langmuir field of high intensity for cold plasma, that is, when the energy density of the field exceeds the density of the thermal energy of the medium $W = |E_0|^2 / 4\pi \gg n_0 T_e$. Particles are in the field of an external wave, the length of which, for simplification of calcula-

¹⁸ By the way, this allows verification of the hydrodynamic description, the description using the equations for the distribution functions of ions, and the description of ions by the "particle in cell" methods.

tions, is set equal to infinity, oscillating with speed $u_{0\alpha} = -(e_\alpha |E_0| / m_\alpha \omega_0) \cos \Phi$. The components of the field strength of the external wave are defined as it follows

$$E_0 = -i(|E_0| \exp[i(\omega_0 t + \phi)] - |E_0| \exp[-i(\omega_0 t + \phi)]) / 2. \quad (20.1)$$

For complex slowly varying components E_n, \bar{E}_n and $n_{i,n} = v_{i,n} / e$, accordingly, the high-frequency electric field, low-frequency electric field and ion density of the excited short-wave spectrum, the following system of equations can be written as (see annex XIV)

$$\frac{\partial E_n}{\partial t} - i \left(\frac{\omega_{pe}^2 - \omega_0^2}{2\omega_0} + \beta n^2 \right) E_n + \theta \frac{n^6}{n_M^6} E_n - \frac{4\pi\omega_{pe} v_{i,n}}{k_0 n} J_1(a_n) \exp(i\phi) - \quad (20.2)$$

$$-i \frac{\omega_0}{2en_0} \sum_m v_{i,n-m} [E_{-m}^* J_2(a_{n-m}) \exp(2i\phi) + E_m J_0(a_{n-m})] = 0,$$

$$\bar{E}_n = -\frac{4\pi i}{k_0 n} v_{i,n} \left[1 - J_0^2(a_n) + \frac{2}{3} J_2^2(a_n) \right] + \frac{1}{2} J_1(a_n) [E_n e^{-i\phi} - E_{-n}^* e^{i\phi}] - \quad (20.3)$$

$$-\frac{ink_0}{16\pi en_0} J_0(a_n) \sum_m E_{n-m} E_{-m}^* -$$

$$-\frac{ik_0}{16\pi en_0} J_2(a_n) \sum_m (n-m) [E_{n-m} E_m e^{-2i\phi} + E_{m-n}^* E_{-m}^* e^{2i\phi}].$$

$$\frac{d^2 x_s}{dt^2} = \frac{e}{M} \sum_n \bar{E}_n \exp(ik_0 n x_s), \quad (20.4)$$

$$\frac{\partial E_0}{\partial t} - i\Delta E_0 = -\frac{\omega_0}{2en_0} \sum_m v_{i,-m} [E_{-m}^* J_2(a_m) \exp(2i\phi) + E_m J_0(a_m)]. \quad (20.5)$$

where the arguments of the Bessel functions are $a_n = nek_0 E_0 / m_e \omega_0^2$, $\Phi = \omega_0 t + \phi$,

$v_{i,n} = en_0 \frac{k_0}{2\pi} \int_{-\pi/k_0}^{\pi/k_0} \exp(-ink_0 x_s(x_0, t)) dx_{s0}$ and $v_{i,n} = en_{i,n}$, are the components of the ion charge density, the RF field of the spectrum is $E = \exp\{-i\omega_0 t\} \cdot \sum_n E_n \cdot \exp\{ink_0 x\}$, and the term $\theta \cdot (n / n_M)^6 E_n$ models the attenuation of the RF mode of the spectrum by electrons, moreover $n_M = 20$, $\Delta = (\omega_{pe}^2 - \omega_0^2) / 2\omega_0$.

In addition, in (20.2) the dispersion term $\beta = k_0^2 v_{Te}^2 / 2\omega_0$ was added, which is proportional to $v_{Te}^2 = T_e / m_e$, x_s is the coordinate of the s -th particle modeling the ion. The expressions are proportional to $J_0(a_n)$ correspond to slow movements in the flows of enthusiasm, and expressions are proportional to $J_{\pm 2}(a_n)$, determined by the contribution to the nonlinearity of the second

harmonic, n_0 is the unperturbed plasma density, T is the electron temperature, and we assume that the ions are cold at the initial moment.

The equations of the hybrid Zakharov model. When $a_n \ll 1$ the equations of the Silin hybrid model, taking into account the representations $J_1(a_n) \approx a_n/2$, $J_0(a_n) \approx 1$, $J_2(a_n) \approx a_n^2/8$ coincide with the equations obtained for non-isothermal plasma of the Zakharov hybrid model [19-18], respectively, accurate to the detuning value and taking into account substitutions $E_0 \rightarrow -iE_0$ and $E_0^* \rightarrow iE_0^*$:

$$\frac{\partial E_n}{\partial t} - i \frac{\omega_{pe}^2 - \omega_0^2 + k_0^2 n^2 v_{Te}^2}{2\omega_0} E_n + \theta \frac{n^6}{n_M^6} E_n - i \frac{\omega_0}{2n_0} \left[n_{in} E_0 + \sum_{m \neq 0} n_{in-m} E_m \right] = 0, \quad (20.6)$$

$$\bar{E}_n = -ik_0 n \tilde{\phi}_n = \frac{-ik_0 n n_{i,n} T}{en_0} + \frac{-ik_0 n e}{4m\omega_p^2} \left[E_n E_0^* + E_0 E_{-n}^* + \sum_{m \neq 0, n} E_{n-m} E_{-m}^* \right], \quad (20.7)$$

$$\frac{d^2 x_s}{dt^2} = \frac{e}{M} \sum_n \bar{E}_n \exp(ik_0 n x_s), \quad (20.8)$$

$$\frac{\partial E_0}{\partial t} - i \frac{\omega_0}{2n_0} \sum_m n_{i,-m} E_m = 0, \quad (20.9)$$

where for the components of the density of ions we have the expression

$$n_{in} = n_0 \frac{k_0}{2\pi} \int_{-\pi/k_0}^{\pi/k_0} \exp(-ink_0 x_s(x_0, t)) dx_{s0}.$$

From the Zakharov equations (20.6) – (20.9) in the linear case, using the representation $\partial E / E \partial t \Rightarrow i\Omega$, we can obtain the dispersion equation for the nonisothermal case in the supersonic limit $\partial^2 n_{i,n} / n_{i,n} \partial t^2 \gg k_0^2 c_s^2 n^2$.

$$-\Omega^2 (\Omega^2 - \Delta^2) + \Delta \cdot A = 0, \quad (20.10)$$

where $\Delta = v_{Te}^2 n^2 k_0^2 / 2\omega_p$ and $A = \frac{1}{2} \frac{m_e}{M} \frac{k_0^2 n^2 v_{Te}^2}{2\omega_{pe}} \frac{|E_0|^2}{4\pi n_0 T_e} \omega_{pe}^3$.

On the other hand, linearizing equations (20.2) – (20.5) we shall obtain the same dispersion equation for the case of cold plasma, where, however, $\Delta = \Delta_0 = (\omega_{pe}^2 - \omega_0^2) / 2\omega_0$ and the magnitude is $A = J_1^2(a_n) \omega_{pe}^3 m / M$. Let us note that the dispersion equations (20.10) with $a_n \ll 1$ and taking into account substitutions $E_0 \rightarrow -iE_0$ and $E_0^* \rightarrow iE_0^*$ with the corresponding choice of detuning in these two cases coincide.

Positive definiteness of the detuning in the Zakharov model $\Delta = v_{Te}^2 n^2 k_0^2 / 2\omega_p$ is obvious; as for the detuning in the Silin model

$\Delta = (\omega_{pe}^2 - \omega_0^2) / 2\omega_0$, it was shown in the book [20-19] that it is also positively defined and the order of the instability increment is $\gamma = \text{Im } \omega$, at least in case of excitation of long-wavelength Langmuir oscillations by a high-current relativistic electron beam.

For normalized quantities $\gamma' = \Omega / \omega_{pe}$ and $A' \rightarrow A / \omega_{pe}^3$ in Table 20-1, values that correspond to two models for describing the modulation instability of Langmuir oscillations are given. In the Zakharov model, the correction $\gamma' = \Omega / \omega_{pe}$ normalized to the Langmuir frequency should be written as

Table 20-1

Parameters of linear theory
for Zakharov and Silin models

Values	Zakharov Model	Silin Model
Correction square to normalized frequency	$(\gamma')^2 = \frac{(\Delta')^2}{2} \pm \sqrt{\frac{(\Delta')^4}{4} + A'(\Delta')}$	
Detuning	$(\Delta')_n = \frac{\omega_{pe}^2 + v_{Te}^2 k_0^2 n^2 - \omega_0^2}{2\omega_{pe}^2} \approx \frac{v_{Te}^2 k_0^2 n^2}{2\omega_{pe}^2}$	$\Delta' = \Delta'_0 = \frac{\omega_{pe}^2 - \omega_0^2}{2\omega_{pe}^2}$
Coefficient A	$A' = A'(n) = \frac{1}{2} \frac{m_e}{M} \frac{k_0^2 n^2 v_{Te}^2}{2\omega_{pe}} \frac{ E_0 ^2}{4\pi n_0 T_e}$	$A' = A'(n) = \frac{m_e}{M} J_1^2(a_n)$

$$(\gamma')^2 = \frac{(\Delta')^2}{2} \pm \sqrt{\frac{(\Delta')^4}{4} + B(\Delta')^2}, \quad (20.11)$$

where $B = m_e |E_0|^2 / 8\pi n_0 T_e M$. Since $[(\Delta')^4 + 4B(\Delta')^2]^{1/2} - (\Delta')^2$, it grows monotonically with the growth Δ' , without having a pronounced maximum, then for small $(\Delta')^2 \ll B$ and $\Omega^2 \approx -(\Delta')\sqrt{B}$. In this case $|\Omega^2| < B$ and the instability increment is

$$\text{Im } \Omega = |\Omega| \approx \left(\frac{k_0^2 n^2 v_{Te}^2}{2\omega_{pe}^2} \right)^{1/2} \left(\frac{1}{2} \frac{|E_0|^2}{4\pi n_0 T_e} \frac{m_e}{M} \right)^{1/4} \omega_{pe}. \quad (20.12)$$

For large $(\Delta')^2 \propto B$, and $\Omega^2 \approx -B$. In this case the instability increment is

$$\text{Im } \Omega = |\Omega| \approx \left(\frac{1}{2} \frac{|E_0|^2}{4\pi n_0 T_e} \frac{m_e}{M} \right)^{1/2} \omega_{pe}. \quad (20.13)$$

This shows that the increment increases with increasing wave number of perturbations, reaching its highest value at large values of the wave number (20.13). In the Silin model, if $(\Delta')^3 = A' / 2$, which is the same as $\Delta' = (m_e 2M)^{1/3} J_1^{2/3}(a_{n_m})$, the relative increment reaches the values

$$\gamma' = \pm \frac{i}{\sqrt[3]{2}} (A')^{1/3} = \pm \frac{i}{\sqrt[3]{2}} \left(\frac{m_e}{M} \right)^{1/3} J_1^{2/3}(a_n). \quad (20.14)$$

Perturbations with a wave number $k_m = k_0 n_m$ for which $a_{n_m} = 1.84$ the value of the Bessel function is maximum and the relative increment for such perturbations reaches its maximum value

$$\delta'_{\max} = \pm 0.44i (m_e / M)^{1/3}. \quad (20.15)$$

Thus, in the Silin model, wave vectors for which $a_{n_m} = 1.84$ have the greatest increment. With the development of instability, the amplitude of the pump wave decreases and the maximum of the increment moves to the short-wavelength region.

It is important to note that the values of the maximum increments of parametric instability in the Zakharov model for supersonic disturbances grow with decreasing scale. Moreover, if in the Zakharov model a decrease in the amplitude of the pump field leads to a decrease in increments in the entire instability region, then in the Silin model a similar process shifts the increment maximum to the short-wave region, without decreasing its value (20.15).

Thus, it should be noted that the process of energy movement in the short-wavelength part of the spectrum in two models is largely due to the linear mechanisms of perturbation growth. In addition, the expected explosive increase in the amplitudes of the instability spectrum modes in the supersonic regime of the decay of an intense Langmuir field in a nonisothermal plasma under conditions $W = |E_0|^2 / 4\pi \ll n_0 T_e$ is caused by large increment values in almost entire instability region. This explosive increase in the spectrum amplitudes at the initial stage of the process was observed in many numerical experiments.

Nonlinear modes of instabilities. An analysis of the dynamics of the process showed [20–20] that, at the nonlinear stage of instability, density caverns were formed in the Silin model, which then were destroyed. Here, the destruction process was no longer accompanied by a breakdown of the count, as it was in the case with the quasi-hydrodynamic description due to the transition to the exacerbation mode [20–21]. The cause of the destruction of the

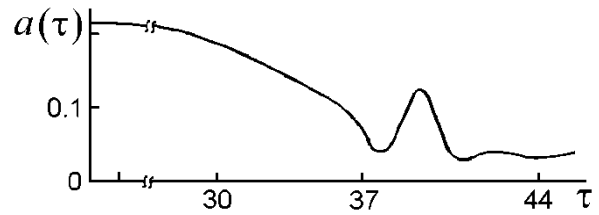


Fig. 20.1. Amplitude of the pump field $a(\tau)$ as a function of time in the hybrid model in the case of weak absorption of energy of short-wave oscillations [20–20]

caverns was the burnout of the field and inertia of the particles modeling the ions, the number of which in the numerical experiment did not exceed 5×10^3 , the number $40 \div 100$ of spectrum modes.

In this case, the largest ionic cavity quickly “collapsed”, the ionic component switched to the regime of intersecting particle trajectories [20–20, 20–22]. The energy taken by the ions turned out to be of the order $(m_e / M)^{1/3}$ of the initial energy of the pump wave [20–20]. At low absorption levels and small initial fluctuations, the behavior of the pump wave is shown in Fig. 20.1. As a result of the instability, most of the energy of the pump field was transformed into the energy of the short-wave Langmuir spectrum, then a partial exchange of energy between the spectrum and the pump wave could be observed, and when $\tau > 40$ the ion cavity “collapsed,” that is, it switched to the regime of intersecting particle trajectories.

An analysis of the hybrid Zakharov model was carried out in [20–23], where the last equation for pumping was substituted by the simple dynamics of weak pump attenuation. The authors of [20–23] chose the mass ratio $m_e / M = 1 / (16 \times 1836)$, the isothermal plasma, the region under consideration was $L = 1,8 \times 10^3 \lambda_{de}$; 600 modes of the spectrum were used for the quasi-hydrodynamic description, 3,000 positions were for the hybrid, that is, the coordinate region is divided into just such a number of sections. The non-self-consistent case of a constant or weakly varying field of an intense Langmuir wave was considered, the influence of the spectrum of excited short-wave perturbations was neglected.

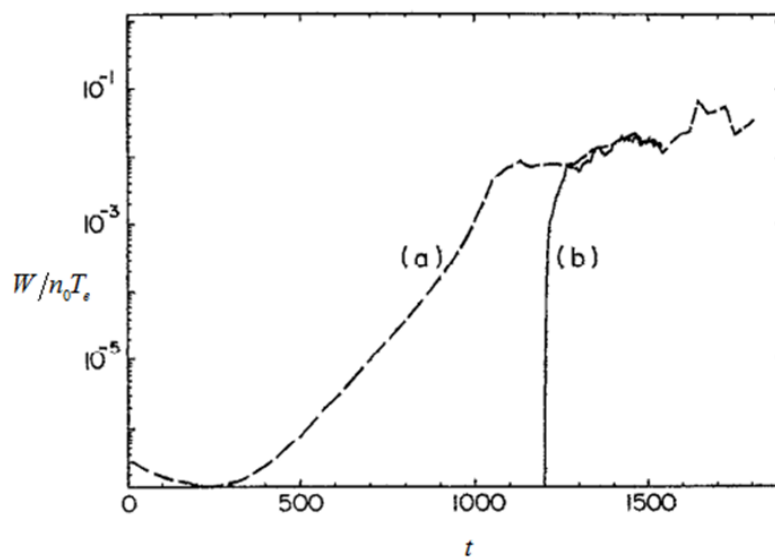


Fig. 20.2. Ratio of the field energy density to the electron thermal Energy density for the cases of hydrodynamic (a) and hybrid (b) Zakharov models [20–23] (along the ordinate axis) versus time t

First, the authors of [20–23] noted a much faster growth of perturbations in the hybrid model, which they explained by large values of perturbations of ion density in their chosen coordinate grid. Integral indicators – the RF energy of the short-wave spectrum at the initial stage of modulation instability for the quasi-hydrodynamic description and the description by the hybrid model, turned out to be similar (Fig. 20.2).

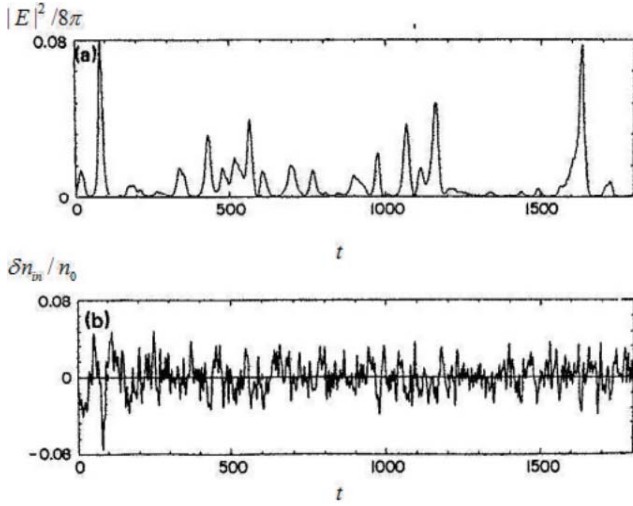


Fig. 20.3. Envelope of the RF field $|E|^2 / 8\pi$ (a) and relative deviations of the ion density $\delta n_{i,n} / n_0$ (b) in the hybrid model, at time $340\omega_{pe}^{-1}$ [20-23]

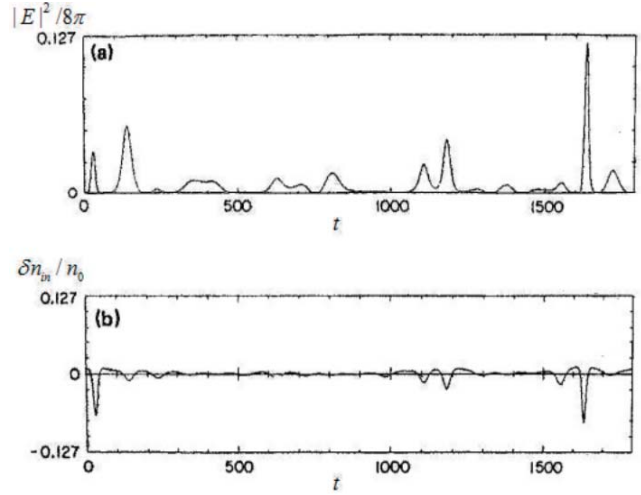


Fig. 20.4. Envelope of the rf field $|E|^2 / 8\pi$ (a) and the relative deviations of the ion density $\delta n_{i,n} / n_0$ (b) in the quasi-hydrodynamic model, at time $1363\omega_{pe}^{-1}$ [20-23]

Here, for the convenience of comparison, similar instability modes were chosen, which are characterized by approximately equal maximum field amplitudes and density perturbations. First of all, a noticeably larger number of plasma density caverns and significant fluctuations in the density of ions should be noted. Accordingly, the number of soliton-like perturbations of the short-wave field density is also larger in the hybrid model. The maximum cavity depth in the hybrid model is always less, the characteristic dimensions along the system are similar. Estimates of ion heating under conditions of constant magnitude or a slow change in the pump field is hardly of interest, as the authors did not consider the effect of a short-wave spectrum on the pumping.

At the initial stage of the developed process mode, it was found that the relation between the relative perturbations of the ion density $\delta n_{i,n} / n_0$ and the integrated energy density of the short-wave field is $\delta n_{i,n} / n_0 \propto |E|^2 / 8$.

References to section 20

- 20-1. Silin V. P. Parametric resonance in plasma // *ZhETF*. 1965. – V. 48. – P. 1679 (in Russian).
- 20-2. Zakharov V.E. Spectrum of weak turbulence in plasma without a magnetic field // *ZhETF*. 1966. – T. 51. – No. 6. – P. 688–696 (in Russian).
- 20-3. Zakharov V. E. Collapse of Langmuir waves // *ZhETF*. 1972. – V. 62. – No. 5. – S. 1745–1759.
- 20-4. Zakharov V. E., Lvov V. S., Rubenchik A. M. On the influence of modulation instability on the relaxation of relativistic electron beams in plasma // *JETP Letters*. 1977. – T. 25. – No. 1. – P. 11–14 (in Russian).
- 20-5. Buchelnikova N. S., Matochkin E. P. Instability and damping of one-dimensional Langmuir waves // *Preprints of the INP SB AS USSR*. 1979. – No. 79–115. – P. 20 (in Russian).
- 20-6. Sagdeev R. Z., Shapiro V. D., Shevchenko V. I. Langmuir turbulence and dissipation of high-frequency energy // *Sov. Plasma Phys.* 1980. – V. 6. – P. 377 (in Russian).
- 20-7. Degtyarev L. M. et al. Langmuir collapse in the presence of pumping and wave energy dissipation // *ZhETF*. 1983. – V. 85. – No. 4. – P. 1221–1231 (in Russian).
- 20-8. Wong A., Cheung P., Waves L. Three-Dimensional Self-Collapse of Langmuir Waves // *Phys. Rev. Lett.* 1984. – V. 52. – No. 14. – P. 1222–1225.
- 20-9. Cheung P. Y., Wong A. Y. Nonlinear evolution of electron-beam-plasma interactions // *Phys. Fluids*. AIP Publishing, 1985. – V. 28. – No. 5. – P. 1538.
- 20-10. Popel S. I., Tsytovich V. N., Vladimirov S. V. Modulational Instability of Langmuir Wave-Packets // *Phys. Plasmas*. 1994. V. 1. – No. 7. – P. 2176–2188.
- 20-11. Zakharov B. E. et al. Kinetics of three-dimensional Langmuir collapse // *ZhETF*. 1989. – V. 96. – No. 4. – P. 591 (in Russian).
- 20-12. Karfidov D. M. and others. Strong Langmuir turbulence excited in plasma by an electron beam // *ZhETF*. 1990. – V. 98. – No. 5. – P. 1592 (in Russian).
- 20-13. Vyacheslavov L. N. and others. Spectra of developed Langmuir turbulence in nonisothermal magnetized plasma // *Sov. Phys. Plasmas*. 1995. – V. 2. – No. 6. – P. 2224–2230 (in Russian).
- 20-14. McFarland M. D., Wong A. Y. Spectral content of strong Langmuir turbulence in the beam plasma interaction // *Phys. Plasmas*. 1997. – V. 4. – No. 4. – P. 945.
- 20-15. Andreev N. E., Silin V. P., Stenchikov G. L. On saturation of parametric instability of plasma in a strong electric field // *Plasma Phys.* 1977. – V. 3. – No. 5. – P. 1088–1096 (in Russian).

20-16. L. M. Kovrizhnykh Modulation instability and nonlinear waves in cold plasma // Plasma Phys. 1977. – V. 3. – No. 5. – P. 1097–1105 (in Russian).

20-17. Dyachenko A. I. et al. Two-dimensional Langmuir collapse and two-dimensional Langmuir cavitons // JETP Letters. Science, 1986. – V. 44. – P. 504.

20-18. Kuznetsov E. A. On the averaged description of Langmuir waves in plasma // Sov. Plasma Phys. The science. 1976. V. 2. – No. 2. – P. 327–333 (in Russian).

20-19. Silin V. P. Parametric effect of high-power radiation on plasma. The science. – 1973.

20-20. Chernousenko V. V, Kuklin V. M., Panchenko I. P. The structure in nonequilibrium media. In book: The integrability and kinetic equations for solitons // AN USSR, ITPh. K. Nauk. Dumka. 1990. – P. 472.

20-21. Kuklin V. M., Sevidov S. M. On the nonlinear theory of stability of intense oscillations of cold plasma // Sov. Plasma Phys. 1988. – V. 14. – No. 10. – P. 1180–1185 (in Russian).`

20-22. Kuklin V. M., Panchenko I. P., Sevidov S. M. Instability of an intense Langmuir wave in cold plasma // Radio engineering and electronics. 1980. – V. 33. – No. 10. – P. 2135–2140 (in Russian).

20-23. Clark K. L., Payne G. L., Nicholson D. R. A hybrid Zakharov particle simulation of ionospheric heating // Phys. Fluids B Plasma Phys. 1992. – V. 4. – No. 3. – P. 708.

SECTION 21.

COMPARISON OF SILIN'S AND ZAKHAROV'S MODELS, HEATING OF IONS

Below, let us compare the dynamics of the development of the modulation instability of an intense Langmuir wave for two cases of significant interest [21-1]. In the first case described by the Silin model, the field energy density is much higher than the thermal energy density of cold plasma. In the second case described by the Zakharov model, the field energy density is noticeably lower than the thermal energy of non-isothermal plasma, where the temperature of the ions is much lower than the temperature of the electrons.

Let us focus on the efficiency of energy transfer to ions and ion disturbances as a result of the development of modulation instabilities in cases of nonisothermal and cold plasma in the framework of hybrid models. For each model, two cases of light ions ($m_e/M=0.5\cdot 10^{-3}$) and heavy ions ($m_e/M=8\cdot 10^{-6}$) are considered. It is also of interest to find out how the attenuation of the RF spectrum and, correspondingly, the field burn in density cavities affect the character of energy transfer to plasma ions.

Number of large particles modeling ions, is chosen to be $0 < s \leq S = 20000$. Particles are uniformly distributed over the interval $-1/2 < \xi < 1/2$, $\xi = k_0 x / 2\pi$, $v_s = d\xi / d\tau$, initial conditions for particles are $d\xi_s / d\tau |_{\tau=0} = v_s |_{\tau=0} = 0$, number of spectrum modes $-N < n < N$, $N = S/100$. The initial normalized amplitude of intense oscillations is $a_0(0) = ek_0 E_0(0) / m_e \omega_{pe}^2 = 0.06$. The initial amplitudes of the HF modes are given by the expression $e_n |_{\tau=0} = e_{n0} = (2 + g)10^{-3}$ in the Silin model and $e_n |_{\tau=0} = e_{n0} = (0.5 + g)10^{-4}$ in the Zakharov model, where $g \in [0;1]$ is a random number, $ek_0 E_n / m_e \omega_{pe}^2 = e_n \exp(i\psi_n)$ and $\psi_n |_{\tau=0}$ are also randomly distributed in the interval $0 \div 2\pi$.

For perturbations of the ion density n_{ni} and slowly varying electric field \bar{E}_n , dimensionless representations

$$M_n = M_{nr} + iM_{ni} = n_{ni} \omega_{pe} / n_0 \gamma = \frac{\omega_{pe}}{\gamma} \int_{-\pi/k_0}^{\pi/k_0} \exp(2\pi n \xi_s) d\xi_s$$

and $ek_0 \bar{E}_n / m_e \omega_{pe}^2 = E_{nr} + iE_{ni}$ are also used.

The density estimation of the energy E_{kin} transferred to ions was determined by the expression

$$\frac{E_{kin}}{W_0} \approx 0.27 \cdot I \cdot \left(\frac{M}{m_e} \right) \frac{\gamma^2}{\omega_{pe}^2}, \quad (21.1)$$

where W_0 is the initial energy density of the intense Langmuir wave, $I = \sum_s (d\xi_s / d\tau)^2$ is the ion energy in the corresponding normalization, γ is the increment of linear instability. The fraction of the energy of the intense Langmuir wave transmitted to ions in the case of a non-isothermal plasma (Zakharov model) was determined by the ratio $W_0 / n_0 T_e$ and in the case of cold plasma (Silin model) by the ratio $(m / M)^{1/3}$.

A program that implements a mathematical model of the problem was created using JCUDA technology [21-2]. JCUDA provides interaction with CUDA technology from a Java program and makes it possible to carry out high-speed computing in parallel on a GPU.

Results of numerical simulation. For the parameters that are responsible for the nature of absorption of the energy of the HF spectrum $n_M = 20$ and $\Theta = \theta / \gamma = 0.05$, the energy of the main wave, the energy of the small-scale Langmuir spectrum, and the energy transferred to plasma electrons and ions, normalized to the initial energy of the main wave, are presented in Fig. 21.1.

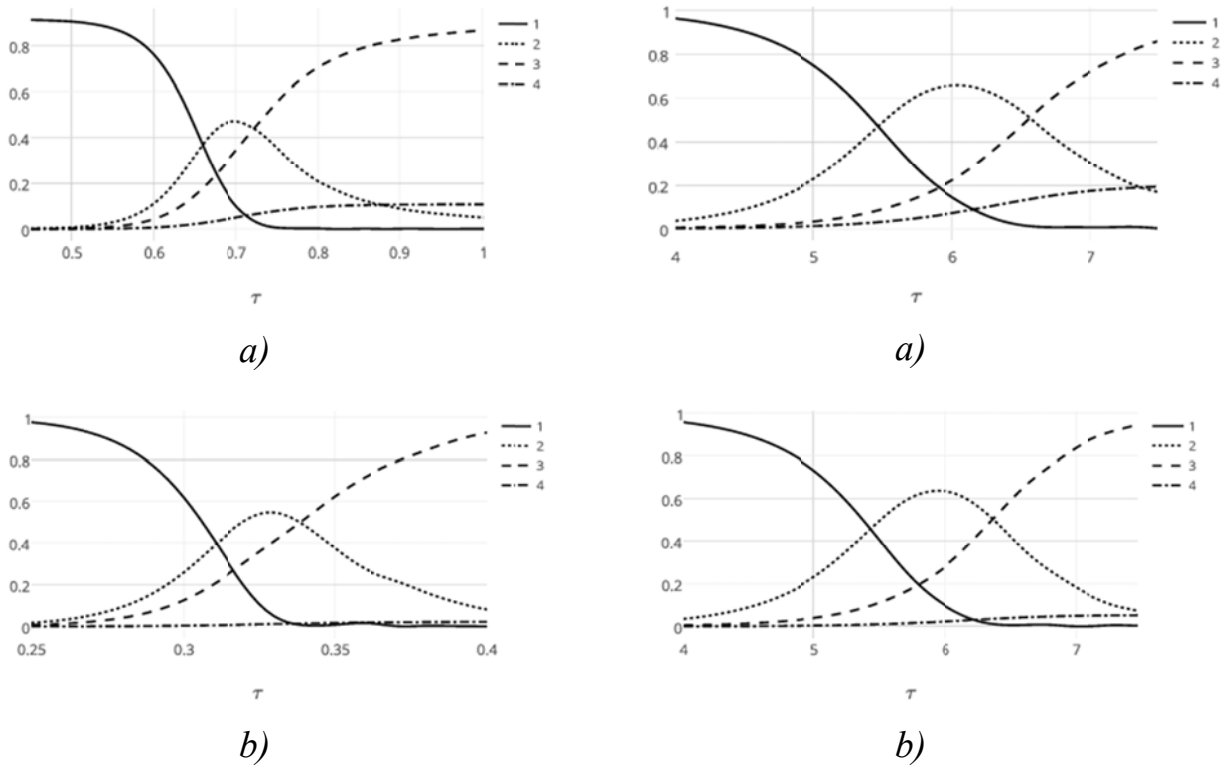


Fig. 21.1. Relative values of the energy of the main wave (1), energy of the small-scale Langmuir spectrum (2), energy transferred to the electrons (3) and ions (4) of the plasma, for the Zakharov model (left) and the Silin model (right) for light ions (a) and heavy ions (b)

The energy of the intensive long-wave Langmuir wave first passes into the energy of the HF Langmuir short-wave spectrum. It is at this stage that plasma density caverns filled with the rf field are formed. Then the rf field due to attenuation by electrons, which is considered phenomenologically in these models, burns out (while transmitting its energy to plasma electrons). Caverns under these conditions “collapse”, LF waves are excited, the ion paths intersect, and the energy of the “collapsed” caverns and the LF spectrum are transferred to the ions.

It is interesting that for the case of Buneman instability in plasma discussed in [21-3], the dynamics of a decrease in the kinetic energy of electrons is similar to the dynamics of the field of a long-wave Langmuir wave (which causes such intense oscillations of the electron velocity in the Silin model).

It is possible to determine the root-mean-square velocity at the end of the numerical simulation $\sigma(v_s) = \sqrt{\sum_s v_s^2 / S}$, while in the Zakharov model we shall obtain $\sigma(v_s) = 0.015$ for light ions and $\sigma(v_s) = 0.006$ for heavy ions. In the Silin model $\sigma(v_s) = 0.002$ is for light ions and $\sigma(v_s) = 0.0005$ is for heavy ones. Total particle energy in the selected normalization $I = \sum_s (d\xi_s / d\tau)^2$ in the Zakharov model for light ions is 4.689, total particle energy for heavy ions is 0.808, in the Silin model for light ions it is 0.086, and for heavy ions 0.005

The differences in total energy values in different models are determined by different values of the linear increment, and for cases of light and heavy ions, by the choice of ion mass. A normal distribution can be built on the basis of the mean square velocity, then particles that are outside it (mainly in the so-called “tails of the distribution function”) in the Zakharov model for light ions have 13.8 % of the total energy, for heavy ions it is 9.2 %, and in the Silin model, it is noticeably larger, that is, for light ions it is 25.6 %, and for heavy ions it is 13 %, respectively. That is, in the case of instability of an intense wave in cold plasma, a significantly larger fraction of fast particles can be expected.

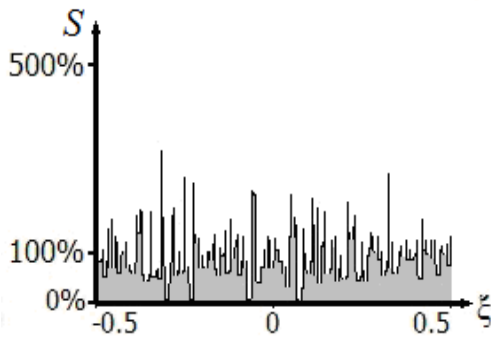


Fig. 21.2. Ion distribution $S(\xi)$ in the developed instability regime in the Zakharov model

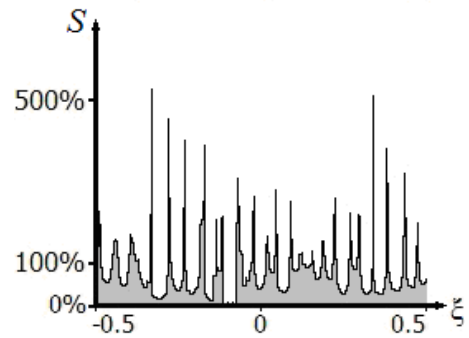


Fig. 21.3. Ion distribution $S(\xi)$ in the developed instability regime in the Silin model

The intensity of the low-frequency spectrum in case of non-isothermal plasma (Zakharov model) is quite large in a wide range of wave numbers, which corresponds to the spectrum of ionic sound after the destruction of density caverns found in numerical experiments [21-4] – [21-7]. On the contrary, in cold plasma, long-wave oscillations dominate in the spectrum. It is worth paying attention to the fact that the energy of the LF field is much lower than the ion energy in all the cases considered. A decrease in the field energy with time occurs due to the transfer of energy to ions and due to the destruction of plasma density caverns, as it was indicated in [21-6].

For both models, the kinetic energy of ions in the normalization selected above is

$$\frac{1}{2} \int_{-1/2}^{1/2} d\xi_{s0} \left(\frac{d\xi_s}{d\tau} \right)^2, \quad (21.2)$$

The selected rate of burn-out of the HF field in the caverns is determined by the value $\Theta = \theta / \gamma$. It is of interest to find out how the calculation results depend on this parameter. Obviously, a decrease in this parameter not only slows down the burnup of the rf field in the caverns, but also broadens the spectrum of rf modes, i.e., increases the fraction of its small-scale components, which leads to deepening of plasma density caverns and to an increase in the kinetic energy

of ions ejected from the caverns. Let us note that with the decrease of the attenuation of the HF modes, the ion velocity distribution function in the two models is getting closer and closer to the normal distribution, i.e. to the Maxwell function, which is shown in Fig. 21.4. If in the Zakharov model for sufficiently strong absorption the differences from the normal velocity distribution reach 19.9 % and in the Silin model they reach 13 %, then for relatively weak absorption, differences from the normal the distributions are only 6.9 % for the Zakharov model and 8.8 % for the Silin model.

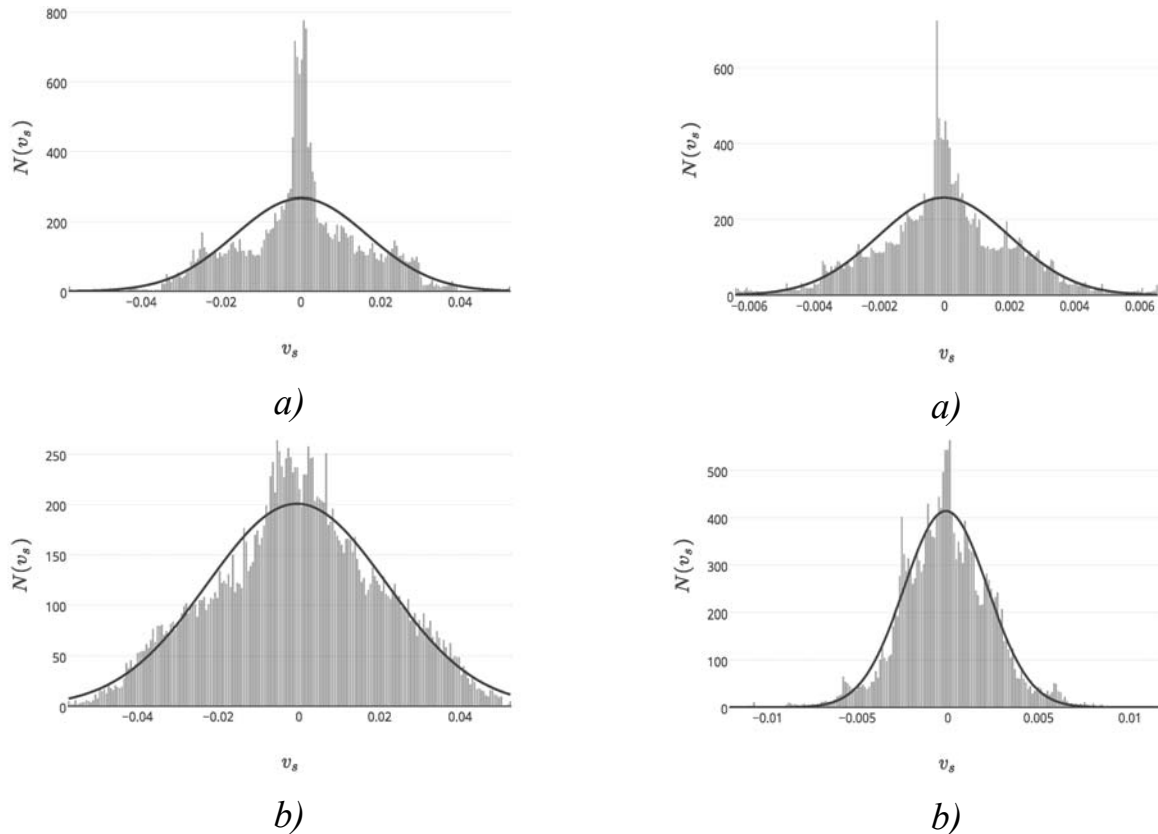


Fig. 21.4. Speed distribution of ions for the Zakharov model (left) and the Silin model (right) for light ions ($a - \Theta = 0.05$, $b - \Theta = 0.001$)

That is, if the deceleration of burning of the RF field in cavities in the Zakharov model significantly brings the velocity distributions of ions closer to the Maxwell distribution, then in the Silin model this is prevented by significant “tails” – the presence of fast particles whose energy is comparable to total ion energy.

As expected, with a decrease in the absorption of the HF spectrum, energy ultimately transferred to ions grows in almost the same proportion in non-isothermal and cold plasma (see Fig. 21.5). For the above conditions [21-1], the fraction of the field energy of long-wave Langmuir oscillations, which is transferred to ions in the Zakharov model does not exceed 6.3 %, and in the Silin model it does not exceed 5.4 %. That is, here, with increasing nonlinearity, the relative efficiency of energy transfer to ions decreases.

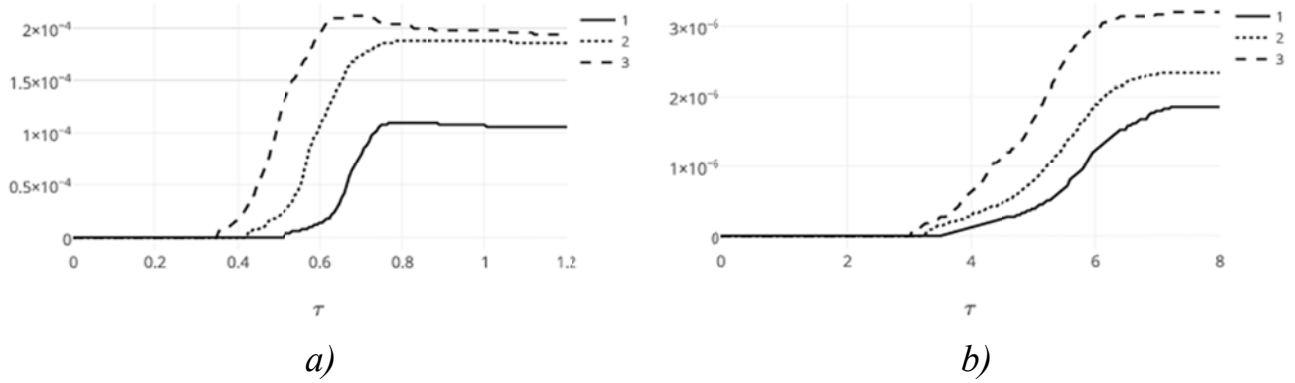


Fig. 21. 5. Kinetic energy of ions in the Zakharov model (left) and in the Silin model (right) for light ions (1 – $\Theta = 0.05$, 2 – $\Theta = 0.015$, 3 – $\Theta = 0.001$) as a function of time τ

Let us note in conclusion that the scales of ion density perturbations smaller than the Debye radius of the ions $r_{Di} = v_{Ti} / \omega_{pi}$ do not contribute to the formation of low-frequency electric fields due to the screening effect. In terms of $r_{Di}k_0 / 2\pi$, the ion Debye radius can be estimated [21-1]:

$$r_{Di}k_0 / 2\pi = R_{Di} \propto \langle v_s \rangle \left(\frac{\gamma}{\omega_{pe}} \right) \left(\frac{M}{m_e} \right)^{1/2}. \quad (21.3)$$

In the developed instability regime, this quantity is of the order of magnitude, and the number of modes of the ion density spectrum does not exceed the value, which does not contradict the analysis performed.

Thus, it is shown that the mechanism of nonlinear absorption of Langmuir oscillations discovered by V. E. Zakharov when the density of the plasma thermal energy is higher than the density of the RF field is also applicable to fields whose energy density significantly exceeds the plasma thermal energy.

However, nonlinear damping of intense Langmuir waves, which leads to plasma heating, is traditionally explained by the Landau damping in the resulting collapsing caverns of plasma density. This apparently only takes place to some extent. It was shown above (see also [21-1]) that the decisive mechanism for the transfer of field energy to ions and their further thermalization is multiple scattering by numerous field inhomogeneities arising from instability.

The processes described in the two models are similar, which should not be surprising, because the equations of the Zakharov model can be obtained from the equations of the Silin model by reducing the field intensity of the Langmuir wave and taking into account the electron temperature.

With a decrease in the attenuation of the rf modes, the ion distribution function is less and less different from Maxwell's, which allows talking about the temperature of the ions, and in the Silin hybrid model the instability process is characterized by the presence of a large fraction of fast particles. It is important to note that with a decrease in the absorption of the HF spectrum, the energy ultimately transferred to ions increases.

References to section 21

21.-1. Kirichok A. V., Kuklin V. M., Zagorodny A. G. One-dimensional modulational instability models of intense Langmuir plasma oscillations using the Silin–Zakharov equations // *Physics–Uspekhi* – 2016. – V. 59. – No. 7. – P. 669–688.

21-2. Gushchin I. V., Kuklin V. M., A. V. Mishin A. V., Priymak A. V. Application of CUDA technology for modeling physical processes. / ed. V. M. Kuklin and A. V. Priymak – Kh. : V. N. Karazin Kharkiv National University. – 2017 (in Russian).`

21-3. Kuzelev M. V., Rukhadze A. A. Electrodynamics of dense electron beams in plasma. – M. : Science. Ch. ed. phys.-mat. lit. 1990. – 336 p. (in Russian).

21-4. Galeev A. A., Sagdeev R. Z., Sigov Yu. S., Shapiro V. D., Shevchenko V. I. Nonlinear theory of modulation instability of Langmuir waves // *Plasma Phys.* 1975. Vol. 1. – No. 1. – P. 10–20.

20-5. Sigov Yu. S., Khodyrev Yu. V. One-dimensional quasi-collapse of Langmuir waves under parametric action on plasma // *DAN SSSR*, 1976. – V. 229. – P. 833–836 (in Russian).

21-6. Sigov Yu. S., Zakharov V. E. Strong turbulence and its computer simulation. // *J. de Physique.* 1979. – V. 40. – #C7. – P. 63–79.

21-7. Robinson P. A., de Oliveira G. I., Effect of ambient density fluctuations on Langmuir wave collapse. *Phys. Plasmas*, 1999. – V. 6. – P. 3057–3065.

CHAPTER 10. Structures of different scales and topologies in a thin layer convection

The process of structural-phase transformations in a thin layer of convectively unstable liquid or gas is discussed within the framework of the Proctor-Sivashinsky description model, which is valid for a low level of heat transfer at the layer boundaries. It is shown that transitions are accompanied by a jump in the state function, and the transition time is inversely proportional to the change in this function and is much shorter than the lifetime of metastable states. The relation between the spectral and visual defects of the convective field in the formation of a stable state is discussed. It is shown that the inclusion of vortices of a different nature in the system, within the framework of the generalized Proctor-Sivashinsky-Pismen model, leads to modulation instability of developed convection and the formation of large-scale poloidal vortices, i.e., to the effect of the regular hydrodynamic dynamo predicted by S. S. Moiseev.

SECTION 22.

STRUCTURAL-PHASE TRANSITIONS IN A THIN LAYER OF CONVECTIVELY UNSTABLE MEDIUM

In a number of applications, such as thin clouds, convection between closely spaced surfaces, the Proctor-Sivashinsky model [22-1, 22-2], which was used to describe the development of convection in a thin liquid layer with poorly heat-conducting boundaries, was of great interest. The authors of [22-3] discovered stationary solutions and studied their stability. The peculiarity of the model is that it distinguishes one spatial scale of interaction, leaving for the evolution of the system the ability to choose the nature of symmetry. All spatial perturbations of the same size, but of different orientations interact with each other. That is, the nonlinearity in the system is vectorial. It turned out that the presence of minima of the interaction potential of modes, the absolute value of the wave number vectors of which is unchanged, determines the choice of symmetry and, accordingly, characteristics of the spatial structure.

By modifying the structure of the mode interaction potential in the framework of a similar generalized Proctor-Sivashinsky model, the symmetry of stable solutions can be changed by the number of minima [22-3]. The prospectivity of the Proctor-Sivashinsky model was also manifested in the possibility to form a generalized Proctor-Sivashinsky-Pismen model, when taking into account the poloidal vortices inside the thin layer [22-4]. This model, as further studies have shown, was able to correctly describe the process of transformation of the energy of the periodic structure of the Proctor-Sivashinsky toroidal vortices into the energy of a large-scale poloidal vortex motion [22-5].

This phenomenon of "hydrodynamic dynamo" is responsible for the formation of large eddies in convective layers, in particular in the atmosphere of planets.

It is shown below that such a process is a consequence of the secondary, already modulating instability of the system of developed convective cells, as a result of which not only a self-similar structure occurs – convective cells of different scales [22-7], but also a large-scale poloidal vortex is formed [22-5, 22- 6].

This phenomenon, which was previously studied only for irregular models (see the detailed review [22–8]), as suggested by S. S. Moiseev, can occur as a result of the instability of the regular spatial convective structure of finite amplitude.

The Proctor-Sivashinsky equation. Assuming that the liquid (or gas) layer is thin, it is possible to integrate all perturbations caused by convection along the layer height and pass to the two-dimensional description [22-1, 22-2] (see also [22-9]). In two-dimensional geometry, the Proctor-Sivashinsky equation for the temperature field of convection takes the form

$$\frac{\partial \phi}{\partial T} + \nabla^4 \phi + \nabla[(2 - \gamma_V \phi - |\nabla \phi|^2) \nabla \phi] + a\phi = 0. \quad (22.1)$$

where $\nabla \phi = \vec{i} \cdot \frac{\partial \phi}{\partial \zeta} + \vec{j} \cdot \frac{\partial \phi}{\partial \vartheta}$ is the two-dimensional operator, in this case \vec{i}, \vec{j} – are unit vectors orthogonal to each other in the plane (ζ, ϑ) of the medium separation. It should be noted that the quadratic nonlocal (i.e., the presence of derivatives with respect to time or coordinate) nonlinearity in the equation is present in the form of a term proportional to γ_V and is due to the dependence of viscosity on temperature along the height of the layer, and the nonlocal cubic is taken into account by the term proportional to ϕ^3 .

Let us assume $k_0 \approx 1$, that is let us restrict to the case of weak excess above the threshold of convective instability. Indeed, for any deviation of the wave number from unity, the perturbation amplitudes rapidly decrease. Here ϕ is the relative temperature at the upper boundary of the layer. An increase in this value indicates an increase in the thermal conductivity of the layer as a whole.

To describe such convection under the same conditions, the simplified Swift – Hohenberg equation is often used [22-10]

$$\frac{\partial \phi}{\partial T} = e\phi - (1 + \nabla^2)^2 \phi - 2\gamma\phi^2 + 3\phi^3, \quad (22.2)$$

where the vector character of the nonlinear terms is replaced by the scalar one. Here $e = (1 - a)$.

The growth of perturbation amplitudes during instability $\phi \propto \exp\{\text{Im } \omega \cdot T\}$ occurs with increment $\text{Im } \omega \approx e - (k^2 - 1)^2$. For $\gamma > 0$ gas flow (this corresponds to gas convection) ascends to the center of the cell, for $\gamma < 0$ (which corresponds to fluid motion) it does vice versa.

The Swift – Hohenberg equation, as noted in the review [22–11], describes a system of clearly defined hexagonal cells after the formation of an amorphous state of random convection as a result of the soft (for liquid) and hard (for gas) instability regimes, which was observed in particular in [22–12]. In this case, the nature of the instability demonstrates all the features of the first-order phase transition – the formation of a clear spatial structure of convection from the amorphous state.

Below let us discuss soft and hard modes of structural-phase transitions in the Proctor-Sivashinsky model. In contrast to the traditionally applied Swift-Hohenberg equations we shall use the Proctor-Sivashinsky 3D equation that is more suitable for the real conditions. This task is obviously three-dimensional in space and non-stationary, which at first glance creates significant problems. However, the Proctor-Sivashinsky model allows reducing the dimension of the description and focus on topological aspects, that is, the type, size, and time of development of spatial structures.

In the case of a more realistic convection model described by the Proctor-Sivashinsky equation (1), both a first-order phase transition and a second-order phase transition can be observed, and it was possible to find a state function that is responsible for the topology of the formed convective structure [22-13].

If the temperature dependence of viscosity is not taken into account $\gamma_v = 0$, in the model, which is commonly called the Proctor-Sivashinsky model, only a nonlocal cubic nonlinearity $\nabla [|\nabla \phi|^2 | \nabla \phi]$ remains

$$\frac{\partial \phi}{\partial T} + \nabla^4 \phi + \nabla [(2 - |\nabla \phi|^2) | \nabla \phi] + a\phi = 0, \quad (22.3)$$

This equation can be represented as $\partial \phi / \partial T = -\delta F[\phi] / \delta \phi$, where $\delta F[\phi] / \delta \phi$ is the variational derivative and is the functional

$$F[\phi] = - \int d\zeta \cdot d\mathcal{G} \cdot \left\{ (\nabla \phi)^2 - \frac{1}{4} (\nabla \phi)^4 - \frac{1}{2} (\nabla^2 \phi)^2 - \frac{a}{2} \phi^2 \right\}$$

The peculiarity of this model is that it also describes Maradoni convection and convection of a layer with one of the free boundaries [22-2].

The most interesting phenomenon in convection of a thin liquid layer is the process of changing the topology and intensity of spatial convective structures, which, as it turned out, were not difficult to study. These processes, as it will be shown below, are analogues of second-order phase transformations,

when the topology and, partly the intensity of the spatial structure of convection change in the system.

Let us restrict to the case of the absence of a dependence of viscosity on temperature ($\gamma_V = 0$). Equation (22.3), which determines the dynamics of the temperature field of this process in the horizontal plane (x, y), can be written in the form:

$$\frac{\partial \Phi}{\partial T} = \varepsilon^2 \Phi - (1 - \nabla^2)^2 \Phi + \frac{1}{3} \nabla \left(\nabla \Phi |\Phi|^2 \right) + \varepsilon^2 f, \quad (22.4)$$

where Φ is the normalized temperature, f is the random function describing the external noise, and the quantity $\varepsilon^2 = e$, determining the excess of the convection development threshold is assumed, as before, to be sufficiently small ($0 < \varepsilon < 1$). Let us represent the solution in the form of a series $\Phi = \varepsilon \sum_j A_j \exp(i\vec{k}_j \vec{r})$ with $|\vec{k}_j| = 1$. When replacing $T \cdot \varepsilon^2 = t$, for slow amplitudes A_j we shall obtain a convenient representation of the Proctor-Sivashinsky model for convection description:

$$\frac{\partial A_j}{\partial t} = A_j - \sum_{i=1}^N V_{ij} |A_i|^2 A_j + f \quad (22.5)$$

where the interaction coefficients are determined by the relations

$$V_{jj} = 1, \\ V_{ij} = (2/3) \left(1 - 2(\vec{k}_i \vec{k}_j)^2 \right) = (2/3) (1 + 2 \cos^2 \mathcal{G}_{ij}), \quad (22.6)$$

and \mathcal{G}_{ij} is the angle between the vectors \vec{k}_i and \vec{k}_j . Expressions (22.5) – (22.6) must be supplemented with initial values of the spectrum amplitudes A_j , i.e. $A_j|_{t=0} = A_{j0}$. In contrast to the Swift-Hohenberg equation (22.2), where the cubic nonlinearity is presented in scalar form for qualitative reasons, the nonlinearity is vectorial, which is the reason for successive changes in the topology of convective structures.

The width of the instability interval in k-space is a ring – the average radius of which is unity, and the width of the order of magnitude of the relative overthreshold ε , i.e. much less than one. During the development of instability due to the growth of nonlinear terms, the effective increment of the modes lying outside very small neighborhood near the unit circle will decrease and may change sign, which will lead to narrowing of the spectrum to the unit circle in k-space.

Since the aim of further research will be to study the stability of spatial structures with a characteristic order size $2\pi/k \propto 2\pi$ and an important characteristic for visualizing simulation results is the clarity of these structures,

then let us restrict ourselves to the consideration of a somewhat idealized model of the phenomenon, assuming that the vibration spectrum is already located on a unit circle in k – space.

From the results of preliminary studies [22-3], it became clear that the system can have at least two stationary solutions in the form of a roll structure (shafts) (see Fig. 22.1 a), and in the form of a square cell field (see Fig. 22.1 b).

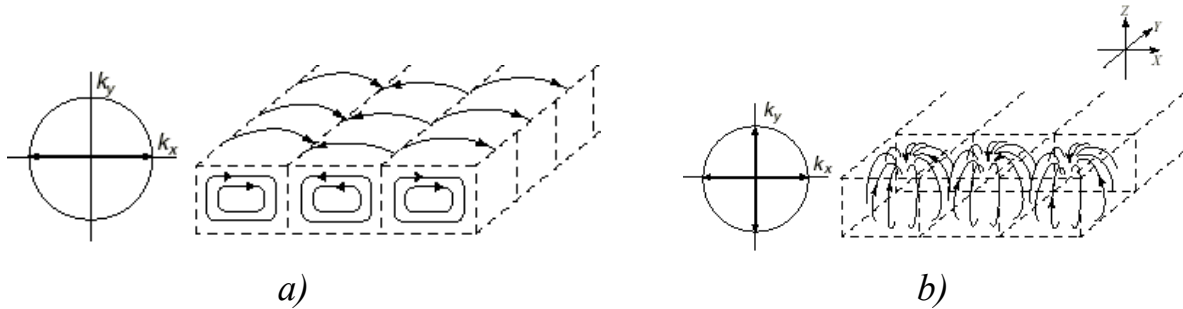


Fig. 22.1. Convective structures: rolls (a) and square cells (b)

The Proctor-Sivashinsky model in the absence of temperature dependence of viscosity ($\gamma = 0$) was studied in detail in [22-9.]. It was shown that after the structural-phase transition of the first kind from the amorphous state of random convection, a quasistable system of convective rolls is formed, which, as a result of their modulation within the structural-phase transition of the second kind, form a stable field of square convective cells. The structural-phase transition of the first kind, noted earlier in [22-11], corresponds to the transition from an amorphous state of convection to a state that has the form of a pronounced spatial structure. It should be emphasized that such a spatial clarity of the structure is observed only in conditions of proximity to the instability threshold. If, as a result of instability, the topology of the structure changes, we can speak of a structural-phase transition of the second kind.

Amorphous state. The mechanism of competition of spectrum modes.

From equations (22.5) – (22.6) under the initial conditions of the form, it can be seen that at the initial moment the development of the process will $A_j |_{t=0} = A_{j0}$ be determined by an explosive exponential increase in the amplitude of the spectrum with the same linear increment equal to unity in a given time scale. The growth rate is limited when it is necessary to take into account the second term (22.5), which corresponds to a nonlinear increment equal to

$$(\text{Im } \omega)_{NL} = 1 - \langle \sum_{i=1}^N V_{ij} |A_i|^2 \rangle \propto 1 - \langle V \rangle \sum_{i=1}^N A_i^2, \quad (22.7)$$

in this case, the average value of the interaction potential is

$$\langle V \rangle \propto \frac{4}{3} \quad (22.8)$$

Whence at the beginning of the process the active stage of interaction of modes, when the amplitudes of the modes of the spectrum are approximately the same, we shall obtain the expression given below for the perturbation density of such an “*amorphous state*”

$$I = \frac{1}{N} \sum_{i=1}^N A_i^2 \approx I_{amor} = \frac{3}{4}. \quad (22.9)$$

Let us show that the amorphous state is unstable. Let us consider the nonlinear rise increment (or attenuation decrement, which depends on the sign of the expression) of the j -th mode (obviously at the beginning of the process $\text{Im } \omega_L = 1$)

$$(\text{Im } \omega)_{jNL} = 1 - \sum_{i=1}^N V_{ij} |A_i|^2. \quad (22.10)$$

At the end of the linear stage of the rapid growth of perturbation amplitudes (of spectrum mode - spectral line) and the achievement of the so-called “*amorphous*” state, when nonlinear increments become much less than unity, the process sharply slows down. As a result of a random ejection of one of the modes (that is, if one of the modes-spectral line turns out to be larger than the others), then for it the second term of the right-hand side of equation (22.5) becomes smaller than that of the neighboring modes. That is, for this mode of larger amplitude, the value (22.10) remains positively determined and largest one, and for neighboring modes, the nonlinear increment turns out to be either less or even negative, which corresponds to their attenuation. The neighborhood of the growing modes decreases rapidly and as a result, only two modes are left shifted by an angle π in the spectrum, and the total energy of such a roll structure is equal to $I = 1$.

This state is unstable, which leads to an increase in the lateral spectrum $\vartheta = \pi/2$ relative to the leader mode, the spectral width of which is inversely proportional to the size of the regions, where the roll modulation occurred. The side spectrum narrows and its amplitude increases, which expands the areas with modulation of the shafts, which in their turn quickly merge. These areas are domains¹⁹ with different orientations (see (Fig. 22.4 c). The modulation of the rolls increases until a field of square convective cells (i.e. toroidal vortices), is formed. This process of forming a new structure is a second-order phase transition.

The energy of this state is equal to $I = 1.2$. Each of these two states is characterized by different values of intensity I and has a different topology.

¹⁹ The domain boundaries do form the initial defects of the structure of the square convective cells. Then the number of defects decrease rapidly (see Annex XXVI).

Let $\mathcal{G}_s(t=0)$ each mode-spectral line be given uniformly from zero to 2π and the interval should be divided into N equal parts (the number of which is equal to the number of basic modes). Then, if we require zero values at the boundaries, the spatial dependence of each n -th mode will be

$$A_{n,m} \text{Sin}(2\pi nx) \text{Sin}(2\pi my), \quad (22.11)$$

where n, m (they can be represented as $n = N \cdot \text{Cos } \mathcal{G}_s, m = N \cdot \text{Sin } \mathcal{G}_s$) are integers, in this case $N^2 = n^2 + m^2$. In the calculations, generally speaking, it suffices to sum over n , since m is determined from the relation $m^2 = N^2 - n^2$. Obviously

$$n \leq N, \quad m = \sqrt{N^2 - n^2} \geq 0. \quad (22.12)$$

That is, in this case (22.11) can be written as

$$A_{n,\sqrt{N^2-n^2}} \text{Sin}(2\pi nx) \text{Sin}(2\pi y\sqrt{N^2-n^2}), \quad (22.13)$$

Structural-phase transitions. The development of disturbances in the system, as shown by a numerical analysis of equation (22.5), proceeds as it follows.

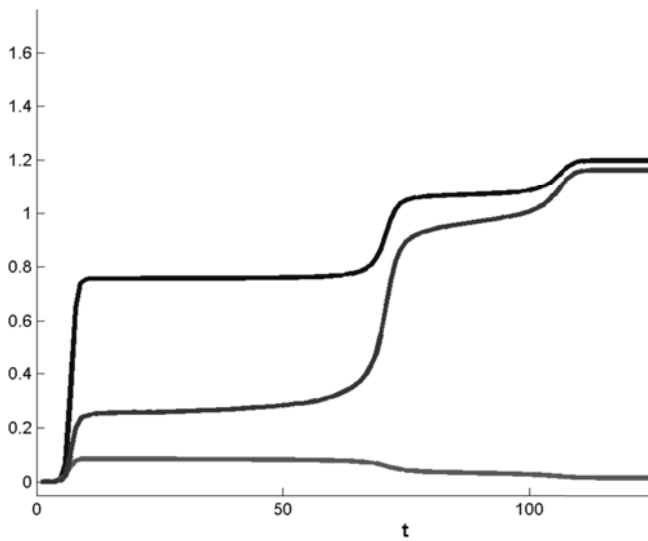


Figure 22.2. The behavior over time of the integral characteristics of the process. The upper curve $\frac{1}{N} \sum_i A_i^2$,

the middle curve $\frac{1}{N} \sqrt{\sum_i (A_i - \bar{A})^2} = \sigma$,

and the lower curve $\frac{1}{N} \sum_i A_i = A_{cp}$

are the average amplitude

follows. From the initial fluctuations, a wide spectrum of \mathcal{G} is rapidly excited. The value of the quadratic form of this spectrum can be estimated $I = \frac{1}{N} \sum_j A_j^2$ by equating the right-hand side of (22.5) to zero, and we will obtain a value close to 0.75. In the case of a large number of modes with high accuracy of calculations, the system is delayed in its development, remaining in dynamic equilibrium. For further development – “crystallization”, one of the modes must receive a portion of energy that exceeds a certain threshold.

That is, under these conditions, a certain level of noise – fluctuations – is necessary $f \neq 0$. This is achieved with a final noise value, or with a decrease in the accuracy of calculations, which, as noted in [22-14], is equivalent. Similar cases when noise is able to provoke or accelerate the process of instability are collected

in the book [22-15.]. Studies of the process revealed the following dynamics of changes in the integral characteristics of the process over time (see Fig. 22.2).

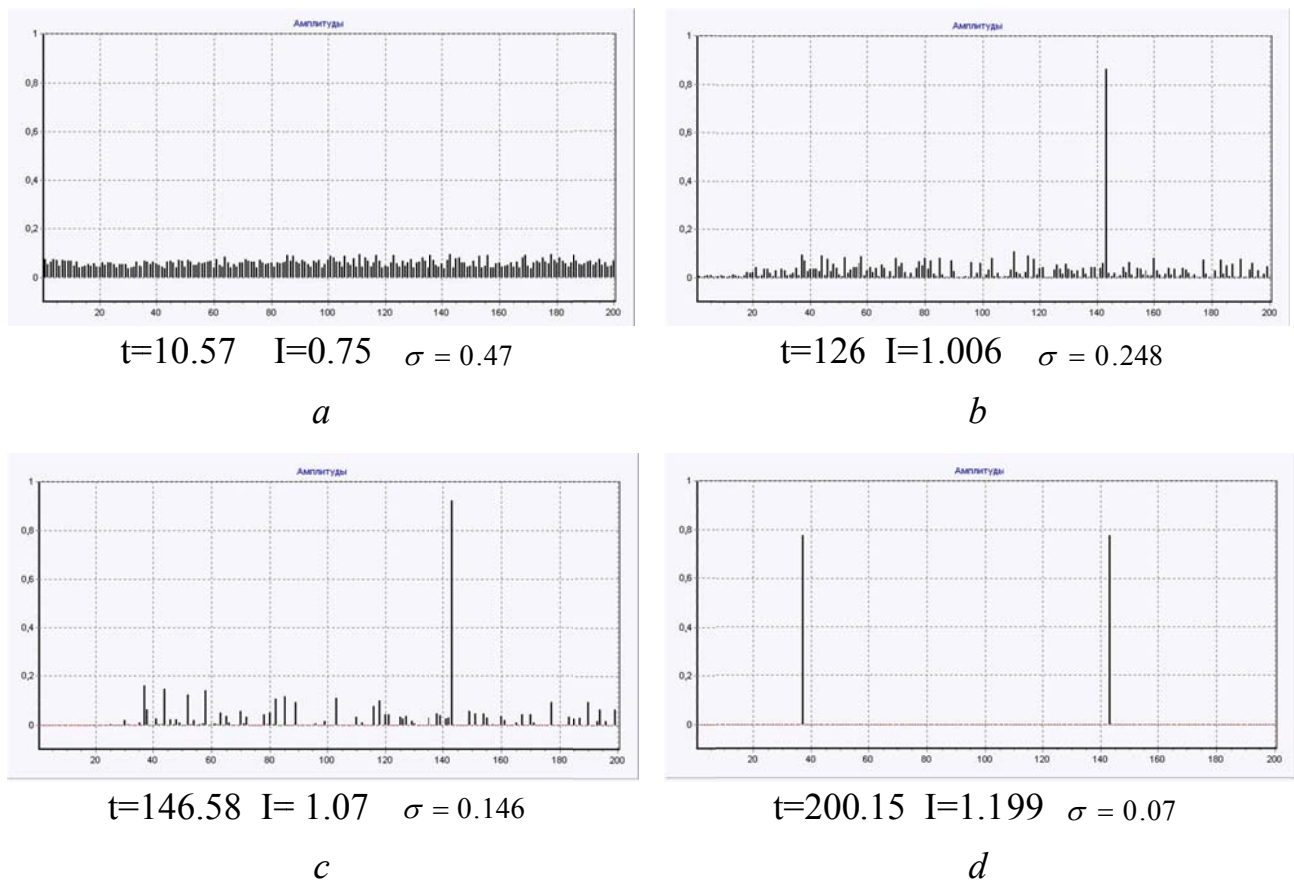


Fig. 22.3. Stages of instability development: spectra of the amorphous state (a) short-lived relatively unstable state (b – convective rolls), intermediate short-lived unstable state (c) – the formation of domains, the boundaries of which determine the initial number of defects in the structure of the cells field) and (d) – a stable state (is the field of convective cells) [22-9]

It is after the first burst of the derivative $\partial I / \partial t$ that an amorphous structure is formed – a system of convective rolls, and up to the second burst the value $I \approx 0.75$ changes little.

The next burst $\partial I / \partial t$ signals the occurrence of an unstable structure (rolls and rolls modulated in the longitudinal direction) with a new value $1 < I \leq 1.07$, after this burst $\partial I / \partial t$ of the derivative, the rolls experience longitudinal modulation, the period of which decreases, and the next third burst $\partial I / \partial t$ of the derivative leads to the appearance of a stable structure of convection cells $I = 1.2$. This behavior of the system convinces of the existence of structural-phase transitions in this system.

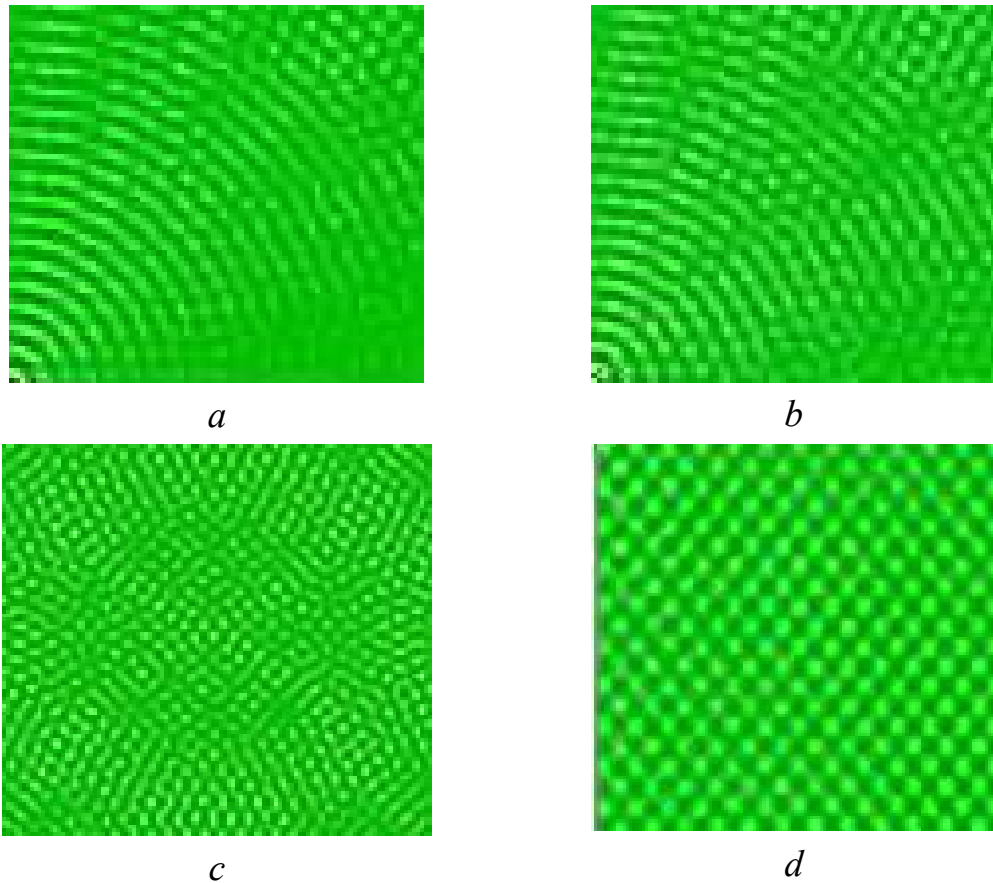


Fig. 22.4. View of the fragments of the spatial structure of the temperature field distribution on the surface of the layer a) after a structural-phase transition of the first kind with the formation of convective rolls, and b) during transverse modulation of the rolls, c) during the formation of domains – a metastable spatial structure, after the destruction of the roll system, d) during the formation of a stable convective structure – square convective cells

The state function, as it is easy to see, is quantity I . It was shown above that the structures that arise during transitions described by a burst of the derivative of this function have distinguishable topologies and are characterized by its fixed values. For each structure there is a certain equilibrium value of the state function. Nevertheless, despite the long existence of each quasistationary structure, there is a mechanism for its destruction and the formation of a structure with a different topology.

Generally speaking, the times of development of relaxation processes when the system moves to a more equilibrium state are usually determined by the difference in the values of the state function after the transition and before it. The larger this difference is, the faster is the process of transition from one state to another. Another thing which is important to note: the sequence of change of states is determined by the times of development of instabilities (playing the role of relaxation processes) that ensure a transition to an increasingly equilibrium state of the system. Moreover, faster relaxation processes due to large differences in the equilibrium values of the state function manifest themselves before.

Let us make sure that in this case all the phenomena occur in a similar sequence and within the framework of a similar scenario [21-16].

It was a *numerical analysis of the model that made it possible to confirm the presence of structural-phase transitions.*

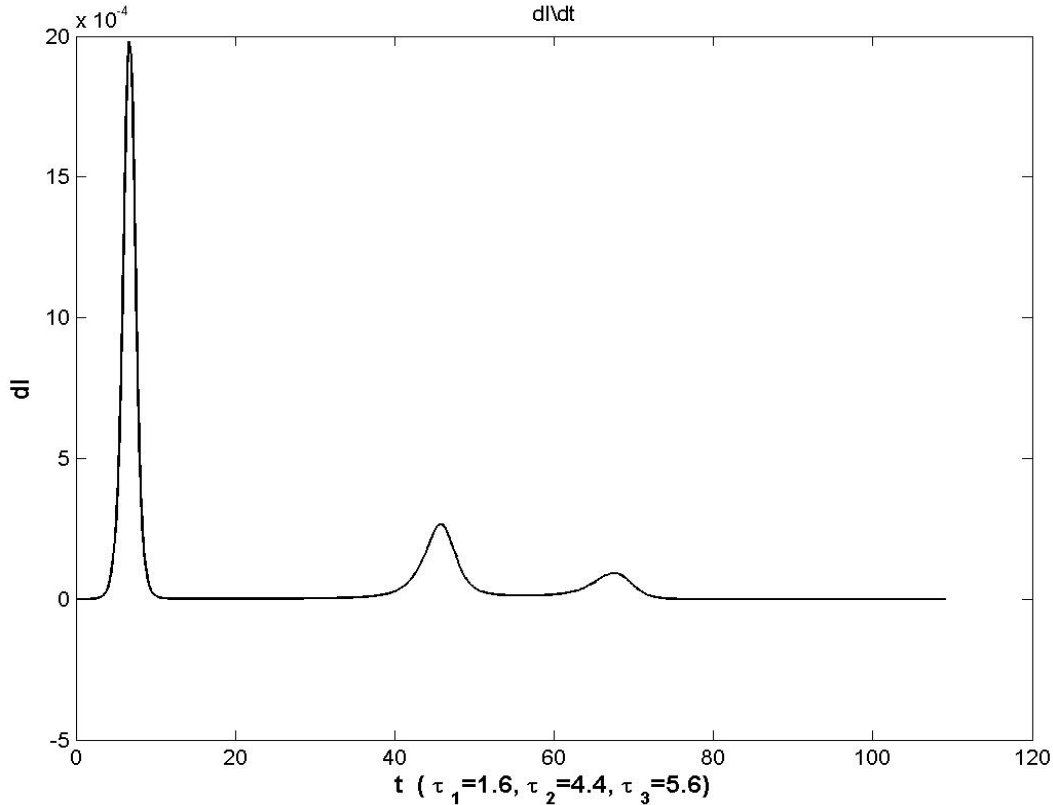


Figure 22.5. The behavior of a derived state function. The characteristic times of transient processes are $\tau_1 = 1.6$ is the time of occurrence of the “amorphous” state, $\tau_2 = 4.4$ is the time of formation of pronounced shaft-like structures, and $\tau_3 \approx 5.6$ is the time of formation of a system of cells for one of the implementations of the process of establishing convective motion.

It is possible to verify that the times of formation of states are inversely proportional to the difference between the values $I = \sum_i A_i^2$ after the structural-phase transition $I_n^{(+)} = (\sum_i A_i^2)_n^{(+)}$ and before this transition $I_n^{(-)} = (\sum_i A_i^2)_n^{(-)}$.
i.e,

$$\tau_n \sim \{(\sum_i A_i^2)_n^{(+)} - \sum_i A_i^2)_n^{(-)}\}^{-1} = \Delta I_n^{-1} \tag{22.14}$$

It is easy to see that

$$\tau_3 / \tau_2 \approx \Delta I_2 / \Delta I_3, \tag{22.15}$$

Thus, based on a numerical study of the Proctor-Sivashinsky model, it was proved that the sum of the squares of the amplitudes of the modes I is a function of a state with a certain topology.

Having a certain topology, each state is characterized by a certain equilibrium value of the state function. Quasistable states are destroyed due to instabilities, the development time of which can be estimated from the magnitude of the momentum in time of the derivative of the state function. It is shown that the characteristic time of instabilities that destroys the former state and forms a new state are inversely proportional to the difference between the values of the state function after and before the structural-phase transition.

It is also shown that faster relaxation processes, i.e. structural phase transitions precede slower ones, as can be seen from fig. 22.2 and fig. 22.

Note that in nature, thin cloud cover also often forms a longitudinally modulated shaft system, which is noted in fig. 22.6



Figure 22.6. Fragment of thin clouds in the form of modulated convective rolls. Kharkiv Ring Road 09/12/2012

The value of I in this case reaches values close to unity ($I \rightarrow 1$). However, this state is not stable: convective shafts undergo modulation along the axis of rotation of the gas (or liquid), whose characteristic size is reduced. In this transition state, the system takes sufficiently long time (which increases slightly within certain limits with an increase in the number of modes), and the value $I \approx 1.07$ is preserved. After sufficiently long time, tens of times greater than the inverse increment of the initial linear instability, only one mode “survives” from the newly formed “side” spectrum, the amplitude of which is compared with the amplitude of the initial leading mode. In the end, a stable convective structure is formed – square cells, in which the quadratic form of the system reaches the value of $I = 1.2$. So, fig. 22.7 shows the spatial structure of convection of a thin cloud layer.



Figure 22.7. A fragment of the spatial structure of convection of a thin cloud layer. White Lake (near Zmiev) 10/06/2012

Thus, a feature of the Proctor-Sivashinsky model for convection description is the presence of three states. The times of structural transitions between metastable states are much shorter than their lifetime. The characteristic size of convective formations in the developed instability mode and the accepted measurement units are $2\pi/k \propto 2\pi$ of the order of magnitude and the length of the wave vectors is of the order of unity.

The interaction potential $V_{ij} = (2/3)(1 + 2\cos^2 \mathcal{G}_{ij})$ of spatial modes has a deep minimum for the angles $\mathcal{G}_{ij} = \mathcal{G}_i - \mathcal{G}_j$ between vectors \vec{k}_i and \vec{k}_j two spatial modes $\mathcal{G}_{ij} = \pm\pi/2$. These are minima V_{ij} , as shown in [22.17], that cause instability of the rolls structure. For the existence of a minimum V_{ij} for modes with relatively small amplitudes allows continuing their growth, while suppressing disturbances that arose before.

When approaching a stable state, the spatial structure gets rid of many defects (arising mostly at the boundaries of homogeneous regions – domains, see Fig. 22.4 c.), and there is a correlation between the relative share of visually (geometrically) structural defects and the defectiveness value, defined as the ratio of the squares of the amplitudes of the spectrum modes that do not correspond to the system of square cells to the total sum of mode squares (see annex XXVI).

Namely, in the case of a more realistic convection model described by the Proctor-Sivashinsky equation (22.1), it is possible to observe the process of both the first-order phase transition and the second-order phase transition and to find the form of the state function that is responsible for the topology of the formed convective structures. Let us note that such a description of phase transitions did not use phenomenological approaches and various speculative considerations, which allows more closely examining the nature of transients, which arouses the greatest interest of researchers, as an example of this model.

The physical nature of the second order phase transition. The onset of longitudinal modulation of convective rolls leads to the occurrence of convective motion in a plane parallel to the direction of the rolls, which adds to the strong convection across the rolls. A decrease in the spatial period of the roll modulation leads to an increase in convection as a whole and its equalization in two perpendicular planes, an increase in the temperature on the upper surface of the layer and, accordingly, in the energy value, that is, in the state function, which indicates a change in the structure and a second-order phase transition.

If we assume that domains with a dominant structure arise and propagate in the convective zone, then we will have to admit that the correlation rate of spatial perturbations in this case is extremely high. This paradox is explained by the fact that the process of a second-order phase transition is described,

at least here, by equations (22.5) – (22.6)²⁰, whose solutions are the set of eigenfunctions (22.4) with different wave vectors

$$\Phi = \varepsilon \sum_j A_j \exp(i\vec{k}_j \vec{r}).$$

The process of phase transformations does not cover individual local regions, but immediately the entire convection zone, where the conditions for the phase transition are satisfied. In this case, the formation of local domains with a homogeneous spatial structure in different places of the convective layer is the result of the interference of these eigenfunctions.

References to section 22

22-1. Chapman, J. and Proctor, M.R.E., Nonlinear Rayleigh-Benard convection between poorly conducting boundaries // *J. Fluid Mech.* 1980. – No 101. – P. 759–765.

22-2. Gertsberg, V. and Sivashinsky G. E., Large cells in nonlinear Rayleigh-Benard convection // *Prog. Theor. Phys.*, 1981. – No 66. – P. 1219–1229.

22-3. Malomed B. A., Nepomnyashchy A. A., Tribelsky M. P. Two-dimensional quasiperiodic structures in nonequilibrium systems. *ZhETF.* 1989. – V. 96. – P. 684–699 (in Russian).

22-4. Pismen, L., Inertial effects in long-scale thermal convection, *Phys. Lett. A.* 1986. – V. 116. – P. 241–243.

22-5. Kirichok A. V., Kuklin V. M., Panchenko I. P., Moiseev S. S., Pismen L. M. The dynamics of the formation of large-scale eddies in the convective instability regime // *Inter. Conf. "Physics in Ukraine"*, Kiev, 22–27 June 1993. *Proc. Contr. Pap. ITP*, 1993. – P. 76–80.

22-6. Kirichok A. V., Kuklin V. M., Panchenko I. P. On the possibility of dynamo mechanism in a nonequilibrium convective medium. *Reports of NASU / 1997.* – No. 4. – P. 87–92 (in Russian).

22-7. Kirichok A. V. and Kuklin V. M. Allocated Imperfections of Developed Convective Structures. *Physics and Chemistry of the Earth Part A* 1999. – № 6. – P. 533–538.

22-8. Vortex dynamo in spiral turbulence. // *Auth.:* Moiseev S. S., Oganessian K. R., Rutkevich P. B., Tur A. V., Khomenko G. A., Yanovskiy V. V. in the book: *Integrability and kinetic equations for solitons ...* Ed. V. G. Bar'yakhtar, V. E. Zakharova, V. M. Chernousenko. *Sat. scientific. tr. Kiev, Naukova Dumka*, 1990. – 472 p. (in Russian).

²⁰ The visually observed almost infinite rate of these correlations is due to phase changes and is not associated with energy-momentum transfer. It is possible that such a high rate of spatial correlations between domains of a new phase for the phenomena of phase transitions can orient researchers to search for such a description.

22-9. I. V. Gushchin, A. V. Kirichok, V. M. Kuklin. Pattern formation in convective media/ «Journal of Kharkiv National University», physical series «Nuclei, Particles, Fields» 2013. issue 1 /57. – V. 1040. – C. 4–27 (in Russian).

22-10. Swift J. B. Hydrodynamic fluctuations at the convective instability / J. B. Swift and P. C. Hohenberg // Phys. Rev. A 1977. – V. 15, – P. 319.

22-11. Rabinovich M. I., Fabrikant A. L., Tsimring L. Sh. Finite Dimensional Disorder. / M. I. Rabinovich A. L. Fabrikant L. Sh. Tsimring / /UFN. – T. 162. – No. 8. – P. 1–42 (in Russian).

22-12. Bodenschatz E. Experiments on three systems with non-variational aspects/ E. Bodenschatz E., J. R. de Bruyn, G. Ahlers, D. Cennell/ Preprint. – Santa Barbara, 1991.

22-13. I. V. Gushchin, A. V. Kirichok, V. M. Kuklin. Structural-phase transitions and state function in unstable convective medium/ Problems of Atomic Science and Technology, 2015. – N 4 – series “Plasma Electronics and New Methods of Acceleration” – P. 252–254.

22-14. Belkin E. V., Gushchin I. V. Mathematical model of convection of liquid layer with a temperature gradient // Kharkov, KhNU, KMNT, 2010. – Vol. 1. – C. 39–40 (in Russian).

22-15. Horsthemke W., Lefebvre R. Noise-induced transitions. Per from English. – M. : Mir, 1987. – 400 p.

22-16. Gushchin I. V., Kirichok A. V., Kuklin V. M. State function in an unstable convective medium. // East Eur. J. Phys. 2015. – V. 2. – no. 1. – P. 32–35.

22-17. Structural transitions in the Proctor-Sivashinsky model / Belkin E. V., Gushchin I. V., Kirichok A. V., Kuklin V. M. // VANT, Ser. “Plasma electronics and new methods of acceleration, 2010. – № 4 (68). – S. 296–298.

SECTION 23.

MODULATION INSTABILITY OF THE SYSTEM OF CONVECTIVE CELLS IN A THIN LAYER. HYDRODYNAMIC DYNAMO EFFECT

Sivashinsky–Proctor–Pismen model. For the first time, the possibility of the occurrence of modulation instability of a system of convective cells in an extremely productive Sivashinsky–Proctor–Pismen model [23-1] was announced in the report [22-2]. This modulation of the system of developed convective cells in a thin liquid layer between poorly heat-conducting horizontal surfaces (the formation of which was discussed above) is caused by the generation of vortices of a different nature than those that form the convective structure.

As a result of the development of modulation instability in the system of the developed regular structure of convective cells, large plane vortices also arise. In other words, this is the effect of the hydrodynamic (vortex) dynamo [23-2 – 23-4], which, in contrast to the well-known physical models considered in a medium with spiral hydrodynamic turbulence (for more details, see review [23-5]), is a regular process and not necessarily due to the presence of uncompensated helicity in the system.

The Proctor-Sivashinsky model, as a result of modification by the author of [23-1], describes convection similar to that considered above, but taking into account the poloidal velocity $\vec{U}_{\text{tor}} = \text{rot}(\vec{e}_z \Psi)$,

$$\dot{\Phi} = \varepsilon^2 \Phi - (1 - \nabla^2)^2 \Phi + \frac{1}{3} \nabla \left(\nabla \Phi |\Phi|^2 \right) + \gamma_{\text{Pr}} \nabla \Phi \times \nabla \Psi, \quad (23.1)$$

$$\nabla^2 \Psi = \nabla \nabla^2 \Phi \times \nabla \Phi, \quad (23.2)$$

Where γ_{Pr} is the reciprocal of the Prandl number $\text{Pr} = \nu/\kappa$, characterizing the nonequilibrium state of the liquid, ν is the kinematic viscosity, here κ is the specific thermal diffusivity, $\varepsilon \ll 1$ in this case.

Modulation instability of a system of convective cells. The threshold of secondary instability is determined by vanishing $\varepsilon_2 = 27b^2\Gamma^2/20 - 1$, where $\Gamma = \varepsilon \cdot \gamma_{\text{Pr}}$, $b = \sqrt{5/3}A$ is the renormalized amplitude of the perturbations of the primary instability considered in the previous section. When the threshold ($\varepsilon_2 > 0$) is exceeded, conditions arise for the existence of secondary instability, with increment maxima

$$\text{Im } \omega_{\text{max}} = 1 - 6b^2/5 + 27\Gamma^2b^4/200 + 2/27\Gamma^2 \quad (23.3)$$

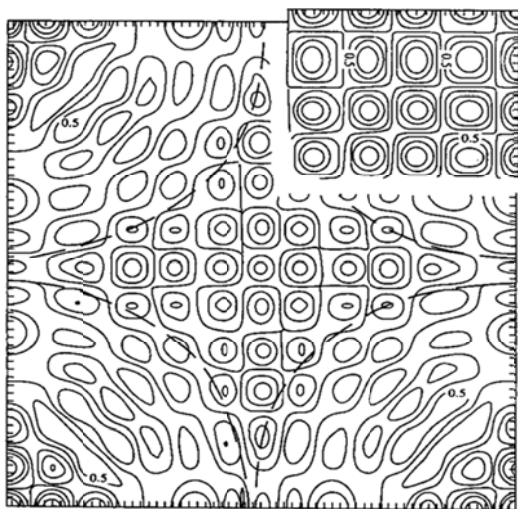


Figure 23.1. Regular defect in convective structure. In the upper right corner there is a fragment of the primary undisturbed structure. The dotted line shows the characteristic streamlines of large-scale vortices [23-3, 23-4]

are close to the main modes of the primary structure ($k_x = \pm 1$, $k_y = 0$ и $k_x = 0$, $k_y = \pm 1$) in mutually perpendicular directions at equal $\Delta = (\sqrt{2}/b\Gamma) |\varepsilon_2| \ll 1$ distances from these points. As the wave numbers approach the modes of the

primary structure in space, the increment of modulation instability tends to zero. The appearance of large-scale vortex disturbances as a result of modulation instability leads to the appearance of shear flows and deforms the convective structure on large scales. The equation, describing the evolution of the instability spectra has the following form:

$$\dot{b}_j = b_j - \sum_j^N V_{ij} |b_i|^2 b_j + \sum_{i,n,m}^N W_{jinm} b_i b_n b_m, \quad (23.4)$$

where the interaction coefficients are determined by the relations below $V_{ij}=1$,

\mathcal{G} is the angle between the vectors \vec{k}_i and \vec{k}_j [22-4],

$$V_{ij} = (2/3) \left(1 - 2 (\vec{k}_i \vec{k}_j)^2 \right) = (2/3) (1 + 2 \cos^2 \mathcal{G}),$$

$$W_{jinm} = (\vec{k}_i \times \vec{k}_n) (\vec{k}_m \times \vec{k}_j) \left[\frac{k_i^2 - k_n^2}{(\vec{k}_i + \vec{k}_n)^2} + \frac{k_i^2 - k_m^2}{(\vec{k}_i + \vec{k}_m)^2} \right] \delta_{\vec{k}_j, \vec{k}_i + \vec{k}_n + \vec{k}_m}.$$

It can be shown that under the conditions of symmetry of the resulting perturbations, the equations for the main modes of convective cells (each of which has an amplitude equal to b) and for the fastest growing modes of the spectrum b_d (in the mode when the rest of the spectrum is suppressed as a result of the above competition mechanisms) of modulation instability have the form

$$\dot{b} = b(1 - b^2 - 4b_d^2), \quad (23.5)$$

$$\dot{b}_d = b_d(1 - b^2 - b_d^2) + \frac{2}{27\Gamma^2} b^2 b_d \theta(\varepsilon_2), \quad (23.6)$$

where the occurrence of the modulation instability threshold is qualitatively described using the theta function $\theta(\varepsilon_2)$. When the threshold of modulation instability is exceeded, as a result of its development, the amplitudes of the primary structure modes decrease from values comparable with unity to values $b_\infty^2 = 20/27\Gamma^2$, while the amplitudes of the main growing modes of the spectra reach values $b_{d\infty} = 1/2(1 - b_\infty^2)^{1/2}$. The intensity (i.e., magnitude) of the primary structure $I = \sum |b_{k_i}|^2$ without the occurrence of modulation instability (when the primary structure is stable) and the intensity of the defective structure, which is the result of the development of this instability, are equal. The defectiveness of the developed structure is equal to ε_2 .

The effect of a regular hydrodynamic dynamo. The interaction between the modes that determine the modulation (distributed defect modes) and the modes of the main structure is due to the existence of large-scale vortices, the streamlines of which in the configuration space can be represented as

$$\Psi \approx \varepsilon \varepsilon_2 b^2 [\cos(l_0 \xi) - \cos(l_0 \eta)], \quad (23.7)$$

where, the ratio of the characteristic linear size of the large-scale vortices L_V and the linear size of the convective cell L_C is equal to $L_V/L_C \approx (b\varepsilon\varepsilon_2)^{-1}$. The occurrence of such large-scale vortices is one of the possible realizations of the hydrodynamic dynamo effect [23-2, 23-3].

Thus, in case of modulation instability of a system of developed convective cells, not only does a self-similar structure occur – convective cells of different scales [23-6], but a large-scale poloidal vortex is formed as well [23-2 – 23-4].

References to section 23

23-1. Pismen L. Inertial effects in long-scale thermal convection, *Phys. Lett. A*. 1986. – V. 116. – P. 241–243.

23-2. Kirichok A. V., Kuklin V. M., Panchenko I. P., Moiseev S. S., Pismen L. M. Dynamics of the formation of large-scale vortices in the convective instability regime. // *Inter. Conf. "Physics in Ukraine"*, Kiev, 22–27 June 1993. *Proc. Contr. Pap. ITP*, 1993. P. 76–80.

23-3. Kirichok A. V., Kuklin V. M., Panchenko I. P. On the possibility of a dynamo mechanism in a nonequilibrium convective medium. *Reports of NASU*. 1997. – No. 4. – C. 87–92 (in Russian).

23-4. Kirichok A. V. and Kuklin V. M. Allocated Imperfections of Developed Convective Structures. *Physics and Chemistry of the Earth Part A*. 1999. – № 6. – P. 533–538.

23-5. Vortex dynamo in spiral turbulence. // Authors: Moiseev S. S., Oganessian K. R., Rutkevich P. B., Tur A. V., Khomenko G. A., Yanovsky V. V. in the book: *Integrability and kinetic equations for solitons*. Ed. V. G. Bar'yakhtar, V. E. Zakharova, V. M. Chernousenko. *Sat. scientific. tr. Kiev, Naukova Dumka*, 1990 – 472 p. (in Russian).

23-6. Kuklin V. M. The role of energy absorption and dissipation in the formation of spatial nonlinear structures in nonequilibrium media. *Ukrainian Physical Journal, Reviews*, 2004. – Vol. 1. – No. 1 – P. 49–81 (in Ukrainian).

PART II

Annexes

ANNEX I

TRADITIONAL THRESHOLD OF INDUCED RADIATION

Let us consider the system of equations (1.1) – (1.3), define the concept of inversion $\mu = (n_2 - n_1)$ and find the integrals of the system

$$N_k + n_2 = Const \quad (1.1)$$

$$n_1 + n_2 = Const \quad (1.2)$$

where we shall get

$$\frac{\partial N_k}{\partial t} = u_{21} \cdot \mu \cdot N_k = u_{21} (2N_k(0) + n_2(0) - n_1(0) - 2N_k) \cdot N_k. \quad (1.3)$$

At low field intensities N_k is

$$\frac{\partial N_k}{\partial t} = u_{21} \cdot \mu_0 \cdot N_k = u_{21} [n_2(0) - n_1(0)] \cdot N_k = \gamma \cdot N_k \quad (1.4)$$

In case of the positive population inversion ($\mu_0 > 0$), we shall find an increase in the number of field quanta N_k at the initial stage $\propto \exp\{\gamma \cdot t\}$ with an increment, which is equal to γ . Then the increase in intensity slows down due to a decrease in the level of inversion. In instability saturation we have $N_{kMAX} = N_k(0) + \mu(0) / 2$.

In case of finite absorption of quantum energy in the system

$$\frac{\partial N_k}{\partial t} = -\delta \cdot N_k + u_{21} \cdot \mu \cdot N_k, \quad (1.5)$$

here δ is the decrement of absorption of the field energy. Typically, losses in active media are due to the removal of radiation from the cavity (resonator) volume. These losses can be correctly set by defining the boundary conditions for the field. However, they can be described approximately in a fairly general way as

$$\delta = \delta_D = \oint_S \frac{\partial \omega}{\partial \vec{k}} \cdot \frac{1}{4\pi} \vec{E} \times \vec{H} \cdot d\vec{s} / \oint_V \frac{\partial [\omega \varepsilon(\omega, \vec{k})]}{\partial \omega} \frac{1}{8\pi} (|\vec{E}|^2 + |\vec{H}|^2) dv, \quad (1.6)$$

that is, in the case under consideration, the flux of electromagnetic energy through the mirrors should be divided by the field energy contained in the resonator. It is important that the value equal to the product of the characteristic time of the change in the field $\{\partial |\vec{E}|^2 / |\vec{E}|^2 \partial t\}^{-1}$ in the resonator by the group

velocity of oscillations $|\partial\omega/\partial\vec{k}|$ is significantly larger than the size L of the resonator. Under these conditions, in theoretical calculations and estimates it is quite possible to substitute losses by mirrors with distributed losses. The traditional instability threshold is determined by the condition

$$\mu > \mu_{TH1} = \delta / u_{21}. \quad (1.7)$$

When approaching the instability threshold, the noise level grows, and when the threshold is exceeded, the process of increasing the number of quanta can become exponential.

ANNEX II

SPONTANEOUS AND INDUCED RADIATION OF THE ELECTRON BEAM. LANDAU DAMPING. EQUATIONS OF KINETIC INSTABILITY OF A HOT ELECTRON BEAM IN PLASMA

Let the beam particles emit and absorb plasmons with energy $\hbar\omega(k)$. In the case of a spontaneous process, the number of quanta emitted per unit time in the wave number interval dk (thereby changing state m to state n) is equal to $N_m A_m^n dk$, for induced radiation process it is equal to $N_m B_m^n E_k dk$. The number of absorbed quanta under the same conditions is equal to $N_n B_n^m E_k dk$. Then, for the number of particles in state m , that is N_m and the number of particles in state n , N_n we can write equations уравнения

$$\frac{\partial N_m}{\partial t} dk = -N_m A_m^n dk - N_m B_m^n E_k dk + N_n B_n^m E_k dk, \quad (II.1)$$

$$\frac{\partial N_n}{\partial t} dk = +N_m A_m^n dk + N_m B_m^n E_k dk - N_n B_n^m E_k dk, \quad (II.2)$$

where E_k and $N(k) = \frac{2\pi}{\hbar\omega(k)} E_k$ are the energy density and the number of quanta in this wave number interval, respectively. Here in the one-dimensional case

$$A_m^n = \frac{1}{2\pi} \cdot \hbar\omega(k) \cdot B_m^n, \quad B_m^n = B_n^m.$$

For the electron charge density $\rho = -e \cdot \delta(v \cdot t - z + s)$, from the Poisson equation we shall obtain the value of the Fourier transform of the electric field

$$E(\omega, k) = 8\pi^2 i e \frac{\delta(\omega - kv)}{k\varepsilon(\omega, k)} \exp\{-iks\}, \quad (II.3)$$

where $\varepsilon(\omega, k) = \varepsilon(\omega) = 1 - \omega_{pe}^2 / \omega(\omega + i\nu_{ei})$, $\omega_{pe} = \sqrt{4\pi e^2 n_0 / m}$, ν_{ei} is the frequency of collisions of electrons with ions, which is assumed to be insignificant. Performing the inverse transformation

$$E(z, t) = (2\pi)^{-2} \int d\omega \cdot \exp\{-i\omega \cdot t\} \int dk \cdot E(\omega, k) \cdot \exp\{ikz\},$$

let us find the value of the electric field

$$E(z, t) = 2ie \int \frac{dk}{k\varepsilon(kv, k)} \exp\left\{-ikv\left(t - \frac{z-s}{v}\right)\right\}. \quad (II.4)$$

The drag force of a particle by the radiation field is

$$F = \frac{1}{2\pi} \int F(k) \cdot dk, \quad (II.5)$$

where $F(k) = 4\pi \cdot ie^2 / [k\varepsilon(kv, k)]$. From here let us obtain the spectral intensity of spontaneous emission of one particle

$$\begin{aligned} w_1(k) &= \text{Re}\{4\pi \cdot ie^2 \cdot v / [k\varepsilon(kv, k)]\} = \text{Re}\{2\pi \cdot ie^2 \cdot v^2 \left[\frac{1}{kv - \omega_{pe}} + \frac{1}{kv + \omega_{pe}} \right]\} = \\ &= 2\pi^2 e^2 \omega_{pe}^2 \cdot \delta(kv - \omega_{pe}) / k^2, \end{aligned} \quad (II.6)$$

that is, for a spontaneous process, the relation holds $N_m A_m^n \cdot \hbar \omega(k) = 4\pi^2 e^2 [\omega^2(k) / k^3] \cdot f_b[\omega(k) / k]$. For $N(k)$ which is determined from the relation $E = \int_{-\infty}^{\infty} dk \cdot E_k = \frac{1}{2\pi} \int_{-\infty}^{\infty} dk \cdot N(k) \cdot h\omega(k)$, the equation takes the form

$$\frac{\partial N(k)}{\partial t} = \{N_m A_m^n + N_m B_m^n E_k - N_n B_n^m E_k\} \quad (II.7)$$

Then for a homogeneous beam with a velocity distribution function $f(v_m)$, let us obtain the relation

$$(N_m - N_n) / N_m = (\hbar k / m) \cdot df(v) / f(v_m) dv|_{v_m} \ll 1, \quad (II.8)$$

where $v_m = \omega(k) / k$.

If the velocity distribution function of the beam $f(v_b)$ has the form

$$f_b = [n_{b0} / \sqrt{\pi} v_{Tb}] \cdot \exp\{-(v - v_{0b})^2 / v_{Tb}^2\}, \quad (II.9)$$

where $v_0; v_{Tb}; n_{b0}$ are average velocity, heat velocity and density of beam particles correspondently, then the equation (II.7) takes the form (2.7)

$$\begin{aligned} dE_k / dt &= 2\pi^2 e^2 [\omega^2(k) / k^3] \cdot f_b[\omega(k) / k] \cdot \\ &\cdot \{1 + N_k (\hbar k / m) \partial f_b(v) / f_b(\omega(k) / k) \partial v|_{v=\omega(k)/k}\} - 2\delta_D \cdot E_k = \\ &= 2\gamma_L \cdot \{E_k + \omega(k) T_b / [kv_{0b} - \omega(k)]\} - 2\delta_D \cdot E_k, \end{aligned} \quad (II.10)$$

where $\gamma_L = (\sqrt{\pi} / 2) \frac{\omega_b^2 \omega(k)}{k^3 v_{Tb}^3} \exp\left\{-\frac{[kv_{0b} - \omega(k)]^2}{k^2 v_{Tb}^2}\right\} [kv_{0b} - \omega(k)]$ is the linear increment of beam-plasma instability in the absence of energy loss ($\delta = 0$) of plasmons $\omega(k) \approx \omega_{pe} = \sqrt{4\pi e^2 n_0 / m}$.

The relationship between the energy density E_k and the electric field strength of plasmons E_k is determined by the ratio $E_k = \frac{\partial \omega \varepsilon(\omega, k)}{8\pi \cdot \partial \omega} |E_k|^2 \approx \frac{\omega_{pe}^2}{4\pi \omega^2(k)} |E_k|^2$. It is not difficult to obtain the Landau

damping decrement [II-1] for the Maxwell plasma [see also damping decrement for electrons from the non-Maxwell plasma [II-2] obtained by A. A. Vlasov somewhat before) for plasmons whose phase velocity is noticeably higher than the thermal velocity plasma. In this case, the role of the particle beam can be played by the high-energy part – the “tail” of the Maxwellian distribution of plasma electrons, and the dispersion characteristics are determined by the bulk of the plasma electrons.

The equation for the spectral intensity of plasmons neglecting spontaneous processes takes the form:

$$dE_k / dt = -2\delta_L \cdot E_k, \quad (II.11)$$

where the value of the Landau damping decrement is

$$\delta_L = -\sqrt{\pi} \cdot \frac{\omega^4(k)}{2k^3 v_{Te}^3} \exp\left\{-\frac{\omega^2(k)}{k^2 v_{Te}^2}\right\}, \quad (II.12)$$

$v_{Te} = \sqrt{T_e / m_e}$ a T_e is the temperature of plasma electrons. In connection with the intensive development of nonlinear physics in distributed systems and media, the main attention is traditionally paid to induced self-consistent processes.

The system of equations that describes the behavior of the field of a plasma wave excited by a beam, for example, (II.7), can be written as

$$\begin{aligned} & \frac{\partial \operatorname{Re}[\omega \cdot \varepsilon(\omega)]}{\partial \omega} \Big|_{\omega_0} \cdot \frac{\partial E_k}{\partial t} + \operatorname{Im}[\omega \cdot \varepsilon(\omega)] \Big|_{\omega_0} \cdot E_k = \\ & = \frac{4\pi e \omega_0}{k_0} \frac{\partial f_0(v)}{\partial v} \Big|_{v=\omega_0/k_0} \cdot \int_{-\pi/k_0}^{\pi/k_0} d\xi_0 \cdot \int_{-\Delta v_m}^{\Delta v_m} d\Delta v_0 \cdot \Delta v \cdot \operatorname{Cos}\{k_0 \xi + \varphi\}, \end{aligned} \quad (II.13)$$

$$\begin{aligned} & \frac{\partial \operatorname{Re}[\omega \cdot \varepsilon(\omega)]}{\partial \omega} \Big|_{\omega_0} \cdot \frac{\partial \varphi}{\partial t} \cdot E_k - \operatorname{Re}[\omega \cdot \varepsilon(\omega)] \Big|_{\omega_0} \cdot E_k = \\ & = -\frac{4\pi e \omega_0}{k_0} \frac{\partial f_0(v)}{\partial v} \Big|_{v=\omega_0/k_0} \cdot \int_{-\pi/k_0}^{\pi/k_0} d\xi_0 \cdot \int_{-\Delta v_m}^{\Delta v_m} d\Delta v_0 \cdot \Delta v \cdot \operatorname{Sin}\{k_0 \xi + \varphi\}, \end{aligned} \quad (II.14)$$

where $\xi = x - v_0 t$, $\Delta v = v - v_0$, $n_{b0} = \int f_0(v) \cdot dv$, $\Delta v_m \propto 6\pi |\gamma| / k_0$, initial conditions are $\xi_0 = \xi(t=0) \in (-\pi/k_0, \pi/k_0)$ и $\Delta v_0 = \Delta v(t=0) \in (-\Delta v_m, \Delta v_m)$. Whence it is easy to obtain equations (2.12) – (2.13).

However, the consideration of spontaneous processes in the general dynamics of the development of many physical phenomena is often necessary to elucidate the role of the intrinsic noise of systems, especially near the threshold of instabilities. This will allow us to adjust our understanding of the dynamics of nonequilibrium processes.

References to annex II

II-1. Landau L. D. On oscillations of electron plasma // JETP, 1946. – V. 16. – No 7. – P. 574-586 (in Russian).

II-2. Rukhadze A. A., Silin V. P. Scientific works. The way to create physical concepts of plasma without collisions // Problems of theoretical physics. Issue 2 / V. A. Butz, A. G. Zagorodniy, A. V. Kirichok, V. M. Kontorovich, V. M. Kuklin, A. A. Rukhadze, V. P. Silin, A. V. Tur, V. V. Yanovskiy; under the general editorship of A. G. Zagorodny, N. F. Shulga, edit. V. M. Kuklin – Kh.: V. N. Karazin Kharkiv National University, 2016. – Issue. 2 – 376 p. (in Russian).

ANNEX III

ON SPONTANEOUS AND INDUCED WAVE RADIATION

The Fourier image of the current at the combination frequency $\omega_2 + \omega_3$ can be written as

$$j_{23}(\omega, k) = (k_2 + k_3) \frac{n_0 e^3 \{E_2 E_3\}_\omega}{m_i^2 \omega_1 \omega_2 \omega_3} \delta(k_1 - k_2 - k_3), \quad (\text{III.1})$$

where for $\{E_2 E_3\}_\omega$ you can use the view of

$$\{E_2 E_3\}_\omega = \{E_2 E_3\}_0 \frac{1}{\Delta_{\Omega 23} \sqrt{\pi}} \exp\{-(\omega - \omega_2 - \omega_3)^2 / \Delta_{\Omega 23}^2\},$$

here $\Delta_{\Omega 23}$ is the spectral width of the packet at the combination frequency, $E_i = |E_i| \exp\{i\varphi_i\}$ is the slowly varying complex amplitude of the i -th wave. For the field accompanying this current, the expression is

$$E_{23}(\omega, k_2 + k_3) = 4\pi \frac{ie(k_2 + k_3) \{E_2 E_3\}_\omega \Omega_i^2}{m_i \omega^2 \omega_2 \omega_3 \varepsilon(\omega, k_2 + k_3)} \delta(k - k_2 - k_3), \quad (\text{III.2})$$

where $\varepsilon(\omega, k) = 1 - \frac{\Omega_i^2}{\omega^2} + \frac{\Omega_i^2}{k^2 v_s^2} = 0$, Ω_i and v_s are the Fourier transformation of the dielectric constant, the ion plasma frequency, and the speed of sound, respectively. Applying the Borel theorem, let us find the work of the field on the current and after the inverse transformation this expression will take the form:

$$E_{23}^{(2)} * j_{23}^{(2)} = -i \left(\frac{e}{m_i v_s} \right)^2 W_2 \cdot W_3 \frac{8}{3} \frac{\omega_1}{\omega_2 \omega_3} [1 - i\alpha] \exp \left\{ -i(\omega_1 - \omega_2 - \omega_3) \cdot t - \frac{(\Delta_{\Omega 23} t)^2}{4} \right\}. \quad (\text{III.3})$$

In order to obtain (III.3), it is necessary to use the relation

$$\frac{1}{\omega \varepsilon(\omega, k_2 + k_3)} = \frac{\omega_1}{3\omega_2 \omega_3} + i\pi \cdot \frac{k_1^2 v_s^2}{2\Omega_i^2} \{\delta(\omega - \omega_1) + \delta(\omega + \omega_1)\}, \quad (\text{III.4})$$

in addition, the following concepts were used: $W_1 = \frac{1}{8\pi} \omega_1 \frac{\partial \varepsilon}{\partial \omega_1} |E_1|^2 = 2 \frac{\Omega_i^2}{8\pi \omega_1^2} |E_1|^2$

is the density of vibrational energy at a frequency ω_1 , $\Delta_{-1,2,3} = (-\omega_1 + \omega_2 + \omega_3) = 3\omega_1\omega_2\omega_3 / 2\Omega_i^2$ is the frequency detuning due to dispersion, and $\alpha = \pi \cdot \frac{3\omega_1\omega_2\omega_3}{2\Omega_i^2} \frac{1}{\Delta_{\Omega_{23}} \sqrt{\pi}} \exp\{-(\omega_1 - \omega_2 - \omega_3)^2 / \Delta_{\Omega_{23}}^2\}$ since $\Delta_{\Omega_{23}} \geq \omega_1 - \omega_2 - \omega_3$, under these conditions, α is the order of unity. Under conditions of insignificant detuning $\Delta_{-1,2,3}$ not exceeding the spectral width of wave packets for sound waves, current (III.1) is able to excite a field at a frequency ω_1 due to the presence of resonance $\varepsilon(\omega_1, k_2 + k_3) = 0$. For small detunings, the change in the field energy at the frequency ω_1 due to the current at the combination frequency can be presented as

$$-(E_{23}^{(2)*} j_{23}^{(2)} + E_{23}^{(2)} j_{23}^{(2)*}) / 2 = \alpha \left(\frac{e}{m_i v_s} \right)^2 W_2 W_3 \frac{8}{3} \frac{\omega_1}{\omega_2 \omega_3}. \quad (III.5)$$

It should be noted that the sign of expression (III.5) does not depend on the waves involved in the interaction, which corresponds to the process of oscillation generation (radiation). Such sign-definiteness is characteristic of spontaneous processes. In addition, radiation at a frequency ω_1 , is caused by extraneous sources (here, waves are at frequencies ω_2 and ω_3) with respect to a wave at the same frequency, which is also characteristic of spontaneous processes. Therefore, such generation with respect to a wave at a frequency ω_1 has the properties of spontaneous processes.

Obviously, with large detunings in the spectral range of interacting modes, the radiation (III.5) is exponentially small. For the vibrational energy at a frequency, the following equation [III-1] is true:

$$\frac{\partial W_1}{\partial t} = \alpha \frac{8}{3} \left(\frac{e}{m_i v_s} \right)^2 \omega_1 \frac{W_2 W_3}{\omega_2 \omega_3} - \text{Re} \frac{2\Omega_i^2 e E_2 E_3 E_1^*}{\pi m_i v_s \omega_2 \omega_3} + \frac{8}{3} \left(\frac{e}{m_i v_s} \right)^2 \omega_1 \left\{ \frac{\alpha' W_1 W_1}{2 \omega_1 \omega_1} + \alpha \frac{W_1}{\omega_1} \left(\frac{W_2}{\omega_2} + \frac{W_3}{\omega_3} \right) \right\}. \quad (III.6)$$

This equation can be written for the number of quanta per unit volume $N_i = W_i / \hbar \omega_i$

$$\frac{\partial N_1}{\partial t} = \alpha \frac{8\hbar}{3} \left(\frac{e}{m_i v_s} \right)^2 N_2 N_3 - \text{Re} \frac{2\Omega_i^2 e E_2 E_3 E_1^*}{\pi m_i \hbar v_s \omega_2 \omega_3 \omega_1} + \frac{8\hbar}{3} \left(\frac{e}{m_i v_s} \right)^2 \left\{ \frac{\alpha'}{2} N_1 N_1 + \alpha N_1 (N_2 + N_3) \right\}. \quad (III.7)$$

The same equation can be written for the slow phase of oscillations at a frequency ω_1 :

$$N_1 \frac{\partial \varphi_1}{\partial t} = \frac{8\hbar}{6} \left(\frac{e}{m_i v_s} \right)^2 N_2 N_3 - \text{Im} \frac{\Omega_i^2 e E_2 E_3 E_1^*}{\pi m_i \hbar v_s \omega_2 \omega_3 \omega_1} - \frac{8\hbar}{6} \left(\frac{e}{m_i v_s} \right)^2 \left\{ \frac{1}{2} N_1 N_1 - N_1 (N_2 + N_3) \right\}. \quad (III.8)$$

The first term on the right-hand side of each of equations (III.7) and (III.8) corresponds to spontaneous effects, the second term determines the interaction of all three waves, and the third term determines the induced effects of self-interaction ($\propto N_1^2$) and cross-modulation, which can be obtained by direct calculations.

Let us note that the coefficient, preceding the product of the number of quanta in equations (III.7) and (III.8) is equal to $\hbar e^2 / (m_i v_s)^2$, can be represented in the form of $\alpha_v \cdot \omega \cdot \tilde{\lambda}_v^2 \cdot k^{-1}$, where $\alpha_v = e^2 / \hbar v_{ph}$ is the analog of the fine structure constant for the case when the phase velocity $v_{ph} = v_s$ and the quantity $\tilde{\lambda}_v = \hbar / m_i \cdot v_{ph}$ are formally similar to the Compton wavelength for $v_{ph} = v_s$ scattering by ion.

On the description of self-interaction processes. The term $\propto N_1^2$ in the right-hand sides of (III.6) – (III.8) describes the result of self-action and, which is noteworthy, can also be formally obtained. For a current at combination frequencies $2\omega_1 - \omega_1$ (it can be shown that the drag current makes a significantly smaller contribution than the account of perturbations at the second harmonic), we can write

$$j_{2\omega_1 - \omega_1}(x, t) E_{2\omega_1 - \omega_1}^*(x, t) = -\frac{W}{2} \cdot N_{2\omega} N_{\omega} (i + \alpha'), \quad (III.9)$$

where the numerical coefficient $\alpha \rightarrow \alpha' = 3 \cdot 4 \frac{\omega_1^3}{\Omega_i^2} \left(\frac{1}{\Delta_{\Omega_{23}} \sqrt{\pi}} \right) \exp \left\{ - \left(\frac{3\omega_1^2}{\Omega_i^2} \right)^2 / \Delta_{\Omega_{23}}^2 \right\}$

is of the order of unity. Similarly, let us write the procedure for obtaining the nonlinear term for self-action

$$-\frac{W}{2} \cdot (i + \alpha') [(N_{2\omega} + 1)(N_{\omega} - 1) - N_{2\omega} N_{\omega}] \cdot N_1 \approx -\frac{W}{2} N_1^2 (i + \alpha'), \quad (III.10)$$

(because $N_{2\omega} \ll N_{\omega}$), the value of which can also be obtained by direct calculation. But since the magnitude of the current at combination frequencies $2\omega_1 - \omega_1$ is determined by values of a higher order of smallness in terms of the amplitudes of oscillations, in this case it is more correct to focus on direct calculations of the terms responsible for the effects of self-action. Similar calculation schemes were actively used by many authors (see, [III-2] and the literature there) to describe wave interactions. However, it should be noted that the application of such operations in the framework of developed phenomenologies, in most cases very successful, can distort the physical meaning of individual elements of the description and should be based on direct calculations. In the absence of detuning, the first term on the right-hand side of (III.6) is responsible for the radiation at a frequency generated only by the combination interaction of two waves with frequencies ω_2 and ω_3 . The second term on the right-hand side of (III.6) defines the well-known collective process of interaction of all three waves. The account of the spontaneous generation process described by the first term of the right-hand side of (III.6), which can be called spontaneous, provides not only the formation of a certain level of fluctuations in the system, but also can significantly affect the dynamics

of multi-wave interaction (similar to the phenomena discussed in [III- 3, III-4]). In particular, the increasing noise level can smooth out amplitude oscillations and equalize the intensity levels of interacting waves, as well as the effect of random phase disturbances [III-5, III-6]. In the homogeneous case, for sufficiently large detuning Δ values, exceeding the spectral width of the waves involved in the interaction, the first term of the right-hand side is negligible, i.e., the effectiveness of such a spontaneous interaction of waves is weakened.

References to annex III

III-1. Kirichok A. V. Kuklin V. M. Theory of Some Nonlinear Processes in Plasma in Terms of Spontaneous and Stimulated Radiation // Phys. Scripta. – 82 (2010) 065506.

III-2. Tsytovich V. N. The theory of turbulent plasma. – M.: Atomizdat, 1971. – 423 p. (in Russian).

III-3. Sitenko A. G. Fluctuations and nonlinear interaction of waves in plasma. – K.: Nauk. dumka, 1977. – 248 p. (in Russian).

III-4. Anishchenko V. S., Neiman A. B., Moss F., Shimansky-Gayer L. Stochastic resonance as a noise-induced effect of increasing the degree of order // Physics Uspehi, 1999. – V. 169. – No. 1. – P. 7–38 (in Russian).

III-5. Akhiezer A. I., Aleksin V. F., Khodusov V. D. To the nonlinear theory of low-frequency oscillations in a weakly turbulent plasma // ZhETF, 1977, vol. 73. – V. 5 (11). – P. 1757–1766 (in Russian).

III-6. Abramovich B. S., Tamoikin V. V. Diffusion approximation in the theory of nonlinear interaction of waves in chaotically inhomogeneous media. – In the book: Nonlinear waves. Dissemination and interaction. – M.: Nauka, 1981. – P. 225–234 (in Russian).

ANNEX IV

ON THE NATURE OF MÖSSBAUER EFFECT

Let us consider the HF oscillator-emitter, trapped in the potential well, which interacts with an external field [IV-1]. Let us show, when the recoil energy during the act of absorption or emission of a field quantum is equal to $\hbar\Omega$ (where Ω is the LF frequency of the oscillatory motion in the potential well), the emission and absorption lines at the HF oscillator-emitter are of the highest intensity, the frequencies of these intense lines are equal to each other and do not differ from the frequency of the resting oscillator-emitter.

Let us discuss the oscillator emission process with an eigenfrequency ω_0 , charge and mass equal to e, m_0 , that oscillates in a potential well oriented along the OZ axis. The vector of the emitted electromagnetic wave is also oriented in the same direction.

Let there be an HF oscillator at the origin of coordinates whose velocity is $v_x = v_{x0} \cos \omega_0 t = a \omega_0 \cos \omega_0 t$. Slow oscillations of such an oscillator in a potential well occur in speed $v_z = b \Omega \cos(\Omega t)$, in this case $\Omega \ll \omega_0$. The conservation laws

during the absorption of a quantum $E_\nu = \hbar(\omega_0 + \Omega)$ of an external field by an oscillator with a rest mass m_0 and charge e have the form $\hbar(\omega_0 + \Omega)/c = m_0 V_\Omega$, $\hbar\Omega = m_0 V_\Omega^2 / 2$.

Under conditions $\alpha = \hbar\omega_0 / m_0 c^2 \ll 1$, the motion of the oscillator along the OZ axis is described by the equation $z = b \sin \Omega t$, where $\Omega = V_\Omega / b$. In this case, an important relation is fulfilled [IV-2]

$$\omega_0 b / c = kb \approx 2. \quad (\text{IV.1})$$

The vector potential of the external field has components $A_x = q(t) \cdot \sqrt{2} \cdot \text{Cos}\{kz + \delta\}$, $A_y = 0$, $A_z = 0$. The phase δ depends on the orientation of the oscillator. The choice of type A_x is determined by normalization conditions, so that the integral of the square of the vector potential in a unit volume is equal to unity, and the quantity $q(t)$ satisfies the equation $\ddot{q} + \omega^2 q = 0$, where ω and $\vec{k} = (0, 0, k)$ is frequency and the wave vector of the electromagnetic field. The total energy of the field in the volume V is equal to $U = V \cdot (\dot{q}^2 + \omega^2 q^2) / 8\pi c^2$, where we can determine the effective mass of the field oscillator $m_{\text{eff}} = V / 4\pi c^2$. The interaction energy of the oscillator with an external field is $H' = -e \cdot v_x A_x / c$. The vector potential at the point where there is an oscillator is

$$A_x = \sqrt{2} \cdot q_0 \exp\{i(\omega \pm \Omega)t + ikb \sin \Omega t\} \cdot \text{Cos}\{\delta\} = \sqrt{2} \cdot q_0 \text{Cos}\{\delta\} \sum_m J_m(kb) \exp\{i(\omega \pm \Omega)t + im\Omega t\},$$

where $v_x = v_{x0} \cdot \text{Cos}\omega_0 t$ is the oscillator speed.

The resonance conditions require that the frequency in the rest frame of the oscillator be equal to, ω_0 that is $\omega \pm \Omega + m\Omega = \omega_0$. The upper sign corresponds to radiation, the lower one corresponds to the absorption of an external quantum. Indeed, at $b=0$ and $m=0$, the frequency of the external field during emission of a quantum is equal to $\omega = \omega_0 - \Omega$ and the frequency of the external field during absorption is $\omega = \omega_0 + \Omega$.

If $b \neq 0$, the system "oscillator in a potential well" is an infinite set of oscillators (see [IV-1], [IV-3]) with an amplitude and frequency $\sim J_m(kb) \cdot \exp\{i\omega_0 t + im\Omega\}$, of which we will be interested only in those that correspond to the values $m = \pm 1$. Thus, in the system there are m energy levels, transitions to each of which can be carried out independently.

In this case, attention should be paid to the change in frequency during recoil $k \cdot t^{-1} \int t dt \cdot (dV_\Omega / dt) \approx \pm k V_\Omega / 2 = \pm \Omega$ in the rest system of the particle-oscillator. In the classical model, the time interval of the momentum and energy transfer to the particle-oscillator is quite long, in the quantum case this process is considered instantaneous. That is, the interaction leads to a change in frequency precisely by an amount Ω .

We can make sure that only for the values of the external field frequency $\omega = (-m \mp 1)\Omega + \omega_0$ the expression for the interaction energy of the oscillator with the field turns out to be nonzero and can be represented as

$$H' = -e \cdot v_x A_x / c = -\frac{e \cdot v_{x0}}{c} q_0 \sqrt{2} \cdot \sum_m J_m(kb) \cdot \cos \delta. \quad (IV.2)$$

Let us note that for an oscillator at rest $b=0$, in expression (IV.2), only one member of $m=0$ series is nonzero. Thus, the frequency of the absorbed radiation $\omega = \omega_0 + \Omega$ differs from the frequency of the emitted $\omega = \omega_0 - \Omega$ by 2Ω , which corresponds to the difference in the energies of the absorbed and emitted quanta in two recoil energies.

When $b \neq 0$ in case of trapped quantum $\omega + m\Omega = \omega_0 + \Omega$, which determines the value $m=1$ at the frequency of external radiation $\omega = \omega_0$. In case of quantum radiation, an oscillator trapped in a potential well is $\omega + m\Omega = \omega_0 - \Omega$, which determines the value $m=-1$ at the frequency of external radiation $\omega = \omega_0$. It is easy to see that when the ratio $\omega_0 b / c = kb \approx 2$ is fulfilled, the radiation and absorption at the natural frequency of the oscillator ω_0 are the most intense (i.e. $J_1^2(kb)|_{kb \approx 2} = J_{-1}^2(kb)|_{kb \approx 2} \gg J_0^2(kb)|_{kb \approx 2}$). To do this, let us represent the matrix element as

$$H_{if} = -\sqrt{2}(e/c) \cdot \omega_0 \cdot x_{ab} \cdot q_{nn'} \cdot J_{\pm 1}(kb) \cdot \cos \delta.$$

Two oscillator states are a, b , which are indicated by lower indices, and the indices n, n' correspond to two states of the radiated $(n, n+1)$ or absorbed $(n, n-1)$ field. Moreover, for the case of absorption $|q_{nn'}|^2 = |q_{n, n-1}|^2 = n |q_{01}|^2$, and for the case of radiation $|q_{nn'}|^2 = |q_{n+1, n}|^2 = (n+1) |q_{01}|^2$, where $|q_{01}|^2 = hc^2 / V \omega_0$ and the mass value $m_{eff} = V / 4\pi c^2$ are used. For the square of the matrix element, let us obtain the expression

$$|H_{if}|^2 = -\frac{2e^2}{c^2} \cdot \omega_0 \cdot (x_{ab}^2 + y_{ab}^2) \cdot \frac{hc^2}{V} J_1^2(kb) \cdot \cos^2 \delta \cdot \left\{ \begin{matrix} n+1 \\ n \end{matrix} \right\}, \quad (IV.3)$$

where the upper value corresponds to radiation (let us restrict to the case $n=0$), and the lower value corresponds to absorption (we set $n=1$). The transition probability can be found by multiplying by $4\pi^2 \rho(\omega_{ab}) / h$, where $\rho(\omega_{ab})$ is the density of oscillations in the frequency range and let us take into account that when averaging over the initial phases $\langle \cos^2 \delta \rangle = 1/2$

$$P_{if} = \frac{4\pi^2}{h^2} |H_{if}|^2 \rho = \frac{8\pi e^2}{hc^3} \omega_0^2 (|x_{ab}|^2 + |y_{ab}|^2) \cdot J_1^2(kb) \cdot \cos^2 \delta. \quad (IV.4)$$

Let us note that the probability of absorption at a frequency $\omega_0 \pm \Omega$ can be obtained by replacing $J_1^2(kb)$ in (IV.3) by $J_0^2(kb)$. The intensity along the OZ direction can be obtained by multiplying (IV.3) by $\hbar\omega_0$, and the total intensity in all directions by integrating along the cone $\theta = \vec{k} \wedge O\vec{Z}$.

It is easy to see that in case of an oscillator in a potential well with the frequency Ω and amplitude of oscillations b , since $J_1^2(kb) \gg J_0^2(kb)$ the intensity of the absorption and emission lines at the natural frequency of the oscillator ω_0 is almost an order of magnitude higher than the intensity of the emission lines at the frequency $\omega_0 - \Omega$ and absorption at the frequency $\omega_0 + \Omega$ [IV-1].

Let us also note that the nature of the high-frequency oscillator, whose vibrational energy in the potential well is equal to the recoil energy, does not affect the nature of the radiation and absorption under discussion at its natural frequency.

Let us mention that when radiation is at the angle of $\theta_0 \approx 50^\circ$ and when $J_1^2(kb \cdot \cos\theta_0) = J_0^2(kb \cdot \cos\theta_0)$, the radiation intensities at the natural frequency ω_0 and at the combination frequency $\omega_0 - \Omega$ are compared, *which makes it possible to experimentally verify this theory*²¹.

Thus, the nature of the Mossbauer effect can be quite simply explained by the peculiarities of radiation of atoms with an excited nucleus oscillating in potential wells of the crystal structure.

The relaxation processes of LF excitations in continuous media. If the system discussed above is in the medium, then the possibility of low-frequency quantum radiation $\Omega = \omega_0(\hbar\omega_0 / 2m_0c^2)$ should be considered.

The relatively low velocity acquired by the oscillator as a result of recoil $v_s \gg c(\hbar\omega_0 / 2m_0c^2)$ often turns out to be noticeably lower than the phase velocity of phonons. This makes it impossible to directly transfer the kinetic energy of the recoil to the phonon. This is also evidenced by the inability to comply with the laws of conservation of energy and momentum. The lifetime of such a low-frequency oscillator should be estimated. If the lifetime of the low frequency oscillator turns out to be noticeably longer than the period of oscillations in the potential well, then the radiation and absorption mechanisms of the isolated system "oscillator – potential well" discussed here are also applicable to the case when such a system is in the medium. In other words, relaxation processes, involving the phonon spectrum, in this case can be neglected. In the three-dimensional case, the characteristic relaxation time of the LF motion [IV-1] of the order $\tau_{LF} \approx 3(\rho_0\lambda_s^3 / m_0)(\omega_0 / \pi^2\Omega)$ is proportional to a very large parameter $\rho_0\lambda_s^3 / m_0$. This parameter is equal to the ratio of the mass of atoms $\rho_0\lambda_s^3$ in a three-dimensional cube, whose side is equal to the wavelength of sound λ_s , to the mass of one atom m_0 . It is also proportional

²¹ There is a fundamental possibility of the refutability of this consideration, that is, Popper's criterion is fulfilled.

to the large parameter ω_0 / Ω . In this case, the lifetime of the HF oscillator may be much less than the relaxation time of the LF motion due to sound radiation [IV-3].

Effect of jitter of a potential well. It can also be shown [IV-1, [IV-4] that the account of fast oscillations-jitter (caused by the action of energetic phonons of the medium) of a potential well with frequency ω_s and amplitude b_s , for which inequalities $b_s^2 \omega_s^2 > b^2 \Omega^2$, are valid leads to a decrease in the amplitude of the vector potential A_x and the interaction energy H' , reduces the transition probability by a factor $\exp\{-W/2\} = (1 - b_s^2/b^2)$. In this case, the probability of transition (IV.3) is decreased by $\exp\{-W\}$ times.

Similarly, the presence of a relatively high-frequency phonon spectrum of the environment will affect the transition probability. In the case of a sufficiently wide spectrum of oscillations of the potential well, the decrease in the transition probability $\exp\{-W\} = (1 - b^{-2} \cdot \sum_i b_i^2)$ will be insignificant if the energy conditions $b^2 \Omega^2 \ll \sum_i b_i^2 \omega_i^2$ and deviation amplitudes $b^2 \gg \sum_i b_i^2$ are satisfied.

So, for example, the absorption of ^{57}Fe and ^{119}Sn by the nuclei of gamma rays of 14.4 keV and 23.8 keV, respectively, according to the expression $\omega_0 b/c \approx 2$ leads to atomic oscillations in the potential well of the crystal with ranges (double amplitude) equal to $0,55 \cdot 10^{-8}$ cm. and $0,33 \cdot 10^{-8}$ cm.

The relaxation time of such an oscillatory motion of iron and tin atoms due to sound generation is defined above about 0.1 and 0.01 seconds, respectively, which is many orders of magnitude longer than the lifetime of an excited atomic nucleus. The above estimates of the attenuation of line intensities $\sim \exp\{-W\}$ remain valid even for Debye temperatures (for example, for iron $\theta_D = 467^0 K$, $\omega_{SMAX} \approx k\theta_D / \hbar \approx 10^{14}$, $b^2 \gg \sum_i b_i^2$).

The process of radiation and absorption at the natural frequency of the nucleus ω_0 is largely determined by the presence of a significant number of atoms, oscillating in the potential wells of the crystal, both with excited and non-excited nuclei. The source of atoms with an excited nucleus, which oscillate in a potential well (at a frequency Ω) at the initial moment, is external radiation with a frequency $\omega_0 + \Omega$, the number of quanta of which $G_k^{(+)}$ comes from the outside per unit time. Obviously, regardless of the fact of excitation of the atomic nucleus, which vibrates in a potential well in the presence of an external field, the system of low-energy levels remains the same. In the work [IV-2] it was shown that the number of quanta at the natural frequency ω_0 of the nucleus at the developed stage of the process exceeds the number of quanta at the frequency $\omega_0 + \Omega$ with respect to $(w_{2*1} \cdot n_{10} / \delta_k) > 1$. Here δ_k is the decrement of the field energy absorption by the medium, $w_{2*1} \cdot n_{10}$ is the rate of change in the number of excited nuclei due to the induced absorption of a quantum at a frequency $\omega_0 + \Omega$ by previously quiescent atoms with unexcited nuclei whose equilibrium density is equal to n_{10} .

References to annex IV

IV-1. Kirichok A. V., Kuklin V. M., Zagorodny A. G. On the emission spectrum of oscillator trapped in a potential well. // XII international workshop "Plasma electronics and new acceleration methods" 26-30 August 2013, Kharkov, Ukraine; VANT, 2013, N. 4 (86). – series "Plasma Electronics and New Methods of Acceleration" issue 8. – P. 256–259; On the spectrum of the trapped oscillator in a potential well // Physical basis of device construction. 2013. – V. 2. – № 3, – P. 56–63; arXiv:1701.06223v1 [quant-ph] – 2017.

IV-2. Kuklina O V, Kuklin V M On the relative role of the phonon spectrum and collisional relaxation in the generation and scattering processes // Bulletin of KhNU im. V. N. Karazina. 2009. – No. 846. – 2 (50). – P. 20–28 (in Russian).

IV-3. Qiong Li, D. Z. Xu, and C. Y. Cai Recoil effects of a motional scatterer on single-photon scattering in one dimension. ar Xiv:1303.1287 [quant-ph].

IV-4. Zagorodny A. G., Kuklin V. M. Features of radiation in nonequilibrium media / Problems of theoretical physics. Scientific works / V. A. Buts, A. G. Zagorodny, V. E. Zakharov, V. I. Karas, V. M. Kuklin, A. V. Tur, S. P. Fomin, N. F. Shulga, V. V. Yanovsky; ed. no. V. M. Kuklin. – Kh. : V. N. Karazin Kharkiv National University, 2014. – V. 1 – 532 p. pp. 13–81 (in Russian).

ANNEX V

DENSITY MATRIX AND EQUATIONS OF THE SEMI-CLASSICAL MODEL

Let us consider a density matrix whose elements for a two-level system are (see, for example, [V-1]) $\rho_{aa} + \rho_{bb} = 1$ and $\rho_{ba} = \rho_{ab}^*$, where ρ_{aa} is the relative population of the upper level. For simplicity of description, we shall restrict ourselves to the one-dimensional case. Matrix elements of interaction (dipole approximation) are $\hat{V} = -\vec{d} \cdot \vec{E}$. Let us define d_{ba} as the projection of the dipole moment on the direction of polarization of the electric field and $P = N(d_{ab}\rho_{ba} + d_{ba}\rho_{ab})$ is written as the polarization of N identical molecules, $\Omega = 2d_{ba}A/\hbar$ is the Rabi frequency. The following equations are valid, where spontaneous emission is not taken into account

$$\frac{d}{dt}\rho_{ba} + (i\omega_{ba} + \frac{1}{T_2})\rho_{ba} = -\frac{i}{\hbar}V_{ba}(\rho_{aa} - \rho_{bb}); \quad (V.1)$$

$$\frac{d}{dt}(\rho_{aa} - \rho_{bb}) + \frac{1}{T_1}[(\rho_{aa} - \rho_{bb}) - (\rho_{aa}^0 - \rho_{bb}^0)] = +\frac{2i}{\hbar}(V_{ba}\rho_{ab} - \rho_{ba}V_{ab}); \quad (V.2)$$

$$V_{ba} = V_{ab}^* = -d_{ba}[A(t) \cdot \exp\{-i\omega t\} + A^*(t) \cdot \exp\{i\omega t\}]; \quad (V.3)$$

where $E = A(t) \cdot \exp\{-i\omega t\} + A^*(t) \cdot \exp\{i\omega t\}$

$$\text{Obviously} \quad \frac{dP}{dt} = N(d_{ab} \frac{d}{dt}\rho_{ba} + d_{ba} \frac{d}{dt}\rho_{ab}) \quad (V.4)$$

assuming $\omega_{ab} = -\omega_{ba} = \omega$, $V_{ab}^* = -d_{ab}^* E = V_{ba} = -d_{ba} E$, $\rho_{ab}^* = \rho_{ba}$, $d_{ab}^* = d_{ba}$

let us write (V.1) in the form

$$\frac{d}{dt} \rho_{ba} = -\left(i\omega_{ba} + \frac{1}{T_2}\right) \rho_{ba} - \frac{i}{\hbar} V_{ba} (\rho_{aa} - \rho_{bb}), \quad (V.5)$$

$$\frac{d}{dt} \rho_{ab} = -\left(i\omega_{ab} + \frac{1}{T_2}\right) \rho_{ab} - \frac{i}{\hbar} V_{ab} (\rho_{bb} - \rho_{aa}), \quad (V.6)$$

then

$$\frac{1}{N} \frac{dP}{dt} = d_{ab} \frac{d}{dt} \rho_{ba} + d_{ba} \frac{d}{dt} \rho_{ab} = i\omega(d_{ab} \rho_{ba} - d_{ba} \rho_{ab}) - \frac{1}{T_2} (d_{ab} \rho_{ba} + d_{ba} \rho_{ab}). \quad (V.7)$$

You can use $\gamma_{12} = 1/T_2$ as the width of the spectral line.

Since $-\frac{2i}{\hbar} \langle V_{ba} \rho_{ab} - \rho_{ba} V_{ab} \rangle = \frac{2}{\hbar\omega N} \langle \frac{dP}{dt} E \rangle$ from equation (V.2) we shall obtain

$$\frac{d}{dt} (\rho_{aa} - \rho_{bb}) + \frac{1}{T_1} [(\rho_{aa} - \rho_{bb}) - (\rho_{aa}^0 - \rho_{bb}^0)] = \frac{2}{\hbar\omega N} \langle \frac{dP}{dt} E \rangle \quad (V.8)$$

or if we determine the population inversion $\mu = N(\rho_{aa} - \rho_{bb})$, then (V.8) can be rewritten as it follows:

$$\frac{d\mu}{dt} + \frac{1}{T_1} (\mu - \mu_0) = \frac{2}{\hbar\omega} \langle \frac{dP}{dt} E \rangle. \quad (V.9)$$

Differentiating equation (V.7) we shall obtain

$$\begin{aligned} \frac{d^2 P}{dt^2} &= -i\omega N \frac{d}{dt} (d_{ba} \rho_{ab} - d_{ab} \rho_{ba}) = -i\omega N d_{ba} \left[-\left(i\omega_{ab} + \frac{1}{T_2}\right) \rho_{ab} - \frac{i}{\hbar} V_{ab} (\rho_{bb} - \rho_{aa}) \right] - \\ &- d_{ab} (-i\omega N) \left[-\left(i\omega_{ba} + \frac{1}{T_2}\right) \rho_{ba} - \frac{i}{\hbar} V_{ba} (\rho_{aa} - \rho_{bb}) \right] = \\ &= (-i\omega N) \left[(-i\omega d_{ba} \rho_{ab} - i\omega d_{ab} \rho_{ba}) - \frac{i}{\hbar} V_{ab} d_{ba} (\rho_{bb} - \rho_{aa}) + \frac{i}{\hbar} V_{ba} d_{ab} (\rho_{aa} - \rho_{bb}) \right] = \\ &- \omega^2 P - 2i\omega \left(-\frac{i}{\hbar}\right) N (\rho_{aa} - \rho_{bb}) d_{ba} d_{ab} E, \end{aligned}$$

i. e.

$$\frac{\partial^2 P}{\partial t^2} + \omega^2 P = -2\omega |d_{ab}|^2 E \mu / \hbar, \quad (V.10)$$

If we add the equation

$$\frac{\partial^2 E}{\partial t^2} + \delta \frac{\partial E}{\partial t} - c^2 \frac{\partial^2 E}{\partial x^2} = -4\pi \frac{\partial^2 P}{\partial t^2} \quad (V.11)$$

to (V.9) and (V.10), where δ is the decrement of field absorption in the medium, we shall obtain the equations of the semi classical model (V.9) – (V.11) used in [V-2].

References to annex V

V-1. Zeiger S. G., Klimontovich Yu. L., Landa P. S., Lariontsev E. G., Fradkin E. E. Wave and fluctuation processes in lasers. Moscow: Nauka, – 1974 (in Russian).

V-2. Landa P. S. Self-oscillations in distributed systems. – M.: Science. 1983. – 320 p. (in Russian).

ANNEX VI

CALCULATION OF PARAMETERS OF PULSES OF INDUCED RADIATION

Calculation of pulse parameters of a quantum source [VI-1]. Let us show how the parameters of the pulses of the induced radiation were determined depending on the degree of approach to the threshold (5.8). Let us assume that the total number of states $N = n_1 + n_2 = 10^{12}$, in this case a threshold inversion is $\mu_{0th} = \sqrt{N} = 10^6$. Let us evaluate the transition to a single time scale according to the relation $T = \tau \cdot \mu_0$, where T is the time in each individual case.

The initial values are determined by $M(T = 0) = M_1(T = 0) = 1$ and $N_{inc}(T = 0) = N_{inc} / \mu_0 = 3 \cdot 10^4 / \mu_0$, also $N_c(T = 0) = N_c / \mu_0 = 3 \cdot 10^4 / \mu_0$, in addition $N_1(T = 0) = N_k / \mu_0 = 3 \cdot 10^4 / \mu_0$. The absorption of field energy is taken into account by the value $\theta = \delta / \mu_0$, where δ is the decrement of field absorption in the medium. In the absence of loss or absorption of quantum energy, the calculation results for different values of the initial inversion are presented in Table VI.1. The pulse size and its shape were determined by its half-width [VI-1].

Table VI.1

№	μ_0	N_c	$N_c \cdot \mu_0$ $\times 10^6$	Half width ΔT	Half width ($\Delta \tau = \Delta T / \mu_0$) $\times 10^{-6}$	Rear to Front Ratio $\Delta \tau_2 / \Delta \tau_1$
1	$\sqrt{2} \cdot 10^6$	0.053	0.075	3.352	2.37	1.04
2	$2 \cdot 10^6$	0.083	0.166	4.743	2.37	1.08
3	$\sqrt{10} \cdot 10^6$	0.204	0.645	7.716	2.44	1.55
4	$\sqrt{20} \cdot 10^6$	0.318	1.422	12.46	2.78	2.46
5	$\sqrt{50} \cdot 10^6$	0.415	2.934	27.26	3.85	5.34
6	10^7	0.454	4.540	52.30	5.23	9.88
7	$\sqrt{2} \cdot 10^7$	0.475	6.716	102.5	7.25	17.6
8	$2 \cdot 10^7$	0.487	9.740	202.8	10.1	31.7
9	$\sqrt{10} \cdot 10^7$	0.494	15.62	503.3	15.9	71.4

In case of fixed absorption, corresponding to the values $\delta = 4 \cdot 10^5$, the calculation results are given in Table VI.2.

Table VI.2

No	μ_0	N_c	$N_c \cdot \mu_0$ $\times 10^6$	Half width ΔT	Half width ($\Delta \tau = \Delta T / \mu_0$) $\times 10^{-6}$	Rear to Front Ratio $\Delta \tau_2 / \Delta \tau_1$
1	$\sqrt{2} \cdot 10^6$	0.034	0.048	3.036	2.15	1.28
2	$2 \cdot 10^6$	0.046	0.092	4.554	2.28	1.05
3	$\sqrt{10} \cdot 10^6$	0.12	0.38	6.641	2.1	1.23
4	$\sqrt{20} \cdot 10^6$	0.211	0.94	8.348	1.87	1.63
5	$\sqrt{50} \cdot 10^6$	0.33	2.33	12.396	1.75	2.64
6	10^7	0.382	3.82	17.14	1.71	3.64
7	$\sqrt{2} \cdot 10^7$	0.418	5.91	24.35	1.72	5.14
8	$2 \cdot 10^7$	0.441	8.82	34.28	1.71	7.19
9	$\sqrt{10} \cdot 10^7$	0.462	14.6	54.77	1.73	10.9

Periodic changes in the luminosity of Cepheid stars. As noted above in Section 6, N_2 can describe the generation of induced radiation, for example, in the photosphere of stars, which is a pulse with a certain constant component. In addition, there is a spontaneous incoherent component of the same source. To this radiation, it is necessary to attach the constant radiation of the rest of the heated material of the star, i.e. the total emission of the star takes the form

$$N(\tau) = N_b + N_2(\tau) \tag{VI-1}$$

The value of the constant component N_b (the spontaneous incoherent component of a quantum source and the constant radiation of the rest of the warmed matter of the star) must be added to N_2 . This addition can be estimated by knowing the relation between the maximum and minimum luminosity of a star $k = (N_b + N_{2\max}) / (N_b + N_{2\min})$, on the other hand, the ratio of the maximum and minimum luminosities of a star is $k = L_1 / L_2 = 10^{0.4(m_2 - m_1)}$ [VI-3], here m_1 is the apparent magnitude at the maximum luminosity of the star, m_2 is the minimum luminosity.

Below let us focus on the values of the apparent magnitude obtained from observations. From the known apparent magnitude m , knowing the distance to the star in parsec d , we can calculate the luminosity L :

$$m = M_{lsun} + 5 \lg(d / 10) - 2.5 \lg(L) \tag{VI-2}$$

To compare the luminosities of stars, the absolute magnitude (visible magnitude from a distance of 10 parsecs) $M_l = m - 5 \lg(d / 10)$ is also often used, here d is the distance in parsecs to the star, $d = 273$ for the Cephei delta and $d = 133$ is for the

North Star. Then the luminosity of the star in units of luminosity of the Sun is equal to $L = 10^{0,4(M_{sun} - M)} L_{sun}$, $L_{sun} = 1$, where $M_{I\odot} = 4.77$ is the absolute magnitude of the Sun.

To obtain the dependence of the luminosity of the star on time $L(\tau)$, let us multiply (VI-1) by the coefficient A , i.e.

$$L(\tau) = A \cdot N(\tau) = A \cdot [N_b + N_2(\tau)] \tag{VI-3}$$

where $A = \frac{L_1}{N_b + N_{2\max}} = \frac{L_2}{N_b + N_{2\min}}$.

Table VI.3 shows the calculation results for the Cepheus delta and the North Star. For this, the values of table 6.1 (section 6) from the first and fifth rows are taken.

Table VI.3

Table VI ations	m_1	m_2	k	$N_{2\min}$	$N_{2\max}$	N_{2av}	N_b	A	L_1^*	L_2^*
delta Cepheus	3.48	4.37	2.27	4	20,188	10	8.748	84.507	2445.3	1077.3
Polar star	2.092	2.125	1.031	9.635	10,374	10	14.315	84.412	2084	2021.6

* calculated by the formula (VI-3)

You can make sure that the average value \bar{L} is determined by the ratio

$$\bar{L} = A \cdot (N_{2av} + N_b). \tag{VI-4}$$

Fig. VI.1 a, b shows the time dependence of the number of quanta and the corresponding luminosity of the Cepheus delta and the North Star. The bottom curve is the number of quanta of induced radiation. The upper curve takes into account the constant component of spontaneous emission due to other elements of the radiation source, in addition to the quantum system.

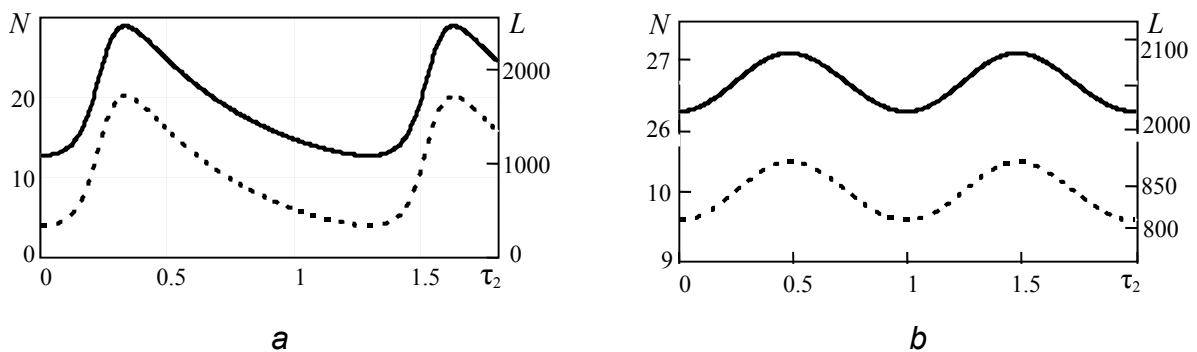


Fig. VI.1. Dependence on time of the relative number of quanta (left scale) and the corresponding luminosity (right scale) of the Cephei delta (a) and the North Star (b)

The lower curve on each fragment represents the number of quanta of induced radiation. The upper curve takes into account the constant component of spontaneous emission due to other elements of the radiation source, in addition to the quantum system.

Figures VI.2 and VI.3 below show the change in the stellar magnitude of the star of the Cepheus delta [VI-4] and the North Star [VI-5] over time. The ordinate shows the values of the apparent magnitude, the abscissa shows time in fractions of the period of change in the brightness of the star.

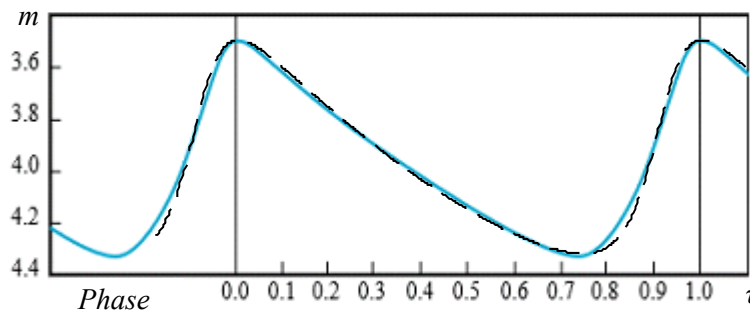


Fig. VI.2. The change in the stellar magnitude of the star of the Cepheus delta over time. (solid curve was obtained in the 1930s by N.F. Florey using a visual photometer) see, for example [VI.-6] and the solution of the equations of system (6.10) – (6.11) in the same variables, when selecting spontaneous emission level and scale (dotted line)

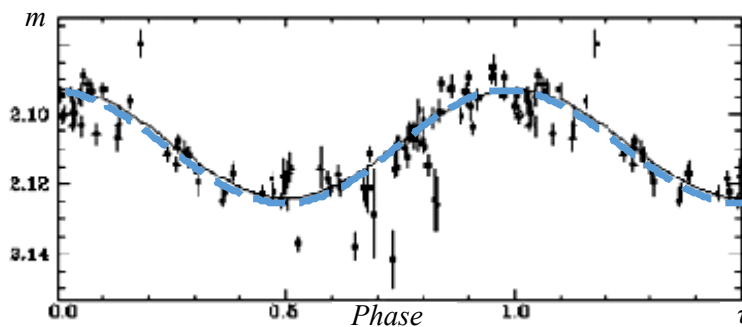


Fig. VI.3. The change in the magnitude of the North Star over time (solid curve) and the solution of the equations of the system (6.10) – (6.11) in the same variables when selecting the level of spontaneous emission and scales (dashed line)

A similar layer with an active medium, which can be described by a quantum two-level system located near equilibrium, can exist in stars and is most likely localized in the photosphere. If there is significant convection in the star atmosphere, conditions can be accomplished to generate pulses of induced radiation. It turns out that the similarity of the obtained solutions with well-known observations of changes in the luminosity of Cepheid stars (Cepheus delta and the North Star) can be seen. In this case, according to table 6.1 the ratio of periods of change in luminosity is also similar (accurate to 2.5 %).

It is important to note that the solutions of equations (6.10) – (6.11) for these two cases are located on the same diagram in Fig. 6.3, which corresponds to one type of object. As well as small amplitude Cepheids (DCEPS) of the North Star type, they belong to the class of classical Cepheids, the brightest representative of which is the Cepheus delta.

References to annex VI

VI-1. On the formation of pulses of coherent radiation in weakly inverted media / Kirichok A. V., Kuklin V. M., Mischin A. V., Pryjmak A. V., Zagorodny A. G. // XII international workshop "Plasma electronics and new acceleration methods" 26-30 August, 2013, Kharkov, Ukraine; VANT, Series "Plasma Electronics and New Methods of Acceleration" 2013. – N. 4 (86). – Issue 8. – P. 267–271.

VI-2. Kirichok A. V., Kuklin V. M., Zagorodny A. G. On the nature of periodically pulsating radiation sources //arXiv preprint arXiv / 1610.04628v1 [quant-ph] – 2016.

VI-3. Rastorguev A. S. Lectures on Galactic Astrophysics
<http://www.astronet.ru/db/msg/1228262> (in Russian).

VI-4. Jim Kaler, Stars and stars of the week. University of Illinois.
<http://stars.astro.illinois.edu/sow/deltacep.html>

VI-5. Jim Kaler, Stars and stars of the week. University of Illinois.
<http://stars.astro.illinois.edu/sow/polaris.html>

VI-6. Samus, N. N. & Durlevich, O. V. (April 2011), GCVS – General Catalog of Variable Stars, Institute of Astronomy of Russian Academy of Sciences and Sternberg State Astronomical Institute of the Moscow State University.

ANNEX VII

EQUATIONS OF TURBULENT WAVE INSTABILITY

Using the results of Section 1, let us obtain a system of equations of turbulent-wave instability similar to (7.2) in a somewhat simplified form for greater clarity. Let us consider the perturbation introduced by an ion-sound wave with an amplitude E_s and frequency $\Omega = Kc_s$, propagating in plasma into the distribution function of the electron beam

$$f_1 = i \frac{eE_s}{m(\Omega - Kv)} \frac{\partial f_0}{\partial v}. \quad (\text{VII.1})$$

If the unperturbed distribution function is Maxwellian $f_b = [n_{b0} / \sqrt{\pi} v_{Tb}] \cdot \exp\{-(v - v_{0b})^2 / v_{Tb}^2\}$, then it is easy to show that $f_1 = (2ieE_s / Kv_0 v_{Tb} m) f_0$, respectively $\partial f_1 / \partial v = (2ieE_s / Kv_0 v_{Tb} m) \cdot \partial f_0 / \partial v$, then equation (2.7) takes the form

$$\partial E_k / \partial t = 2(\gamma_0 - \delta_D) E_k - \frac{i4\gamma_0 e E_s}{Kv_0 v_{Tb} m} \cdot E_k - \frac{e}{Mc_s} E_s \cdot E_k + Q \cdot \left(1 - \frac{i2eE_s}{Kv_0 v_{Tb} m}\right), \quad (\text{VII.2})$$

where the source of spontaneous emission in the absence of a wave is $Q = 2\pi^2 e^2 [\omega^2 / k^3] \cdot f_b$, the increment of beam instability is

$$\gamma = \frac{2\pi^2 e^2 \omega}{mk^2} \frac{\partial f_0(v)}{\partial v} \Big|_{v=\omega/k}, \text{ and the third term on the right-hand side of (VII.2)}$$

is responsible for the drift of the energy of the rf turbulence in the field of the ion-sound wave in the plasma with the velocity $V_i = -ieE_s / M\Omega$, where M is ion mass and $c_s = \sqrt{T_e / M}$ is the speed of sound.

From the equation for perturbations of plasma density in the fields of RF turbulence (see section 20)

$$\frac{\partial^2 n}{\partial t^2} - c_s^2 \frac{\partial^2 n}{\partial x^2} = \frac{1}{16\pi M} \frac{\partial^2 |E|^2}{\partial x^2}, \quad (\text{VII.3})$$

using the relation $n = +en_p E_s / M \cdot c_s$, let us obtain equations for a slow change in the amplitude of the ion-sound wave

$$\frac{\partial E_s}{\partial t} = -\frac{K}{8en_p} \tilde{E}_k, \quad (\text{VII.4})$$

where the energy density is represented as

$$\begin{aligned} E_k &= E_{k0}(t) + \tilde{E}_k \cdot \exp\{-i\Omega t + iKx\} + \tilde{E}_k^* \cdot \exp\{i\Omega t - iKx\} = \\ &= E_0 [W_0(t) + W_1 \cdot \exp\{-i\Omega t + iKx\} + W_1^* \cdot \exp\{i\Omega t - iKx\}]. \end{aligned} \quad (\text{VII.5})$$

The system of equations (VI.2) (VI.4) can be written as

$$\partial W_0 / \partial \tau = -\varepsilon_0 \cdot W_0 + i\alpha(A^* \cdot W_1 - A \cdot W_1^*) - \lambda(A^* \cdot W_1 + A \cdot W_1^*) + q, \quad (\text{VII.6})$$

$$\partial W_1 / \partial \tau = -\varepsilon_0 \cdot W_1 + 2i\alpha A \cdot W_0 - 2\lambda A \cdot W_0, \quad (\text{VII.7})$$

$$\partial A / \partial \tau = -\mu W_1. \quad (\text{VII.8})$$

using the following notation $\tau = \delta_D \cdot t$, $2(\gamma_0 - \delta_D) = -\varepsilon_0 \cdot \delta_D$,
 $A = E_s / |E_s(\tau = 0)|$, $\alpha = 2\gamma_0 e |E_{s0}| / K v_0 v_{Tb} m \delta_D$, $\lambda = e |E_{s0}| / 2 M c_s \delta_D$,
 $q = Q / E_0 \delta_D$, $\mu = K E_0 / 8en_p \delta_D |E_{s0}|$.

Thus, up to certain numerical coefficients it is not difficult to obtain a similar system of equations, describing the interaction of turbulence with an LF wave that can change the degree of deviation from the instability threshold.

ANNEX VIII

SPATIAL AND TEMPORARY DYNAMICS

OF INSTABILITY DURING A THREE-WAVE INTERACTION

The system of equations (7.2), which describes the decay of the pump field into two waves, can be represented as a single equation

$$\left\{ \left(\frac{\partial}{\partial t} + v_1 \frac{\partial}{\partial x} \right) \left(\frac{\partial}{\partial t} + v_2 \frac{\partial}{\partial x} + \delta_2 \right) - \alpha_1 \alpha_2 \right\} A_{1,2} = 0 \quad (\text{VIII.1})$$

To obtain the solution (VIII.1) with some initial conditions in the domain $-\infty < x < \infty$ on the interval $0 < t < \infty$, we shall use the Fourier transforms in the coordinate and the Laplace transform in time

$$A_i(\Omega, K) = \int_0^\infty dt \cdot \exp(i\Omega t) \int_{-\infty}^\infty dx \cdot A_i(t, x) \cdot \exp(-iKx) \quad (\text{VIII.2})$$

To obtain the Fourier component of the wave amplitude, let us use the equation

$$D_L(\Omega, K) \cdot A_i(\Omega, K) = [(\Omega - Kv_1)(\Omega - Kv_2 + iv_2) + \alpha_1 \alpha_2] \cdot A_i(\Omega, K) = A_{i0}(K) \quad (\text{VIII.3})$$

where $A_{i0}(\mathbf{K})$ are the functions determined by the initial conditions:

$$A_{i0}(0, x) = \frac{1}{2\pi} \int_{-\infty}^{\infty} A_{i0}(\mathbf{K}) \cdot \exp(i\mathbf{K}x) \cdot d\mathbf{K} \quad (\text{VIII.4})$$

In this case, in a moving with speed V reference frame ($\xi = x - Vt, t$), $v_2 < V < v_1$ the dispersion equation $D(\Omega, \mathbf{K})$ for perturbations of the form $\sim \exp\{-i\Omega t + i\mathbf{K}\xi\}$ that corresponds to the system of equations (VII.1) under the accepted assumptions will have the following form

$$D(\Omega, \mathbf{K}) = (\Omega - \mathbf{K}v_1 + \mathbf{K}V)(\Omega + \mathbf{K}V - \mathbf{K}v_2 + i\nu_2) + \alpha_1\alpha_2. \quad (\text{VIII.5})$$

Obviously the dispersion equation in a laboratory frame of reference is

$$D(\Omega, \mathbf{K})|_{V=0} = D_L(\Omega, \mathbf{K}). \quad (\text{VIII.6})$$

Performing the inverse transformation, we shall find

$$A_i(t, x) = \frac{1}{(2\pi)^2} \int_{C_\Omega} d\Omega \int_{-\infty}^{\infty} d\mathbf{K} \frac{A_{i0}(\mathbf{K})}{D(\Omega, \mathbf{K})} \exp\{-i\Omega t + i\mathbf{K}\xi\} = \int_{-\infty}^{\infty} d\xi' \cdot G_i(\xi - \xi', t) \cdot A_{i0}(\xi, 0),$$

where $G_i(\xi, t) = \frac{1}{(2\pi)^2} \int_{C_\Omega} d\Omega \int_{-\infty}^{\infty} d\mathbf{K} \frac{\exp\{-i\Omega t + i\mathbf{K}\xi\}}{D(\Omega, \mathbf{K})}$ is the Green's function, the form of which does not depend on the initial conditions, but is determined only by the properties of the system. The integration loop C_Ω is parallel to the axis $\text{Re}\Omega = 0$ and is above all the features of the integrand. Closing it in the lower half-plane Ω we shall get

$$G(\xi, t) = \frac{i}{2\pi} \int_{-\infty}^{\infty} d\mathbf{K} \sum_n \frac{\exp\{-i\Omega_n(\mathbf{K}) \cdot t + i\mathbf{K}\xi\}}{D'_\Omega[\Omega_n(\mathbf{K}), \mathbf{K}]} \quad (\text{VIII.7})$$

where $D'_\Omega[\Omega_n(\mathbf{K}), \mathbf{K}] = \frac{\partial}{\partial \Omega} D(\Omega, \mathbf{K})|_{\Omega=\Omega_n(\mathbf{K})}$ and $\Omega = \Omega_n(\mathbf{K})$ are the roots of the dispersion equation $D(\Omega, \mathbf{K}) = 0$.

If $\text{Im}\Omega_n(\mathbf{K}) < 0$ is for all branches of oscillations, then the system is stable. If $\text{Im}\Omega_n(\mathbf{K}) > 0$ is for any root, then we should expect the development of instability, although the type of instability remains undefined. For the case of the interaction of two waves (VII.1), there are only two roots:

$$\Omega_1 = \sqrt{\alpha_1\alpha_2} \cdot \left[-1 - \theta \frac{v_1 - V}{2V - v_1 - v_2}\right], \quad \Omega_2 = \sqrt{\alpha_1\alpha_2} \cdot \left[-\frac{v_1 - V}{v_1 - v_2} - \frac{1 - \theta}{1 + \theta^2} \cdot \frac{V - v_2}{v_1 - v_2}\right]. \quad (\text{VIII.8})$$

Generally speaking, the integral can be calculated using the residue theorem. To do this, let us supplement the integration loop with an arc of infinitely large radius. For large values of $|K|$, $\Omega_1(\mathbf{K}) \rightarrow \mathbf{K}(v_1 - V)$ and $\Omega_2(\mathbf{K}) \rightarrow \mathbf{K}(v_2 - V)$, it is possible to close the circuit only at $\text{Im}\Omega_n(\mathbf{K}) < 0$. Then $(v_1 - V) > 0$ and $(v_2 - V) > 0$ will have to close the circuit in the lower half-plane, and for $(v_1 - V) < 0$ and $(v_2 - V) < 0$, respectively, in the upper half-plane of the complex variable K . The roots under these conditions are in the inner region covered by the contour. You can make sure

that in any single area there is $\lim_{t \rightarrow \infty} G(\xi_0, t) \rightarrow 0$. That is, under these conditions, absolute instability is not realized.

If $v_2 < V < v_1$, it is impossible to use the residue theorem, because the integral over the arc of a large radius diverges. Therefore, the integral should be calculated in another way, for example, by the saddle-point method.

The perturbation, which is the envelope of the oscillation field, is proportional to $\exp\{-i\Omega_0 t\}$, where Ω_0 is the value of the root of the dispersion equation $D(\Omega, K) = 0$, corresponding to the instability at the point, where the derivative vanishes $\partial\Omega / \partial K$. Pass points determined from the equation

$$\partial\Omega / \partial K \Big|_{D(\Omega, K)=0} = 0 \tag{VIII.9}$$

are also the branch points of the function $\Omega = \Omega_n(K)$, in addition this is a condition for the development of instability under which the group envelope velocity vanishes

$$V_g = \partial\Omega / \partial K \Big|_{D(\Omega, K)=0} = -\left[\frac{\partial D(\Omega, K)}{\partial K}\right] \Big|_{D(\Omega, K)=0} / \left[\frac{\partial D(\Omega, K)}{\partial \Omega}\right] \Big|_{D(\Omega, K)=0} = 0. \tag{VIII.10}$$

ANNEX IX

SPACE-TEMPORAL DEVELOPMENT OF BEAM INSTABILITY IN PLASMA

Let us show that if the V speed of the reference frame we have chosen does not fall into the velocity range $v_g < V < v_0$, at least at a low absorption level, then absolute instability in this reference frame does not occur. An integral of type (VIII.7) can be calculated, using the residue theorem. We shall supplement, as before, the integration contour with an arc of an infinitely large radius. When $|K| \rightarrow \infty$ $\Omega_1(K) \rightarrow K(v_1 - V)$ and $\Omega_2(K) \rightarrow K(v_g - V)$, since you can close the circuit only if $\text{Im}\Omega_n(K) < 0$, then $(v_1 - V) > 0$ and $(v_g - V) > 0$ will close the circuit in the lower half-plane, and when $(v_1 - V) < 0$ and $(v_g - V) < 0$, respectively, in the upper half-plane of the complex variable. The integral in this case is equal to the sum of the residues of the integrand in the region covered by the contour. To find the sum of these residues, let us solve the equations together

$$\frac{\partial}{\partial \Omega} D(\Omega, K) = 0 \quad \text{and} \quad D(\Omega, K) = 0,$$

as a result, we shall find найдем

$$\Omega_n = \frac{i\delta(v_0 - V)}{v_g - v_0} + \gamma_0 \frac{[2(v_g - V) - (v_0 - V)]}{3(v_g - v_0)} \exp\{2\pi ni / 3\}, \tag{IX.1}$$

$$K_n = \frac{i\delta}{v_g - v_0} + \gamma_0 \frac{\exp\{\pi i / 3\}}{3(v_g - v_0)} \exp\{2\pi ni / 3\}. \tag{IX.2}$$

Let us choose from the roots $n = 0; 1; 2$ those ones that are in the inner region. In all cases when $t \rightarrow \infty$, $G(\xi, t) \rightarrow 0$, that is $(v_1 - V)(v_g - V) > 0$, only convective instability can develop.

Obviously $(v_1 - V)(v_g - V) < 0$, using the residue theorem is impossible due to the divergence of an integral of the form (IX.7), which nevertheless can be calculated by the saddle-point method. The envelope of the oscillation field, in case of instability, grows proportionally to $\exp\{-i\Omega_0 t\}$, where Ω_0 is the value of the root of the dispersion equation $D(\Omega, K) = 0$, at the point where the derivative $\partial\Omega / \partial K$ vanishes. Thus, the saddle points (9.7) and (9.8), which ensures the growth of the field, can be determined using equations (9.6) and

$$\partial\Omega / \partial K \Big|_{D(\Omega, K)=0} = 0, \quad (\text{VIII.3})$$

ANNEX X

MULTIMODE INTERACTION OF A NON-RELATIVISTIC ELECTRON BEAM WITH PLASMA

The equation for the description of the process of interaction between a beam and plasma can be represented as

$$\frac{\partial}{\partial t} E + 4\pi\{J_L + J_b\} = 0, \quad (\text{X.1})$$

where J_L is the plasma current linear in the perturbation amplitudes and J_b is the beam current. Since the phase velocity of the beam significantly exceeds the thermal velocity of plasma particles, equation (X.1) can be represented as

$$\begin{aligned} i\omega\varepsilon(pk_{00}v_{b0}, pk_{0b})E_{0p} + \frac{\partial}{\partial\omega}\omega\varepsilon(\omega, k) \Big|_{\substack{\omega=pk_{00}v_{b0} \\ k=pk_{00}}} \left(\frac{\partial}{\partial t} E_{0p} - \delta \cdot E_{0p}\right) = \\ = +4\pi en_{b0} \frac{1}{L} \int_{-L/2}^{L/2} dx_0 v_b \exp\{ipk_{00}(x - v_{b0}t)\} dx, \end{aligned} \quad (\text{X.2})$$

where $\varepsilon(\omega, k) = 1 - \omega_{pe}^2 / \omega^2$ and δ is the linear decrement of absorption of vibrational energy $p = 1, 2, 3 \dots P$, $\omega_{pe}^2 = 4\pi e^2 n_0 / m_{e0}$, n_0 , n_{b0} are unperturbed plasma and beam densities, e is the electron charge, m_{e0} is rest mass, v_b is the beam electron velocity, and at the initial moment the beam is assumed to be monoenergetic $v_b|_{t=0} = v_{b0}$, $p_0 k_{00} v_{0b} = \omega_{pe}$, integration in (X.2) is carried out over initial positions of the beam particles $x|_{t=0} = x_0$. Obviously, here k_{00} is the interval between the modes of the spatial spectrum. The electric field of long-wave perturbations, whose phase velocity coincides with the beam velocity, has the form

$$E = \sum_{p>0} E_{0p} \exp\{-ipk_{00}(x - v_{0b}t)\}, \quad (\text{X.3})$$

where $\varepsilon(pk_{0b}v_{b0}, pk_{00}) = 1 - \omega_{pe}^2 / (pk_{00}v_{b0})^2 = 1 - p_0^2 / p^2$, $\frac{\partial}{\partial \omega} \omega \varepsilon(\omega, k) \Big|_{\substack{\omega=pk_{00}v_{b0} \\ k=pk_{00}}} = 1 + p_0^2 / p^2$.

The equations of motion of particles, simulating a beam can be represented as

$$\frac{dx_b}{dt} = v_b, \quad (\text{X.4})$$

$$\frac{dv_b}{dt} = -\text{Re} \sum_p \frac{eE_{0p}}{m_{e0}} \exp\{-ipk_{00}[x - v_b t]\}. \quad (\text{X.5})$$

Let us also give the total long-wave field excited by the beam, acting on the plasma particles

$$\begin{aligned} E_0 \exp\{i\omega_{pe}t\} &= |E_0| \exp\{i\omega_{pe}t + i\phi_0\} \approx \sum_p E_{0p} \exp\{ipk_{00}v_{0b}t - ipk_{00}x\} \approx \\ &\approx \sum_{p_{\min}}^{p_{\max}} E_{0p} \exp\{ipk_{00}v_{0b}t\} = \sum_{p_{\min}}^{p_{\max}} |E_{0p}| \exp\{ipk_{00}v_{0b}t + i\phi_{0p}\}, \end{aligned} \quad (\text{X.6})$$

where we shall neglect the deviations $pk_{00}\Delta x \sim \Delta x / \lambda_0 \ll 1$, where λ_0 is the characteristic wavelength of the intense Langmuir oscillations excited by the beam, and disturbances whose frequency differs markedly from the Langmuir frequency. The amplitude of the long-wavelength Langmuir oscillations excited by the electron beam turns out to be equal to

$$|E_0| = \sqrt{\left[\sum_{p_{\min}}^{p_{\max}} |E_{0p}| \cdot \text{Cos}\{\phi'_{0p}\} \right]^2 + \left[\sum_{p_{\min}}^{p_{\max}} |E_{0p}| \cdot \text{Sin}\{\phi'_{0p}\} \right]^2}, \quad (\text{X.7})$$

and for the phase ϕ_0 the equation is

$$\begin{aligned} |E_0| \frac{\partial \phi_0}{\partial t} &= \text{Cos}\{\phi_0\} \sum_{p_{\min}}^{p_{\max}} \left[\frac{\partial |E_{0p}|}{\partial t} \text{Sin}\{\phi'_{0p}\} + |E_{0p}| \text{Cos}\{\phi'_{0p}\} \frac{\partial \phi'_{0p}}{\partial t} \right] - \\ &- \text{Sin}\{\phi_0\} \sum_{p_{\min}}^{p_{\max}} \left[\frac{\partial |E_{0p}|}{\partial t} \text{Cos}\{\phi'_{0p}\} - |E_{0p}| \text{Sin}\{\phi'_{0p}\} \frac{\partial \phi'_{0p}}{\partial t} \right], \end{aligned} \quad (\text{X.8})$$

where such expressions are used $\phi'_{0p} = \phi_{0p} + (pk_{00}v_{0b} - \omega_{pe})t$,

$$\text{Cos}\{\phi_0\} = \frac{1}{|E_0|} \sum_{p_{\min}}^{p_{\max}} |E_{0p}| \cdot \text{Cos}\{\phi'_{0p}\}, \quad (\text{X.9})$$

$$\text{Sin}\{\phi_0\} = \frac{1}{|E_0|} \sum_{p_{\min}}^{p_{\max}} |E_{0p}| \cdot \text{Sin}\{\phi'_{0p}\}. \quad (\text{X.10})$$

Neglecting the nonlinearity of the plasma, the system of equations (X.2) – (X.5) describes the excitation by a beam of nonrelativistic electrons of long-wave oscillations.

It can be shown that under these conditions the relation is satisfied, which is the integral of the system of equations (X.2) – (X.5)

$$\sum_p \frac{1}{4\pi R_p} \{ |E_{0p}|^2 - \theta \int_0^t dt' |E_{0p}(t')|^2 \} + m_{e0} v_{0b} n_{b0} \cdot \frac{k_{00}}{2\pi} \int_{-\pi/k_{00}}^{\pi/k_{00}} v_b dx_0 = Const, \quad (X.11)$$

where $\frac{\partial}{2\partial\omega} \omega \varepsilon(\omega, k) \Big|_{\substack{\omega = m k_{00} v_{b0} \\ k = m k_{00}}} = R_p^{-1}$.

ANNEX XI

DISSIPATIVE GENERATION MODE IN A RESONATOR FILLED WITH AN ACTIVE MEDIUM

For local variables E_j , P_j and M_j , truncated equations of the semiclassical description model are valid (see Section 4)

$$\frac{\partial P_j}{\partial \tau} + \Gamma_{12} P_j = -i M_j E_j, \quad (XI.1)$$

$$\frac{\partial M_j}{\partial \tau} = \frac{i}{2} [E_j P_j^* - E_j^* P_j], \quad (XI.2)$$

where $E_j(\tau) = \left(\sqrt{\frac{2}{S}}\right) \cdot |E(\tau)| \cdot \text{Sin} \left\{ 2\pi \frac{j}{S} + \alpha \right\}$, $\frac{1}{2} \sum_{j=1}^S (M_j + M_j^*) = M$.

For the number of field quanta, the equation (conservation law) can be written as

$$\frac{\partial M}{2\partial \tau} + \frac{\partial \langle E(\tau) \rangle^2}{\partial \tau} + 2\Theta \langle E(\tau) \rangle^2 = 0 \quad (XI.3)$$

It should be noted that the case $\Gamma_{12} > 1$ corresponds to low levels of electric field intensity or small values of population inversion. In contrast, with the opposite inequality $\Gamma_{12} < 1$, the radiation intensities and population inversions are very significant.

Let us consider the solutions of the system (XI.1), (XI.2), and (XI.3), using the following notation

$$N(\tau) = \frac{1}{S} \sum N_j(\tau), \quad M(\tau) = \frac{1}{S} \sum M_j(\tau), \quad E_j(\tau) = \sqrt{2N(\tau)} \cdot \text{Sin} \left(2\pi \frac{j}{S} \right). \quad (XI.4)$$

Under the conditions let us set $N(0)=0.001$ $M(0)=1$ $S=100$, $\Gamma_{12} = 0$. In this case, let us discuss the effect of external field energy absorption, for example, due to energy output ($\Theta \neq 0$).

Here the following notation are used: $\mu / \mu_0 = M$, $\Omega_0 = |d_{ab}| \cdot |E_0| / \hbar = |d_{ab}| \cdot [4\pi\omega \cdot \mu_0 / \hbar]^{1/2}$ is the Rabi frequency corresponding to the value

of the amplitude of the electric field $|E_0| = [4\pi\hbar\omega\mu_0]^{1/2}$, $E = E(t)/[4\pi\hbar\omega\mu_0]^{1/2}$, $P = 4\pi\omega P(t)/\Omega_0[4\pi\hbar\omega\mu_0]^{1/2}$, $\tau = \Omega_0 t$, $\Gamma_{12} = \gamma_{12}/\Omega_0$, $\Theta = \delta/\Omega_0$.

Let us imagine the time dependence of N at different absorption levels Θ , and also consider the change in the linear increment of the process $dN/Nd\tau$, as well as the maximum attainable relative field intensity N_{MAX} and the maximum energy flux from the system $\Theta \cdot N_{MAX}$ as functions of Θ , which are responsible for the energy output from the waveguide [XI-1].

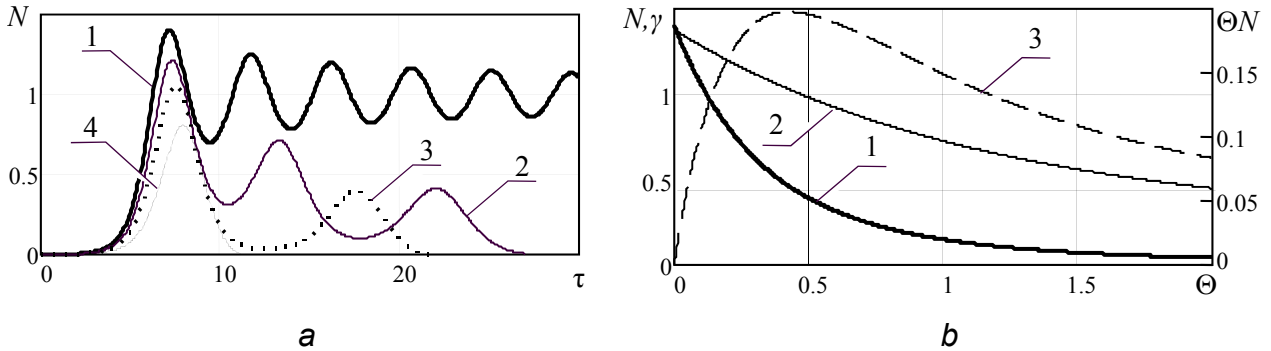


Fig. XI.1. a). Dependence of N on time for different Θ .

1 – $\Theta = 0$; 2 – $\Theta = 0.05$; 3 – $\Theta = 0.1$; 4 – $\Theta = 0.2$; b) Linear increment

of the process is $\gamma = dN/Nd\tau$, maximum achievable field intensity is N_{MAX} , as well as maximum energy flux from the system $\Theta \cdot N_{MAX}$ as a function of Θ . 1 – N_{MAX} ; 2 – γ_{max} ; 3 – $\Theta \cdot N_{MAX}$. In all cases, the line width is negligible $\Gamma_{12}=0.1$

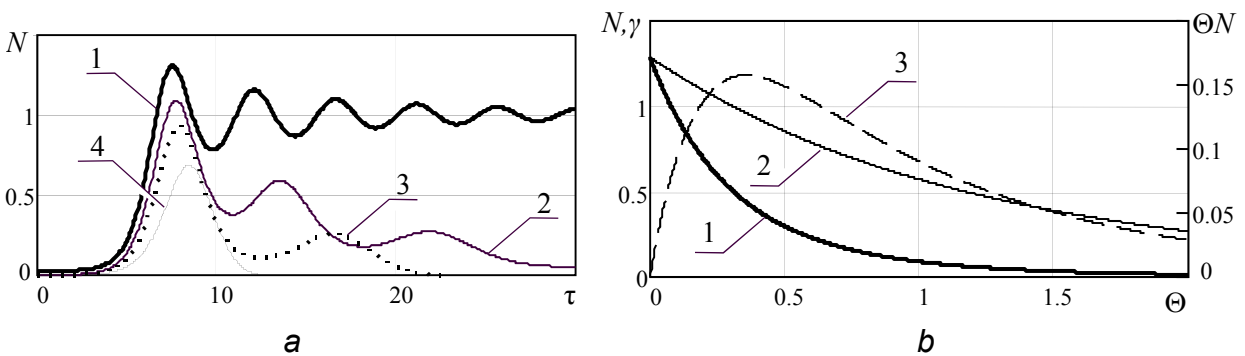


Fig. XI.2. a). Dependence of N on time for different Θ .

1 – $\Theta = 0$; 2 – $\Theta = 0.05$; 3 – $\Theta = 0.1$; 4 – $\Theta = 0.2$; b) Linear increment

of the process is $\gamma = dN/Nd\tau$, maximum achievable field intensity is N_{MAX} , as well as maximum energy flux from the system $\Theta \cdot N_{MAX}$ as a function of Θ . 1 – N_{MAX} ; 2 – γ_{max} ; 3 – $\Theta \cdot N_{MAX}$. In all cases, the line width is defined by expression $\Gamma_{12}=0.1$

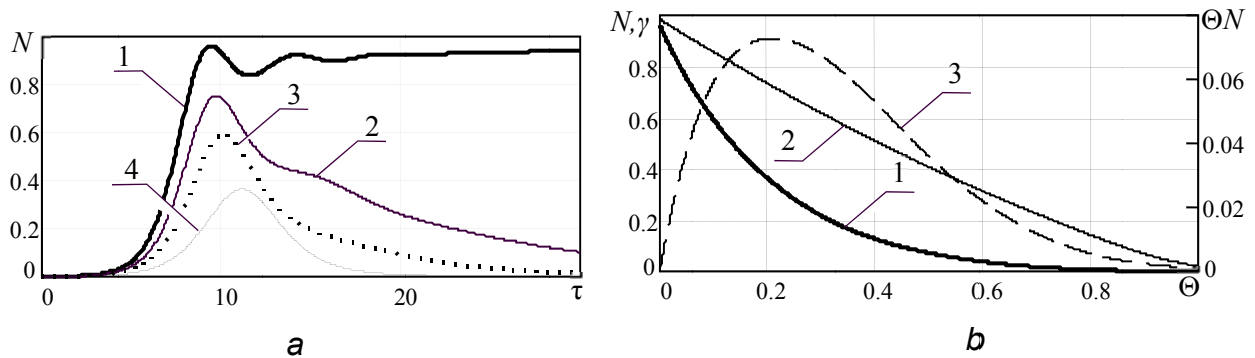


Fig. XI.3. a). Dependence of N on time for different Θ .

1 – $\Theta = 0$; 2 – $\Theta = 0.05$; 3 – $\Theta = 0.1$; 4 – $\Theta = 0.2$; b) Linear increment of the process is $\gamma = dN / Nd\tau$, maximum achievable field intensity is N_{MAX} , as well as maximum energy flux from the system $\Theta \cdot N_{MAX}$ as a function of Θ . 1 – N_{MAX} ; 2 – γ_{max} ; 3 – $\Theta \cdot N_{MAX}$. In all cases, the line width is defined by expression $\Gamma_{12}=0.5$

A feature of the solutions of system (XI.1) – (XI.3) for large values of Θ (when the energy is efficiently removed from the system) is the presence of only one field maximum. It is possible due to a rapid decrease in the inversion level in the waveguide. In fig. XI.4. the diagram of the maximum field amplitude as a function of two variables Θ and Γ_{12} is presented:

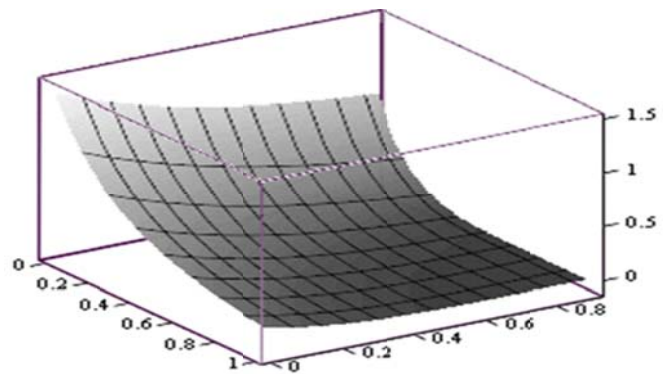


Fig. XI.4. Dependence of N_{max} on Θ and Γ_{12}

References to annex XI

XI-1. Kostenko V. V. Kuklin V. M., Poklonskiy V. M. On generation of a wave package in a waveguide, filled active medium / VANT, 2020. – N 3 (127). – P. 105–109.

ANNEX XII

CAVITONS, FORMED IN THE PLASMA RESONANCE REGION

The phenomenon of electromagnetic field conversion in the region of plasma resonance in the inhomogeneous region at the plasma boundary leads to the transfer of part of the external field energy to short-wave Langmuir oscillations, propagating in the direction of decreasing plasma density [XII-1] – [XII-3]. In this section, let us restrict to the consideration of only one-dimensional case, since we will only be interested in the consequences of the formation of cavitons and their influence on the course of relaxation processes.

It was found in [XII-4] – [XII-7] that the nonlinear damping decrement of electromagnetic oscillations due to absorption of their energy (conversion to other types of oscillations) in the plasma resonance region with an increase in the intensity of the electromagnetic field decreases inversely with its amplitude. As an illustration of this position, let us consider the attenuation of a surface wave at a diffuse boundary of homogeneous plasma (the field of which penetrates into plasma to a depth substantially exceeding the size of the boundary inhomogeneity).

In an inhomogeneous region in the vicinity of plasma resonance, short-wave plasma oscillations are excited, the group velocity of which is directed toward the plasma boundary. This process leads to a partial conversion of the surface wave to plasma oscillations. So, in particular, the linear decrement of oscillations of a surface wave propagating along the blurred plasma boundary – the vacuum due to this conversion, has the form [XII-8, XII-9] (see also [XII-10])

$$\delta_L = (\pi k_z \omega / 4)(d\varepsilon / dx) |_{\omega=\omega_{pe}} \quad (\text{XII.1})$$

In this case, the X axis is oriented along the inhomogeneity of the plasma, and the Z axis lies in the plane parallel to the plasma surface, $\varepsilon = 1 - \omega_{pe}^2(x) / \omega^2$ is the dielectric constant of the plasma. Other designations are generally accepted. The presence of the conversion of an external field or a surface wave field into longitudinal plasma oscillations in the plasma resonance region allows correctly describing the process of field penetration into strongly inhomogeneous plasma with a finite temperature (a linear theory is presented in [XII-11]). The envelope of Langmuir oscillations excited near the plasma resonance obeys the equation [XII-12]:

$$i\partial A / \partial \tau + \partial^2 A / \partial \xi^2 + A |A|^2 = \alpha_N + \alpha_N^{3/2}(\xi - i\sigma), \quad (\text{XII.2})$$

where $\tau = \omega t / 2[\alpha_N (k_D x_D)^{-2/3}]$, $\xi = 2\alpha_N^{-1/2} (k_D x_D)^{2/3} [(2x / x_D) - 1]$, $v_{Te} = T_e / m_{e0}$, $k_D = \omega / \sqrt{6} v_{Te}$, $\sigma = (v_e / \omega \alpha_N^{1/2}) (k_D x_D)^{2/3}$, E_0 is the amplitude of the surface wave.

Let us consider the condition $\alpha_N \ll 1$ to be fulfilled. Let us select the solution in the form of [XII-13.]:

$$A = a_s c h^{-1} \frac{a_s}{\sqrt{2}} (\xi - v\tau) \exp \left\{ i \left(\frac{a_s^2}{2} + \frac{v^2}{2} \right) \tau + \frac{i}{2} v (\xi - v\tau) \right\} \quad (\text{XII.3})$$

This is an exact solution to equation (XII.2), where $\alpha_N = 0$ [XII-14]. Under the conditions $\alpha_N \ll 1$, the inclusion of the right-hand side of (X.2) leads to a slow change in the amplitude a_s and velocity v of the perturbation, similar to how it was done for hydrodynamic solutions [XII -13]. The effect of inhomogeneity on the behavior of the plasma wave field was also previously discussed in [XII-15]

At the initial moment $\tau < [2 / \pi^2 \alpha_N^2]^{1/3}$, there is a linear growth of the caviton “sliding” to the plasma boundary (and an increase in its velocity) $a_s \cong \pi \alpha_N \tau$, $v = -\alpha_N^{3/2} \tau$ which is replaced by an oscillating regime (energy exchange between the caviton and the surface wave field). Dividing the average energy flux of the Langmuir wave by the energy of the surface wave, we shall obtain

$$\delta_{NL} = \delta_L (\alpha_N^{1/2} / 2^{3/2}). \quad (\text{XII.4})$$

That is, the decrement is inversely proportional to the amplitude of the field of the electromagnetic wave. In addition, nonlinear attenuation is less than linear. It should be noted that the use of a stationary description of the behavior of the mean field near the plasma resonance also gives a decrease in energy absorption inversely with the amplitude of the external penetrating radiation [XII-16] – [XII-18].

In case of a nonlinear theory, intense radiation can change the conditions for the penetration of a field into plasma. Penetration into plasma, the density of which n_{e0} slightly exceeds the critical value $n_{ecr} = \omega^2 m_{e0} / 4\pi e^2$, of sufficiently powerful radiation when its amplitude exceeds a certain threshold value [XII-19] can also be accompanied by the formation of cavitons – regions with a reduced plasma density filled with plasma oscillations. A similar problem was also considered later in [XII-20]. It was shown that at sufficiently high intensities of the external field, the forming cavitons periodically arise and move deep into the plasma.

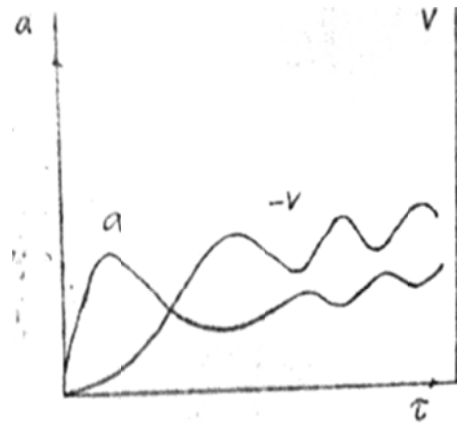


Fig. XII.1. The linear growth of a caviton “sliding” to the plasma boundary is replaced by an exchange of energy between the caviton and the surface wave field

References to annex XII

XII-1. Denisov N. G. On one feature of the field of an electromagnetic wave propagating in an inhomogeneous plasma // ZhETF, 1956. – V. 31. – No. 4. – P. 609–618 (in Russian).

XII-2. Piliya A. D. On the transformation of waves in an inhomogeneous plasma. // ZhTF, 1966. – vol. 36. – No. 5. – C. 818–826 (in Russian).

XII-3. Erokhin N. S., Moiseev S. S. In the book: Questions of the theory of plasma. Issue 7. – M.: Atomizdat, 1973. – P. 146–198 (in Russian).

XII-4. Kondratenko A., N. Kuklin V. M., Tkachenko V. I., Peneva I. Ch. On the change of beam instability nature in the plasma waveguide with diffuse boundaries. Conf. on Surface waves in plasma. Blagoevgrad Bulg., Sept.28 – Oct. 3 1981. Inv. talk and contr. papers. Sofia, 1983. – P. 325–327 (in Russian).

XII-5. Davydova T. A. Parametric instabilities and the formation of cavitons in the vicinity of plasma resonance // Plasma Phys. 1982. – V. 8. – No. 4. – S. 850–856 (in Russian).

XII-6. Taranov V. B. Shamray K. P. Nonlinear saturation of resonant damping of surface waves excited by an electron beam in a semi-bounded plasma // Plasma Physics, 1984. – Vol. 1. – B. 5. – C. 961–967 (in Russian).

XII-7. Taranov V. B., Shamrai K. P. Resonance damping of intense surface wave in a semi – bounded plasma // Plasma Phys. and Contr. Fusion., 1985. – V. 27. – N 8. – P. 925–929.

XII-8. Romanov Yu.A. On the theory of characteristic losses in thin films // ZhETF, 1964. – V.47. – No. 6. – P. 2119–2133 (in Russian).

XII-9. Stepanov K. N. On the influence of plasma resonance on the propagation of surface waves in an inhomogeneous plasma // *ZhTF*, 1965. – V. 35. – No. 6. – P. 1002–1014 (in Russian).

XII-10. Kondratenko A.N. Surface and bulk waves in confined plasma. – M. : Energoatomizdat, 1985. – 320 s. (in Russian).

XII-11. Kondratenko A. N., Kuklin V. M. On the question of effective boundary conditions in a hot plasma with a diffuse boundary // *Radiotekhnika i Elektronika*, 1981. – V. 26. – No. 8. – P. 1708–1709 (in Russian).

XII-12. Morales G. I., Lee Y. C. Generation of density cavities and localized electric fields in a nonuniform plasmas // *Phys. Fluids*, 1977. – V. 20. – N 7. – P. 1135–1147.

XII-13. Andronov A. A., Fabrikant A. L. Landau damping, wind waves and whistle. – in the book: *Nonlinear waves*. M., Nauka, 1979. – P. 63–104 (in Russian).

XII-14. Chen H. H., Liu C. S. Langmuir solitons and resonance absorption in laser irradiated plasmas // *Plasma Physics*, Edited by H. Whihelmsson, N.Y. – 1977.

XII-15. Guildenburg V. B., Fraiman G. M. Deformation of the plasma resonance region in a strong electromagnetic field. *ZhETF*, 1975. – V. 69. – No. 5 (11). – P. 1601–1606 (in Russian).

XII-16. Gildenburg V. B., Litvak A. S., Fraiman G. M. Deformation of the density profile and the efficiency of resonant absorption of laser radiation in an inhomogeneous plasma // *JETP Letters*, 1978. – V. 28 – P. 433–436.

XII-17. Gildenburg V. B. Plasma density jump in the field of a strong electromagnetic wave and its influence on the efficiency of resonant absorption // in collection of papers. works "Interaction of strong electromagnetic waves with collisionless plasma" Gorky, 1980. – P. 51–83 (in Russian).

XII-18. Karpman V. I. *Nonlinear waves in dispersive media*. – Moscow: Nauka, 1973. – 175 p. (in Russian).

XII-19. Reztsov A. S. Penetration of a powerful electromagnetic wave into a plasma // *Sov. Plasma Phys.* 1986. – T. 12, B. 4. – P. 496–499 (in Russian).

ANNEX XIII

ATTENUATION OF A WAVE PACKAGE IN A RESONATOR FILLED WITH AN ACTIVE MEDIUM

Let us consider attenuation processes of wave packets of finite amplitude in bounded systems that impose a possible set of wavelengths of such packets and form the spatial field structure in waveguides. The waveguide is filled with an active two-level medium (a system of dipoles). For description it is possible to use a semiclassical model of the interaction of the field and particles (see, for example, [XIII-1]).

In this case, the quantum-mechanical description of the medium is combined with the classical representation of the field. In this approach, the Rabi frequency plays an important role, which determines the probabilities of induced radiation or absorption of field quanta [XIII-2, XIII-3] and the oscillatory change in population inversion (nutaton). Depending on the relation between the values of the Rabi frequency $\Omega = |d_{ab}| |E(t)| / \hbar$ (where d_{ab} and E are the dipole moment of the

particle and the amplitude of the electric field, respectively) and the line width γ_{12} of the wave packet, the process can change the nature of the field behavior. Here, the line width is inversely proportional to the lifetime of states (the lifetime of energy levels), which is due to relaxation processes.

For local variables E_j , P_j and M_j the truncated equations of the semiclassical description model are valid (see Section 4)

$$\frac{\partial P_j}{\partial \tau} + \Gamma_{12} P_j = -i M_j E_j, \quad (\text{XIII.1})$$

$$\frac{\partial M_j}{\partial \tau} = \frac{i}{2} [E_j P_j^* - E_j^* P_j], \quad (\text{XIII.2})$$

where $E_j(\tau) = \left(\sqrt{\frac{2}{S}}\right) \cdot |E(\tau)| \cdot \text{Sin}\left\{2\pi \frac{j}{S} + \alpha\right\}$, $\frac{1}{2} \sum_{j=1}^S (M_j + M_j^*) = M$.

For the number of field quanta, one can write the equation (conservation law)

$$\frac{\partial M}{2\partial \tau} + \frac{\partial \langle E(\tau) \rangle^2}{\partial \tau} + 2\Theta \langle E(\tau) \rangle^2 = 0 \quad (\text{XIII.3})$$

Let us recall that the case $\Gamma_{12} > 1$ corresponds to low levels of electric field intensity or small values of population inversion. In contrast, with the opposite inequality $\Gamma_{12} < 1$, the radiation intensities and population inversions are very significant. Let us consider the solutions of the system (XIII.1), (XIII.2), (XIII.3) using the following notation:

$\mu / \mu_0 = M$, $\Omega_0 = |d_{ab}| \cdot |E_0| / \hbar = |d_{ab}| \cdot [4\pi\omega \cdot \mu_0 / \hbar]^{1/2}$ is Rabi frequency corresponding to the value of the amplitude of the electric field $|E_0| = [4\pi\hbar\omega\mu_0]^{1/2}$, $E = E(t) / [4\pi\hbar\omega\mu_0]^{1/2}$, $P = 4\pi\omega P(t) / \Omega_0 [4\pi\hbar\omega\mu_0]^{1/2}$, $\tau = \Omega_0 t$, $\Gamma_{12} = \gamma_{12} / \Omega_0$, and

$$N(\tau) = \frac{1}{S} \sum N_j(\tau), \quad M(\tau) = \frac{1}{S} \sum M_j(\tau), \quad E_j(\tau) = \sqrt{2N(\tau)} \cdot \text{Sin}\left(2\pi \frac{j}{S}\right). \quad (\text{XIII.4})$$

Let us discuss the effect of line width Γ_{12} on the nature of wave absorption by active particles. External mechanisms of energy absorption will not be considered ([XIII-4]).

Results of numerical simulation. Let us use equations (XIII.1) – (XIII.4) for calculations. Below, the initial conditions $N_0 = 1.45$, $M_0 = -1$, $S = 100$, $\Theta = 0$ are used. Attention should be paid to the oscillations caused by the interference of the processes of induced radiation and absorption of field quanta in different parts of the waveguide (see Fig. XIII 1.). The nature of this phenomenon was discussed in Section 5 (see also[XIII-4])

The population inversion oscillation frequency corresponds to the Rabi frequency and is proportional to the electric field in this local region. It turns out in our case with different line widths over time $N \rightarrow 0.95$, In this case $M \rightarrow 0$.

With an increase in the line width, the field intensity oscillations (the number of quanta) and population inversions weaken (see Fig. XIII 2.)

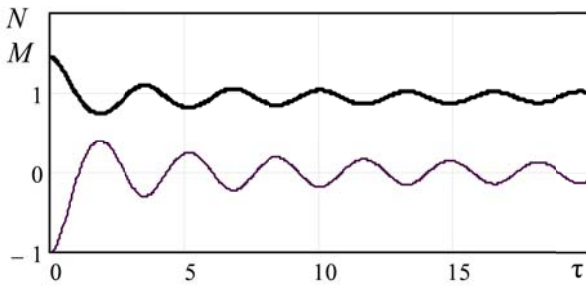


Fig. XIII.1. The behavior of the relative number of quanta (bold line) and relative population inversion (thin line) over time with a negligible line width $\Gamma_{12} = 0$

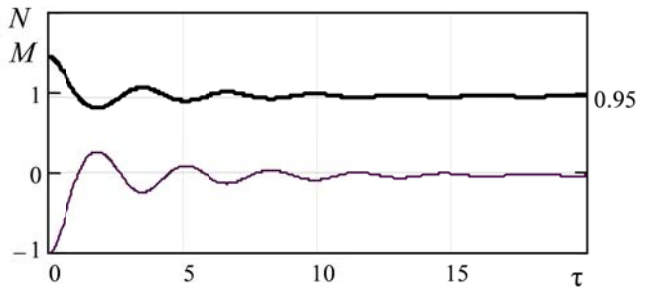


Fig. XIII.2. The behavior of the relative number of quanta (bold line) and relative population inversion (thin line) over time with a small line width $\Gamma_{12} = 0.25$

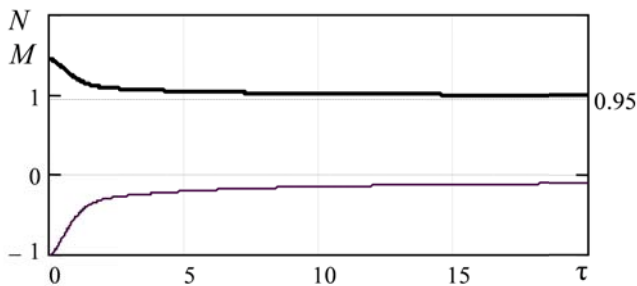


Fig. XIII.3. The behavior of the relative number of quanta (bold line) and the relative population inversion (thin line) over time with the line width $\Gamma_{12} = 3$

In case of a sufficiently large line width, the regime for changing the field intensity (number of quanta) and population inversion becomes monotonic (see Fig. XIII-3.)

This monotonic change in the number of quanta and the population inversion of a two-level system in the presence of an electric field is characteristic of the case of the description of the process by balanced equations. It is important to note that the finite

width of the wave packet is able to suppress the interference of population inversion sections oscillating with different local Rabi frequencies in the field of a standing waveguide wave.

References to annex XIII

XIII-1. Landa P. S. Self-oscillations in distributed systems. -- M. : Science. 1983 (in Russian).

XIII-2. Davydov A. S. Quantum Mechanics Fizmatgiz. 1963. – 748 p. (in Russian).

XIII-3. Allen L., Eberly J. Optical resonance and two-level atoms. Wiley-Interscience Publication John Wiley and Sons. New York – London – Sydney – Toronto. 1975. -- 222 p.

XIII-4. Kuklin V. M, E V. Poklonskiy E. V., Sevidov S. M, On the attenuation of a wave packet in limited systems filled with an active medium and plasma / East Eur. J. Phys. 1. 37--46 (2020) DOI:10.26565/2312-4334-2020-1-02.

ANNEX XIV

ATTENUATION OF A WAVE PACKAGE IN A RESONATOR FILLED WITH NON-ISOTHERMAL PLASMA

The line width of the wave packet can be defined as result of dissipative processes (in a quantum system this is the reciprocal of the lifetime of energy levels) or as consequence of reactive processes of wave packet formation (in classical waveguide systems this is the spectral width of the packet).

When considering the field damping in plasma (Landau damping by electrons), the role of population inversion is taken by the quantity $\mu = n_2 - n_1 = f(v_0 + \hbar k / m) - f(v_0) = (\hbar k / m) \cdot \partial f(v) / \partial v|_{v=v_0}$, where $f(v)$ is the velocity distribution function of electrons, n_2, n_1 are the number of electrons whose velocity is less or greater than the phase velocity of the wave [XIV-1, XIV-2]. In this case, it is the final spectral width of the wave packet that can affect the character of the velocity distribution of particles. With a large packet width, as is well known from [XIV-3], the so-called quasilinear relaxation process can be observed, which leads to the formation of a "plateau" on the particle distribution function in the velocity space.

By the way, here the role of the Rabi frequency is played by the oscillation frequency of the trapped particles in the potential well of the field $\Omega_{tr} = \sqrt{ekE / m_e}$ (here e, m_e are the charge and mass of the electron, and k is the wave number of oscillations, $v_{ph} = \omega / k$ is the phase velocity of the wave). If the spectral width of the packet is small $\Delta k \cdot v_{ph} \approx \Delta \omega \ll \Omega_{tr}$, the process of wave attenuation acquires a characteristic oscillatory form, associated with the exchange of energy between the wave and plasma electrons captured by its field. In the case of the reverse inequality, an almost monotonous character of the field attenuation is observed with the formation of a characteristic "plateau" in the vicinity of the phase velocity of the wave on the electron velocity distribution function, corresponding to the state with zero population inversion in this case presented in the form $\mu = (\hbar k / m) \cdot \partial f(v) / \partial v|_{v=v_0} = 0$.

Let us consider the process of attenuation of plasma (Langmuir) waves on plasma electrons. Electrons effectively interact with the wave, moving at a speed V close to the phase velocity of the wave packet. For simplicity, let us restrict ourselves to the one-dimensional case [XIV-4] (see also [XIV-5]). It follows from the materials of Section 2 that the complex equation for the field, which describes the process of induced absorption of the plasma wave field by plasma electrons, can be written as

$$\frac{\partial(\omega \varepsilon)}{\partial \omega} \frac{\partial E_n}{\partial t} + i\omega \varepsilon \cdot E_n = \frac{4\pi e \omega}{k} \frac{\partial f}{\partial v} \Big|_0 \cdot \int_{-\pi/k}^{\pi/k} d\xi_0 \int_{-v_m}^{v_m} v_0 dv_0 \exp(ik_n \xi + i\varphi_n) \quad (\text{XIV.1})$$

where $\xi = x - v_0 t$, $\Delta v = v - v_0$, $n_{b0} = \int f_0(v) dv$, $\Delta v_m \propto 6\pi |\gamma| / k_0$, and the initial conditions are

$$\xi_0 = \xi(t=0) \subset (-\pi / k_0, \pi / k_0) \quad \text{и} \quad \Delta v_0 = \Delta v(t=0) \subset (-\Delta v_m, \Delta v_m).$$

Results of numerical simulation [XIV.6]. For calculations, let us use the equations already for the wave packet

$$\frac{\partial A_n}{\partial \tau} + i(n - n_0)A_n = -8\pi \int_{-0.5}^{0.5} d\xi \int_{-\eta}^{+\eta} d\eta \cdot \eta \cdot \exp\{-2\pi n i \xi\} \quad (\text{XIV.2})$$

$$2\pi \cdot \frac{\partial^2 \xi}{\partial \tau^2} = -\text{Re} \left[\sum_3^6 A_n \cdot \exp\{2n\pi i \xi\} \right] \quad (\text{XIV.3})$$

where the modes of the wave packet are $A_n = |A_n| \exp\{i\varphi_n\}$, the main wave is $n_0 = 5$, the satellites are $n = 3; 4; 6; 7$, under the following initial conditions: $A_5 = 1.0$ – the amplitude of the main wave, the amplitudes of the satellites are $A_3 = A_7 = 0.2$; $A_4 = A_6 = 0.7$, and the number of particles is 5000, $\xi \in (0, 1)$

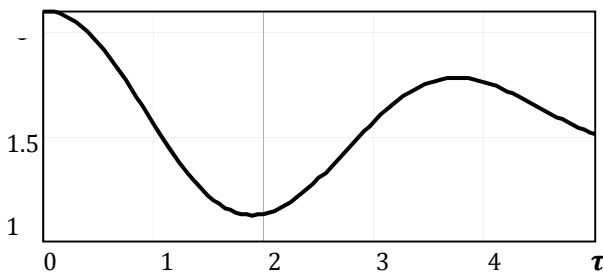


Fig. XIV.1. The behavior over time and intensity of wave I in a single mode

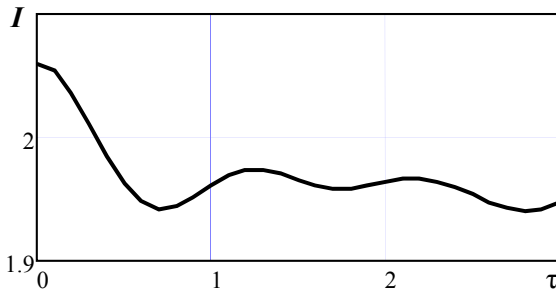


Fig. XIV.2. The behavior of the intensity of wave I over time for the wave packet

and $\eta = \frac{1}{2\pi} \cdot \frac{d\xi}{d\tau}$, $\xi = \frac{kx}{2\pi}$.

Let us study the behavior of the wave packet in time by changing the sum of the squares of the modules of all amplitudes $|A_n|^2$. This value

determines the intensity $I = \sum_{n=3}^7 |A_n|^2$

of the resulting wave of our package. In the single-mode mode (the case of a narrow line width of the wave packet – one mode is $n_0 = 5$), oscillation of the wave intensity is observed. This initial wave attenuation mode is known as Landau attenuation. In the design scheme, the intensity of the monochromatic wave is $I = |A_5|^2$. In the deve-

loped regime, the process acquires a nonlinear character with weakly damped field oscillations (see Fig. XIV. 4).

For the packet ($A_3 = A_7 = 0.2$; $A_5 = 1.0$; $A_4 = A_6 = 0.7$), a decrease in the intensity of the wave packet is observed, associated with the energy exchange between the field and the plasma electrons captured by the wave (see Fig. XIV.2).

The electron distribution function in the vicinity of the phase wave velocity $f(\eta)$ for different time instants for wave packets with different line widths is presented below. In the single mode, the distribution function changes strongly during oscillations of the wave amplitude (see Fig. XIV.3).

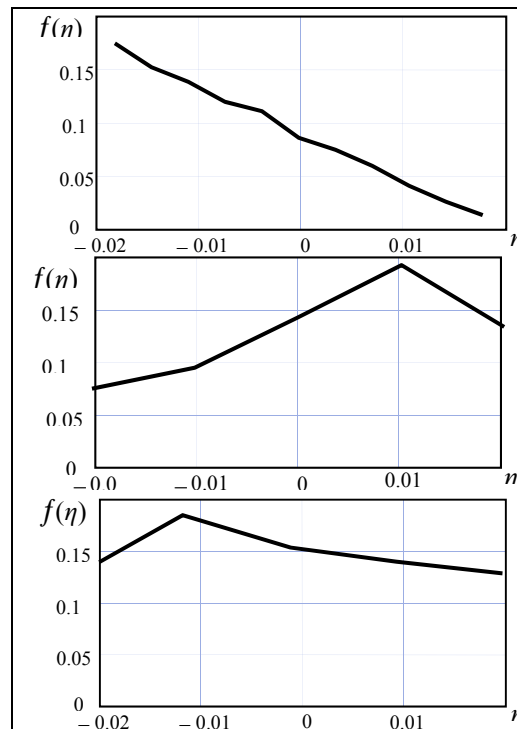


Fig. XIV.3. The electron distribution function in the vicinity of the wave phase velocity $f(\eta)$ for time instants $\tau = 0; 3; 4$ in single mode

Attenuation of the packet leads to the formation of a stable state of the electron velocity distribution function with a practically zero velocity derivative near the phase velocity of the packet (see Fig. XIV.4)

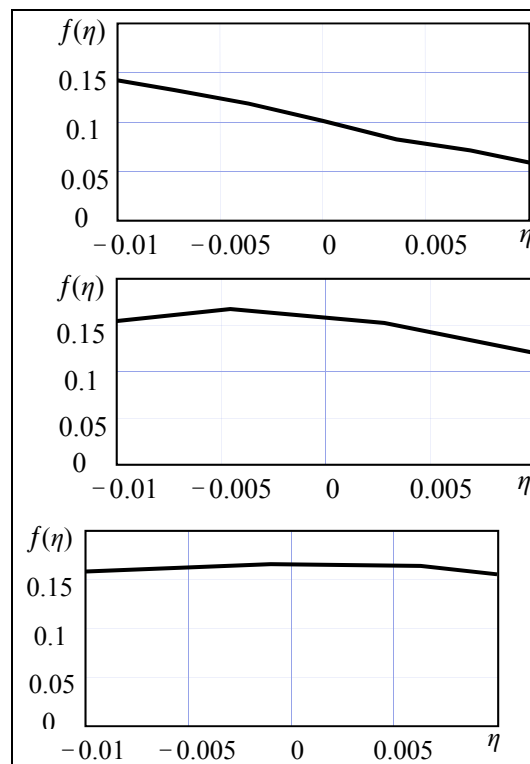


Fig. XIV.4. The distribution function of electrons in the vicinity of the phase velocity of the wave for time instants $\tau = 0; 2; 5$ in case of attenuation of the wave packet

In case of a small spectral width of the packet $\Delta k \cdot v_{ph} \approx \Delta \omega \ll \Omega_{tr}$, the process of wave attenuation acquires a characteristic oscillatory form associated with the exchange of energy between the wave and plasma electrons captured by its field. In the case of the reverse inequality, the field attenuation is monotonous with the formation of a characteristic “plateau” in the vicinity of the phase velocity of the wave on the electron velocity distribution function corresponding to the state with zero population inversion, which is presented in this case $\mu = (\hbar k / m) \cdot \partial f(v) / \partial v|_{v=v_0} = 0$.

References to annex XIV

XIV.1. Andronov A. A. On the issue of attenuation and growth of plasma waves // Izv. Universities. Radiophysics, 1961. -- V. 4. -- No. 5. -- P. 861--866 (in Russian).

XIV.2. Kondratenko A. N., Kuklin V. M. Fundamentals of Plasma Electronics. – M. : Energoatomizdat, 1988. -- 320 p. (in Russian).

XIV.3. Akhiezer A. I. Plasma Electrodynamics. / A. I. Akhiezer, I. A. Akhiezer, A. G. Sitenko, K. M. Stepanov, R. V. Polovin. N.-Y.: Pergamon, 1975. -- 431p.

XIV.4. Landau L. D. On oscillations of electron plasma // JETP, 1946. – vol 16. – V. 7. -- P. 574--586 (in Russian).

XIV.5. Rukhadze A. A., Silin V. P. The way of creating physical concepts of plasma without collisions // Problems of Theoretical Physics. Scientific works. Issue 2 / V. A. Butz, A. G. Zagorodniy, A. V. Kirichok, V. M. Kontorovich, V. M. Kuklin, A. A. Rukhadze, V. P. Silin, A. V. Tur, V. V. Yanovskiy; under the general editorship of A. G. Zagorodny, N. F. Shulga, edit. V. M. Kuklin – Kh. : V. N. Karazin Kharkiv National University, 2016. – Issue. 2 -- 376 p. (in Russian).

XIV.6. Kuklin V. M, E V. Poklonskiy E. V., Sevidov S. M, On the attenuation of a wave packet in limited systems filled with an active medium and plasma / East Eur. J. Phys. N.1. 37--46 (2020) DOI: 10.26565 / 2312-4334-2020-1-02.

ANNEX XV

WAKE FIELD OF AN ELECTRON BUNCH, MOVING IN PLASMA

To obtain the wake field of a bunch, we needed to find the wake field of an individual particle. It is important to note that if we consider an infinite periodic arrangement of individual particles, as it is often done, and then increase the period indefinitely, the transition to the wake field of an individual particle of a bunch will be difficult. Let us draw attention to the fact that in the periodic system the field is present both in front and behind an individual particle. As for a single particle, the radiation field in front of it in the direction of its motion is absent.

To obtain the correct result, a different method of calculating the wake field of an individual particle is needed. Let us imagine the charge density of an electron moving with speed $v > 0$ in the following form $\rho = -e \cdot \delta(-v \cdot t + x - s) = -e \cdot \delta(\xi - s)$. We shall use the Poisson equation $\partial D / \partial x = \partial \hat{\epsilon} E / \partial x = 4\pi\rho$, which we can write in the Fourier representation in the form [XV-1]

$$-ik \epsilon(\omega, k) \cdot E(\omega, k) = 4\pi\rho(\omega, k) \quad (XV.1)$$

Performing the inverse transformation of the left side of the equation, we shall obtain

$$-i \int_{-\infty}^{\infty} \exp\{-ik\xi\} \cdot dk \cdot [k \cdot \varepsilon(k) \cdot E(k)] = k_0 \cdot \frac{\partial \varepsilon(k)}{\partial k} \Big|_{k_0} \cdot \frac{\partial E(\xi)}{\partial \xi} \cdot \exp\{-ik_0\xi\}. \quad (\text{XV.2})$$

Here we took advantage of the fact that the wave packet is located in the space of wave vectors near k , and then $d(k_0 + K) = dK$, in addition

$E(\xi) = \int_{-\infty}^{\infty} \exp\{-iK\xi\} \cdot dK \cdot E(K)$ is the amplitude of the electric field strength slowly varying in space. Let us also use the fact that the equation $\varepsilon(\omega, k) = \varepsilon(kv, k) = \varepsilon(k) = 1 - \omega_{pe}^2 / k v (kv + i\nu) = 0$ has the roots $k_{1,2}v = k_0v = \pm \omega_{pe} - i\nu/2$ in the moving frame of reference. The Poisson equation in this case takes the form:

$$(\partial E(\xi) / \partial \xi) \cdot \exp\{-ik_0\xi\} = -4\pi e \cdot \{k_0 \cdot \partial \varepsilon(k) / \partial k \Big|_{k_0}\}^{-1} \cdot \delta(\xi - s), \quad (\text{XV.3})$$

moreover, in this case the relation $k_0 \cdot \partial \varepsilon(k) / \partial k \Big|_{k_0} = \partial \omega \varepsilon(\omega) / \partial \omega \Big|_{\omega=k_0v}$ holds. Note that it was not necessary to transform the right-hand side of (XV.1) at all. For further transformation of equation (XV.3), he will use the representation $\delta(x) = d\theta(x) / dx$, where $\theta(x)$ is the symmetric unit function, which is equal to zero at $x < 0$, and is equal to unity at $x > 0$. Given the presence of the delta function, equation (XV.3) can be represented as

$$\partial E(\xi) / \partial \xi = \alpha \cdot \delta(\xi - s), \quad (\text{XV.4})$$

where $\alpha = -4\pi e \cdot \{k_0 \cdot \partial \varepsilon(k) / \partial k \Big|_{k_0}\}^{-1} \cdot \exp\{ik_0s\}$. We are looking for a solution in the form $E = C + \alpha \cdot \theta(\xi - s)$, where C is the indefinite constant. Since the field strength has the form

$$E(\xi) \cdot \exp\{-ik_0\xi\} = [C + \alpha \cdot \theta(\xi - s)] \cdot \exp\{-ik_0\xi\}, \quad (\text{XV.5})$$

then in the region of large values $\xi > 0$ the expression tends to infinity, which is unacceptable. Therefore, you should choose $C = -\alpha$. Thus, the final field strength of the wake of a particle moving in the positive direction is

$$E(\xi) = -4\pi e \cdot \{k_0 \cdot \partial \varepsilon(k) / \partial k \Big|_{k_0}\}^{-1} \cdot \theta(s - \xi) \cdot \exp\{ik_0(s - \xi)\}. \quad (\text{XV.6})$$

It is not difficult to see that, with appropriate normalization, the sum of such spontaneous fields of particles is represented by expression (12.3).

On the applicability of the description. It is important to note that the field (XI.6) describes the total field of an individual particle in plasma. That is, the Coulomb field of a previously resting particle during its motion was transformed precisely into this field. Therefore, summing up all such fields of the bunch particles, we obtain the total bunch field, which can be represented as the sum of the field, accompanying the bunch and the radiation field lagging behind the bunch [XV-2]. It is the accompanying field – this is the eigenfield of the bunch or the inverse Coulomb field of the bunch – that focuses the bunch. Equation (XV.4) is obtained for a uniformly moving charge.

More rigorous calculations [XI-3] make it possible to obtain a similar formula for the charge field with an arbitrary law of motion $t = t_L(x)$:

$$E = E_0 \theta[t - t_L(x)] \exp[i\omega_p(t - t_L(x))]. \quad (\text{XV.7})$$

Here is the so-called Lagrangian time, i.e. the time of particle arrival at a point (in the laboratory reference frame). Expression (XV.7) has a transparent physical meaning: a particle flying through a point excites a longitudinal field with amplitude. Subsequently, the field at this point of the cold plasma oscillates with the plasma frequency and does not depend on the subsequent evolution of the particle. It is important to emphasize that the phase of the field created by the charge at a point depends only on the difference between the current time and the time of flight of the charge through this point. In the case of uniform motion of the charge, expressions (XV.6) and (XV.7) are equivalent, since , where and are the current coordinate of the particle in the laboratory frame of reference and the frame of reference associated with the particle, respectively. From this it is easy to obtain an estimate of the applicability of expression (XV.6) to use it in a self-consistent model of excitation of a wake field by a bunch, taking into account the uneven motion of the particles of the bunch due to the influence of a self-consistent field:

$$\frac{\varphi_t - \varphi_x}{2\pi} = \frac{\varphi_x}{2\pi} \left[\frac{v_0}{v(t,x)} - 1 \right] = \frac{\varphi_x}{2\pi} \left[1 - \frac{\bar{v}(t,x)}{v_0} \right] \approx \frac{\varphi_t}{2\pi} \frac{\Delta v}{v} \ll 1, \quad (\text{XV.8})$$

where $\varphi_t = \omega_p(t - t_L(x))$, $\varphi_x = k_0(x(t) - x)$, $\bar{v}(t,x) = (x(t) - x)/(t - t_L(x))$, and $\Delta v(x,t)$ are the average velocity and variation of the particle velocity in the region $[x, x(t)]$, respectively. Thus, the equation for the field (XV.6) and the resulting model (11.2) – (11.3) have certain limitations. The applicability of these equations is limited by the spatial (or time) domain in which the velocity variation is negligible compared to the initial velocity of the bunch (in most applications it can be considered close to the speed of light). Let us clarify the limits of applicability of model (12.2) – (12.3) in the dimensionless units we have adopted. We will proceed from a more rigorous model [XV-3.], using Lagrangian time. The equation for the Lagrangian time has the form in the above notation:

$$\frac{d\tau_{L\alpha}(\xi)}{d\xi} = \frac{\Delta}{1 + \Delta \cdot v_{L\alpha}(\xi)}, \quad (\text{XV.9})$$

to which the equation of motion should be added:

$$\left(\frac{1 + \Delta \cdot v_{L\alpha}}{\Delta} \right) \frac{dv_{L\alpha}(\xi)}{d\xi} = E(\xi, \tau) \quad (\text{XV.10})$$

and the equation for the field

$$E(\xi, \tau) = -\frac{2}{N} \sum_{\alpha}^N f_{\alpha} \cos[\tilde{\omega}_p(\tau - \tau_{L\alpha}(\xi))] \cdot \Theta(\tau - \tau_{L\alpha}(\xi)). \quad (\text{XV.11})$$

Here $\tau_{L\alpha}(\xi)$ is the time when the particle with the number α passes through the point ξ , $v_{L\alpha}(\xi)$ is its speed at this moment. Integrating equation (XV.9) in the ξ interval $[\xi, \xi_{\alpha}]$, we shall obtain:

$$\tau_{L\alpha}(\xi) = \tau - \Delta \cdot \int_{\xi}^{\xi_{\alpha}} \frac{d\xi}{1 + \Delta \cdot v_{L\alpha}(\xi)}. \quad (\text{XV.12})$$

To close this equation, we need to know $v_{L\alpha}(\xi)$. Considering that in a laboratory reference system a particle travels very quickly over a distance $[\xi, \xi_{\alpha}]$ (with a speed of about Δ^{-1}), it can be assumed that in this interval its velocity varies slightly and, therefore, the value $v_{L\alpha}(\xi)$ can be expanded in a series with $\xi_{\alpha} - \xi$ respect to the current position of the particle:

$$v_{L\alpha}(\xi) \approx v_{\alpha} + \frac{dv_{\alpha}}{d\xi}(\xi - \xi_{\alpha}) + \dots = v_{\alpha} + \frac{\Delta}{1 + \Delta \cdot v_{\alpha}} \frac{dv_{\alpha}}{d\tau}(\xi - \xi_{\alpha}) + \dots (\text{XV.13})$$

substituting this expansion in (XI.12), we shall obtain

$$\tau_{L\alpha}(\xi) = \tau - \Delta \int_{\xi}^{\xi_{\alpha}} \frac{d\xi}{1 + \Delta \cdot v_{L\alpha}(\xi)} \approx \tau - \Delta(1 - \Delta \cdot v_{\alpha})(\xi - \xi_{\alpha}) + \frac{1}{2} \Delta^3 (1 - \Delta \cdot v_{\alpha}) \frac{dv_{\alpha}}{d\tau} (\xi - \xi_{\alpha})^2 + \dots (\text{XV.14})$$

It is easy to show that if we keep only the linear term $\xi_{\alpha} - \xi$ in the obtained expression and substitute it in (XV.11), then we will get equation (XV.5). The difference arises when terms of a higher order are taken into account. This implies the applicability condition for equation (XV.5). Based on the requirement that the quadratic term is small

$$\frac{1}{2} \Delta^3 (1 - \Delta \cdot v_{\alpha}) \frac{dv_{\alpha}}{d\tau} (\xi - \xi_{\alpha})^2 \ll 1 \quad (\text{XV.15})$$

we shall obtain the boundary of the spatial domain of applicability of the model in question [XV-2.]

$$\xi \gg \xi^* = -\frac{2}{\Delta^{3/2} |E|}. \quad (\text{XV.16})$$

Since it is always $|E| \leq 2$, but for relativistic bunches it is $\Delta \ll 1$, we can assume that the simplified model we have proposed is applicable in a fairly wide spatial domain and can be used in practical calculations. The applicability limits of the model can be defined as it follows: if even $|E| \approx 2$, then for $\Delta = 0$, $\xi^* \rightarrow -\infty$ is equivalent to an infinite beam velocity, because the beam velocity in the selected units is proportional to Δ^{-1} , for $\Delta = 0.1$, $\xi^* \approx -31$ is the most problematic case, for $\Delta = 0.01$, $\xi^* \approx -1000$. The model (12.2) – (12.3) proposed in this paper has an important advantage compared to the more rigorous model [XI-3] from the point of view of computational resources, since it contains only time-dependent equations, and the model [XV-3] is a more complex spatio-temporal problem. There are other features of model (12.2) – (12.3) that make its use preferable in studying the dynamics of beams with a relatively low density, the consideration of which allows us to use a linear description of the perturbations of the surrounding plasma.

First of all, you can ignore the magnetic field created by the beam current, because the currents in the rest system of the beam-bunch are negligible. Moreover, all disturbances in the system can be considered potential, ignoring electromagnetic effects, which is unacceptable when describing the dynamics of moving bunches of charged particles in a laboratory frame of reference. This circumstance becomes even more important in the transition to three-dimensional modeling [XV-4] – [XV-6].

References to annex XV

XV-1. Zagorodny A. G., Kuklin V. M. Features of radiation in nonequilibrium media / Problems of theoretical physics. Scientific works / V. A. Buts, A. G. Zagorodny, V. E. Zakharov, V. I. Karas, V. M. Kuklin, A. V. Tur, S. P. Fomin, N. F. Shulga, V. V. Yanovsky; ed. no. V. M. Kuklin. – Kh. : V. N. Karazin Kharkiv National University, 2014. – Issue. 1–532 p. (Series "Problems of Theoretical and Mathematical Physics"; under the general editorship of A. G. Zagorodny, N. F. Shulga). – C.13–81 (in Russian).

XV-2. Kuklin V. M. One-dimensional moving bunches of charged particles in plasma // UFZh, 1986. -- V. 31. – No. 6. – P. 853--857 (in Russian).

XV-3. Balakirev V. A., Karbushev N. I., Ostrovsky A. O., Tkach Yu. V. Theory of Cherenkov amplifiers and generators on relativistic beams. – Kiev: Naukova Dumka, 1993. -- 208 p. (in Russian).

XV-4. Kirichok A. V., Kuklin V. M., Mishin A. V., Priymak A. V. 1D model of a bunch of charged particles moving in plasma // Physical foundations of instrument engineering. 2013. -- V. 2. -- No. 3. -- P. 80--93.]

XV-5. Alterkop B. A., Zheksemin S. R., Rukhlin V. G. Tarakanov V. P. Two-dimensional dynamics of a compensated electron bunch in a dense plasma // Preprint of the Institute of High Temperatures of the Academy of Sciences of the USSR, 1986, N 6–193, -- P. 35--45 (in Russian).

XV-6. Kuklin V. M., Moiseev S. S., Panchenko. I. P. 3-D short Beam Dynamics // Moscow. Reprint of Institute of Space Research, N 1619, 1989. – 11 P.

ANNEX XVI

SUPERRADIANCE MODE OF OSCILLATOR SYSTEM

Fields of a single particle and particle bunch. Let us consider the mode of superradiance when the cavity field or the waveguide field are absent. You can also determine the total radiation field of the oscillators in the same volume. First, let us find the field of one oscillator. For slowly changing amplitude of radiation field E in space the equation is

$$\frac{\partial E_x}{\partial z} = \frac{2\pi}{c} \cdot e \cdot a \cdot \omega \cdot \exp\{+i\psi \pm ikz\} \cdot \delta(\pm z \mp z_0) = \lambda \cdot \delta(\pm z \mp z_0). \quad (\text{XVI.1})$$

Its solution is $E_x = C + \lambda \cdot U(z - z_0)$, where $U(z < 0) = 0$, $U(z \geq 0) = 1$. Since for the wave emitted by the oscillator, the equation is $D(\omega, k) \equiv (\omega^2 \varepsilon_0 - k^2) = 0$, which roots are $k_{1,2} = \pm(\omega_0 \text{Re } \varepsilon_0 / c)(1 + i \text{Im } \varepsilon_0 / \text{Re } \varepsilon_0) \approx \pm(\omega_0 / c \varepsilon_0)(1 + i0)$, then for the wave propagating in the direction $z > z_0$, the wave number $k = k_1 > 0$ and

constant value C should be chosen equal to zero, in order to avoid unlimited growth of the field at infinity. For a wave propagating in the direction $z < z_0$, the wave number is $k=k_2 < 0$, the value of a constant should be chosen equal to $-\lambda$ for the same reasons. The amplitude of the electric field in

$$E_x = 2\pi e a \omega M \cdot c^{-1} \exp\{-i\omega t + i\psi\} [\exp\{ik(z - z_0)\} \cdot U(z - z_0) + \exp\{-ik(z - z_0)\} \cdot U(z - z_0)] \quad (\text{XVI.2})$$

where $U(z) = 1$ at $z \geq 0$ and $U(z) = 0$ at $z < 0$, F or one particle in such a volume of unit cross section and cavity length is b , M is numerically equal to unity.

We can represent the equations of motion in the form

$$\frac{d}{dt} \frac{v_i}{\sqrt{1 - \frac{|v_i|^2}{c^2}}} + \omega^2 x_i = -\frac{e}{m} E_x(z_i, t) \quad (\text{XVI.3})$$

where

$$x_i(t) = i \cdot a_i \cdot \exp\{-i\omega t + i\psi\} = iA \cdot \exp\{-i\omega t\}, \quad v_i = \omega \cdot a_i \cdot \exp\{-i\omega t + i\psi\} = \omega A \cdot \exp\{-i\omega t\}.$$

The equation of motion for an oscillating electron has the form (XVII.3).

Using the above notation, let us write (XVI.3) in the form

$$\begin{aligned} \frac{dA_j}{dt} - i \frac{|3A_j|^2 \cdot \omega^3}{4c^2} A_j = \\ = -\frac{\pi \cdot e^2 \cdot M}{mc} \cdot \frac{1}{N} \sum_{s=1}^N A_s \left(e^{ik(z_j - z_s)} \cdot U(z_j - z_s) + e^{-ik(z_j - z_s)} \cdot U(z_s - z_j) \right) \end{aligned} \quad (\text{XVI.4})$$

or in the dimensionless form

$$\begin{aligned} \frac{dA_j}{dt} - i\Delta_j A_j = -\frac{1}{N} \sum_{s=1}^N A_s [e^{2\pi i(Z_j - Z_s)} \cdot U(Z_j - Z_s) + \\ + e^{-2\pi i(Z_j - Z_s)} \cdot U(Z_s - Z_j)] - E_0 \cdot e^{2\pi i Z_j} = \frac{1}{2} E_x(Z_j, \tau) - E_0 \cdot e^{2\pi i Z_j}; \end{aligned} \quad (\text{XVI.5})$$

where

$$\begin{aligned} \gamma = \gamma_0^2 / \delta_D = \pi e^2 M / mc; \quad E = eE / m\omega\gamma a_0, \quad A = A / a_0; \\ kz_j = 2\pi Z_j \quad \tau = \gamma t; \quad \Delta_j = \alpha |A_j|^2 A_j, \\ \gamma_0^2 = \pi e^2 n_0 / m = \omega_{pe}^2 / 4, \quad \alpha = \frac{3\omega}{4\gamma_0} (ka_0)^2. \end{aligned}$$

The account of the nonlinearity of the oscillator is necessary [XVI-1, XVI-2]. The electric field strength of the oscillator radiation in dimensionless units can be described by the expression

$$E_x(Z_j, \tau) = \frac{2}{N} \sum_{s=1}^N A_s [e^{2\pi i(Z_j - Z_s)} \cdot U(Z_j - Z_s) + e^{-2\pi i(Z_j - Z_s)} \cdot U(Z_s - Z_j)] \quad (\text{XVI.6})$$

in this case, the expression for the energy conservation law is the same as (13.21)

$$\frac{d}{d\tau} |A_j|^2 = -\text{Re}\{E_x(Z_j, \tau) A_j^*\} \quad (\text{XVI.7})$$

Obviously, the field can be represented as

$$|E(Z, \tau)| = \sqrt{[\text{Re} E(Z, \tau)]^2 + [\text{Im} E(Z, \tau)]^2}. \quad (\text{XVI.8})$$

Representing the field in the form $|E(Z, \tau)| \cdot \exp\{i\varphi(Z, \tau)\}$, we can distinguish the phase of the field $\varphi(Z, \tau)$ from the relations

$$\begin{aligned} \text{Cos}[\varphi(Z, \tau)] &= \text{Re} E(Z, \tau) / |E(Z, \tau)|, \\ \text{Sin}[\varphi(Z, \tau)] &= \text{Im} E(Z, \tau) / |E(Z, \tau)|, \end{aligned} \quad (\text{XVI.9})$$

where

$$\begin{aligned} \text{Re} E(Z, \tau) &= \frac{1}{N} \sum_{s=1}^N A_s \cdot [\text{Cos}\{2\pi |Z - Z_s| + \psi_s\} \cdot U(Z - Z_s) + \text{Cos}\{-2\pi |Z - Z_s| + \psi_s\} \cdot U(Z_s - Z)], \\ \text{Im} E(Z, \tau) &= \frac{1}{N} \sum_{s=1}^N A_s \cdot [\text{Sin}\{2\pi |Z - Z_s| + \psi_s\} \cdot U(Z - Z_s) + \text{Sin}\{2\pi |Z - Z_s| + \psi_s\} \cdot U(Z_s - Z)] \end{aligned}$$

References to annex XVI

XVI-1. Il'inskii Yu. A., Maslova N. S. Classical analog of superradiance in a system of interacting nonlinear oscillators // Zh. Eksp. Teor. Fiz. – 1988. – Vol. 91. – No. 1. – P. 171-174.

XVI-2. Kuklin V. M., Litvinov D. N., Sevidov S. M., Sporov A. E. Simulation of synchronization of nonlinear oscillators by the external field. // East European Journal of Physics 2017. – V. 4. – N 1. – P. 75–84.

ANNEX XVII

PLASMA GYROTRON EQUATIONS

Transition (14.6) is carried out on the basis of the following transformation:

$$\exp\{in\theta_{12}\} \cdot J_n(x_1) = \sum_{q=-\infty}^{\infty} J_{n-q}(x_2) \cdot J_q(x_3) \cdot \exp\{in\theta_{23}\} \quad (\text{XVII.1})$$

here x_i are the sides of the triangle ($i = 1, 2, 3$), $\theta_{12} = \angle x_1 x_2$ is the angle between the sides x_1 and, x_2 accordingly, $\theta_{23} = \angle x_2 x_3$ is the angle between the sides x_2 and x_3 of the triangle.

Figure XVII.1 below shows the Larmor orbit of the electron in the section of the waveguide. It is easy to see that x_1, x_2, x_3 can be defined as r, r_B, r_C , respectively.

Here the radius r_W of the waveguide determines the position of the electron beam, r_C is the position of the center of the Larmor rotation of the electron, r_B is the

$$(B_r, E_\theta) = \left(J'_m(k_\perp r) + \frac{\omega^2 \varepsilon_2}{c^2 k_\perp^3} \frac{m}{r} J_m(k_\perp r) \right) \exp(-i\omega t + ik_z z + im\theta) \times \left(\frac{1}{k_\perp} \frac{\partial b}{\partial z}, -i \frac{\omega}{ck_\perp} b \right) \quad (\text{XVII.6})$$

It is rational to use such a representation of fields to obtain the stationary gain regime along the waveguide. Here there is the expression for the components of the permittivity tensor of the medium $\varepsilon_{ij}(\omega, \vec{k})$: $\varepsilon_{11} = \varepsilon_{22} = \varepsilon_1 = 1 - \omega_{pe}^2 / (\omega^2 - \Omega_B^2)$, $\varepsilon_{12} = -\varepsilon_{21} = i\varepsilon_2 = i\omega_{pe}^2 \Omega_B / \omega(\omega^2 - \Omega_B^2)$, $\varepsilon_{33} = \varepsilon_3 = 1 - \omega_{pe}^2 / \omega^2$. In this case, the conditions $(k_z / k_\perp) < 1$ and $g = (\omega^2 \varepsilon_{xy} / c^2 k_\perp^2) = \omega^2 \varepsilon_2 / c^2 k_\perp^2 < 1$ are considered to be fulfilled and the dependence on the coordinate z has not yet been determined. The transverse component of the wave vector $k_\perp = k'_{ms} = x'_{ms} / r_w$ is determined from the boundary condition

$$J'_m(x'_{ms}) + \frac{\omega^2 \varepsilon_2 r_w^2}{c^2 x'_{ms}{}^2} \frac{m}{x'_{ms}} J_m(x'_{ms}) = 0. \quad (\text{XVII.7})$$

The field equation takes the form

$$\left(\frac{\partial^2}{\partial z^2} + \frac{\omega^2 \varepsilon_1}{c^2} - k'_{ms}{}^2 \right) b = -\frac{4N_{b0} e \omega_B k'_{ms}{}^2}{c} \left[x'_{ms}{}^2 J_m{}^2(x'_{ms}) + J_m^2(x'_{ms})(x'_{ms}{}^2 - m^2) \right]^{-1} \times \times J_{n-m}(k_{ms} r_c) \frac{1}{N} \sum_{j=1}^N \left[a_j J'_n(a_j) + g \frac{n}{a_j} J_n(a_j) \right] \exp(-2i\pi \zeta_j). \quad (\text{XVII.8})$$

Upon transition to a coordinate system whose center coincides with the center of rotation of an individual electron in the beam, the fields are transformed as it follows

$$b'_z = b_z, \quad b'_\phi = b_\phi + igb_R, \quad b'_R = b_R - igb_\phi, \quad e'_R = e_R - ig e_\phi, \quad e'_\phi = e_\phi + ig e_R. \quad (\text{XVII.9})$$

Given relativism for the particles of the beam

$\Omega_B = eB_0 / m_e c = \omega_B (1 - \beta_{\perp 0}^2 - \beta_{z0}^2)^{-1/2}$, let us present the equations of their motion

$$2\pi \frac{d\zeta}{dz} = \frac{n\omega_{B0} - \omega}{v_z} + \frac{n\omega_{B0}}{2v_z} \left[\beta_{\perp 0}^2 - \beta_\perp^2 - 2\beta_{z0}(v_z - v_{z0}) / c \right] + n \frac{e}{m_e c v_z} J_{n-m}(k'_{ms} r_c) \exp(2i\pi \zeta) \left\{ \left[\left(1 - \frac{n^2}{a^2} \right) J_n(a) - g \frac{n}{a} J'_n(a) \right] b - \frac{in^2 v_z}{\omega a^2} \times \right. \quad (\text{XVII.10})$$

$$\left. \times \left[J_n(a) + g \frac{a}{n} J'_n(a) \frac{\partial b}{\partial z} \right] \right\},$$

$$\frac{da}{dz} = in \frac{e\omega}{m_e c \omega_B v_z} J_{n-m}(k_{ms} r_c) \left[J'_n(a) + g \frac{n}{a} J_n(a) \right] \exp(2i\pi \zeta) \left[b + i \frac{v_z}{\omega} \frac{\partial b}{\partial z} \right], \quad (\text{XVII.11})$$

$$\frac{d}{dz} \left(\frac{1}{v_z} \right) = -\frac{e\omega_B}{k_{ms}^2 v_z^3 m_e c} \frac{\partial b}{\partial z} J_{n-m}(k_{ms} r_c) a \left[J'_n(a) + g \frac{n}{a} J_n(a) \right] \exp(2i\pi \zeta), \quad (\text{XVII.12})$$

For the case of a sufficiently large Larmor radius, the equations of the amplification regime can be represented as

$$\left(\frac{d^2}{d\xi_P^2} + i \frac{\partial}{\partial \tau_P} + \gamma_P^2 \right) E_P = -\frac{1}{N} \sum_{j=1}^N a_j \left[J'_n(a_j) + g \frac{n}{a} J_n(a_j) \right] \exp(-2i\pi\zeta_j), \quad (\text{XVIII.13})$$

$$2\pi \frac{d\zeta}{d\xi_P} = \sigma \left[\Delta_P + \frac{a_0^2 - a^2}{2\varepsilon' n^2} + \beta_{z_0}^2 \frac{(\sigma - 1)}{\sigma \varepsilon'} \right] + \exp(2i\pi\zeta) \times$$

$$\times n \left\{ \left[\left(1 - \frac{n^2}{a^2} \right) J_n(a) - g \frac{n}{a} J'_n(a) \right] \sigma E_P - \frac{i\varepsilon' n^2}{a^2} \left[J_n(a) + g \frac{a}{n} J'_n(a) \right] \frac{\partial E_P}{\partial \xi_P^2} \right\}, \quad (\text{XVII.14})$$

$$\frac{da}{d\xi_P} = in \left[J'_n(a) + g \frac{n}{a} J_n(a) \right] \exp(2i\pi\zeta) \left[\sigma E_P + i\varepsilon' \frac{\partial E_P}{\partial \xi_P} \right], \quad (\text{XVII.15})$$

$$\frac{d\sigma}{d\xi_P} = -R_P \sigma^3 \frac{\partial E_P}{\partial \xi_P} a \left[J'_n(a) + g \frac{n}{a} J_n(a) \right] \exp(2i\pi\zeta), \quad (\text{XVII.16})$$

where $\xi_P = z\rho_P$, $E_P = \frac{e}{m_{e0} c \rho_P v_{z0}} J_{n-m}(k'_{ms} r_c)$, $\sigma = \frac{v_{z0}}{v_z}$, $R_P = \rho_P \omega_B / k'_{ms}{}^2 v_{z0}$,

$$\varepsilon' = \frac{\rho_P v_{z0}}{\omega}, \quad \Delta_P = \frac{n\omega_{B0} - \omega}{\rho_P v_{z0}}, \quad G = \frac{(\omega^2 - \Omega_B^2)^2 + \omega_{pe}^2 \Omega_B^2}{(\omega^2 - \Omega_B^2)^2}, \quad \gamma_P^2 = \frac{1}{\rho_P^2} \left[\frac{\varepsilon_1 \omega^2}{c^2} - k'_{ms}{}^2 \right],$$

$$\rho_P^3 = \frac{4N_{b0} e^2 \omega_B k'_{ms}{}^2}{m_e c^3 \beta_{z0}} \left[x'_{ms}{}^2 J_m^2(x'_{ms}) + J_m^2(x'_{ms})(x'_{ms}{}^2 - m^2) \right]^{-1} J_{n-m}^2(k'_{ms} r_c),$$

and on the left side of the equation the time derivative $\frac{\partial}{\partial \tau_P}$ is taken into account,

where $\tau_P = \rho_P^2 c^2 / 2\omega G$.

With a small argument of Bessel functions, using the new variable $\xi_G = \beta_{\perp}^2 \omega_{B0} z / 2v_z$, one can obtain modified Gaponov equations (14.21) – (14.22).

References to annex XVII

XVII-1. Kuklin V. M. Grant Report / PST EV N 978763, NATO Science Programm Cooperative Science & Technology Sub-Programme, Hamburg. 2002.

ANNEX XVIII

INTEGRALS OF EQUATION SYSTEMS, WHICH DESCRIBE CYCLOTRON INSTABILITIES

Let us note that the integrals are valid for these two waves TE and TM

$$R \cdot a^2 - 2n \cdot \eta = Const, \quad (\text{XVIII-1})$$

$$|E|^2 - (2/R) \cdot N^{-1} \sum_{j=1}^N \eta_j = Const, \quad (\text{XVIII-2})$$

$$|E|^2 - n^{-1} \cdot N^{-1} \sum_{j=1}^N a_j^2 = Const, \quad (\text{XVIII-3})$$

In this case, the last integral (XXIII.3) is valid for $\theta=0$, if $\theta \neq 0$ on its right-hand side $Const \rightarrow Const + \theta \cdot \int_0^t dt' |E(t')|^2$. It is useful to pay attention to the corollary of the integrals [14-7, 15-2] in the absence of field energy loss ($\theta=0$): changes in the energy of transverse motion

$$\Delta W_{\perp} = \frac{\omega_B \cdot m_e \cdot N_{b0}}{2k_{ms}^2} N^{-1} \sum_{j=1}^N (a_j^2 - a_{j0}^2) \text{ and changes in the energy of longitudinal}$$

motion $\Delta W_{\parallel} = \frac{v_{z0} \cdot m_e \cdot N_{b0}}{k_z} N^{-1} \sum_{j=1}^N (\eta_j - \eta_{j0})$ are related to each other as

$\Delta W_{\perp} / \Delta W_{\parallel} = n\omega_B / k_z v_{z0}$, and changes in the field energy and changes in the energy of transverse motion as $\omega / n\omega_B$.

The consideration of the case $n < 0$ for particles moving in the direction of wave propagation corresponds to the anomalous Doppler effect and is not accomplished for particles that do not move in this direction. Taking into account relativism (negative mass effect, see, for example, [XVIII-3]) leads to the appearance of nonlinearity in the equations of motion (14.13) and (15.12). Indeed, in equations (14.13) and (15.12) η_i should be replaced by $\eta_i - \alpha(a_j^2 - a_{j0}^2)$, where $a_{j0}^2 = a_j^2 |_{\tau=0}$, $\gamma_0 = (1 - v_{\Phi}^2 / c^2)^{-1/2} |_{\tau=0}$, $\alpha = n\omega_B^3 \cdot \gamma_0^2 / 2k_{ms}^2 c^2 \delta_h$.

References to annex XVIII

XVIII-1. Kuklin V. M. Grant Report / PST EV N 978763, NATO Science Programm Cooperative Science & Technology Sub-Programme, Hamburg. 2002.

XVIII-2. Kuklin V. M., Puzyrkov S. Yu., Schunemann K., Zaginaylov G. I. Influence of low-density plasma on Gyrotron Operation. / Ukr. J. Phys. 2006. – V. 51. – № 4. – P. 358--366.

XVIII-3. Zaginailov G. I., Kuklin V. M., Panchenko I. P., Shunemann K. On the change in the mechanism of particle bunching in beam cyclotron instabilities / G. I. Zaginailov // Bulletin of KhNU im. V. N. Karazina. Ser. Kernels, particles, fields. – 2003. -- No. 585. – B. 1 (21). -- P. 73--75 (in Russian).

ANNEX XIX

MODULATION INSTABILITY OF A FLAT WAVE IN A TWO-DIMENSIONAL CASE

For two-dimensional instability of a plane intense wave, the system of equations is

$$\frac{d\varphi_0}{dt} = -u_0^2 - 4 \sum_{s>0}^S \sum_{m>0}^N (u_{m,s}^2 + u_{-m,-s}^2) - 2 \sum_{s>0}^S \sum_{m>0}^N u_{m,s} u_{-m,-s} \cos\Phi_{m,s}, \quad (\text{XIX-1})$$

$$\frac{d}{dt} u_0 = \{-\delta - 2 \sum_{s=-S}^S \sum_{m>0}^N u_{m,s} u_{-m,-s} \sin\Phi_{m,s}\} + G, \quad (\text{XIX-2})$$

$$\frac{du_{n,s}}{dt} = u_{n,s} \left\{ -\delta + u_0^2 \frac{u_{-n,-s}}{u_{n,s}} \sin\Phi_{n,s} + 2 \frac{u_{-n,-s}}{u_{n,s}} \sum_{\substack{z>0 \\ z \neq s}}^S \sum_{\substack{m \neq n \\ m > 0}}^N u_{-m,-z} u_{m,z} \sin\Psi_{snmz} \right\}, \quad (\text{XIX-3})$$

$$\frac{d\varphi_{n,s}}{dt} = (K_{n,s}^2 + K_{n,s}^2) - 2[u_0^2 + \frac{1}{2}u_{n,s}^2 + u_{-n,-s}^2 + 2\sum_{\substack{z>0 \\ z\neq s}}^S \sum_{\substack{m>0 \\ m\neq n}}^N (u_{m,z}^2 + u_{-m,-z}^2)]$$

$$-u_0^2 \frac{u_{-n,-s}}{u_{n,s}} \cos\Phi_{n,s} - 2 \frac{u_{-n,-s}}{u_{n,s}} \sum_{\substack{z>0 \\ z\neq s}}^S \sum_{\substack{m\neq n \\ m>0}}^N u_{-m,-z} u_{m,z} \cos\Psi_{snmz},$$

(XIX -4)

where $\Phi_{n,s} = 2\varphi_0 - \varphi_{n,s} - \varphi_{-n,-s}$ and $\Psi_{snmz} = \Phi_{n,s} - \Phi_{m,z}$, for wave numbers in two directions we have

$$K_{n,s}^2 = \{1 + (\frac{2|n|-N}{N})\sqrt{1-\delta}\} - K_{n,s}^2, \quad K_{m,s} = 0.1 \cdot s.$$

For a slowly changing field, the expression is

$$E_M(\xi, \eta, t) = [u_0 + \sum_{s>0}^S \sum_{m>0}^N [u_{m,s} \exp\{-iK_{m,s}\xi - iK_{m,s}\eta + i(\varphi_{m,s} - \varphi_0)\} + u_{-m,-s} \exp\{iK_{m,s}\xi + iK_{m,s}\eta + i(\varphi_{-m,-s} - \varphi_0)\}]]$$

(XIX -5)

In case if it is necessary to view the fine structure of the field, that is, individual waves we have

$$E_M(\xi, \eta, t) = \exp\{-ik_0\xi + i\varphi_0\} \times$$

$$\times \left(u_0 + \sum_{s>0}^S \sum_{m>0}^N \left(u_{m,s} \exp(-iK_{m,s}\xi - iK_{m,s}\eta + i(\varphi_{m,s} - \varphi_0)) + u_{-m,-s} \exp(iK_{m,s}\xi + iK_{m,s}\eta + i(\varphi_{-m,-s} - \varphi_0)) \right) \right)$$

(XIX -6)

In the rest system of modulation for such a fine field structure, the expression is

$$E_M(\xi, \eta, t) = \exp\{-ik_0((\xi + 2k_0t)) + i\varphi_0\} \cdot [u_0 +$$

$$+ \sum_{s>0}^S \sum_{m>0}^N [u_{m,s} \exp\{-iK_{m,s}\xi - iK_{m,s}\eta + i(\varphi_{m,s} - \varphi_0) - 2K_m \cdot k_0t\} +$$

$$+ u_{-m,-s} \exp\{iK_{m,s}\xi + iK_{m,s}\eta + i(\varphi_{-m,-s} - \varphi_0) + 2K_m \cdot k_0t\}]]$$

(XIX-7)

ANNEX XX

SELF-SIMILAR STRUCTURES ON THE SURFACE AND IN THE VOLUME OF CRYSTALS

Any crystal lattice in the bulk and on the surface of a solid is formed as a result of a certain process – the ordering process – primary instability, which has certain inverse characteristic development time and is saturated with non-linearity. This nonlinearity is due to a deviation from the equilibrium position of a fairly homogeneous subsystem of atoms, inside which interactions with the nearest neighboring atoms prevail.

Very often, the nonlinearity is cubic or higher (often there are more neighboring atoms, but their contribution to the interaction is not always equivalent and that is why

only some types of interactions dominate). The source of nonequilibrium is perturbation of the density of the medium due to overheating, and a significant absorption of energy in the process of ordering - instability is due to the transfer of energy by elastic waves from this region.

The process of the emergence of primary structure as a whole is determined, first of all, by the dominant mechanism of interaction of elements, which forms its geometry, characteristic dimensions, and orientation.

It can be assumed that at the stage of the primary process, the formation of a periodic structure occurs due to the narrowing of the spectrum of density perturbations due to the nonlinear mechanism of perturbation competition, similar to those considered above.

However, in addition to the main mechanism of interaction of elements, a number of weaker interactions are often present in the system, manifesting themselves only under conditions when the process of constructing the main (primary) structure is close to completion.

The crystal surface structure has always attracted the attention of researchers.

First of all, because the differences in the structure of the surface layer from the internal structure of the crystal were undoubted, in particular, there were regular surface formations whose linear sizes significantly exceeded the corresponding sizes of the unit cells of the crystal. It was believed [XX-1, XX-2] that a solid body always strives to lower its surface (and therefore total) free energy, while forming at the same time its "mountain" structure of hills and valleys, where there are 12 convexities of electron density corresponding to the positions of individual atoms [XX-2]).

For example, surface large-scale diamond-shaped regular formations on the surface of a silicon single crystal are known (the so-called "7X7 cell", where 12 convexities of electron density, corresponding to the positions of individual atoms are located [XX-3]). The surface layers of atoms, the nature of the interaction and the corresponding arrangement of which differ from similar parameters of the atoms that make up the bulk layers of the lattice, already at scales comparable to the size of the unit cell, exhibit deviations in regularity, noted, for example, in experiments [XX-3].

Periodic deviations in the positions of local maximums of electron density were observed at distances significantly exceeding the characteristic unit cell size, but no distortions of the boundary in the direction normal to the sample surface were discussed.

Below there are the results of experimental studies [XX-4] of the graphite surface by scanning tunneling microscopy (STM). The studies were carried out in air using a STM – 1 scanning tunneling microscope described in [XX-5].

Resolution in the horizontal XY plane is less than 1.4 \AA , and vertical resolution is 0.7 \AA . As a probe, needles prepared by the method of electrochemical etching with a hood were used. The graphite surface was cleaned by chipping the upper layer immediately before the measurement. Fig. XX.1. "a", "b", "c" shows topographic images of highly oriented graphite portions at various magnifications obtained by scanning in tunnel current stabilization mode. The time for scanning sections is 10–20 sec. Fig. XX.1. "a" presents an image of a highly oriented graphite at maximum magnification.

The ordered rows of the hexagonal structure of graphite are observed: the hexagon consists of atoms with different levels of local density of states. Let us

note that the unit cell parameters are consistent with the data presented in the works of other authors.

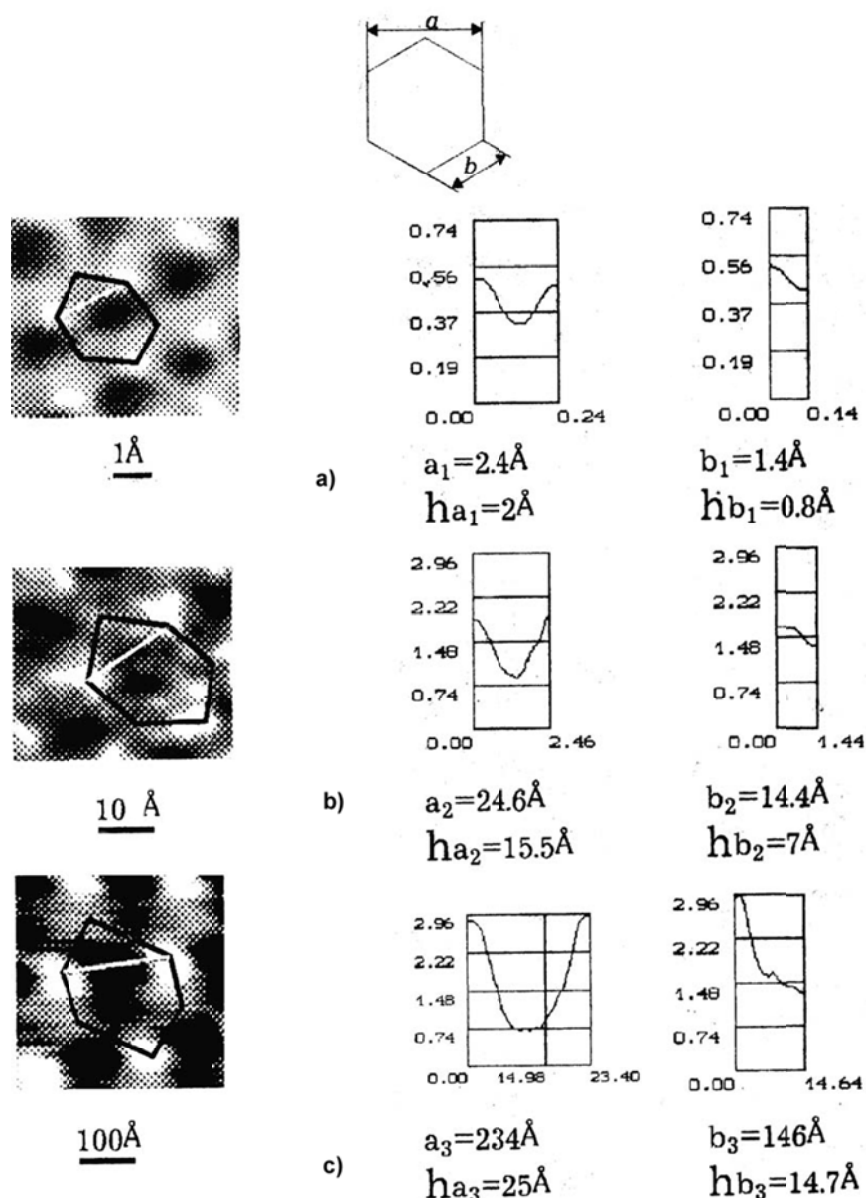


Fig. XX.1. Topographic images of highly oriented graphite at various magnifications obtained by scanning tunneling microscopy

Periodic modulation of surface electron density (large-scale corrugation) was found in individual sections of the samples, the character of which is similar (with a similarity coefficient close to 10) of small-scale modulation of electron density within a unit cell on the surface of graphite (see Fig. XX.1. "b").

On another sample (see Fig. XX.1. "c"), surface corrugation was found, the longitudinal linear dimensions of which are two orders of magnitude greater than the corresponding unit cell sizes (the size of the vertical modulation of the surface is only twice as large as in the previous case shown in Fig. XX.1. "b"). Let us note that the linear modulation scale of surface electron density, discussed in [XX-6], corresponds to the longitudinal corrugation scale shown in Fig. XX. "b".

The longitudinal scale of the corrugation shown in Fig. XX.1 "c" is an order of magnitude more. The observed differences in the characteristic sizes of the modu-

lation of the graphite surface are apparently associated with various modifications of its internal structure. It is possible that the case shown in fig. XX.1. "b", presents the most common allotropic form of carbon – graphite with a hexagonal structure.

Fig. XX.1. "c" corresponds, as it can be assumed, to the rhombohedral packing of graphite. The undoubted similarity of the primary structure – the unit cell and the secondary structure – modulation of the electron density surface is more important than the vertical component of the modulation for the obtained experimental data, at least in the case shown in Fig. XX.1. "b".

The cause of modulation instability, which forms self-similar structures, may be shear stresses due to the nonlinear interaction of the primary structure with improper perturbations of a non-divergent type, which can change near the surface. The approach [XXI-6, XXI-7] to the description of the lattice stability can be constructive. You can consider a simpler model.

Graphite is a multilayer structure, each layer of which represents carbon atoms, united by strong covalent bonds. The bond between the layers is determined by weaker Van der Waals interactions. The surface of each layer can be considered inextensible, and the van der Waals forces only lead to its corrugation. It is not difficult to build a model that can qualitatively clarify the appearance of large-scale corrugation on the surface of graphite. Let us consider a simpler two-dimensional case, with the OX axis directed along the inextensible layer, and the OY axis defined perpendicular to the sample boundary. Then the corrugation wave number inside the graphite sample can be written as $k_0 = k_{00} + a_0^2 k_0^3 / 4$, where the ratio between the spatial period λ and the wave number of the periodic structure is $k = 2\pi / \lambda$, k_{00} is the wave number in the absence of corrugation, a_0 is the amplitude of the corrugation, and the above expression is valid for $(k_0 a_0)^2 < 1$. For a perturbed system, we can write the equation

$$(k - i \frac{\partial}{\partial y}) \cdot a = k_{00} + \frac{k^3 |a|^2}{4} a. \quad (XX.1)$$

Let the corrugation perturbations have wavenumbers $k_{\pm} = k_0 \pm K$ and amplitudes a_{\pm} , then for these perturbations one can write the equation

$$\frac{\partial}{\partial y} a_{\pm} \pm i K a_{\pm} = i \frac{k_0^3 a_0^2}{4} a_{\mp}^*, \quad (XX.2)$$

from where it is not difficult to find a solution $\sim \exp\{-iKy\} \cdot \exp\{k_0^3 a_0^2 y / 4\}$ growing to the surface, where, due to the oscillating factor, the amplitudes of large-scale corrugation disturbances are limited. An approximate equality $(k_0 a_0)^2 \approx (ka)^2 + (a_{\pm} K)^2$ is performed, where the value $(k_0 a_0)^2$ is in the depth of the sample. On the surface $(ka)^2 \approx \alpha \cdot (a_{\pm} K)^2$ it can be assumed that $\alpha \approx 1$ is for the allotropic form, and $\alpha \approx 0.2$ is for the rhombohedral packing of graphite.

Instead of one stable position of a single atom in the surface layers, two or more such positions can appear. The shift of the atomic layers in the interior of the

crystal is noticeably weakened; therefore, overlapping of the same type of periodic lattices can occur near the surface, followed by rotation of one of them with respect to a more deeply lying one at a small angle. Such structures are called Moire structures, and the period of large-scale modulation is completely determined by the angle of rotation ϕ when decreasing ϕ period increases. The surface layer of the crystal may be deployed on a small angle relative to the next layer facing the surface of a sufficient number of dislocations of the same sign [XX-7] – [XX-9]. In this case, the so-called superlattice, i.e. a lattice having the same topology as the main one, but this lattice has a longer period, which depends on the angle of rotation. The mismatch of the scales of the primary structure (lattice period) in the planes tangent to the surface of each of the crystalline layers can lead to the appearance of stresses normal to this surface near the crystal boundary. These forces, acting both in the vertical and horizontal directions (that is, parallel to the macroscopic surface of the sample), can, with a relatively low level of fluctuations, introduce some equilibrium state. This equilibrium state must have a certain depth of vertical modulation of the crystal surface in order to combine the scales on the surface and in volume.

Obviously, the formation of spatial modulation of the surface layer occurs under the influence of a weaker physical mechanism, so the role of fluctuations that accompany this process may be significant. In some cases, fluctuations can disrupt the secondary instability, and deep vertical modulation of the surface may not be introduced. Thus, in the first case (Fig. XX.1. "b") $\varepsilon_2 \propto 10^{-1}$, and in the second (Fig. XX.1. "c") it is $\varepsilon_2 \propto 10^{-2}$. The characteristic time of formation of a regular surface structure should be expected to be 10 and 100 times, respectively, longer than the formation time of the atomic structure of graphite.

Volumetric violations. When a single crystal is formed, the arising regular periodic microstructure – the atomic lattice of the crystal in a nonlinear medium is unstable in the bulk of the sample. The development of this instability (i.e., a secondary weaker process compared to the process of forming a single crystal lattice) leads to large-scale regular displacement of atoms from the positions characteristic of a perfect lattice (an analog of modulation instability). In places of the greatest deviation of atoms, a spatial shift of atomic rows occurs and characteristic defects – dislocations appear.

The ratio of the scales of the unit cell of the crystal and the large-scale dislocation network – the Frank network – is of the order of 10^{-4} . If we assume that the mechanism of the formation of the Frank mesh is similar to the processes considered above, then $\varepsilon_2 \propto 10^{-4}$. It can also be expected that the characteristic time of the formation of the Frank network is 10^4 times longer than the formation of a regular atomic lattice. The forces of interaction, which form small-scale and large-scale structures, are in the same proportion.

References to annex XX

XX-1. Christian J. W. Transformations in metals and alloys. – Pergamon Press, 1975.

XX-2. Ramstad A., Brocks G., Kelly P. J. Theoretical study of Si (100) surface reconstruction // Phys. Rev. 1995. – V. 51 – N. 20. – P. 14504.

XX-3. Investigation of the asymmetry of the atomic image of the surface lattice of graphite by the STM method. // Authors: Alekperov S. D., Vasiliev S. I., Leonov V. B., Panov V. I., Semenov A. E. // Reports of the Academy of Sciences of the USSR, Physics, 1989. -- V. 307. -- No. 5. -- P. 1104--1109 (in Russian).

XX-4. On distributed defects on the surface and in the bulk of the crystal. // Auth: Babaskin A. A., Kamenskiy Yu. V., Kirichenko V. G., Kirichok A. V., Kuklin V. M., Tvardovskiy A. // Bulletin of KhNU im. V. N. Karazin, 2000. – № 49. -- B. 4 (12). -- p. 23--28 (in Russian).

XX-5. Kamensky Yu., Limansky A., Limanskaya O. Imaging of oligonucleotides and DNA by Scanning Tunneling Microscopy. "Nano-2" Second International Conference on Nanometer Scale Science and Technology Aug. 2–6. – 1993.

XX-6. Hill R. On the elasticity and stability of perfect crystals at finite strain // Math. Proc. Camb. Phill. Soc., 1975. – V. 77. – P. 225–234

XX-7. Thompson J. M. T. Instabilities and catastrophes in science and engineering. – John Willey & Sons, 1982. – 320 p.

XX-8. Fridel J. Dislocations. – Pergamon Press. 1964.

XX-9. Eshelby J. D. Solid State Physics v. 3. NY, – 1956.

ANNEX XXI

NATURE OF FORCED INTERFERENCE

At various initial amplitudes of the modes u_n and u_{-n} , for which the value of the wave numbers K_n^2 falls into the interval $1 + (\frac{2|n|-N}{N})\sqrt{1-\delta}$, their nonuniform growth occurs at $\{-\delta + u_o^2 \sin \Phi_n^*\} = \gamma > 0$. A mode with a larger amplitude grows more slowly than a mode with a smaller amplitude. For the amplitude difference from equation (16.22) we shall obtain

$$\frac{\partial(u_m - u_{-m})}{\partial t} = \{-\delta - u_o^2 \sin \Phi_n^*\} \cdot (u_m - u_{-m}), \quad (\text{XXI.1})$$

which describes the dynamics of the alignment of the growing amplitudes of the modes. Alignment of amplitudes and their growth occur already in the process of the development of instability. To correctly determine the behavior of the phase difference of these modes, it is useful to use the equations of the system (16.18) – (16.23), whence we can obtain

$$\frac{d(\phi_n - \phi_{-n})}{dt} = 2 \frac{d(\phi_n - \phi_0)}{dt} = 2(u_n^2 - u_{-n}^2) \cdot \left\{ 1 + \frac{(K_n^2 - u_0^2)}{(u_n^2 + u_{-n}^2)} + \frac{2}{(u_n^2 + u_{-n}^2)} \sum_{m>0}^N u_m u_{-m} \cos \Phi_m \right\}. \quad (\text{XXI.2})$$

It should be noted that when the mode amplitudes are equalized, the phase difference does not change at the initial stage of developed instability. Thus, despite the synchronization of the total phases of the spectrum modes by the main wave $\Phi_n \rightarrow \Phi_n^*$, each pair of modes at the nonlinear stage of the process preserves the phase difference, which leads to the interference imposed by the main wave.

But this does not mean that each standing wave formed by a pair of modes does not change its position relative to the main wave. Let us consider in more detail the behavior of the phases of the growing modes. It is useful to switch to a frame of reference in which the phase of the main wave does not change. In this reference frame we have

$$\frac{d\phi_n}{dt} - \frac{d\phi_0}{dt} = K_n^2 - u_0^2 \left\{ \frac{u_{-n}}{u_n} \cos\Phi_n + 1 \right\} + \left\{ u_n^2 + 2 \sum_{m>0}^N u_m u_{-m} \cos\Phi_m \right\}. \quad (XXI.3)$$

Assuming that the total phase in the process of instability development adjusts to its quasi-stable position Φ_n^* and taking advantage of the fact that the amplitudes of the symmetric modes are aligned $u_m \approx u_{-m}$, we can obtain accurate to quadratic terms in u_n^2

$$\frac{d\phi_n}{dt} - \frac{d\phi_0}{dt} = K_n^2 - u_0^2 \left\{ \frac{u_0^2 - u_n^2 - K_n^2 + u_0^2 + 2u_n^2}{u_0^2 + 2u_n^2} \right\} + \left\{ u_n^2 + \sum_{m>0}^N u_m^2 \frac{u_0^2 - K_m^2}{u_0^2} \right\} \approx 2(K_n^2 - u_0^2), \quad (XXI.4)$$

moreover, let us note that due to asymmetry $-\sum_{m>0}^N u_m^2 \frac{u_0^2 - K_m^2}{u_0^2}$ at the initial moment it is equal to zero and remains small at the initial stage. Shifting the phase of the main wave by $\pi/4$, let us represent the wave packet of the spectrum in the form

$$a - u_0 \exp[i\pi/4] \propto 2 \sum_{m>0}^N u_m \cdot \text{Cos} \{ -K_m \xi + 2(K_n^2 - u_0^2)t + \alpha_n \} \quad (XXI.5)$$

where $\alpha_n = \left(\frac{\Phi_n^* - \pi/2}{2} \right)$. Expression (XXI.5) is a collection of standing waves. The phases α_n of the longer $K_m < u_0$ disturbances are located in the negative region and move, as it follows from (XXI-5), in the positive direction, and the phases α_n of the shorter disturbances are in the positive region and move in the negative direction. That is, longer standing waves $K_m < u_0$ move towards shorter ones $K_m < u_0$, and with a decrease in the amplitude of the main wave, the energy is more concentrated in the long-wavelength part of the envelope spectrum.

The more the length of a standing wave formed by a pair of modes differs from the length of a disturbance growing with a maximum increment, the greater is the rate of change of its phase. The interference of these standing waves imposed by the main wave is forced [XXI-1, XXI-2] and accelerated with a change in the amplitude of the main wave. The process of interference of a set of standing waves forming an anomalous envelope can be seen in the observations presented in [XXI-3].

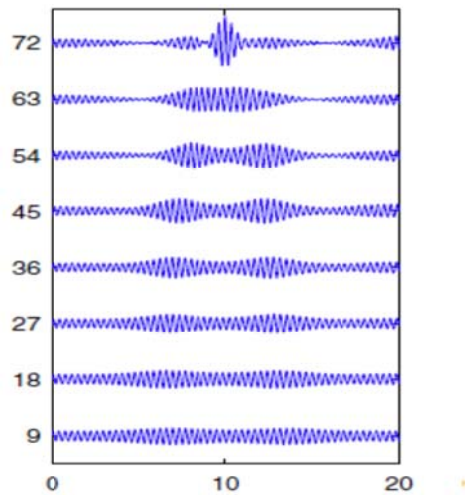


Fig. XXI-1 The evolution of the wave profile of anomalous amplitude in the experiment [XXI-3]. The ordinate is the time of each segment (in seconds), the abscissa is the distance estimate (in meters)

References to annex XXI

XXI-1. Kuklin V. M. On the interference nature of the formation of a fine structure of laser pulses and anomalous bursts of the amplitude of oscillations in the Lighthill model / VIII Khariton Scientific Readings. March 21–24, 2006 Sarov, Russia, Sat. reports. – Sarov, 2006. -- S. 450–456 (in Russian).

XXI-2. Kuklin V. M. Effect of induced interference and the formation of spatial perturbation fine structure in nonequilibrium open-ended system // Issues of Atomic Science and Technique (BAHT) Ser. «Plasma Electronics and Methods of Acceleration. – 2006. – No 5 (5). – P. 63–68.

XXI-3. Chabchoub A., Hoffmann N, Onorato M. and Akhmediev N. Super Rogue Waves: Observation of a Higher-Order Breather in Water Waves./ Physical Review X 2, 011015 (2012).

ANNEX XXII

WAVES OF ANOMALOUS AMPLITUDE IN THE OCEAN

An urgent problem of the safety of shipping and oil and gas production in the oceans and seas is the determination of the conditions for the occurrence of surface waves of anomalous amplitude that can lead to major disasters and accidents. Previously, when the intensity of shipping and oil and gas production was not so intense, the occurrence of such waves was considered rather rare, and there was no need to take into account their appearance and impact. With the increase in the number of vessels and their personnel, there is numerous evidence of the occurrence of such anomalous waves.

However, people are not only worried about the detection of such waves of anomalous amplitude, it is necessary to find out the features of the life cycle of such waves, how long they can exist and whether they can move. It is useful to find out the time of existence of waves of anomalous amplitude, the nature of their appearance and the dynamics of propagation.

Abnormally high waves as they are (extreme waves, rogue waves, abnormal waves, exceptional waves, giant waves, steep wave events) on the surface of deep water (these are so-called gravitational surface waves, the length of which is much less than the depth of the ocean, by the way, with decreasing depth, the speed of the wave slows down) are divided into three main types: “white wall”, “three sisters” (a group of three waves)²², and a single wave (“single tower”) [XXII-1 – XXII-4]. The height (swing) of the wave is usually indicated precisely as the distance from the highest point of the crest to the lowest point of the trough. The width of a train of giant waves can reach from several hundred meters to a kilometer, which is longer than the lengths of such waves.

In some cases, the direction of propagation of such waves, which often stray into groups of two or three waves, differed from the main direction of wave motion up to tens of degrees.

²² The used simple model presented above, which is quite adequate for the correct description of nonlinear ocean waves - the wave packets of the Three Sisters type. The appearance of waves of other type is quite possible (see, for example, the discussion of this issue in [XXII-8, XXII-9.]) but the reasons for their appearance are discussed in section 19.

Anomalously high waves are waves whose height is more than two times the significant wave height. The significant wave height is calculated for a given period in a given region.

For this, a third of all the recorded waves, which have the highest height, is selected, and their average height is found. Most modern vessels can withstand up to 15 tons per square meter, and in the case of even strong waves, this corresponds to more than double margin of safety, however abnormally large waves can cause pressure up to hundreds of tons per square meter [XXII-5]. All this inspires concern for maritime workers. Therefore, attempts are being made to find out the areas of their emergence, to determine the frequency of occurrence of such waves, and to develop methods how to warn about their appearance.

Based on the data received from satellites, it was possible to draw up an approximate map that will help skippers avoid dangerous areas. Europeans are primarily concerned about the eastern coast of South Africa, the Bay of Biscay, and the North Sea. There are other dangerous regions – this is the southern part of the coast of Latin America. Doubting the possibility of early warning, Swedish experts recommend creating virtual maps of the oceans with the designation of moving "triangles of death" on them – sections where, at certain times of the year and under certain conditions, the appearance of killer waves is most likely. The areas of sea currents were previously considered as the areas of the most probable appearance of killer waves [XXII-6]. The authors of [XXII-4, XXII-7], believe that the probability of random elevations of the sea surface $P(H)$ obeys the Rayleigh distribution:

$$P(H) = \exp\left\{-2\frac{H^2}{H_s^2}\right\}, \quad (\text{XXII.1})$$

where H_s is the average height-swing of one third of the highest waves²³. It can be shown that such waves can appear quite often. According to their calculations, a wave with a height-swing $2H_s$ is a wave of approximately $3 \cdot 10^3 - 10^4$ waves (waves in the ocean far from the coast have lengths of up to 100 meters and higher, and velocities of the order of 10 m/s), which did not contradict some experimental data. However, if we use the value of this probability, then for $3H_s$ we shall get that a wave of this height can be observed once every 20 years. In comparison with the estimate (19.11), waves with an amplitude exceeding $2H_s$ were quite frequent.

However, according to the observation of the MaxWave project of the sea surface from space, the wave $H/H_s = 2.9$ was observed. Over 793 hours of wave observation in the North Sea, a wave with $H/H_s = 3.19$ [XXII-10] was recorded. Such unexpectedly frequent recording of extreme waves has led to the need for a serious review of approaches to the applicability of the classical statistical model in the high-wave region. The random mechanism of the formation of anomalous waves was not correct, therefore, the main attention was paid to other mechanisms, which are mostly based on the results of the development of modulation instability of gravitational surface waves in deep water. In particular, it is similar to the above study.

²³ W. Munk, Proposed uniform procedure for observing waves and interpreting instrument records, SIO Wave Project. Translations by D D Bidde and R L Wiegel can be found in Translations of Four French, 1944.

To determine the zones of the oceans where abnormal waves are most likely to occur, it is necessary to determine the conditions, frequency and values of anomalous waves using the developed environmental models based on the developed mathematical models. Monitoring, which consists of checking a number of critical indicators, should be based on the results of simulations similar to the simulations performed above. For the observed anomalously large waves, the doubled amplitude-range of which is estimated from the empirical relation $(2 \div 3) \frac{2|A_0|}{2\pi} k_0 \propto 0,13$, where there is no collapse (breaking) yet [XXII-10, XXII-12], the average height (from undisturbed surface, $2A \approx H$) of the dangerous wave generating the killer wave is comparable to $|\bar{A}_0| \leq 0.04\lambda$ and for waves whose wavelength is 200 m. the amplitude can reach 8 meters. The wavelength is related to the oscillation period by the relation $\lambda \propto 1,6 \cdot T^2$ for two hundred meter waves with a period of 11 sec. Such ocean waves correspond to a wavelength of about 15 m. The ratio of the maximum increment of modulation instability to the oscillation frequency is of the order α , where $\alpha = \text{Im}\omega / \omega = (|A_0|k)^2 / 2 \approx 0.01$ under the conditions discussed above. The phase velocity of such waves reaches 18 m/s, the group velocity is half of that.

In other words, the characteristic process time (reverse increment) can be estimated as 3–4 minutes. In less than an hour, it will be possible to observe instability at its developed nonlinear stage. In case of wind excitation (the wind speed should exceed the phase velocity of gravitational surface waves equal to about 15–20 m/s, but if there is a counter current, then the wind speed can be even less than this value by the value of the current velocity), the zone of developed modulation instability is 20–50 km from the border of the zone of active wind excitation. The number of such waves in areas of strong wind exposure was on the one hand significantly larger than that allowed by statistics of random interference processes. But on the other hand, a simple calculation of such waves by means of space monitoring may also be inaccurate due to the small viewing area (frame). Once formed, such waves are able to drift at a speed (half the group) at significant distances. Moreover, they can fall into the next viewing frame, which unjustifiably increases the number of such waves in the entire observation zone.

Modeling of the dynamics of anomalous amplitude waves. Here we used the description in the framework of the so-called modified S-theory [XXII-12], and the interaction occurs only between the spectrum modes that are symmetric with respect to the pump ($k_n + k_{-n} = 2k_0$, $k_S + k_{-S} = k_n + k_{-n}$). In section 19 and in [XXII-13] it is shown that a direct calculation of equation (19.1a) and S - theory lead to qualitatively the same results.

In the presented model, the characteristic spatial scale is correlated with the wavelength $k_0 \xi = \zeta$, that is, the time scale is determined by the ratio $\tau = t \cdot \alpha \cdot \omega$, that is, the unit of measurement in space is the wavelength, and the unit of time is the inverse increment, that is, the characteristic process time.

For each moment of time, the amplitude (remind, here it is wave height or swing, i.e. distance from ridge to trough) H was calculated – the difference between the neighboring maximum and minimum, at $-1047 < \zeta < 1047$ (about 333 wavelengths). For each moment of time, the relative maximum amplitude

H_{rel} was calculated: the ratio of the maximum amplitude H_{max} to the average H_{av} over the entire space

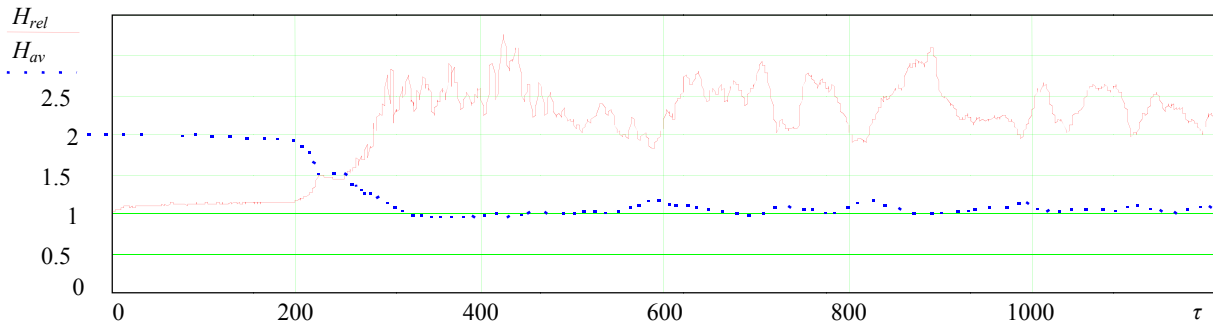


Fig. XXII.1 The behavior of the relative maximum amplitude of the waves H_{rel} in the interval $-1047 < \zeta < 1047$

At the initial stage of instability development, a quasistationary regime is reached with an average range of wave motion close to unity, which is approximately two times less than the initial value for the main wave. The largest wavelengths are achieved at the time $\tau = 425$ in the region near $\zeta = -482$ and also at the time $\tau = 888$ near $\zeta = 956$. For example, one can imagine phase diagrams and the form of the field in the vicinity of the maxima of the ranges (see Fig. XXII.2).

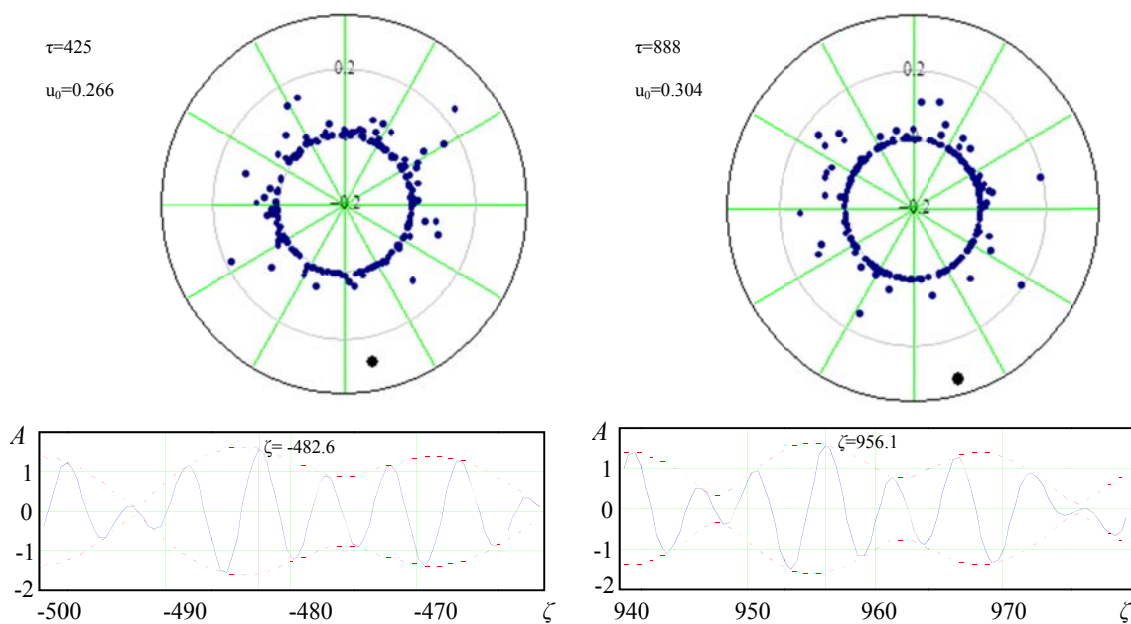


Fig. XXII.2. Phase diagrams and field views near the maximums of the amplitude for the first maximum $H_{max1} = 3.118, H_{rel1} = 3.253$ (left) and $H_{max1} = 3.035, H_{rel1} = 3.094$ (right)

It should be noted that, the amplitude of the main wave (the bullet point) is not so small, it controls the instability to a lesser extent, Indeed, in the developed regime, the energy of the main wave turns out to be half the energy of the spectrum

(see Fig. XXII.3), which, by the way, is characteristic of developed modes of modulation instability in other cases [XVII-14].

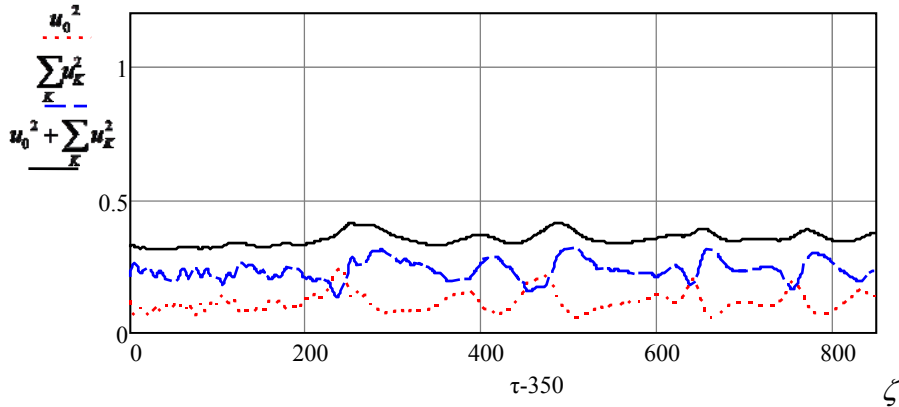


Fig. XXII.3. The behavior in the developed regime of the energy of the main wave u_0^2 (lower curve), the energy of the spectrum $u_0^2 + \sum_K u_K^2$ (middle curve) and total energy $u_0^2 + \sum_K u_K^2$ (upper curve)

It is of interest to consider the movement of wave packets with a maximum amplitude in space and in time (Fig. XXII. 4.)

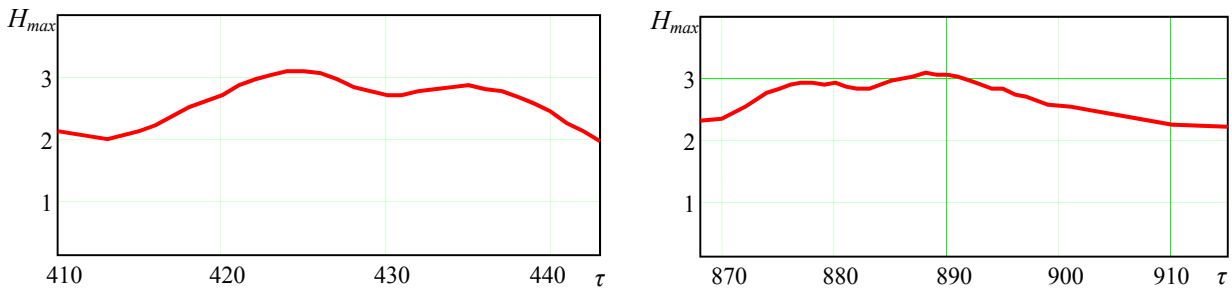


Fig. XXII.4. Change over time of the maximum amplitude of the wave packets (in their rest frame) near the maxima of the swings for the first maximum $H_{max1} = 3.118$ $H_{rel1} = 3.253$ (left) and $H_{max1} = 3.035$ $H_{rel1} = 3.094$ (right)

For the first packet (left), the maximum speed in the adopted units is 21.6, for the second package (right) the maximum speed is 21.7. That is, the movement of the crest of the anomalous wave occurs at the same speed. This speed is the group velocity of the packet, which is easy to see by considering the ratio

$$\frac{\partial \zeta}{\partial \tau} = 21.6 = \frac{\partial x}{\partial t} \cdot \frac{k_0}{\omega \cdot (\alpha / 2)} = \frac{v_g}{v_{ph}} \cdot \frac{2}{\alpha}, \text{ from where } \frac{v_g}{v_{ph}} \approx 0.54. \quad (\text{XXII.2})$$

In the laboratory system, the change in the amplitude of the crest of the wave of anomalous amplitude is more pronounced (see Fig. XXII 5). This qualitatively corresponds to the duration of the Peregrin autowave [XXII-15] in the laboratory frame of reference. Although it should be noted that the Peregrin autowave corresponds to a different physical reality, where the dispersion of the wave is weak. Gravitational

surface waves have a strong dispersion, and the NSE equation (19.1a) in this case is strongly modified. However, in a wave moving relative to the laboratory system of rest, the wave lifetime is much longer. Figure XXII.4 shows that the time of existence of a wave of anomalous amplitude in a reference frame moving with a group velocity of a packet does not exceed 40 time units in the model under consideration. Given its speed, a wave can travel hundreds of wavelengths. It is worth noting that in the numerical experiment considered at one moment in time, two waves of anomalous amplitude of 333 waves appeared in the observation area (see Fig. XXII.1) and during the order of 40 units there were no new waves; people in the sea can meet the same wave more than once.

Waves of anomalous amplitude, as it turned out, are long-lived formations drifting in the direction of wave motion with the group velocity of the wave packet, which is half the phase velocity of the main wave. The longitudinal size of the wave packet practically does not change, the amplitude of the maximum amplitude first increases, then gradually decreases. The distance that a wave packet travels with a persisting anomalous range is at least equal to several hundred wavelengths and for it can reach hundreds of kilometers for 200 meter waves.

It is important to note that a wave excited as a result of wind exposure as a result of modulation instability forms a disturbance spectrum whose energy is twice the energy of the main wave in the developed instability regime. It is the mode interference of this spectrum that forms a bizarre wave pattern, where waves of anomalous amplitude appear from time to time.

On the one hand, the number of such waves in areas of strong wind exposure is much larger than the statistics of random interference processes allow. This is due to the influence of the main wave (its amplitude remains noticeably greater than the amplitudes of each of the modes of the wave packet) on the behavior of each pair of modes from the wave packet of the perturbation. This is the effect of forced interference imposed by the main wave. However, the simple calculation of such waves by means of space monitoring due to the small viewing area (frame) may also be inaccurate. Once formed, such waves are able to drift over significant distance. Moreover, they may well fall into the next viewing frame, which unreasonably increases the number of such waves in the entire observation zone. That is, evaluation of the number of such modes can be overestimated.

The shape of the packet, which contains a wave of anomalous magnitude, and which is more than three times the average value of the magnitudes of the wave motion, is a train of three waves, similar to the Peregrin autowave [XXII-15]. The remark of V. E. Zakharov that there are other types of anomalous waves of this nature [XXII-8, XXII-9], based on the observations of [XXII-1 – XXII-10], is explained by the results of [XXII-16], where it is shown that converging wave fronts can certainly generate more powerful anomalous perturbations of a slightly different topology.

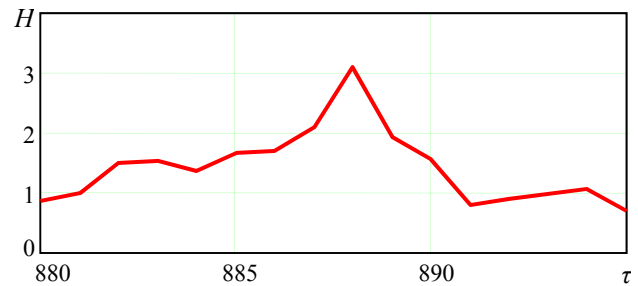


Fig. XXII.5. Change in the swing of anomalous amplitude wave for the second packet, the maximum values of which were

$$H_{\max 1} = 3.035, \quad H_{\text{rel}1} = 3.094$$

References to annex XXII

XXII-1. Kurkin A. A., Pelinovsky E. N. Killer waves: facts, theory and modeling. -- Nizhny Novgorod: UNN, 2004 (in Russian).

XXII-2. Kharif C., Pelinovsky E. Physical mechanisms of the rogue wave phenomenon // *Eur. J. Mech. B-Fluid.* – 2006. – V. 22 (6). – P. 603--633 (in Russian).

XXII-3. Yeom D.-I., Eggleton B. J. Photonics: rogue waves surface in light // *Nature.* 2007. – V. 450. – P. 953--962.

XXIII-4. Kharif C., Pelinovsky E., Slunyaev A. *Rogue Waves in the Ocean.* – Berlin, Heidelberg: Springer-Verlag, 2009.

XXII-5. Berdichevsky A. Giant killer waves still pose a danger to shipping. – RIA news, 2007. – Access mode: <http://transbez.com/info/sail/wave-killer.html>. (in Russian).

XXII-6. Lavrenov I. V. The wave energy concentration at the Agulhas current of South Africa // *Natural Hazards.* 1998. – Vol.17. – P. 117--127.

XVII-7. Badulin S., Ivanov A., Ostrovsky A. Influence of giant waves on the safety of offshore production and transportation of hydrocarbons // *Technologies, Fuel and Energy Complex.* 2005 – No. 2 (in Russian).

XXII-8. Zakharov V. E. Statistical theory of gravity and capillary waves on the surface of a finite-depth fluid. Three-dimensional aspects of air-sea interaction // *Eur. J. Mech. B Fluids.* – 1999. – Vol. 18 (3). – P. 327--344.

XXII-9. Dyachenko AI, Zakharov V. E. Modulation instability of stokes wave – Freak wave // *JETP Lett.* 2005. – Vol. 81 (6). – P. 255--259 (in Russian).

XXII-10. Stansell P. Distributions of extreme wave, crest and trough heights measured in the North Sea // *Ocean Engineering.* – 2005. – Vol. 32. – No. 8–9. – P. 1015--1036.

XVII-11. Schwartz L. W., Fenton J. D. Strongly nonlinear waves // *Ann. Rev. Fluid. Mech.* – 1982. – Vol. 14. – P. 39--60.

XXII-12. Chernousenko V. M., Kuklin V. M., Panchenko I. P., Vorob'ev V. M. Spatial Dissipative Structures. // *Nonlinear World (IV Int. Workshop on Nonlinear and Turbulent Proc. In Physics.)*. Singapore, World Scientific 1990. – V. 2, – P. 776–803 (in Russian).

XXII-13. Belkin, E. V., Kirichok, A. V., Kuklin V. M., Priymak A. V. Anomalous waves in a modulationally unstable wave field // *East Eur. J. Phys.* – 2014. – V. 1 – No. 2. – P. 4–39; Kuklin V. M. On frequency and spatial periodicity of the waves of the anomalous amplitude in the ocean / V. M. Kuklin, E. V. Poklonskiy. // *East European Journal of Physics* 2019. – V. 6. – N 4. – P. 41–46 (in Russian).

XXII-14. Chabchoub A., Hoffmann N., Akhmediev N. Rogue wave observation in a water wave tank / *Physical Review Letters* 106 (20) (2011) 204502.

XXII-15. Peregrine D. Water waves, nonlinear Schrodinger equations and their solutions / *Journal of the Australian Mathematical Society Series* 25 (1) (1983) 16–43.

XXII-16. Chabchoub A., Hoffmann N, Onorato M and Akhmediev N. Super RogueWaves: Observation of a Higher-Order Breather in Water Waves./ *Physical Review X* 2, 011015 (2012).

ANNEX XXIII
COLD PLASMA.
ONE-DIMENSIONAL SILIN EQUATIONS

Let us first consider the case of parametric instability of an external long-wavelength Langmuir field of high intensity for cold plasma, that is, when the energy density of the field exceeds the density of the thermal energy of the medium $W = |E_0|^2 / 4\pi \gg n_0 T_e$.

The equations of quasi-hydrodynamics for particles of a variety are known to have the form

$$\begin{aligned} \frac{\partial v_\alpha}{\partial t} + u_{0\alpha} \frac{\partial}{\partial x} v_\alpha - \frac{e_\alpha}{m_\alpha} E &= -v_\alpha \frac{\partial}{\partial x} v_\alpha, \\ \frac{\partial n_\alpha}{\partial t} + u_{0\alpha} \frac{\partial}{\partial x} n_\alpha + n_{0\alpha} \frac{\partial}{\partial x} v_\alpha &= -\frac{\partial}{\partial x} (n_\alpha v_\alpha), \\ \frac{\partial}{\partial x} E &= 4\pi \sum_\beta e_\beta n_\beta, \end{aligned} \quad (\text{XXIII.1})$$

where $\alpha = e$ and $\alpha = i$ correspond to electrons and ions. Particles are in the field of an external wave, the length of which, for simplification of calculations, is set equal to infinity, oscillating with speed $u_{0\alpha} = -(e_\alpha |E_0| / m_\alpha \omega_0) \cos \Phi$.

It is important to note that the initial variable field exciting the instability spectrum in the volume of consideration is uniform in space. This leads to oscillations of plasma electrons in such a spatially uniform field, that gave reason to call this process the parametric excitation of the wave spectrum. Traditionally, parametric instabilities are usually called processes, the cause of the development of which was a periodic change in an individual parameter (or part thereof), responsible, for example, for low-frequency motion, as in the cases described by the Mathieu equation. However, the last equation did not contain the inverse effect of the developing process on the source, causing high-frequency modulation of the parameter. That is, such a system was not self-consistent. In the case discussed below, the entire system is self-consistent, which is usual for the description of phenomena in plasma. The spectrum of this instability is similar to the spectrum of the modulation instability of a wave motion with a finite wavelength. In addition, the effect of this spectrum leads to modulation of the density of the medium. All this gave reason to consider such a parametric instability as a type of modulation instability (or, on the contrary, consider such a modulation instability as a type of parametric one).

The components of the field strength of the external wave are defined as it follows

$$E_0 = -i(|E_0| \exp[i(\omega_0 t + i\phi)] - |E_0| \exp[-i(\omega_0 t - i\phi)]) / 2.$$

Getting rid of $E_n = -4\pi i e (n_{i,n} - n_{e,n}) / k_0 n$, let us rewrite the first equation of the system (XXIII.1) in the following form

$$\frac{\partial v_{\alpha,n}}{\partial t} + u_{0\alpha} i k_0 n v_{\alpha,n} + \frac{4\pi e_\alpha i}{k_0 n m_\alpha} \sum_\beta e_\beta n_{\beta,m} = -i k_0 \sum_m m v_{\alpha,n-m} v_{\alpha,m}. \quad (\text{XXIII.2})$$

We use the following variables переменные $v_{\alpha,n} = e_{\alpha} n_{\alpha,n} \exp(-ia_{\alpha,n} \sin \Phi)$, $\theta_{\alpha,n} = v_{\alpha,n} \exp(-ia_{\alpha,n} \sin \Phi)$, where $a_{\alpha,n} = ne_{\alpha} k_0 E_0 / m_{\alpha} \omega_0^2$, $\Phi = \omega_0 t + \phi$. In this case, the first two equations (XXIII.1) can be written as

$$\frac{\partial v_{\alpha,n}}{\partial t} + \theta_{\alpha,n} ik_0 ne_{\alpha} n_{\alpha,0} = -ik_0 n \sum_m v_{\alpha,n-m} \theta_{\alpha,m}, \quad (\text{XXIII.3})$$

$$\frac{\partial \theta_{\alpha,n}}{\partial t} + \frac{4\pi e_{\alpha} i}{k_0 n m_{\alpha}} \sum_{\beta} v_{\beta,n} \exp(i(a_{\beta,n} - a_{\alpha,n}) \sin \Phi) = -ik_0 \sum_m m \theta_{\alpha,n-m} \theta_{\alpha,m}. \quad (\text{XXIII.4})$$

Obviously $a_{i,n} - a_{e,n} = n(ek_0 E_0 / M \omega_0^2) + n(ek_0 E_0 / m_e \omega_0^2) \approx n(ek_0 E_0 / m_e \omega_0^2) = a_n$, where $k_n = nk_0$, the quantity determines the discrete set of wave numbers of the modes of the short-wave spectrum. For electrons, equations (XXIV.3) – (XXIV.4) can be written as

$$\frac{\partial v_{e,n}}{\partial t} - \theta_{e,n} ik_0 nen_0 = -ik_0 n \sum_m v_{e,n-m} \theta_{e,m}, \quad (\text{XXIII.5})$$

$$\frac{\partial \theta_{e,n}}{\partial t} - \frac{4\pi e i}{k_0 n m_e} (v_{e,n} + v_{i,n} \exp(ia_n \sin \Phi)) = -ik_0 \sum_m m \theta_{e,n-m} \theta_{e,m}. \quad (\text{XXIII.6})$$

We shall use representation

$$v_{e,n} = \sum_s u_n^{(s)} \exp(is\omega_0 t) = u_n^{(0)} + u_n^{(1)} e^{i\omega_0 t} + u_n^{(-1)} e^{-i\omega_0 t} + u_n^{(2)} e^{i2\omega_0 t} + u_n^{(-2)} e^{-i2\omega_0 t}, \quad (\text{XXIII.7})$$

$$\theta_{e,n} = \sum_s v_n^{(s)} \exp(is\omega_0 t) = v_n^{(0)} + v_n^{(1)} e^{i\omega_0 t} + v_n^{(-1)} e^{-i\omega_0 t} + v_n^{(2)} e^{i2\omega_0 t} + v_n^{(-2)} e^{-i2\omega_0 t}, \quad (\text{XXIII.8})$$

and the known expansion $\exp(ia \sin \Phi) = \sum_{m=-\infty}^{\infty} J_m(a) \exp(im\Phi)$, where $J_m(x)$ is the Bessel function, in this case $J_0(x) = J_0(-x)$, $J_1(x) = -J_1(-x) = J_{-1}(-x)$, $J_2(x) = J_{-2}(x) = J_2(-x)$ [XXIV-2], after which we can find the non-resonant values of the density $u_n^{(0)}, u_n^{(2)}, u_n^{(-2)}$ and velocity $v_n^{(0)}, v_n^{(2)}, v_n^{(-2)}$ perturbations in the oscillating reference frame:

$$v_n^{(0)} = \frac{k_0}{\omega_0} \sum_m (n-m) \left[v_{n-m}^{(1)} v_m^{(-1)} - v_{n-m}^{(-1)} v_m^{(1)} \right] = \frac{1}{i\omega_0} \left[\frac{\partial v^{(1)}}{\partial x} v^{(-1)} - \frac{\partial v^{(-1)}}{\partial x} v^{(1)} \right]_n, \quad (\text{XXIII.9})$$

$$u_n^{(0)} = -v_{i,n} J_0(a_n) + \frac{k_0^2 n^2 m_e}{4\pi e} \sum_m v_{n-m}^{(1)} v_m^{(-1)} = -v_{i,n} J_0(a_n) - \frac{m_e}{4\pi e} \frac{\partial^2}{\partial x^2} \left[v^{(1)} v^{(-1)} \right]_n, \quad (\text{XXIII.10})$$

$$v_n^{(\pm 2)} = \pm \frac{2\omega_0}{3k_0 nen_0} v_{i,n} J_{\pm 2}(a_n) \exp(\pm 2i\phi) \mp \frac{k_0}{\omega_0} \sum_m m v_{n-m}^{(\pm 1)} v_m^{(\pm 1)} = \pm \frac{2\omega_0}{3k_0 nen_0} v_{i,n} J_{\pm 2}(a_n) \exp(\pm 2i\phi) \mp \frac{1}{i\omega_0} \left[\frac{\partial v^{(\pm 1)}}{\partial x} v^{(\pm 1)} \right]_n, \quad (\text{XXIII.11})$$

$$\begin{aligned}
u_n^{(\pm 2)} &= \frac{1}{3} v_{i,n} J_{\pm 2}(a_n) \exp(\pm 2i\phi) - \frac{k_0^2 n e n_0}{\omega_{pe}^2} \sum_s s v_s^{(\pm 1)} v_{n-s}^{(\pm 1)} = \\
&= \frac{1}{3} v_{i,n} J_{\pm 2}(a_n) \exp(\pm 2i\phi) + \frac{e n_0}{\omega_{pe}^2} \frac{\partial}{\partial x} \left[\frac{\partial v^{(\pm 1)}}{\partial x} v^{(\pm 1)} \right]_n.
\end{aligned} \tag{XXIII.12}$$

Expressions (XXIII.9) and (XXIII.10.10) proportional to $J_0(a_n)$ correspond to slow movements, and expressions (XXIII.11) and (XXIII.12) proportional to $J_{\pm 2}(a_n)$ are determined by the contribution to the nonlinearity of the second harmonic. For resonant quantities, the equation is

$$\begin{aligned}
\pm 2i\omega_0 \left[\frac{\partial u_n^{(\pm 1)}}{\partial t} \mp i \frac{\omega_{pe}^2 - \omega_0^2}{2\omega_0} u_n^{(\pm 1)} \mp i v_{i,n} \frac{\omega_{pe}^2 J_{\pm 1}(a_n) \exp(\pm i\phi)}{2\omega_0} \right] = \\
+k_0^2 n e n_0 \sum_m m \left[v_{n-m}^{(0)} v_m^{(\pm 1)} + v_{n-m}^{(\pm 1)} v_m^{(0)} \right] - ik_0 n (\pm i\omega_0) \sum_m \left[u_{n-m}^{(0)} v_m^{(\pm 1)} + u_{n-m}^{(\pm 1)} v_m^{(0)} \right] + \\
+k_0^2 n e n_0 \sum_m m v_{n-m}^{(\mp 1)} v_m^{(\pm 2)} - ik_0 n (\pm i\omega_0) \sum_m \left[u_{n-m}^{(\pm 2)} v_m^{(\mp 1)} \right].
\end{aligned} \tag{XXIII.13}$$

The representation of $u_n^{(\pm 1)} = \pm k_0 n e n_0 v_n^{(\pm 1)} / \omega_0 = ik_0 n E_n^{(\pm 1)} / 4\pi$, was used, where $v_n^{(\pm 1)} = \pm i e E_n^{(\pm 1)} / m \omega_0$. In this case, collecting the terms responsible only for electronic nonlinearity on the right-hand side (XXIII.1), we can rewrite this equation for short-wave perturbations in the form

$$\begin{aligned}
\pm 2i\omega_0 \left[\frac{\partial u_n^{(\pm 1)}}{\partial t} \mp i \frac{\omega_{pe}^2 - \omega_0^2}{2\omega_0} u_n^{(\pm 1)} \mp i v_{i,n} \frac{\omega_{pe}^2 J_{\pm 1}(a_n) \exp(\pm i\phi)}{2\omega_0} \right] e^{\pm i\omega_0 t} + \\
+ \frac{\omega_0^2}{e n_0} n e^{\pm i\omega_0 t} \sum_m \frac{v_{i,n-m}}{m} \left[u_m^{(\mp 1)} J_{\pm 2}(a_{n-m}) \exp(\pm 2i\phi) + u_m^{(\pm 1)} J_0(a_{n-m}) \right] = \\
= (k_0 n e n_0 / \omega_0) I.
\end{aligned} \tag{XXIII.14}$$

where the contribution of electronic nonlinearity can be represented as

$$\begin{aligned}
I &= -\frac{\partial}{\partial x} \left(v^{(\pm 1)} \left[\frac{\partial v^{(1)}}{\partial x} v^{(-1)} - \frac{\partial v^{(-1)}}{\partial x} v^{(1)} \right] \right) \mp v^{(\pm 1)} \frac{\partial^2}{\partial x^2} \left[v^{(1)} v^{(-1)} \right] - \\
&- \frac{\partial v^{(\pm 1)}}{\partial x} \left[\frac{\partial v^{(1)}}{\partial x} v^{(-1)} - \frac{\partial v^{(-1)}}{\partial x} v^{(1)} \right] \pm v^{(\mp 1)} \frac{\partial}{\partial x} \left[\frac{\partial v^{(\pm 1)}}{\partial x} v^{(\pm 1)} \right] \pm \\
&\pm v^{(\mp 1)} \frac{\partial}{\partial x} \left[\frac{\partial v^{(\pm 1)}}{\partial x} v^{(\pm 1)} \right]
\end{aligned}$$

Obviously, the right-hand side of equation (XXIII.14) corresponding to the contribution of electronic nonlinearity in the considered one-dimensional case turns out to be zero, which was previously independently noted in the works by V.P. Silin [XXIII-3] and V. E. Zakharov [XXIII-4]. Let us rewrite (XXIII.14) in the form [XXIII-5]

$$\frac{\partial u_n^{(\pm 1)}}{\partial t} \mp i \frac{\omega_{pe}^2 - \omega_0^2}{2\omega_0} u_n^{(\pm 1)} \mp i v_{i,n} \frac{\omega_{pe}^2 J_{\pm 1}(a_n) \exp(\pm i\phi)}{2\omega_0} \mp$$

$$\mp i \frac{\omega_0 n}{2en_0} \sum_m \frac{v_{i,n-m}}{m} \left[u_m^{(\mp 1)} J_{\pm 2}(a_{n-m}) \exp(\pm 2i\phi) + u_m^{(\pm 1)} J_0(a_{n-m}) \right] = 0. \quad (\text{XXIII.15})$$

If we use the representation for the resonance field in the form $(E_n^{(1)} \cdot e^{i\omega_0 t} + E_n^{(-1)} \cdot e^{-i\omega_0 t}) / 2$, as it was done in the work by E. A. Kuznetsov [XXIII-6], then $E_n^{(pm1)} \rightarrow E_n^{(\pm 1)} / 2 = -4\pi i u_n^{(\pm 1)} / k_0 n$, and the equation (XXIII.15) can be written differently

$$\frac{\partial E_n^{(\pm 1)}}{\partial t} \mp i \frac{\omega_{pe}^2 - \omega_0^2}{2\omega_0} E_n^{(\pm 1)} \mp \frac{8\pi\omega_{pe} v_{i,n}}{2k_0 n} J_{\pm 1}(a_n) \exp(\pm i\phi) \mp$$

$$\mp i \frac{\omega_0}{2en_0} \sum_m v_{i,n-m} \left[E_m^{(\mp 1)} J_{\pm 2}(a_{n-m}) \exp(\pm 2i\phi) + E_m^{(\pm 1)} J_0(a_{n-m}) \right] = 0. \quad (\text{XXIII.16})$$

We can also give the equation for the pump wave

$$\frac{\partial E_0^{(\pm 1)}}{\partial t} \mp i \frac{\omega_{pe}^2 - \omega_0^2}{2\omega_0} E_0^{(\pm 1)} \mp$$

$$\mp \frac{8\pi\omega_0}{2en_0 k_0} \sum_m \frac{v_{i,-m}}{m} \left[u_m^{(\mp 1)} J_{\pm 2}(a_{-m}) \exp(\pm 2i\phi) + u_m^{(\pm 1)} J_0(a_{-m}) \right] = 0. \quad (\text{XXIII.17})$$

From the representation of the pump wave corresponding to the chosen oscillation velocity $u_{0\alpha} = -(e_\alpha E_0 / m_\alpha \omega_0) \cos \Phi$, we shall obtain²⁴ $E_0 \rightarrow iE_0$ and $E_0^* \rightarrow iE_0^*$ and for E_0 we can rewrite equation (XXIII.17) [XXIII-5, XXIII-7]:

$$\frac{\partial E_0}{\partial t} - i\Delta E_0 = \frac{8\pi i \omega_0}{2en_0 k_0} \sum_m \frac{v_{i,-m}}{m} \left[u_m^{(-1)} J_2(a_{-m}) \exp(+2i\phi) + u_m^{(+1)} J_0(a_{-m}) \right], \quad (\text{XXIII.18})$$

where $\Delta = (\omega_{pe}^2 - \omega_0^2) / 2\omega_0$, or expressing density perturbations through the electric field strength of the modes

$$\frac{\partial E_0}{\partial t} - i\Delta E_0 = -\frac{\omega_0}{2en_0} \sum_m v_{i,-m} \left[E_m^{(-1)} J_2(a_m) \exp(2i\phi) + E_m^{(+1)} J_0(a_m) \right]. \quad (\text{XXIII.19})$$

Here, the terms on the right-hand side (XXIV-19) are also proportional to $J_0(a_n)$ and correspond to slow movements, as well as the proportional terms $J_{\pm 2}(a_n)$ are determined by the contribution to the nonlinearity of the second harmonic.

Slowly changing in time electric field strength

²⁴ In fact, this means that $|E_0| \exp(i\phi) \rightarrow |E_0| \exp(i\phi - i\pi/2)$, because the phase $\phi_0 = i\pi/2$ is connected with the choice of the form of the oscillation velocity.

$$\begin{aligned}
\bar{E}_n &= -\frac{4\pi i}{k_0 n} \left(\langle v_{en} \exp(-ia_n \sin \phi) \rangle + v_{i,n} \right) = \\
&= -\frac{4\pi i}{k_0 n} \left(v_{i,n} \left[1 - J_0^2(a_n) + \frac{2}{3} J_2^2(a_n) \right] + \left[u_n^{(1)} J_1(a_n) e^{-i\phi} + u_n^{(-1)} J_{-1}(a_n) e^{i\phi} \right] - \right. \\
&\quad \left. - \frac{n^2}{en_0} J_0(a_n) \sum_m \frac{u_{n-m}^{(1)} u_m^{(-1)}}{(n-m)m} - \frac{n}{en_0} J_2(a_n) \sum_m \frac{1}{m} \left[u_{n-m}^{(1)} u_m^{(1)} e^{-2i\phi} + u_{n-m}^{(-1)} u_m^{(-1)} e^{2i\phi} \right] \right). \quad (\text{XXIII.20})
\end{aligned}$$

may be presented differently

$$\begin{aligned}
\bar{E}_n &= -\frac{4\pi i}{k_0 n} v_{i,n} \left[1 - J_0^2(a_n) + \frac{2}{3} J_2^2(a_n) \right] + \frac{1}{2} \left[E_n^{(1)} J_1(a_n) e^{-i\phi} + E_n^{(-1)} J_{-1}(a_n) e^{i\phi} \right] - \\
&\quad - \frac{ink_0}{16\pi en_0} J_0(a_n) \sum_m E_{n-m}^{(1)} E_m^{(-1)} - \quad (\text{XXIII.21}) \\
&\quad - \frac{ik_0}{16\pi en_0} J_2(a_n) \sum_m (n-m) \left[E_{n-m}^{(1)} E_m^{(1)} e^{-2i\phi} + E_{n-m}^{(-1)} E_m^{(-1)} e^{2i\phi} \right].
\end{aligned}$$

which allows describing ions in large particles, equations of motion for which are

$$\frac{d^2 x_s}{dt^2} = \frac{e}{M} \sum_n \bar{E}_n \exp(ik_0 n x_s), \quad (\text{XXIII.22})$$

and the ion density is determined by the expressions

$$v_{i,n} = en_{in} = en_0 \frac{k_0}{2\pi} \int_{-\pi/k_0}^{\pi/k_0} \exp(-ink_0 x_s(x_0, t)) dx_{s0}. \quad (\text{XXIII.23})$$

Let us note that the description of ions by large particles, as shown in [XXIII-7], among other things, allows increasing the stability of the calculation scheme. Using equations (XXIII.1) for ions in which the right-hand sides can be neglected due to their smallness, we can proceed to the hydrodynamic description of ions. The equation for ion density in this case has the form [XXIV-5] [XXIII-5]

$$\begin{aligned}
\frac{\partial^2 v_{i,n}}{\partial t^2} &= -\Omega_i^2 \left(v_{i,n} \left[1 - J_0^2(a_n) + \frac{2}{3} J_2^2(a_n) \right] + \left[u_n^{(1)} J_1(a_n) e^{-i\phi} + u_n^{(-1)} J_{-1}(a_n) e^{i\phi} \right] - \right. \\
&\quad \left. - \frac{n^2}{en_0} J_0(a_n) \sum_m \frac{u_{n-m}^{(1)} u_m^{(-1)}}{(n-m)m} - \frac{n}{en_0} J_2(a_n) \sum_m \frac{1}{m} \left[u_{n-m}^{(1)} u_m^{(1)} e^{-2i\phi} + u_{n-m}^{(-1)} u_m^{(-1)} e^{2i\phi} \right] \right), \quad (\text{XXIII.24})
\end{aligned}$$

or

$$\begin{aligned}
\frac{\partial^2 v_{i,n}}{\partial t^2} &= -\Omega_i^2 \left(v_{i,n} \left[1 - J_0^2(a_n) + \frac{2}{3} J_2^2(a_n) \right] + \frac{ik_0 n}{8\pi} \left[E_n^{(1)} J_1(a_n) e^{-i\phi} + E_n^{(-1)} J_{-1}(a_n) e^{i\phi} \right] - \right. \\
&\quad + \frac{n^2 k_0^2}{64\pi^2 en_0} \sum_m J_0(a_n) E_{n-m}^{(1)} E_m^{(-1)} + \quad (\text{XXIII.25}) \\
&\quad \left. + \frac{nk_0^2}{64\pi^2 en_0} J_2(a_n) \sum_m (n-m) \left[E_{n-m}^{(1)} E_m^{(1)} e^{-2i\phi} + E_{n-m}^{(-1)} E_m^{(-1)} e^{2i\phi} \right] \right).
\end{aligned}$$

You can verify that the complex conjugate equation (XXIV.16) with the lower sign takes the form (when summing, you can replace the dumb index $m \rightarrow -m$)

$$\frac{\partial (E_{-n}^{(-1)})^*}{\partial t} - i \frac{\omega_{pe}^2 - \omega_0^2}{2\omega_0} (E_{-n}^{(-1)})^* - \frac{4\pi\omega_{pe} v_{i,-n}^*}{k_0 n} J_1(a_n) \exp(i\phi) -$$

$$-i \frac{\omega_0}{2en_0} \sum_m u_{i,-n+m}^* \left[(E_{-m}^{(1)})^* J_{-2}(a_{-n+m}) \exp(2i\phi) + (E_{-m}^{(-1)})^* J_0(a_{-n+m}) \right] = 0. \quad (\text{XXIII.26})$$

At the same time, for positive indices, the same equation can be written as

$$\frac{\partial E_n^{(1)}}{\partial t} - i \frac{\omega_{pe}^2 - \omega_0^2}{2\omega_0} E_n^{(1)} - \frac{4\pi\omega_{pe} v_{i,n}}{k_0 n} J_{\pm 1}(a_n) \exp(i\phi) -$$

$$-i \frac{\omega_0}{2en_0} \sum_m v_{i,n-m} \left[E_m^{(-1)} J_2(a_{n-m}) \exp(2i\phi) + E_m^{(1)} J_0(a_{n-m}) \right] = 0. \quad (\text{XXIII.27})$$

It is easy to see that for $E_{-n}^{(-1)} = (E_n^{(1)})^*$ and $v_{i,-n} = v_{i,n}^*$, equations (XXIV-26) and (XXIV-27) are identical. In the same way, one can verify that from such transformations follows $E_n^{(-1)} = (E_{-n}^{(1)})^*$ and $v_{i,n} = v_{i,-n}^*$. That is, ion charge perturbations have symmetry $n_{i,-n} = n_{i,n}^*$. Moreover, in order to correctly describe the instability process, it is sufficient to use the components of the rf field поля $E_n^{(1)}$, $E_{-n}^{(1)}$ и $E_0^{(1)}$ as well as perturbations of the ion charge $v_{i,n}$ at positive definite values of the index. Since the remaining values are expressed through them, that is, you can refuse to use the superscript. Using these simplifications, from (XXIII.19), (XXIII.25), and (XXIII.27) we can obtain the system of equations of the Silin hydrodynamic model, and from (XXIII.19), (XXIII.21), (XXIII.22), (XXIII.23), (XXIII.27) – the system of equations of the Silin hybrid model.

References to annex XXIII

- XXIII-1. Silin V. P. Parametric effect of high-power radiation on plasma. -- Science, 1973 (in Russian).
- XXIII-2. Dwight G. B. Integral tables and other mathematical formulas. Edition 5. – Science, 1978 (in Russian).
- XXIII-3. Silin V. P. Parametric resonance in plasma // ZhETF. 1965. -- V. 48. – P. 1679 (in Russian).
- XXIII-4. Zakharov V. E. Spectrum of weak turbulence in plasma without a magnetic field // ZhETF. 1966. -- T. 51. -- No. 6. – S. 688--696 (in Russian).
- XXIII-5. Kuklin V. M. Similarity of 1D Parametric Instability description of Langmuir waves // Journ. Kharkiv Nat. Univer., Phys. Ser. Nuclei, Part. Fields. 2013. – V. 1041. – № 2 (58). – P. 20–32 (in Russian).
- XXIII-6. Kuznetsov E. A. On the averaged description of Langmuir waves in plasma // Plasma Phys. The science. 1976. -- V. 2. -- No. 2. – P. 327--333 (in Russian).
- XXIII-7. Chernousenko V. V., Kuklin V. M., Panchenko I. P. The structure in nonequilibrium media. In book: The integrability and kinetic equations for solitons. AN USSR, ITPh. K. Nauk. Dumka. 1990. – 472 p. (in Russian).

ANNEX XXIV

ANOMALOUS OSCILLATIONS OF THE COEFFICIENT OF REFLECTION
OF AN ELECTROMAGNETIC WAVE FROM A PLASMA SURFACE [XXIV-1]

Intense electromagnetic fields acting on the plasma surface lead to significant oscillations of the electronic component. Let us consider fairly cold plasma. The nature of the effect of such an external electromagnetic field on the surface of cold plasma is described in the book by V. P. Silin [XXIV-2]. Let us generalize this approach to the case of a self-consistent description of the effect of external electromagnetic radiation normally incident on the plasma boundary with the excitation of a wide spectrum of surface oscillations.

Let the electromagnetic wave be with components $(0, H_y, E_z)$, where $|H_y| = |E_z| = E_0$ is normally incident on the plasma half-space ($x < 0$) with an unperturbed constant plasma density n_0 . Moreover, the intensity of the field of the incident wave will be considered large enough ($E_0^2 > 4\pi n_0 T_e$) and the thermal spread of plasma electrons will be neglected. For perturbations of the surface charge density $\sigma_\alpha = \lim_{\rho \rightarrow 0} \int_{-\rho}^{\rho} n'_\alpha dx$, where $e_\alpha, m_\alpha, n_\alpha$ are the charge, mass and perturbed charge density of the particles of the variety, we can use the system of equations [XXIII-2]

$$\exp[ia_{\alpha n} \cdot \sin(\omega_0 t + \varphi)] \cdot \frac{\partial^2}{\partial t^2} v_{\alpha n} + \frac{\omega_\alpha^2}{2} \sum_{\beta} v_{\beta n} = 0 \quad (\text{XXIV.1})$$

where $v_{\alpha n} = e_\alpha \cdot \sigma_{\alpha n} \exp[-ia_{\alpha n} \sin(\omega_0 t + \varphi)]$, $a_{\alpha n} = e_\alpha n \cdot E_z(k_z = 0) / m_\alpha \omega_0 c$, $\omega_\alpha^2 = 4\pi e^2 n_0 / m_\alpha$, $\omega_0 t + \varphi$ the phase of the field $k_z = 0$ in the plasma, ω_0 is the frequency of the incident wave. The wave number of such disturbances are $k_{zn} = n\omega_0 / c$. The solution (XXIV-1) will be sought in the form of series

$$v_{\alpha n} = \sum_{s=-\infty}^{+\infty} u_{\alpha n}^{(s)} \cdot \exp\{is\omega_0 t\} \quad (\text{XXIV.1})$$

When describing surface ion density perturbations, only the first member of the series can be retained. The summands for v_{en} , proportional to $\exp\{\pm i\omega_0 t\}$, exceed the other members of the series, however, for correctness, it is necessary to keep the terms corresponding to the "zero" and second harmonics. We restrict ourselves to taking into account symmetric perturbations of ions $u_{in}^{(0)} = u_{i-n}^{(0)}$; in this case, relations hold $u_{en}^{(0)} = u_{e-n}^{(0)}$, $u_{en}^{(\pm 2)} = u_{e-n}^{(\pm 2)}$, $u_{en}^{(\pm 1)} = -u_{e-n}^{(\pm 1)}$, $(u_{en}^{(1)})^* = u_{en}^{(-1)}$.

The self-consistent generalized system of Silin's equations, taking into account the inverse effect of the field of the excited short-wavelength spectrum of surface oscillations on the reflected wave (the parameters of the incident wave obviously do not change), has the form:

$$\frac{du_{en}}{dt} + (\theta_n - i\Delta_1\omega_0)u_{en} = i\frac{\omega_0}{2}J_1(a_n) \cdot u_{in} \exp\{i\varphi\}, \quad (\text{XXIV.2})$$

$$\frac{d^2u_{in}}{dt^2} = -\omega_0 \frac{m_e}{m_i} J_1(a_n) \cdot [u_{en} \exp\{-i\varphi\} + u_{en}^* \exp\{i\varphi\}], \quad (\text{XXIV.3})$$

$$D(R - R_0) = \frac{8\pi}{e_0 E_0} \sum_n u_{in} [J_0(a_n) \cdot u_{en}^* \exp\{i\varphi\} - J_2(a_n) \cdot u_{en} \exp\{-i\varphi\}], \quad (\text{XXIV.4})$$

where $1 + R = |1 + R| \exp\{-i\varphi\} = a_n \exp\{-i\varphi\} / \beta_0 n$, $\omega_0 = (1 - \Delta_1) \cdot \omega_{pe} / \sqrt{2}$,

$$\beta_0 = 2eE_0 / m_e c \omega_0, \quad R_0 = -D_0^* / D_0, \quad D_0 = \frac{\varepsilon_0}{\kappa_0} + i \frac{c}{\omega_0}, \quad \varepsilon_0 = 1 - \omega_{pe}^2 / \omega_0^2,$$

$\kappa_0^2 = -\omega_0^2 \varepsilon_0 / c^2$, $\Delta_1 = (m_e / m_i)^{1/3} \Delta$, R is the amplitude reflection coefficient

$$u_{en} = u_{en}^{(1)}, \quad u_{in} = u_{in}^{(0)}.$$

The terms are proportional to $J_0(a_n)$ and $J_2(a_n)$ correspond to the contribution to the nonlinear interaction, respectively, the “zero” and second harmonics. From the equations of the system (XXIV.2) – (XXIV.4), we can obtain the relation

$$1 - |R|^2 = \frac{16\pi}{e\beta_0 n_0 c E_0} \sum_n \frac{1}{n} \left(\frac{d|u_{en}|^2}{dt} + 2\theta_n |u_{en}|^2 \right), \quad (\text{XXIV.5})$$

which is the law of conservation of energy.

For the numerical solution of equations (XXIV.2) – (XXIV.4), let us pass to the variables $\tau = (m_e / m_i)^{1/3} \omega_0 t$, $\theta_n = n\theta_0 (m_e / m_i)^{1/3} \omega_0$, $u_{en} = |u_{en}| \exp\{i\varphi_n\}$,

$$N_n = 4\pi(m_e / m_i)^{1/6} E_0^{-1} \cdot |u_{en}| \beta_0^{1/2}, \quad M_n = 4\pi(m_e / m_i)^{-1/6} E_0^{-1} \cdot |u_{in}| \beta_0^{1/2}.$$

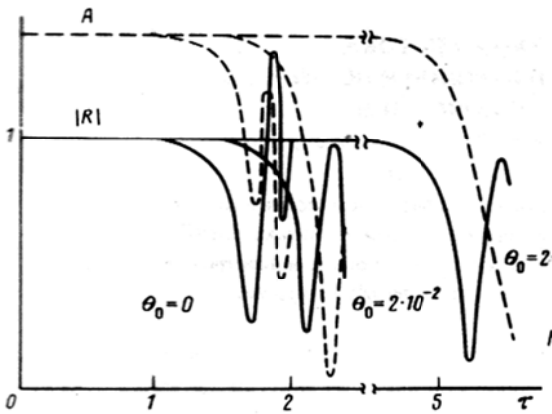


Fig. XXIV.1. The reflection coefficient R and the field in the plasma AE_0 for $\theta_0 = 0$ and $\theta_0 = 0.02$ [XXIV-1]

The features of the attenuation of surface waves are such that it grows with increasing wave number of oscillations [XXIV-3]. In the process of instability development, the phase spread φ_n rapidly decreases over several units τ , forming regions of surface electron and ion density of rapidly decreasing scale. The same mode locking effect leads to a strong interaction of the short-wavelength instability spectrum with the reflected wave and gives rise to significant oscillations of the reflection coefficient for small dissipation in the interval

$R = 0.5 \div 1.3$. The spatial spectrum of the instability narrows accounting for losses, reduces the integral energy level of the spectrum, delays the development of instability, and when the reflection coefficient fluctuates, the latter does not exceed unity.

instability narrows accounting for losses, reduces the integral energy level of the spectrum, delays the development of instability, and when the reflection coefficient fluctuates, the latter does not exceed unity.

References to annex XXIV

XXIV-1. Kuklin V. M., Panchenko I. P. Excitation of short-wavelength spectrum of surface waves in plasma by powerful electromagnetic radiation. Letters to ZhETF, 1986. -- Vol. 43. -- B. 5. -- P. 237--239 (in Russian).

XXIV-2. Silin V. P. Parametric effect of high-power radiation on plasma. -- M., Science, 1973. -- 287 p. (in Russian).

XXIV-3. Kondratenko A. N. Surface and bulk waves in confined plasma. -- M. Energoatomizdat. 1985 -- 208 p. (in Russian).

ANNEX XXV

PHASE TRANSITIONS IN THE PROCTOR-SIVASHINSKY MODEL UNDER THE CONDITIONS OF DEPENDENCE OF VISCOSITY ON TEMPERATURE [XXV-1]

During substitutions $T \cdot \varepsilon^2 = t$, for slow amplitudes A_j in the absence of noise, we can obtain the mathematical expression of the Proctor-Sivashinsky model to describe convection

$$\frac{\partial A_j}{\partial t} = A_j - \gamma A_{j+j_0} A_{j+2j_0} - \sum_{i=1}^N V_{ij} |A_i|^2 A_j, \quad (\text{XXV.1})$$

where the interaction coefficients are determined by the relations

$$V_{jj} = 1$$

$$V_{ij} = (2/3) \left(1 - 2(\vec{k}_i \vec{k}_j)^2 \right) = (2/3) (1 + 2 \cos^2 \vartheta),$$

and ϑ is the angle between the vectors \vec{k}_i and \vec{k}_j with the initial values of the spectrum amplitudes, and $A_j|_{t=0} = A_{j_0}$, $\vartheta_{j_0} = 2\pi/3$. The solution (XXV.1) will be presented as before in the form $\Phi = \varepsilon \sum_i A_j \exp(i\vec{k}_j \vec{r})$ of $|\vec{k}_j| = 1$.

Soft mode of excitation of a hexagonal convective structure. The account of the temperature dependence of viscosity demonstrates the possibility of realizing soft (at $\gamma < 0$) and hard (that is, with setting the initial perturbation already in the form of the desired structure 20 % higher average values of the amorphous state at $\gamma > 0$) excitation of hexagonal convective cells, the state function of which is almost equal to the state function of the shaft system. The time of the structural-phase transition of the first kind from the amorphous state is practically the same. For negative $\gamma < 0$, the mode of soft excitation of hexagonal convective cells is observed, as in the Swift-Hohenberg model (see Fig. XXV.1)

The time interval of the first-order phase transition is equal to τ_2 , however, despite the fact that the values of the state function are equal to unity, which in the former case of the absence of temperature dependence of viscosity $\gamma = 0$

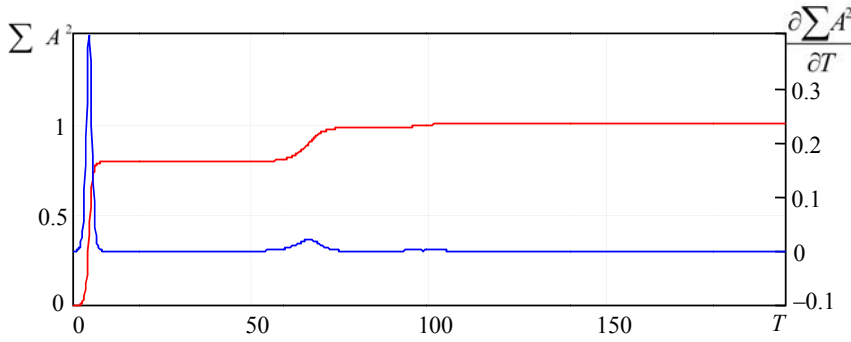


Fig. XXV.1. Value behavior ΣA^2 (upper curve) and $\partial \Sigma A^2 / \partial T$ depending on its time derivative T in the mode soft excitement with $\gamma = -0.25$

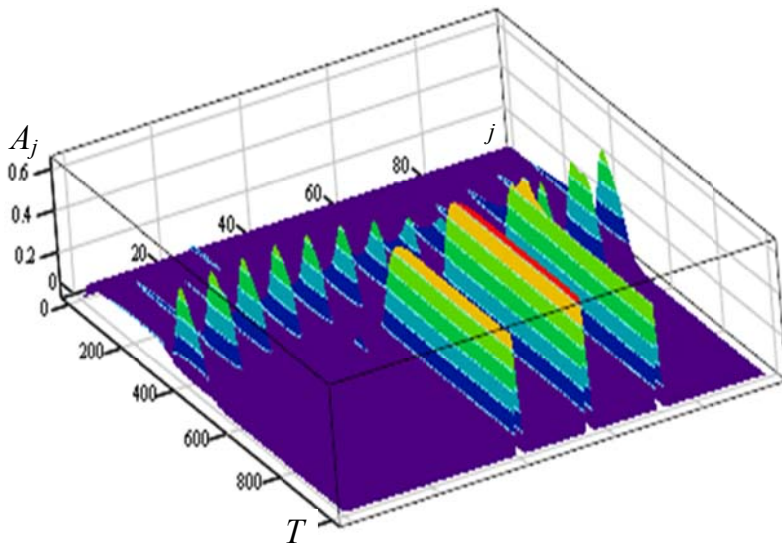


Fig. XXV. 2. Instability spectrum dynamics in soft instability mode ($\gamma = -0.25$)

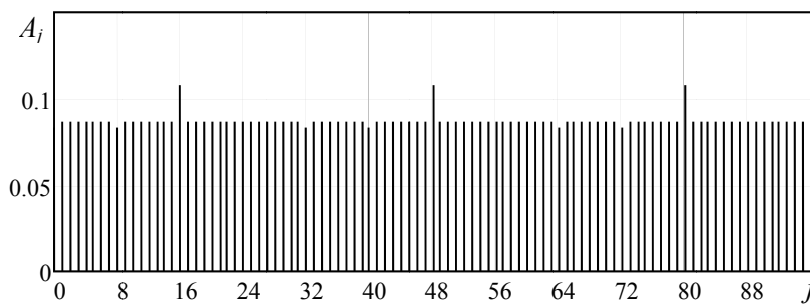


Fig. XXV. 3. The initial state of the mode spectrum against the background of the amorphous state of the system before a phase transition in a gas medium ($\gamma > 0$)

corresponded to a system of convective rolls, a system of hexagonal cells is formed here, as it can be seen in Fig. XXV.2, which shows the dynamics of the instability spectrum.

Hard mode convective hexagonal structure. In the case $\gamma > 0$, the regime of only hard excitation is possible, that is, the initial conditions must be specified in the form of hexagonal convective perturbations, clearly expressed against the background of fluctuations. Under these conditions, all process characteristics are similar to the case of soft excitation at the same values $|\gamma|$. Otherwise, the dynamics of the process, even in the case of nonzero $\gamma > 0$ is similar to the case of the absence of the dependence of viscosity on temperature, discussed above.

To implement the hard regime against the background of an amorphous state, a structure was formed, its amplitude was 20% higher than the average mode amplitudes (see Fig. XXV.3)

The behavior of the state function ΣA^2 and the time derivative

$\partial \Sigma A^2 / \partial T$ is shown in Fig. XXV.4 and fig. XXV.5 respectively.

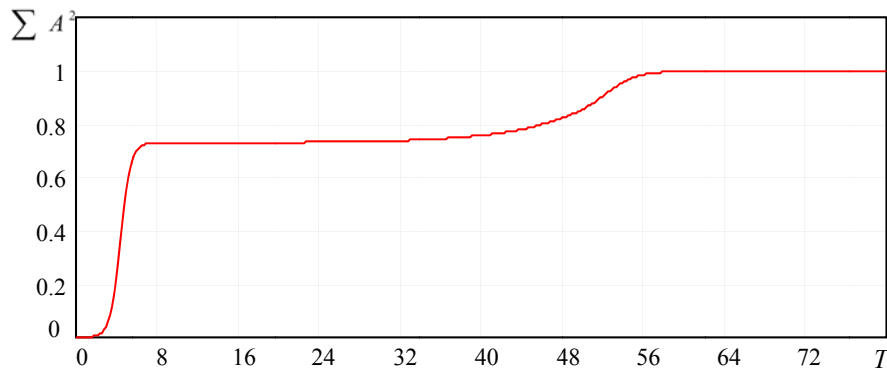


Fig. XXV. 4. The behavior of the value $\sum A^2$ depending on time T in hard excitation mode at $\gamma = 0.2$

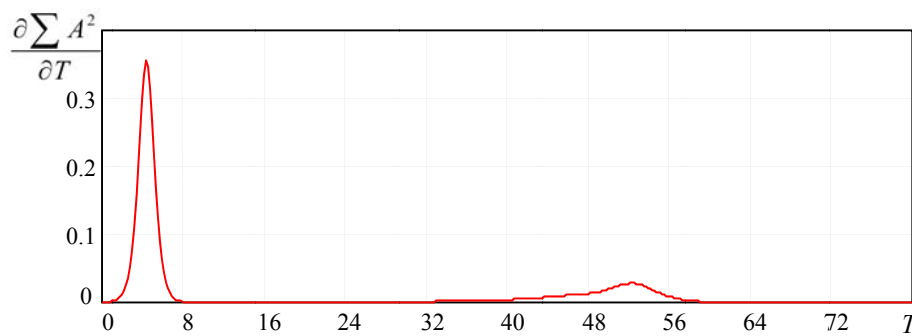


Fig. XXV. 5. The behavior of the value $\partial \sum A^2 / \partial T$ depending on time T in hard excitation mode at $\gamma = 0.2$

The dynamics of spectrum formation is shown in Fig. XXV. 6. The values $1 < j < 100$ correspond to the values of the angle $0 < \vartheta < 2\pi$. The appearance in the spectrum of three modes shifted by $2\pi/3$ corresponds to the formation of hexagonal cells.

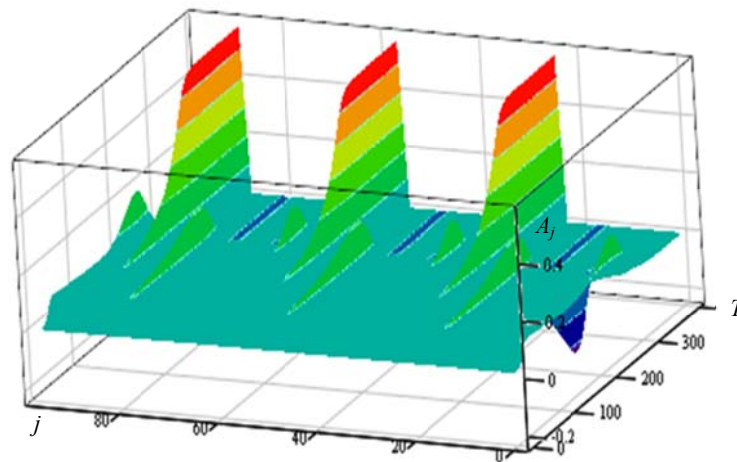


Fig. XXVI. 6. Instability Spectrum Dynamics in hard instability mode ($\gamma = 0.2$)

References to annex XXV

XXV-1. Gushchin I. V. Phase transitions in convection/ I. V. Gushchin, V. M. Kuklin, E. V. Poklonskiy // East European Journal of Physics, 2019. – V. 6. – No 4. – P. 34–40. <http://periodicals.karazin.ua/eejp/article/view/8561>

ANNEX XXVI DEFECTIVENESS CRITERIA OF SPATIAL PERIODIC STRUCTURES

Spectral and visual defectiveness's. It is useful to connect the discussion of this issue with the process of the formation of a stable state – a stable structure of convective cells. In the process of forming the structure of convective cells we shall

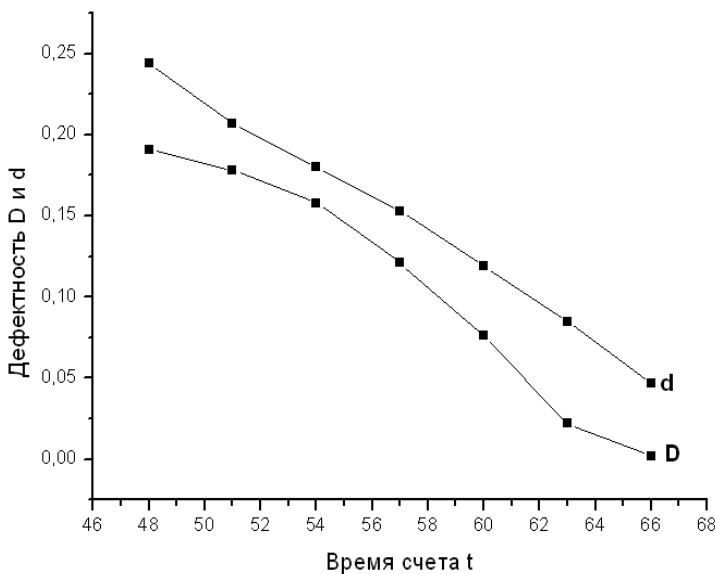


Fig. XXVI.1. Comparative analysis of spectral D and visual d defectiveness. The number of mods is 50

study the dynamics the “spectral imperfection (defectiveness)” of the structure $D = \sum_{j \neq 1,2} a_j^2 / \sum_j a_j^2$

based on the ratio of the squared amplitudes of the spectrum modes that do not correspond to the system of square cells to the total sum of the squared modes. Also we shall study the changes of so-called “Visual defectiveness” $d = N_{def} / N$, where N_{def} is the number of defective spatial cells (the area of the structure occupied by irregular cells) and N is the number of cells in an ideal regular structure (total area of the structure) [XXVI-1, XXVI-2].

The criteria by which to consider the cell correct and the method that allows calculating the number of these cells are as it follows. The resulting picture for the field is converted to 8-bit image mode. That is, the maximum number of displayed colors is reduced to 256. Thus, the formed structure becomes more clearly distinguishable. When enlarging such an image, one can quite clearly distinguish which of the structural units is the correct cell we need and which is not. The correct cell has a regular geometric shape with a uniformly dark center and four heights commensurate with the center in size of a lighter uniform color. Despite the qualitative nature of the description of the quantities, characterizing the spectral and visual imperfection of the structure, one can note (Fig. XXVI.1) their similar behavior when approaching the completion of the structural transition.

External noise and instability of system boundaries. Let us make a few comments regarding the implementation of the discussed process development scenarios. In case of a sufficiently high noise level, both additive ($f \neq 0$) and multiplicative (the random component in the first term ε^2 of the right-hand side of

(22.4)), the level of mode amplitudes from the very beginning can turn out to be significant. The initial conditions can also be such that the starting state of the system can be considered “amorphous” with a high degree of disorder, that is, if the amplitudes of the perturbations are sufficiently large and differ from each other according to a random law.

It is important to find out at what noise levels it is possible to maintain the “amorphous” state, characterized by the presence of a large number of spatial modes. Apparently, noise of very high intensity can prevent the system from forming convective structures, but the results of numerical calculations indicate that noise of even noticeable intensity is not able to prevent the formation of successively metastable (shafts) and stable (square cells) states. On the contrary, with a significant decrease in the amplitude of the noise, the process of transition from a metastable to a stable state is able to slow down when the system is delayed for a long time (“frozen”) in a metastable state. This is consistent with the ideas (see, for example, [XXVI-3]) that in some cases, it is noise that contributes to structural transitions.

The effect of the instability of the boundaries of the convection region is more interesting; it can be qualitatively modeled by changing the angle \mathcal{G}_{ij} between the vectors, which determine here the full set of functions that describe this boundary-value problem. The account of this effect, as it was noted by I. V. Gushchin, showed a much stronger effect of the instability of the system boundaries on the development of convection as a whole and on the nature of structural phase transitions. The models under discussion with a rather small modification are of interest for widespread use for the purpose of simulation modeling of processes of formation of structures and second-order phase transitions.

The presence of a larger number of minima at the period of the angle change (for example, six) will ultimately lead to the appearance of a spatial structure in the form of a polyhedron inscribed in the unit circle with a large number of edges (hexagon). By changing the spatial structure of local potential minima and their magnitude, it is possible to achieve the formation of any symmetric spatial structure, moreover, observing successively the formation of metastable states and all stages of structural transitions. This makes it possible to use a model modified in a similar way for a qualitative description of the processes of formation of at least two-dimensional spatial structures in systems where there is one distinguished scale, in particular, in condensed matter.

References to annex XXVI

XXVI-1. Gushchin I. V., Kirichok A. V., Kuklin V. M. Pattern Transitions in Unstable Viscous Convective Medium //arXiv preprint arXiv: 1311. 3884. – 2013.

XXVI-2. I. V. Gushchin, A. V. Kirichok, V. M. Kuklin. Pattern formation in convective media/ «Journal of Kharkiv National University», physical series «Nuclei, Particles, Fields», 2013. – issue 1 /57. – V. 1040. – C. 4-27

XXVI-3. Horsthemke W., Lefebvre R. Noise-Induced Transitions. Per from English. – M. : Mir, 1987. – 400 s. (in Russian).

ANNEX XXVII

ON THE APPLICABILITY OF THE PROCTOR-SIVASHINSKY-PISMEN MODEL TO THE DESCRIPTION OF THE MODULATION INSTABILITY OF THE DEVELOPED STRUCTURE OF CONVECTIVE CELLS

Despite the fact that the Proctor-Sivashinsky-Pismen model [XXVII-1] was derived for Prand numbers for the order of unity, it turns out to be true for describing the evolution of the developed structure of convective cells, for which, as shown before $\Phi \propto \varepsilon$. Moreover, the modulation instability of this structure arises only at small Prandl numbers [XXVII-2].

The fact is that when deriving equations (23.1) and (23.2) above, it was assumed that $\gamma \cdot \Psi \propto \gamma \cdot \Phi^2 \propto \varepsilon^2$, in this case $\gamma \propto 1$. When considering the modulation instability of the developed structure of convective cells, it turns out that non-zero values are $\Psi \propto \left(\frac{\Delta k}{k}\right) \cdot \Phi^2$, where in its turn $\left(\frac{\Delta k}{k}\right) \propto \varepsilon$. Thus, the model [XXII-1] can be used to describe the modulation instability of the already developed structure of convective cells only when $\gamma \propto 1/\varepsilon$, since only in this case the condition $\gamma \cdot \Psi \propto \varepsilon^2$ is satisfied.

References to annex XXVII

XXVII-1. Pismen L. Inertial effects in long-scale thermal convection, Phys. Lett. A. 1986. – V. 116. – P. 241--243.

XXVII-2. Kuklin V. M. The role of energy absorption and dissipation in the formation of spatial nonlinear structures in nonequilibrium media. Ukrainian Physical Journal, Reviews, 2004. -- V. 1. -- № 1. -- P. 49--81 (in Ukrainian).

ANNEX XXVIII

SEMICLASSIC SUPERRADIATION MODEL

At the end of Section 13, we considered the interaction of emitters with the field of a waveguide or resonator, and the emitters did not directly affect each other. In this case, each emitter generates its eigenfield, acting on other emitters. This interaction mode, with emerging self-synchronization of field generation sources, can be considered a superradiance mode.

Let us consider the behavior of quantum emitters, the wave functions of which do not overlap and their interaction is determined only by the electromagnetic field. In this case, a semiclassical description model based on the use of a density matrix is applicable. Neglecting relaxation processes, the equations for the components of the density matrix can be written in the form

$$\frac{d}{dt}(\rho_{aa} - \rho_{bb}) = -\frac{2i}{\hbar} [d_{ba}\rho_{ab} - d_{ab}\rho_{ba}]E, \quad (\text{XXVIII.1})$$

where the electric field is represented in the form $E + E^* = A(t) \cdot \exp\{-i\alpha t\} + A^*(t) \cdot \exp\{i\alpha t\}$, and the rapidly changing polarization of one emitter has the form $d_{ba}\rho_{ab} + d_{ab}\rho_{ba}$. From $\rho_{ab} = \bar{\rho}_{ab} e^{-i\omega_{ab}t} = \bar{\rho}_{ab} e^{-i\alpha t}$ let us determine slowly varying quantities for the polarization $\bar{p} = d_{ba} \cdot \bar{\rho}_{ab}$ and $d_{ab}\bar{\rho}_{ba} = d_{ba}^* \bar{\rho}_{ab}^* = \bar{p}^*$ of the emitter and also let us write down the system of equations for the inversion of one emitter $\bar{\mu} = (\rho_{aa} - \rho_{bb})$ and \bar{p} :

$$\frac{d}{dt}(\rho_{aa} - \rho_{bb}) = -\frac{2i}{\hbar}[d_{ba}\bar{\rho}_{ab}A^* - d_{ab}\bar{\rho}_{ba}A] = -\frac{2i}{\hbar}[\bar{p}A^* - \bar{p}^*A], \quad (\text{XXVIII.3})$$

$$\frac{d}{dt}\bar{p} = -\frac{i}{\hbar}(\rho_{aa} - \rho_{bb})|d_{ba}|^2 A. \quad (\text{XXVIII.4})$$

The equation for the field of an individual radiator is

$$\frac{\partial^2 E}{\partial t^2} - c^2 \frac{\partial^2 E}{\partial z^2} = 4\pi\omega^2 \cdot \bar{p} \cdot e^{-i\omega t} \cdot \delta(z_0), \quad (\text{XXVIII.5})$$

whence we can find the value

$$A(z, t) = \frac{i \cdot 2\pi \cdot \omega \cdot M}{c} \cdot \frac{1}{N} \sum_s \bar{p}(z_s, t) \cdot e^{ik|z-z_s|}, \quad (\text{XXVIII.6})$$

where $M = n_0 \cdot b$ is the total number of emitters, and n_0 is the density of emitters per unit length. From equations (XXVIII.1) – (XXVIII.2) we can obtain a system of equations for polarization and inversion of the j -th emitter

$$\frac{d}{dt}(\rho_{aa} - \rho_{bb}) = \frac{2i}{\hbar}[\bar{p}^*A - \bar{p}A^*], \quad (\text{XXVIII.7})$$

$$\frac{d}{dt}\bar{p} = -\frac{i}{\hbar}(\rho_{aa} - \rho_{bb})|d_{ba}|^2 A, \quad (\text{XXVIII.8})$$

using the ratios $P_j = P(z_j, \tau)$, $M_j = M(z_j, \tau)$, and also $\mu_1 = (\rho_{aa} - \rho_{bb})$ is the inversion of an individual radiator $\mu_{01} = \mu_j(\tau = 0)$, where $\mu_0 = \mu_{01} \cdot n_0$ is the initial

inversion per unit length $z = \frac{2\pi}{k}Z$, $\mu = \mu_{01} \cdot M$, $\bar{p} = |d_{ab}| \cdot \mu_{01} \cdot P$, $t = \tau/\gamma$,

$\Gamma_{12} = \frac{\gamma_{12}}{\gamma}$, $n_0 \cdot b = M$, $\gamma = \frac{2\pi \cdot \omega \cdot |d_{ba}|^2 \cdot \mu_0 \cdot n_0 \cdot b}{\hbar c}$ is the process increment, let us

write the system (XXVIII.7) – (XXVIII.8) in the form

$$\frac{d}{dt}M_j = -2 \cdot [P_j^* A_j + P_j A_j^*], \quad (\text{XXVIII.9})$$

$$\frac{d}{dt}P_j = M_j \cdot A_j, \quad (\text{XXVIII.10})$$

where for $A_j = A(Z_j, \tau)$ the relation

$$A(Z, \tau) = \frac{1}{N} \sum_s P(Z_s, \tau) \cdot e^{i2\pi|Z-Z_s|} \tag{XXVIII.11}$$

is true. The last expression can be represented as $A(Z, \tau) = |A(Z, \tau)| \cdot e^{i\phi_A}$. It should be borne in mind that for the dimensionless representation of the field we divided (XXVIII.6) by $\gamma \hbar / |d_{ba}|$. Then, for the total amplitude of the electric field in this normalization, the expression $2|A(Z, \tau)|$ is valid. It is important to note that the growth rate $\gamma = 2\pi \cdot \omega \cdot |d_{ba}|^2 \cdot \mu_{01} \cdot n_0 \cdot b / \hbar c$ in the semiclassical model of superradiance corresponds to the growth rate of dissipative instability $\gamma = \tilde{\gamma}_0^2 / \delta_D$ (see Section 13).

For 4000 emitters distributed at the wavelength at $P_j(\tau = 0) = P_0 \exp(i\varphi)$, φ is a random variable $\varphi \in (0 \div 2\pi)$, $P_0 = 0.1$, $M(\tau = 0) = 1$, $\Gamma_{12} = 0$, we obtain the following results of the numerical solution. In fig. XXVIII.1, XXVIII.2 we show the time dependences of the field amplitude to the left, to the right of the system and the maximum inside the emitter and the average inversion of the system.

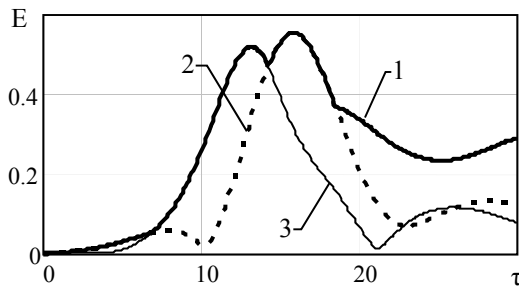


Fig. XXVIII.1 Field amplitude versus time

1 – $\max_Z(E(Z, \tau))$, 2 – $E(Z = 0, \tau)$,
3 – $E(Z = 1, \tau)$.

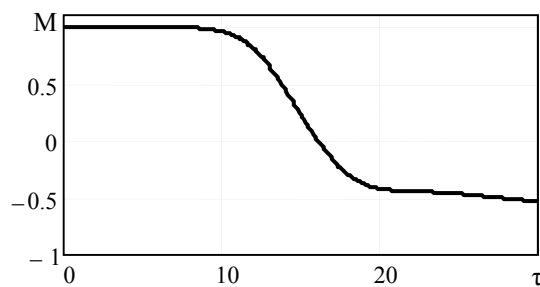


Fig. XXVIII.2 Dependence of the mean inversion of the system

$M = \frac{1}{N} \sum_j M(Z_j, \tau)$ on time

As it can be seen from figures XXVIII.1, XXVIII.2, the energy of the inverted system is pumped into the field. The field strength has two approximately equal maxima at times $\tau = 13.2$ ($E = 0.52$) and $\tau = 15.8$ ($E = 0.555$). The first maximum is on the right edge of the system ($Z = 1$), the second one is on the left ($Z = 0$). This asymmetric behavior of the field is associated with the choice of the initial conditions. Since $E = \sqrt{N}$, where $N = 4(\delta_D^2 / \tilde{\gamma}_0^2) \cdot (N / \mu_0)$, $N = \langle E \rangle^2 / 4\pi\hbar\omega$ (see the notation before formula (13.31)), the two values of the maxima in Fig. XXVIII.1 correspond to values N equal to 0.27 and 0.31, respectively.

References to annex XXVIII

XXVIII-1. Kuklin V. M., Poklonsky E. V. Semiclassical models of dissipative instability and superradiance of a system of quantum emitters // East European Journal of Physics 2020 – V. 7 (in press).

SUBJECT INDEX

Abnormal growth of the wave energy density due to the development of modulation instability. (Section 18).

Absolute and convective instability in moving frames of reference (Sections 8, 9).

Allowance for low-density plasma in the gyrotron equations. (ANNEX XVII).

Anomalous energy losses during dissipative beam instability (Section 10).

Anomalous radiation of a bunch moving in plasma during its self-profiling (Section 12).

Attenuation of a wave packet in a resonator filled with an active medium (ANNEX XIII).

Attenuation of a wave packet in a resonator filled with non-isothermal plasma (ANNEX XIV).

Beam instability with negative dissipation (Section 11).

Comparison of models of instability of Langmuir oscillations in the plasma of Silin and Zakharov, heating of ions (Section 21).

Density matrix and equations of the semiclassical model (ANNEX V).

Dissipative lasing in a resonator filled with an active substance (ANNEX XI).

Formation of a line spectrum of modulation instability near the threshold (Sections 16, 17).

Formation of stable clusters of fast particles in plasma (Section 12).

Generation of coherent pulses near the threshold of stimulated emission (Sections 5, 6).

Generation of self-similar structures by modulation instability near its threshold. (Section 17).

Hydrodynamic dynamo effect (Section 23).

Integrals of systems of equations describing cyclotron instabilities (ANNEX XVIII).

Intense oscillations of the reflection coefficient of an electromagnetic wave from a plasma surface (ANNEX XXIV).

Killer waves on the ocean surface (Section 19, ANNEX XXIII).

Mode of superradiance of a bunch of oscillators (ANNEX XVI).

Modulation instability of a system of convective cells in a thin layer (Section 23).

Nature of forced interference (ANNEX XXI).

Negative macroscopic dielectric constant (clause 12).

New threshold for stimulated emission (Section 5).

On the nature of the Mössbauer effect (ANNEX IV).

Periodic changes in the luminosity of quantum sources (Section 4, ANNEX VI).

Phase transitions in the Proctor-Sivashinsky model under conditions of viscosity versus temperature (ANNEX XXV).

Self-modulation of a bunch of particles moving in plasma (Section 12).

Self-similar structures on the surface and in the bulk of crystals (ANNEX XX).

Semiclassical model (Section 4).

Semiclassical model of superradiance (ANNEX XXVIII)

Silin's model describing the parametric instability of Langmuir oscillations in a plasma. (ANNEX XXIII).

Similarity of the phenomena of superradiance and dissipative instability (Section 13).

Simple connection between the expressions for spontaneous and induced emission of particles (Sections 1 and 2) and waves (Section 3).

Structural phase transitions in a thin layer of a convectively unstable medium (Section 22)

Transitions of dissipative instabilities into reactive regimes with nonlinear dissipation (Section 11).

Turbulent-wave instability (Section 7).

INSTEAD OF CONCLUSION

Every person who is keen on science would like to write what occurred to him, what he/she planned and what he/she managed to do independently and with the help of his/her like-minded colleagues. But, definitely about what he/she was directly involved. The search for new phenomena, effects and knowledge is the whole meaning of life in science. The reward for exhausting work will be the attention of a few colleagues, who showed interest, or perhaps recognition of the author's involvement in the achievements that will be noticed by contemporaries or already descendants.

More often, the achievements of individual scientists and even collectives are a part of separate constructions of the theory being created or already created. Their contribution becomes noticeable by colleagues and has a chance to get into textbooks only if these constructions bear the main load and ensure the stability of “the theory building”, and of course, if these achievements prove to be clearly useful in the creation of other theories. That is why it is especially important to achieve the completeness and consistency of the theory, the completion of its construction, which is rarely possible and only then deserves the recognition of the scientific community.

Only those topics are included in the book, which drove into thoughtfulness, which obscured ordinary life, and if it happened to see and understand something early and more clearly of other people, who were equally enthusiastic, ambitious and was lost for the outside world, it was only because they had to spend a little more vitality and time. Although luck, capricious and inconstant, sometimes glancing favorably, didn't even suggest, but rather hinted where to stop and look around. And only when the discovered and thought over meanings, like good wine matured in numerous discussions, it is worth undertaking writing books. And then we can hope that both the author and the reader will feel the taste of awareness of these meanings and the satisfaction of this awareness.

The author does not expect the reader to read carefully the book from beginning to end. It is quite enough if each of those who opens this book will find for him/her at first something interesting and then useful. Even the author does not know what will turn out to be the most curious, as everything in this life is subjective, even the recognition of truth, of true knowledge. The only question is how many fans the true knowledge and the truth will find among us.

У книзі розглянуто спонтанне і вимушене випромінювання частинок і хвиль. Вивчається формування когерентних імпульсів поблизу виявленого нового порога індукованого випромінювання. Показано, як модуляційні нестійкості породжують самоподібні структури й аномальні хвилі. Представлено порівняння динаміки нестійкості ленгмюровських коливань в плазмі і нагрівання іонів у моделях Сіліна і Захарова. Розглядається турбулентно-хвильова нестійкість і представлено новий підхід до опису ефекту Месбауера. Відзначено подібність процесів суперлюмінесценції і дисипативної нестійкості. Досліджуються структурні переходи в конвективному шарі і виникнення великомасштабних вихорів при модуляційної нестійкості розвиненої конвекції й інші актуальні завдання. Для фахівців, аспірантів і студентів фізичних факультетів.

Наукове видання

Куклін Володимир Михайлович

**ВИБРАНІ ГЛАВИ
(ТЕОРЕТИЧНА ФІЗИКА)**

(Англ. мовою)

Комп'ютерне верстання *В. В. Савінкова*
Макет обкладинки *І. М. Дончик*
Переклад з російської *А. Котова*

Формат 60x84/16. Ум. друк. арк. 15,24. Наклад 300 пр. Зам. № 25/21.

Видавець і виготовлювач
Харківський національний університет імені В. Н. Каразіна,
61022, м. Харків, майдан Свободи, 4.
Свідоцтво суб'єкта видавничої справи ДК № 3367 від 13.01.2009

Видавництво ХНУ імені В. Н. Каразіна
Тел. 705-24-32